UNIVERSIDADE DE LISBOA

FACULDADE DE CIÊNCIAS

DEPARTAMENTO DE QUÍMICA E BIOQUÍMICA

GEOGRAPHICAL ORIGIN DISCRIMINATION OF THE GREEN COFFEE BEAN AND ANALYTICAL QUALIFICATION OF THE ROASTING PROFILES

Carla Isabel Igreja Rodrigues

DOUTORAMENTO EM QUÍMICA
(Especialidade Química Analítica)

2011

UNIVERSIDADE DE LISBOA

FACULDADE DE CIÊNCIAS

DEPARTAMENTO DE QUÍMICA E BIOQUÍMICA

GEOGRAPHICAL ORIGIN DISCRIMINATION OF THE GREEN COFFEE BEAN AND ANALYTICAL QUALIFICATION OF THE ROASTING PROFILES

Carla Isabel Igreja Rodrigues

DOUTORAMENTO EM QUÍMICA
(Especialidade Química Analítica)

Tese orientada pela Profª Doutora Cristina Maria Filipe Máguas Hanson e pelo Prof. Doutor José Manuel F. Nogueira

2011

To my parents,
Bruno and André

"Caíra a conversa nesta moleza, exclama o José António Laertes:

- Recordam-se do velho Costa Cardoso, avô do Evaristo Branco! Era como eu. Não precisou de provar para saber que não gostava.

Quando teimavam com ele, prove lá senhor Cardoso, ia às do cabo. Caladão, sempre de cara dura, tinha um génio enresinado. Certo dia, explodiu numa grande danação contra o neto, que à fina força teimava que ele havia de beber café.

-Posso lá com tal bebida! – gritou-lhe o Costa Cardoso. – Uma planta que só nasce em regiões doentias da África e do Brasil, onde se morre de febres medonhas! E o grão? Quantos trabalhos para trazê-lo, ao lombo, sob o fogo do Sol, até à costa? Quantos trabalhos para embarcá-lo, atravessar as tempestades do oceano, desembarcá-lo, torrá-lo, moê-lo. Pois, após tantas canseiras, tantas, mal mergulham o pó na cafeteira, zás deitam-no fora! E essa mixórdia deixa a água tão suja e amarga que só com açúcar conseguem bebê-lo! Não! Nunca hei-de tocar-lhe sequer!"

em *À Lareira, Nos Fundos da Casa Onde o Retorta Tem o Café*

de Manuel da Fonseca (Editoral Caminho, 2000)

Acknowledgement

First of all, I would like to express my gratitude to Professor Cristina Máguas for all the support during this work, which defined 10 years of achievements, support, projects, dreams, fortunate and less fortunate moments. Thank you for all.

I also want to thank Professor J.M.F. Nogueira for all the advice and for pointing out my faults. I have learnt very important lessons from him. I gratefully acknowledge his down-to-earth, sincere, straightforward way of helping me evolve.

A special thank to my dear Professor Thomas Prohaska from BOKU University in Vienna (Austria) for investing his effort and knowledge in my work. We met in the beginning of 2007 in Vienna when I was attending a SIBAE Spring School and immediately decided we had to work together. His contribution transformed and shaped my work into directions that I did not expect.

I gratefully acknowledge the support of *Comendador* Rui Nabeiro, and the commitment from the Research & Development team of the coffee company Novadelta, S.A. (Portugal), especially of Marco Miranda and Miguel Ribeirinho. Without Novadelta this work would have never been possible. This team recognized the importance of this work at national and international level since the very beginning and has always kept an open door to me. Financial support from Novadelta Company through the Oritocafe project (ADI Agency) triggered the work of these PhD studies.

I want to thank Professor Peter Hildebrandt from the Technical University of Berlin (Germany), for his interest in my work and for the nice collaboration. We met when I was his student in a short course on Raman spectroscopy and we could not resist applying the technique to study coffee. The results revealed many possibilities of research that I hope we will be able to develop.

A special thank to Professor Loren Gautz from Hawai'i University (US) and Shawn Steiman from Coffea Consulting (US). In spite of the distance between us, they persisted in our collaboration, giving all their support, ideas, sending coffee samples, and participating in the IsoGeoCoffee project. They proved that the physical distance between people is not a hindrance to good scientific collaborations.

A special thank to my colleague Rodrigo Maia for all the teachings and motivation. Rodrigo always helped, supported and gave me a kind word, especially in times of difficulty and doubt.

I gratefully acknowledge all the support from Professor José Cochicho, from IICT (Portugal). I always remember his appreciation and motivation.

I want to thank Professor Marco Lauteri from CNR (Italy) for the nice collaboration. I also hope we can continue working together.

I thank Professor Mário Gonçalves from the Geology Department of Faculty of Sciences of University of Lisbon for introducing me to applied computation and for his appreciation of my work.

I would like to thank Professor José Cardoso Menezes from the Biological and Chemical Engineering Department of IST/UTL (Portugal) for accepting me in his group. The first time I applied spectroscopy to study coffee was in collaboration with his team. All colleagues from his group were very supportive.

A special thank to my colleagues from Center for Environmental Biology of Faculty of Sciences of University of Lisbon.

I also want to thank my colleagues from VIRIS laboratory, at BOKU University, Vienna: Marion, Johanna, Monika, Christopher, Lubna, Patrick, all the students, you have always welcomed me and made all your efforts to make my stay in Vienna the most pleasurable possible.

I also want to write a kind word for my colleagues Fátima, Rita, Alexandra, Rosa, Nuno and Rute from the Center for Chemistry and Biochemistry of Faculty of Sciences of University of Lisbon, for having integrated me in their group and for their support and good humor. We had a nice time working together.

At last, thank you mum and thank you dad, thank you my dear Bruno and André for all the support, motivation and patience. This PhD studies were a joint effort from all of us. Thank you for your understanding when I had no time to share, during my absence from home for extended periods, and for helping me to persist during difficult times. Without your support I would have never achieved all the accomplishments of this work.

I wish to thank the financial support of:

ADI Agency (Agência de Inovação) for the Project POCTI Med. 2.3 - Projecto ORITOCAFÉ (2004-2006).

Fundação para a Ciência e a Tecnologia (FCT) for a grant (SFRH/BD/28354/2006) and for the project PTDC/AGR-AAM/104357/2008 (IsoGeoCoffee) (2010-2012).

Foreword

Since the very beginning, this work was considered divided in two distinct parts. The first one, related to the analysis of the green coffee bean in order to achieve its geographical origin discrimination, and the second, targeted to the analysis of the volatile fraction of roasted coffee. The way the work plan for these studies was conceived demanded a multidisciplinary approach involving two scientific areas in the Faculty of Sciences of University of Lisbon, namely the Plant Biology and the Chemistry and Biochemistry Departments. However, during the time of this work, this multidisciplinary approach extended beyond these two departments through scientific collaborations with other abroad groups with different know-how's in the field of Analytical Chemistry.

The main goals of this work were the study of the isotopic composition of different elements of the green coffee bean and how this could contribute to the development of an analytical tool allowing the geographical origin discrimination of coffee. The results of the present work were also applied to the study of isotope effects related with climate and geology influencing the isotope abundance ratios of certain bio-elements and geo-elements in the coffee bean. In parallel a study of how the coffee roasting conditions influenced aroma quality and composition of coffee blends was also addressed. Although the distribution of goals by the two parts of the work was not equitative, both are relevant in what respects to the possible applications to the coffee industry.

C. I. I. Rodrigues

Resumo

No presente trabalho, foram aplicadas diversas técnicas espectroscópicas para a discriminação de diferentes tipos de café, da sua origem geográfica e, também, na caracterização da composição da fracção volátil do café torrado. Numa primeira abordagem, começou por se estudar a aplicação da espectroscopia de Raman no sentido da diferenciação do tipo de café (*Arábica* e *Robusta*), baseada na determinação do teor em "kahweol", tendo os resultados obtidos permitido a respectiva discriminação. Posteriormente, aplicou-se a técnica de espectrometria de massa de razão isotópica (IRMS) para determinação da composição isotópica dos elementos carbono (C), azoto (N) e oxigénio (O) do grão verde do café, o que permitiu a diferenciação dos cafés a nível continental. Demonstrou-se ainda que o O é o elemento fundamental para esta diferenciação, uma vez que reflecte a hidrologia do local de produção do café. Seguidamente, combinou-se IRMS com espectrometria de massa acoplada a plasma indutivo (ICP-MS), permitindo a determinação da composição isotópica do estrôncio (Sr) no grão verde do café, em particular a razão dos isótopos 87 e 86 ($^{87}Sr/^{86}Sr$). Os resultados obtidos demonstraram que, as razões isotópicas do Sr e O, se mostram promissoras para a autenticação da proveniência do café, reflectindo a geologia e hidrologia de cada origem geográfica. Porém, no sentido de expandir a compreensão da forma como os factores ambientais determinam a composição isotópica dos diferentes elementos do grão verde de café, tornou-se necessário estudar uma região modelo de produção, tendo sido seleccionado o Havai. Este estudo realizado à micro-escala, com cafés provenientes de diferentes ilhas, permitiu analisar em detalhe a forma como os diversos factores ambientais, prevalecentes no local e tempo de produção de café, se reflectem na composição isotópica elementar do grão. Esta abordagem permitiu ainda a discriminação dos cafés provenientes das diferentes ilhas do Havai. Verificou-se igualmente que, a composição isotópica do O, Sr e S no grão verde de café se relaciona com factores ambientais conhecidos, nomeadamente, a composição isotópica do O da precipitação ($\delta^{18}O_{prec}$), a distância ao mar e a actividade vulcânica característica desta região. A técnica analítica de IRMS foi ainda aplicada na análise da composição isotópica do O da molécula de cafeína ($\delta^{18}O_{caff}$), préviamente extraída do grão verde de café, tendo os resultados obtidos demonstrado boa correlação entre $\delta^{18}O_{caff}$ e $\delta^{18}O_{prec}$. Uma vez os isótopos de O da molécula de caféina terem somente origem na água metabólica dos tecidos onde ocorre a biossíntese deste metabolito, esta abordagem analítica poderá ser uma alternativa para estudos de ecofisiologia da planta do café. Por último, caracterizou-se o perfil aromático do café torrado com diferentes valores cromáticos, combinando diversas técnicas de microextracção no modo de "headspace" estático com cromatografia gasosa acoplada a espectrometria de massa. O recurso às espumas de poliuretano como fases poliméricas inovadoras, revelou-se uma alternativa promissora na caracterização do aroma e discriminação de diferentes "blends" de café.

Palavras-chave: Isótopos, Grão verde de café, Proveniência geográfica, Café torrado, Perfil aromático

Abstract

In the present work, several spectroscopic techniques were applied for the discrimination of different types of coffee, of their geographical origin, and also in the characterization of the volatile fraction of roasted coffee. In a first approach, a study on the application of Raman spectroscopy to the differentiation of coffee type (*Arabica versus Robusta*) was developed, based on the determination of kahweol content, wherein the results obtained allowed their discrimination. Then, isotope ratio mass spectrometry (IRMS) was applied for the determination of the isotopic composition of carbon (C), nitrogen (N) and oxygen (O) of the green coffee bean, allowing coffee differentiation at continental level. It was also shown that O was the fundamental element to achieve this differentiation, reflecting the hydrology of the coffee-producing regions. Subsequently, IRMS was combined with inductively coupled plasma mass spectrometry (ICP-MS), to determine the isotopic composition of strontium (Sr) in the coffee bean, in particular the ratio of the isotopes 87 and 86 ($^{87}Sr/^{86}Sr$). The results obtained demonstrated that the isotope ratios of Sr and O were promising for coffee authenticity, as these elements reflect the local geology and hydrology. However, in order to expand the understanding of how environmental factors determine the isotopic composition of the different elements on the green coffee bean, it was necessary to study a model region of production, in which Hawai'i was selected. This study performed at micro-scale, with coffees from different islands, allowed the detail analysis of how the various environmental factors prevailing in the location and time of coffee production, were reflected in the elemental isotopic composition of the coffee beans. This approach allowed the discrimination of coffees from the different islands of Hawai'i. It was also shown that the isotopic composition of O, Sr and S in the green coffee beans is related to known environmental factors, namely the isotopic composition of the O of local precipitation ($\delta^{18}O_{prec}$), the distance to the coast, and the volcanic activity characteristic of that region. In addition, IRMS was applied to measure the isotopic composition of the caffeine molecule ($\delta^{18}O_{caff}$) previously extracted from the green coffee bean. As O isotopes of caffeine molecule originate from the metabolic water of plant tissues, where this metabolite is biosynthesized, this analytical approach constitutes an alternative for studies on the ecophysiology of the coffee plant. Finally, a characterization of the aroma profile of roasted coffees with different chromatic values was performed by combining several microextraction techniques with gas chromatography coupled to mass spectrometry. The use of polyurethane foams as innovative polymeric phase proved to be a promising alternative in the aroma characterization and discrimination from different coffee blends.

Key-words: Isotopes, Green coffee bean, Geographical provenance, Roasted coffee, Aromatic profile

Index

Abbreviations list

AAS-Atomic absorption spectroscopy

AES-Atomic emission spectroscopy

CAR-Carboxen

CE-Capillary electrophoresis

CF-IRMS-Continuous flow isotope ratio mass spectrometry

CRM-Certified reference material

CW-Carbowax

DVB-Divinylbenzene

GC-Gas chromatography

GC-MS-Gas chromatography coupled to mass spectrometry

HPLC-High performance liquid chromatography

HS-Headspace

ICP-AES-Inductively coupled plasma atomic emission spectroscopy

ICP-MS-Inductively coupled plasma mass spectrometry

IR-Infrared

IRMS-Isotope ratio mass spectrometry

iWUE-Intrinsic water use efficiency

LD-Liquid desorption

MORBs-Mid-ocean-ridge basalts

MS-Mass spectrometry

NMR-Nuclear magnetic ressonance

OIB-Ocean-island chains

PA-Polyacrilate

PCB-Polymerase chain reaction

PDMS-Polydimethylsiloxane

PEP-Phosphoenolpyruvate

PTR-MS-Proton transfer reaction mass spectrometry

PU-Polyurethane

RH-Relative humidity

SBSE-Stir bar sorptive extraction

SPME-Solid phase microextraction

TD-Thermal desorption

TCD-Thermal conductivity detector

TIC-Total ion chromatogram

1. General introduction

1.1. Coffee history

From its origins in Africa, coffee cultivation wandered east and west, eventually forming a belt roughly bounded by the Tropics of Cancer and Capricorn (Smith, 1985). Nowadays, the top ten coffee-producing countries are Brazil, Colombia, Indonesia, Vietnam, Mexico, Ethiopia, India, Guatemala, Ivory Coast and Uganda. Today Brazil is responsible for about a third of all coffee production (figure 1).

Figure 1. Coffee cultivation zone (the ten top coffee producers are shown in yellow) (map from www.nationalgeographic.com/coffee/ax/frame.html).

According to the legend, coffee originated from Africa in A.D. 800. Kaldi, a legendary Ethiopian goatherd, noticed his herd dancing from one coffee shrub to another, grazing on the cherry-red berries containing the beans and picked some cherries to him and soon felt the effect of this plant. However, coffee, as we know it, originated in Arabia where the first roasted coffee beans were brewed around A.D. 1000. By the 13th century, Muslims were drinking coffee religiously and wherever the Islam went, coffee went too: North Africa, the eastern Mediterranean, and India. A merchant of Venice introduced Europe to coffee in 1615 but the first European-owned coffee estate, on colonial Java, now part of Indonesia, was only founded by the Dutch in 1696. In 1714, the Dutch offered Louis XIV a coffee tree for Paris's Royal Botanical Garden, the *Jardin des Plantes*. Several years later, Gabriel Mathiew de Clieu, a naval officer, steals a sprout of this tree and takes it to Martinique causing the spread of this plant in Latin America. In 1727, coffee blooms in Brazil and by 1800, Brazil's large harvests turn coffee from an elite indulgence to an everyday elixir, a drink for the people. Since then, coffee has become one of the most important merchandises commercialized in the world. It is the only food merchandise produced globally (except in Europe) associated with many sustainability, fair trading, health care and education projects implemented at the regions where it is cultivated. For this reason, there is no

doubt of the importance of the coffee market for global economy. From the early 1970s onwards public concerns over the social aspects of coffee production in producing countries rose in the Netherlands, sometimes forcing retailers and roasting companies to stop selling coffee from countries with dictatorial regimes, such as Angola (Boons, 2009). This is a political matter that, although very interesting for its complexity, is beyond the scope of this work. Nonetheless, to whom it may interest, the reading of the recent work of the sociologist Daniel Jaffee (*Brewing Justice, Fair Trade Coffee, Sustainability, and Survival*) (Jaffe, 2007), and also the work of Goodman and co-authors (*Confronting the Coffee Crisis, Fair Trade, Sustainable Livelihoods and Ecosystems in Mexico and Central America*) (Goodman, 2008) is recommended. At the same time the international organic movement developed which promoted agricultural practices in harmony with nature. During the 1980s the Max Havelaar and EKO standards[1] were introduced. As a result of the market trend for developing specialties, products with labels such as Fair Trade were able to penetrate the regular distribution channels. For producers, a major issue is to get access to the global market through channels that ensure a reasonable price. One way is to grow high quality coffee, which is only possible if local ecosystems are permitting this. An alternative is to grow organic coffee but this involves a choice for one standard or another. Adopting a standard requires substantial additional fieldwork as well as administrative responsibilities, as well as up to three years of operating under more strict principles before a certificate can be obtained (Boons, 2009). This made coffee authenticity confirmation through chemical/physical analysis important also because consumers started to value products with label of origin, even if commercialized by fair trade commerce or produced organically. In addition, coffee importing companies were interested in developing analytical tools that could be applied to demonstrate that the imported coffee had not been adulterated along the commercial chain. These different factors influencing coffee production and consumption had an impact in coffee research field. Coffee has been a case-study in a large number of research studies in many different fields, *e.g.* biology, genetics, agronomy, ecology, plant physiology and analytical chemistry. Several studies have been developed in the last ten to fifteen years in order to achieve the geographical origin discrimination of coffees. Recently, several news concerning the effects of climate change on coffee cultivation came to public (Reuters Agency). Rising temperatures and erratic weather patterns are changing historic trends in the coffee season (Ford, 2008; Grainger, 2010). Farmers also report high-altitude plants are maturing at times more typically of their low-land counterparts (Ford, 2008; McPhaul, 2008). This is generating a complete productive disorder (Ford, 2008), and shifting the attention of coffee producer countries to the problematic of climate change. Today, coffee producing communities struggle to sustain their ecosystems, cultures, and knowledge systems and this will have a major impact on the future of coffee production and consumption.

[1] Max Havelaar quality label for Fair Trade guarantees that products or raw materials were purchased on the basis of Fair Trade principles. EKO quality label represents the use of organic production methods in the country of origin.

1.2. The coffee plant

The genus *Coffea* belongs to the family *Rubiaceae.* This family comprises many genera including *Gardenia*, *lxora*, *Cinchona* (quinine) and *Rubia*. The two main species of coffee tree cultivated on a worldwide scale are *Coffea arabica* and *C. canephora* var. *robusta*. Minor cultivated species include *C. liberica* and *C. excelsa*, which are mainly restricted to West Africa and Asia, and account for only 1-2 % of global production (Wintgens, 2004a). The coffee plant takes approximately 3 years to develop from seed germination to first flowering and fruit production (figure 2).

Figure 2. (a) coffee seedlings, (b) adult coffee plant, (c) ripen coffee cherries, and (d) coffee bean samples for analysis: (1) green coffee beans, (2) grinded green coffee beans, (3) green coffee beans with parchment, (4) dry coffee cherries with coffee bean still inside.

A well-managed coffee tree can be productive for up to 80 years or more, but the economic lifespan of a coffee plantation is rarely more than 30 years (Wintgens, 2004a). The shrub is perennial evergreen dicotyledonous which can reach a height of 10 m in wild state, but plantation coffee is pruned to a maximum of about 3 m to facilitate harvesting and to maintain optimum tree shape. The primary branches are opposed, horizontally or drooping, and the leaves grow in pairs on short stalks. They are about 15

cm in length in *C. arabica* and longer in *C. canephora*, oval or lanceolate, and shiny dark green in appearance. The first flowers are produced at an age of 3 to 4 years, creamy white and sweetly scented, appearing in clusters in the axis of the leaves. After flowers fade, the ovaries slowly develop into oval drupes up to 18 mm in length and 10 to 15 mm in diameter, at first green, ripening to a bright red (referred to as 'cherries'), at which stage they are ready for harvesting. It is common to find blossoms, green fruit and red cherries flourishing on the same branch, especially in regions where there is an even annual rainfall distribution. The coffee 'beans' are the seeds, of which two are normally found in each fruit (Smith, 1985; Wintgens, 2004a). Each bean is covered with a thin closely fitting tegument known as the silverskin, outside of which is a looser, yellowish skin called the parchment, the whole being encased in a mucilaginous pulp which forms the flesh of the 'cherry' (figure 2). The beans which develop inside the cherry are used as the basic element for producing roast and ground coffee, soluble coffee powders, and coffee liquor. Although it is possible to propagate coffee by grafting or by taking cuttings, the usual commercial practice is to raise the plants from seeds. On the plantation the seeds are sown in carefully prepared seed beds, sometimes covered by a layer of sand, with protection from strong sunlight. The seedlings may then be transplanted into nursery beds for final planting in the field when they are 20 to 30 cm high (figure 2a). A density of 2500 to 3000 plants per hectare is typical (Smith, 1985).

The main constituent parts of the coffee berry are shown in figure 3.

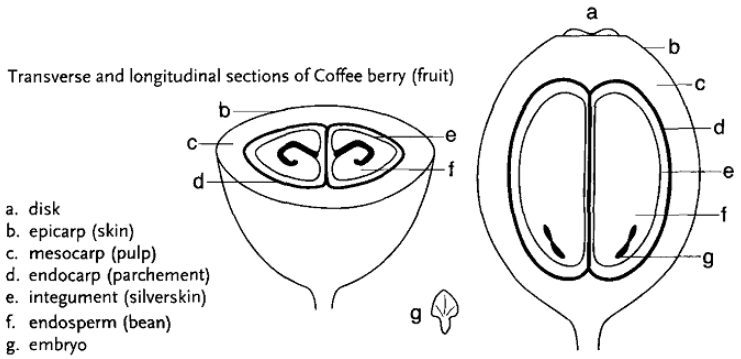

Figure 3. Coffee berry (fruit) (*in* Wintgens, 2004a).

1.3. The specificities of the coffee plant seed

The coffee bean consists of an endosperm containing an embryo, which is wrapped in two husks: the outer parchment and the silverskin (or integument) just underneath (figure 4). The seed, called the green coffee bean, is hard and bluish-green

in color. The silverskin adheres tightly to the seed and above this, follows the parchment and the mucilage. The parchment is rough and papery and, for that reason, is often called 'the pergamin' (Eira *et al.*, 2006). Before being shipped to a roaster, coffee is typically stored with the parchment attached since it serves as a protective barrier.

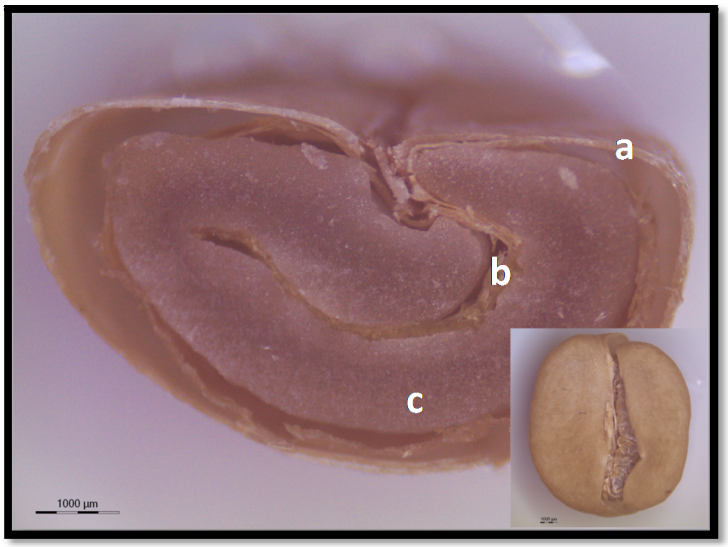

Figure 4. Section of a green coffee bean. Legend: parchment (a), silverskin (b) and endosperm (c).

The coffee flower ovary, which contains the two fertilized ovules, starts to develop immediately following fertilization. During the first 2 months, however, the ovary grows very slowly, but eventually becomes definitely visible in a dormant pinhead stage (figure 5). From the second to third month of development, the ovary increases in size more rapidly and the integument occupies almost the entire space in each ovule (figure 6a and b). The embryonic sac grows and fills with endosperm (figure 6c and d). From the third to the fifth month after fertilization, the fruit increases significantly in weight and volume. The endosperm slowly replaces the integument that is forced back to the periphery of the ovule. Between the sixth and the eighth month after fertilization, the fruit reaches maturity (figure 6f). The integument is now only represented by the silverskin. In the endosperm that fills the whole grain, the zygotic embryo has evolved to the "two-cotyledon" stage. During the last month of maturation, the fruit completes its growth, and, depending on the variety, acquires a red or yellow color. The time taken from flowering until the maturation of the coffee berries varies according to the variety, climatic conditions, and agricultural practices. As a general rule, *C. arabica* takes 6-9 months and *C. canephora* takes 9-11 months to mature, although this period can increase at higher altitudes, where the air temperature drops by 1°C per 180 m of elevation (Wintgens, 2004a).

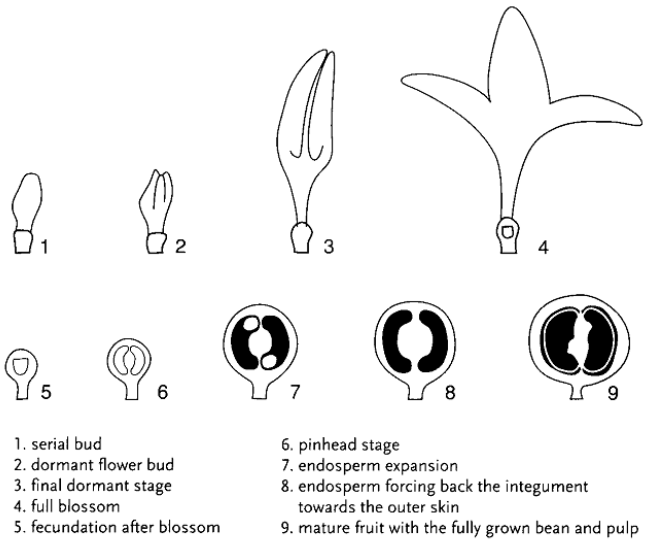

Figure 5. From bud to bean (*in* Wintgens, 2004a).

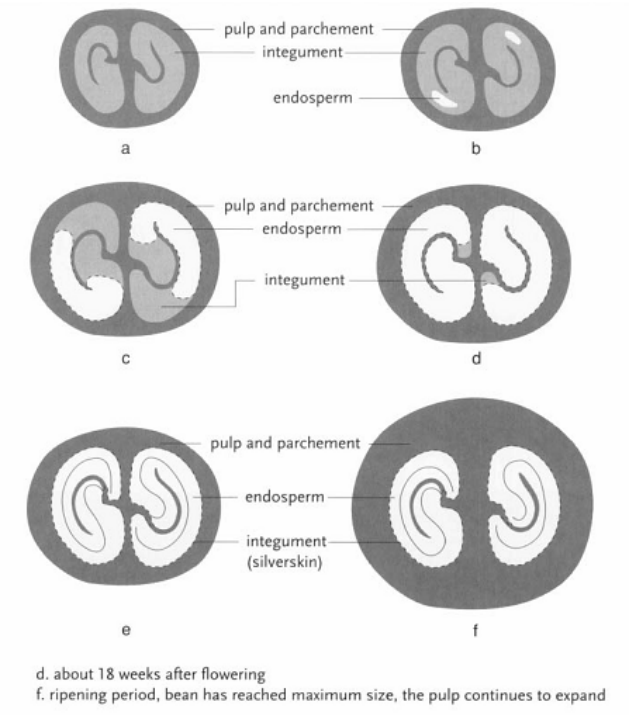

Figure 6. Growth of the endosperm within the space formed by expansion of the integument (Wormer, 1964 *in* Wintgens, 2004a).

1.4. Coffee processing

Once the cherries have been harvested, coffee processing begins. The cherries are pulped (the seed is removed from the fruit), the mucilage is removed and the seeds are dried. There are two different methods of coffee processing: the "wet method" and the "dry method" (Steiman, 2008). The wet method is the most commonly used in the world. It begins with the removal of the pulp and the separation of the seed, after which the mucilage is disposed of by fermenting the coffee in water. Once free of the mucilage, the beans are rinsed and laid out on wood or concrete drying floors where they will air-dry (figure 7).

Figure 7. Air-drying of coffee beans.

The objective of drying is to lower the moisture content of parchment or cherry coffee to about 12%, in order to preserve the beans safely in storage. This moisture level is set in industry as a global standard (Steiman, 2008). Coffee is dried by increasing the temperature of the bean to evaporate water, either by direct exposure to the sun or by exposures to radiation from a heated surface (in the case of drying grounds). Convection and wind move the saturated air away, thus effectively drying the coffee (Brando, 2004). The dry method is an alternative process where the pulping and fermenting stages are skipped and the coffee cherries are dried with their seeds still inside (figure 8). Even within the cherry, the seed moisture content will reach the appropriate level. It is a less commonly used method comparing to the wet method. For instance, in Hawai'i, no one dry-processes coffee deliberately (Steiman, 2008).

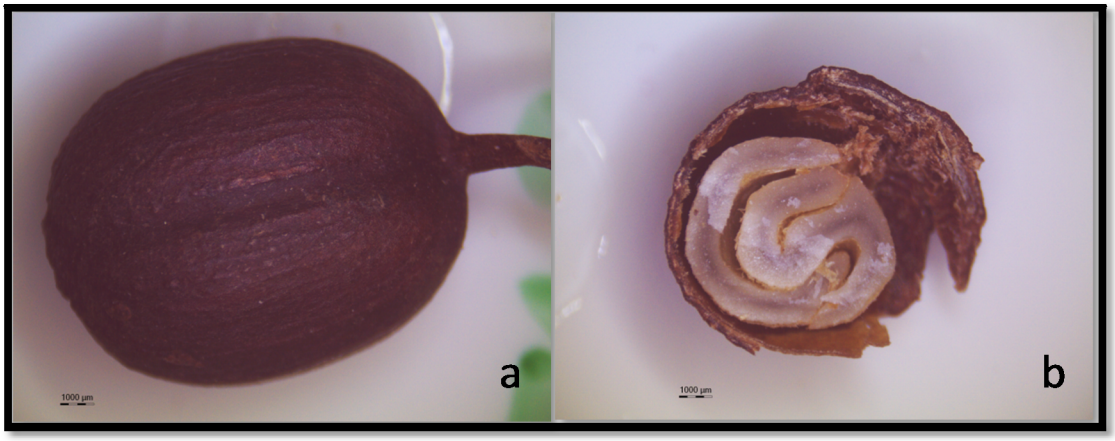

Figure 8. Dried coffee cherry and correspondent transversal section.

1.5. Coffee distribution and main climatic characteristics associated with coffee production

Coffee-growing areas extend from 25° N to 25° S of latitude (Smith, 1985). The appropriateness of the climate for the cultivation of coffee depends on the latitude and the height above sea level. Every 100 m of altitude corresponds to a decrease in temperature of approximately 0.6 °C (Wintgens, 2004b). The positive effect of altitude on coffee quality is well known. Beans produced at higher altitude are harder, and, therefore, more appreciated. In Guatemala, Costa Rica, El Salvador, Honduras and Mexico, coffee classification is based on altitude. Coffees cultivated at higher altitudes develop more acidity, aroma and flavor. Appropriate sites for coffee growing are selected based on six basic environmental factors, *i.e.* temperature (associated with altitude), water availability, sunshine intensity, wind, type of soil and topography of the land. The environmental factors suitable for *Arabica* and *Robusta* coffee cultivation (Descroix & Snoeck, 2004) are summarized in tables 1 and 2, respectively. The information included in these two tables justifies why coffee is cultivated in tropical and sub-tropical regions of the globe. Temperature values and their fluctuations have a significant impact on the behavior of coffee plants (Silva *et al.*, 2004). No coffee species can survive in temperatures bordering on 0 °C. Sensitivity to cold, as well as to high temperatures, can vary between coffee species and varieties and even between individual plants.

Table 1. Environmental factors suitable for *Arabica* coffee cultivation (*in* Descroix & Snoeck, 2004).

Levels of suitability[1]			***S1***	***S2***	***S3***	***N1***	***N2***
Degree of limitation		***0***	***1***	***2***	***3***	***4***	***4***
Climatic characteristics							
Temperatures (ºC)	Mean annual	18-20	16-18	15-16	14-15		<14
		19-20	20-22	22-24	24-26		>26
	Mean maximal annual	25-26	26-28	28-30	30-32		>32
	Mean daily minimal	24-25	22-24	20-22	18-20		<18
		15-17	17-19	19-21	21-23		>23
	Temperature of the coldest month	14-15	10-14	7-10	4-7		<4
Rainfall (mm)	annual	1600-1800	1800-2000	2000-2200	>2200		
		1400-1500	1200-1400	1000-1200	800-1000		<800
	Length of dry season (months)	2.5-3	3-4	4-5	5-6		>6
		2-2.5	1-2	0-1			
Relative humidity (%)	Mean RH of driest month	50-60	60-70	70-80	80-90		>90
		50-55	40-50	30-40	20-30		<20
Soil characteristics							
Slope (%)	Without irrigation	0-4	4-8	8-16	16-30	30-50	>50
	With irrigation	0-2	2-4	4-8	8-16		>16
Hydrous conditions	Drainage	good	good	moderate	imperfect	Poor, but drainable frequent	Poor, but drainable frequent
	submersion	none	none	none	occasional		
Physical characteristics of the soil	Depth of soil (cm)	>200	150-200	100-150	100-50		<50
	texture	Clay	Loam	Silty-sandy	Sandy-silty	sand	Sand
		Clayey-silty	Silty-clayey-sandy				
		Silty-clayey					
	% of coarse elements >2mm	0-3	3-15	15-35	35-55		>55
Chemical characteristics of the soil	pH (H_2O)	5.5-6.0	5.3-5.5	5.0-5.3	4.5-5.0	<4.5	
	Apparent CEC (meq/100g clay)	>24	16-24	<16+	<16-		
	Saturation in cations of layer 0-15 cm (%)	>80	50-80	35-50	20-35	<20	
	Organic carbon layer 0-15 cm (%)	>2.4	1.2-2.4	0.8-1.2	<0.8		

[1]S1 = Best suited units with very few (three or four) slight restrictive factors or none at all; S2 = Average units with more than three or four slight restrictive factors and/or no more than two or three moderately restrictive factors; S3 = Marginally suitable units with more than two or three moderately restrictive factors and/or no more than one serious restrictive factor provided it does not totally exclude farming; N1 = Unsuitable units with one or more serious restrictive factor and no more than one very serious restrictive factor which totally excludes farming. Potentially suitable if improvements were implemented; N2 = totally and potentially unsuitable units.

Table 2. Environmental factors suitable for *Robusta* coffee cultivation (*in* Descroix & Snoeck, 2004).

Levels of suitability[1]			***S1***	***S2***	***S3***	***N1***	***N2***
Degree of limitation		***0***	***1***	***2***	***3***	***4***	***4***
Climatic characteristics							
Temperatures (ºC)	Mean annual	22-28	22-25	20-22	18-20		<18
	Mean maximal annual	>29	27-29	24-27	22-24		>22
	Mean daily minimal	>20	18-20	16-18	14-16		<14
Rainfall (mm)	annual	2000-2500	1600-2000	1400-1600	1200-1400		<1200
	Length of dry season (months)	2-2.5	2.5-3	3-3.5	3.5-4		>4
Relative humidity (%)	Mean RH of driest month	70-75	75-80	80-90	>90		
		60-65	45-60	35-45	30-35		<30
Soil characteristics							
Slope (%)	Without irrigation	0-4	4-8	8-16	30-50		>50
	With irrigation	0-2	2-4	4-8	8-16		>16
Hydrous conditions	Drainage	good	good	moderate	imperfect	Imperfect, but drainable frequent	Imperfect, but drainable frequent
	submersion	none	none	none	occasional		
Physical characteristics of the soil	Depth of soil (cm)	>200	150-200	100-150	50-100		<50
	texture	Clay Clayey-silty Silty-clayey	Loam Silty-clayey-sand	Silty-clayey	Sandy-silty	sand	Sand
	% of coarse elements >2mm	0-3	3-15	15-35	35-55		>55
Chemical characteristics of the soil	pH (H_2O)	5.5-6.0	5.3-5.5	5.0-5.3	4.5-5.0	<4.5	
	Apparent CEC (meq/100g clay)	>16	<16+	<16-			
	Saturation in cations of layer 0-15 cm (%)	>35	20-35	<20			
	Organic carbon layer 0-15 cm (%)	>1.5	0.8-1.5	<0.8			

S1 = Best suited units with very few (three or four) slight restrictive factors or none at all; S2 = Average units with more than three or four slight restrictive factors and/or no more than two or three moderately restrictive factors; S3 = Marginally suitable units with more than two or three moderately restrictive factors and/or no more than one serious restrictive factor provided it does not totally exclude farming; N1 = Unsuitable units with one or more serious restrictive factor and no more than one very serious restrictive factor which totally excludes farming. Potentially suitable if improvements were implemented; N2 = totally and potentially unsuitable units.

Both wind and air humidity can greatly influence the effect of air temperatures. The optimum mean annual temperature range for *Arabica* coffee is 18-21 °C (DaMatta & Ramalho, 2006). Above 23 °C, development and ripening of fruits are accelerated, often leading to loss of quality (DaMatta *et al.*, 2006). It should be noted, however, that selected cultivars under intensive management conditions have allowed *Arabica* coffee plantations to be spread to marginal regions with average temperatures as high as 24–25 °C, with satisfactory yields, such as in the northeast of Brazil (DaMatta, 2004). For *Robusta* coffee, the optimum annual mean temperature ranges from 22 to 26 °C (DaMatta *et al.*, 2006). *Robusta* is much less adaptable to lower temperatures than *Arabica* coffee. As altitude relates to temperature, *Robusta* coffee can be grown between sea level and 800 m, whereas *Arabica* coffee grows best at higher altitudes and is often grown in hilly areas, as in Colombia and Central America. Coffee can also be grown at lower altitudes further from the equator, unless limited by frost, as is the case of *Arabica* coffee in Brazil (DaMatta *et al.*, 2006). Another important environmental factor is rainfall, which is the most important restrictive factor for coffee growing. Coffee requires sufficient and well-distributed rainfalls. Two inseparable elements must be taken into consideration: the total annual rainfall and its monthly or, better still, weekly distribution. A total annual rainfall between 1400 and 2000 mm is favorable for *Arabica* growing, whereas *Robusta* needs about 2000-2500 mm. Rates below 800-1000 mm for *Arabica* and 1200 mm for *Robusta*, even if they are well distributed, can be hazardous to the productivity of the coffee plantation, particularly if artificial irrigation is not possible (Wintgens, 2004a). The rainfall pattern must include a few months with little or no rain as this period is necessary to induce and concentrate flowering. However, water shortage during the critical period from week 6 to 16 after the fecundation may cause huge losses due to the development of empty beans, as the physiologic activity decreases during dry periods (Wintgens, 2004b). A dry season of 2-3 months, coincident with the harvest period, is ideal. The atmospheric humidity or relative humidity (RH) of the air also has a marked influence on the behavior of the coffee plant, particularly in the case of *Robusta* (DaMatta *et al.*, 2006; Wintgens, 2004a). Coffee species are evergreen so transpiration is continuous (Descroix *et al.*, 2004). A high level of RH will reduce water loss, whereas a low level will increase plant evapotranspiration.

Initially, coffee was farmed under natural or artificial shading conditions, in order to recreate the original forest environment, but nowadays coffee plantations are often established under direct sunlight. For best results, coffee requires an average of 2200-2400 h of sunlight per year (Descroix *et al.*, 2004). However, shade still remains useful and even necessary in certain conditions, as it helps to attenuate the effects of extreme high and low temperatures. A further beneficial effect of shade has been revealed by recent studies which indicate that it improves the quality of coffee. Shading also diminishes the risk of erosion, restricts weed growth and generates mulch which protects and enriches the soil with organic matter. In sun-exposed plantations, the

temperatures of air, leaves and soil can be substantially higher than in shaded plantations, sometimes by more than 10 °C. High temperatures can reduce plant performance and coffee quality. In contrast, in almost environments, plants under at least 50 % shade experience optimum air temperatures during the whole day, barely exceeding 25 °C at noon (Wintgens, 2004b). Also, the further the coffee fields are distant from the ideal altitude for coffee growing (either higher or lower), the more severely these microclimatic constraints will affect the coffee trees and, as a result, the need for shade will be greater.

The agronomy of the coffee plant is a complex matter and is related to many aspects, from disease control to the ecophysiology of the plant. This introduction does not intend to be comprehensive but, instead, provide only the necessary background information for understanding the basics underlying the information presented in the chapters that follow. However, to access a more detailed description of the coffee plant, its botany and genetics, as well as the breeding practices, the work of Sondahl and Baumann (Sondahl & Baumann, 2001), Van der Vossen (Van der Vossen, 2001), and Wintgens (Wintgens, 2004a), should be consulted.

1.6. Geographical origin discrimination of food products: where do we step with coffee?

A growing number of consumers demanding diversity and distinctiveness in food, an increasing public concern over issues such as health and ecology, and a series of food scares have undermined public confidence in conventional food production. This makes standards and certification a mean of demonstrating quality and obtaining the trust of consumers with whom the producer did not have a direct relationship. In other words, certification is a way of communicating with consumers living outside the region of production (Higgins *et al*, 2008). Certification is argued to have a number of benefits for consumers and producers. It responds to the growing demand that exists in western nations for foods that are produced in ethical, environmentally sustainable and socially just ways and it is hailed as also yielding 'substantial benefits for producers' (Hatanaka *et al.*, 2005). This is also reflected in the scientific research field that urges to correspond to the increasing demand for developing analytical tools to prove food authenticity and/or quality. Research has been developed with a large number of food products such as olive oil (Alonso-Salces *et al.*, 2010; Camin *et al.*, 2010; Downey *et al.*, 2003; Mannina *et al.*, 2001), meat (Horacek & Min, 2010; Nakashita *et al.*, 2008), vegetables and fruits (Ariyama *et al.*, 2006; Perez *et al.*, 2006), tea and coffee (Anderson & Smith, 2002; Krivan *et al.*, 1993; Pilgrim *et al.*, 2010; Serra *et al.*, 2005; Techer *et al.*, 2011; Weckerle *et al.*, 2002; Wieser *et al.*, 2001), orange juice (Rummel *et al.*, 2008), wine (Almeida & Vasconcelos, 2001; Almeida & Vasconcelos, 2004; Barbaste *et al.*, 2001; Barbaste *et al.*, 2002; Coetzee *et al.*, 2005b), cider and vinegar (Cocchi *et al.*, 2007; García-Ruiz *et al.*, 2007), rice (Suzuki *et al.*, 2008), milk (Critteren

et al., 2007), cheese and butter (Fortunato *et al.*, 2004; Rossmann *et al.*, 2000), asparagus (Swoboda *et al.*, 2008), paprika (Brunner *et al.*, 2010), whiskey (Rhodes *et al.*, 2009), among others.

In the case of coffee, several attempts have been made to determine the origin of green and roasted coffee beans. Analytical methods such as gas chromatography-mass spectrometry (GC-MS) (Costa Freitas *et al.*, 2001) and near infrared spectroscopy (NIR spectroscopy) (Bertrand *et al.*, 2005) were applied for the determination of organic compounds such as fatty acids profiles (Martín *et al.*, 2001), tocopherols and triglycerides (González *et al.*, 2001). Stable isotope ratios of carbon, nitrogen and oxygen of specific compounds extracted from green coffee beans (Weckerle *et al.*, 2002) were studied with promising results. Krivan and co-authors (Krivan *et al.*, 1993) demonstrated the potential of measuring elemental fingerprints in *Coffea arabica* coffee beans and quantified magnesium (Mn) along with carbon (C), cobalt (Co), cesium (Cs), sodium (Na) and rubidium (Rb) in order to discriminate between green coffees from 8 different origins. That study was complemented by Anderson and Smith (Anderson & Smith, 2002) with the determination of the multi element composition of roasted coffee beans from 8 different origins from Central and South America, Indonesia and East Africa. Other authors studied variations in the boron (B) isotope composition of *Coffea arabica* beans, showing that the measured variation in B isotopic composition values among different coffee beans is significant and relates to differences between local growing conditions (Wieser *et al.*, 2001). Based on previous studies, Serra and co-authors (Serra *et al.*, 2005) determined the isotopic composition of C, N and B in green coffees from 19 different countries, showing that the isotopic composition of these three elements is a good indicator of geographical-dependent parameters, and therefore a useful tool to infer the region of production of green coffee. The authors suggested that the use of stable isotope ratios might be improved by the use of climatic data as an additional variable for the construction of a statistical model. However, the research articles above mentioned are described as 'preliminary' as the authors acknowledge the relatively small number of authentic samples they have included in their studies of geographical origin. Recently, Techer and co-authors (Techer *et al*., 2011) have characterized the Sr isotopic composition of all components of a cultivation system *i.e.* plants, rocks, soils and water in the frame of an intensive coffee-growing project on the Réunion Island, East of Madagascar. What these studies indicate is that measuring elemental concentrations and isotopic variation in regional coffees is arguably the best analytical strategy for accurately verifying geographical origin. This approach results from global variations of isotopes abundance of 'light' bio-elements and 'heavy' geo-elements (*see* section 1.8).

1.7. Analytical techniques associated with food authenticity studies

Reports on analytical methods for determining the geographical origin of agricultural products have been increasing since the 1980s (Luykx & van Ruth, 2008). The development of new techniques is highly desirable for consumers, agricultural farmers, retailers and administrative authorities. It is an analytical challenging problem that has been the focus of much attention within Europe and the USA. Various analytical techniques have been studied based on organic constituents, mineral composition, light- and heavy-element isotope ratios, or combinations thereof. Chemometric analysis of the data provided by the analytical instrumentation which has the ability to determine more than one component at a time in a sample can be a support to establish links to the food origin. The analytical techniques that have been applied for the geographical origin discrimination of food may be subdivided in several groups mainly including spectroscopic techniques and separation techniques. For more detailed description concerning other techniques, the Luykx and van Ruth review (Luykx *et al.*, 2008) and references therein are a good reference. In general, mass spectrometry (MS) is applied to elucidate the composition of a sample by generating spectral information of the components and can be combined with other techniques. For instance, isotope ratio mass spectrometry (IRMS) is a technique that can distinguish chemically identical compounds based on their isotope content. Continuous flow IRMS (CF-IRMS) is the most common type of IRMS used in food analysis. The sample introduction technique consists of a helium gas that carries the analytes in gaseous phase into the ion source of the IRMS. The CF-IRMS offers on-line sample preparation and the possibility of interfacing with other preparation techniques, including elemental analysis, gas chromatography (GC) and high performance liquid chromatography (HPLC). IRMS combined with other techniques (*e.g.*, elemental analysis, NMR or GC) or chemometric methods has been applied to determine the geographical origin of a variety of food products (Kelly *et al.*, 2005; Luykx *et al.*, 2008). Another MS technique that is frequently applied for the geographical origin discrimination of food is inductively coupled plasma mass spectrometry (ICP-MS). ICP-MS is a powerful tool for the quantitative determination of a range of metals and non-metals (inorganic elements) in a wide variety of samples at trace (ppb-ppm) and ultra-trace (ppt-ppb) concentration levels (Luykx *et al.*, 2008). ICP-MS encompasses four main processes, including introduction and aerosol generation, ionization by argon plasma source, mass discrimination, and the detection system. ICP-MS can screen the geographical origin of food products by the analysis of the element pattern with or without isotope abundance ratio measurements (*e.g.*, $^{87}Sr/^{86}Sr$). This technique has been successfully applied for the geographical origin discrimination of vegetables (Ariyama *et al.*, 2006) and wines (Coetzee & Vanhaecke, 2005; Coetzee *et al.*, 2005b). It has also been used for geographical origin determination of food products based on their $^{87}Sr/^{86}Sr$ in wines (Almeida & Vasconcelos, 2004; Almeida *et al.*, 2001; Barbaste *et al.*, 2002), cheese

(Fortunato *et al.*, 2004), cider (García-Ruiz *et al.*, 2007), paprika (Brunner *et al.*, 2010) and asparagus (Swoboda *et al.*, 2008). It was also combined with IRMS for milk (Critteren *et al.*, 2007), butter (Rossmann *et al.*, 2000) and orange juice (Rummel *et al.*, 2008) geographical origin differentiation. Other mass spectrometry techniques like the proton transfer reaction mass spectrometry (PTR-MS) and gas chromatography coupled to mass spectrometry (GC-MS) have also been used for assessing the geographical origin of foods with promising results. In spite of the large number of studies in food analysis that apply MS techniques, other spectroscopy techniques are also relevant for the determination of the geographical origin of foods. That is the case of nuclear magnetic resonance (NMR) and of infrared (IR) spectroscopy. Another type of spectroscopy that has been applied for food analysis is fluorescence spectroscopy. Molecular fluorescence is the optical emission from molecules that have been excited to higher energy levels by absorption of electromagnetic radiation. Fluorescence spectroscopy has allowed the geographical origin discrimination of cheese and milk (Karoui *et al.*, 2005) and olive oils (Dupuy *et al.*, 2005). Raman spectroscopy has also been applied for food authentication. For instance, Fourier Transform (FT) Raman spectroscopy has been successfully applied for discriminant analysis of edible oils (Yang *et al*., 2005) and for the discrimination and classification of beet and cane inverts in honey (Muik *et al*., 2005). Other spectroscopy techniques such as the atomic spectroscopy conventional methods (*e.g.* atomic absorption spectroscopy (AAS) and atomic emission spectroscopy (AES)) as well as inductively coupled plasma AES (ICP-AES) with or without chemometrics have also been applied for the determination of geographical origin of food products. Applications of ICP-AES, with higher reproducibility and quantitative linear range comparing to AAS and AES, allowed the discrimination of certain geographical growing origins of coffee (Anderson et al., 2002). Separation techniques such as HPLC, GC and capillary electrophoresis (CE) have also given a good contribution for the classification of food products. GC is one of the most universal separation techniques used in food analysis, mainly in volatile and semi-volatile composition studies. By analyzing the GC profiles of various compounds present in wine it was possible to classify samples according to their geographical origin (Etiévant *et al.*, 2006). The same has been reported for milk (Collomb *et al.*, 2002), olive oils (Ollivier *et al.*, 2003) and orange juices (Ruiz del Castillo *et al.*, 2003). At last, other analytical techniques used in food authenticity are electronic nose technology, methods based on DNA and sensory analysis. The above mentioned techniques have advantages and limitations. Table 3 summarizes the main characteristics related to each analytical technique applied to food authenticity. An accurate determination of the geographical origin of food products may depend on the combination of various parameters measured in the food product and, thus, of different analytical techniques. Such a multi-analytical approach demands a careful interpretation of data and cross-validation with chemometric tools might be required.

Table 3. Main characteristics of the analytical techniques used for the determination of the geographical origin of food products (adapted from Luikx *et al.*, 2008).

Technique	Sensitivity	Simplicity	Time analysis	Costs	Target-compounds
Spectroscopy					
IRMS	+	+/-	+/-	-	Various
ICP-MS	+	+/-	+	+/-	Elements
PTR-MS	+	+	+	-	Volatile
GC-MS	+	+	+/-	-	Volatile, semi-volatile
NMR	-	+/-	+/-	-	Various
IR	+/-	+	+	+	Various
Fluorescence	+	+	+	+	Various
Atomic	+/-	+/-	+/-	+/-	Elements
Separation					
HPLC	+/-	+	+/-	+	Various
GC	+	+	+/-	+	Volatile, semi-volatile
CE	-	+	+/-	+	Various
Other					
PCR	+	+/-	+/-	+	DNA
Sensory analysis	+/-	+/-	-	-	Various

(+) Favorable; (+/-) Moderate; (-) Unfavorable.
Abbreviations – *see* Abbreviations list.

1.8. Isotope ratio analysis as a tool for geographical origin discrimination

We now know that impacts and alternations that result in changes to modern environments are also seen as changes to the hydrogen (H), sulfur (S) and C, N, O, and Sr isotope ratios of atmospheric gases, animal and plant tissues, soil organic matter and its diverse chemical substrates, the carbonates of teeth, corals and soils, the organic matter deposited in sediments, as well as water sources in the hydrosphere and the atmosphere. Any type of sample that is analyzed for its isotope composition, particularly over some period, can therefore serve as an archive of change. Isotopes integrate ecological processes in space and time (Bowen *et al.*, 2009a). The isotope ratios of plant and animal tissues represent a temporal integration of significant physiological and ecological processes on the landscape. The timescale of this integration depends on the element turnover rate of the tissue or pool in question (Cerling *et al.*, 2007). Additionally, isotopes indicate the presence and magnitude of key ecological processes (Bowen *et al.*, 2009b; Dawson *et al.*, 2002; West *et al.*, 2010). The presence or absence of such processes and even their magnitude in relation to other processes are indicated by the stable isotope ratio value relative to known background levels. Many ecological processes produce a distinctive isotope fingerprint, and for that reason, it becomes possible to discriminate the geographical origin of the plant or animal tissues (Barbour *et al.*, 2001; Bowen *et al.*, 2005; Bowen *et al.*, 2009b; Dawson *et al.*, 2002; West *et al.*, 2006). The use of this physical parameter allows the discrimination between samples that may be identical from the chemical point of view. Also, isotopes record biological responses to Earth's changing environmental condition. For cases in which substances or residues accumulate in an incremental fashion, such as tree rings, animal hair and ice cores, isotope ratios can be used as a record of system response to changing environmental conditions or a proxy record for environmental change. The aim of this section is to describe the most important environmental and biological factors influencing isotope ratios of the different elements in Nature.

1.8.1. Stable isotope notation

All the elements discussed in the following chapters are composed of at least two different stable isotopes (one at very high relative abundance, most often the lighter isotope, and the other(s) at much lower relative abundances) (table 4), and the ratio of the rare-to-common (or heavy-to-light) stable isotope in any particular material can very often contain valuable information about both processes and sources.

Table 4. Example of abundances of isotopes from terrestrial sources. The dashed line separates the 'light' isotopes from the 'heavy' isotopes (*in* Dawson et al. 2007).

Element	Isotope	Abundance	Ratio measured	Reference standard
Carbon	^{12}C	98.982	$^{13}C/^{12}C$	PDB[a]
	^{13}C	1.108		
Nitrogen	^{14}N	99.630	$^{15}N/^{14}N$	N_2-atm[b]
	^{15}N	0.366		
Oxygen	^{16}O	99.763	$^{18}O/^{16}O$	VSMOW, PDB[c]
	^{17}O	0.0375	$^{18}O/^{17}O$[d]	VSMOW
	^{18}O	0.1995		
Sulfur	^{32}S	95.02	$^{34}S/^{32}S$	CDT[e]
	^{33}S	0.756		
	^{34}S	4.210		
Strontium	^{84}Sr	0.560	$^{87}Sr/^{86}Sr$	NBS-987[f]
	^{86}Sr	9.860		
	^{87}Sr	7.020		
	^{88}Sr	82.56		

[a] The original carbon isotope standard, the fossil belemnite from the PeeDee geological formation is no longer available and instead the IAEA establishesan equivalent carbon standard in Vienna of a similar isotope value (VPDB) though for carbon isotope analyses it is still referred to as PDB.

[b] The IAEA standard is N_2 gas in the atmosphere because N_2 comprises ~78% of the Earth's atmosphere and there is no known additional source of N_2 of significance to dilute this atmospheric source, it is assumed that N_2-atm is not changing enough to warrant developing a different standard.

[c] In the case where investigators desire to know the $\delta^{13}C$ of a carbonate, the standard VPDB is used instead of VSMOW.

[d] The ^{17}O composition of air or water is also referenced to VSMOW.

[e] Sulfur isotope values are expressed relative to the FeS in a meteoritic troilite from Meteor Crater in Arizona (US) known as the Cañon Diablo Troilite or CDT.

[f] A widely used standard for strontium isotope analyses is the National Bureau of Standards No. 987 (now called the National Institute of Standards and Technology, NIST; http://nist.gov/), a carbonate powder. $^{87}Sr/^{86}Sr$ and $^{86}Sr/^{88}Sr$ ratios are determined with a TIMS and unlike the other light isotopes the ratio measured is not expressed as the rare-to-abundant ratio (or heavy-to-light ratio) but as the ratio of the two isotopes that are most easily measured, $^{87}Sr/^{86}Sr$. A common practice is to normalize $^{87}Sr/^{86}Sr$ values against the $^{86}Sr/^{88}Sr$ (a light-to-heavy ratio of 0.1194) present in seawater because of fractionations that occur during thermal ionization.

However, because of the very small absolute abundances of the rare isotopes in any particular material, stable isotope composition is, by definition, expressed as the difference in isotope abundances relative to an international standard. This led to the now widely accepted use of the so-called 'delta' (δ) notation (eq. 1), where the isotope ratio of the analyzed sample (SA) is expressed relative to an internationally accepted standard (STD) as (Dawson & Siegwolf, 2007):

$$\delta^{XX} E = (R_{SA}/R_{STD} - 1) \times 1 \qquad \text{Equation 1}$$

where *E* is the element of interest (H, C, N, O, S), 'XX' is the atomic mass of the heaviest isotope in the ratio, *R* is the absolute ratio of the element of interest (*e.g.*, $^{13}C/^{12}C$), and the subscripts SA and STD are as noted above. As the isotope abundances are often very small, the δ value is multiplied by 1000 to allow the expression of small differences in units that are convenient to use. Thus, the δ values are expressed in units of parts per thousand (ppt), or the more commonly used 'per mil' and the notation ‰ is used. By definition, the accepted standard (STD) has a δ value of 0 ‰. Therefore, any substance with a positive δ value has a ratio of the heavy to light isotope, R_{SA}, which is higher than the standard, R_{STD}. By analogy, a negative δ value has the opposite meaning. Substances with positive δ values are often said to be 'heavier' or 'enriched' relative to the standard. The reason underlying different observed abundances between the heavier and lighter isotopes is that heavier atoms have a lower vibration frequency than lighter ones. Therefore, heavier atoms/molecules react more slowly than their lighter counterparts because the bond strength of the heavier substances is greater. Thus more energy is needed to break the bonds that contain heavier isotopes, since the potential energy for the heavier isotope is lower than that for the lighter element (O'Leary *et al.*, 1992). This results in lower turnover rates as soon as a heavier substance is involved. This ultimately leads to uneven isotope distributions that are denominated as fractionation (Dawson *et al.*, 2007; West *et al.*, 2010). Changes in the isotopic composition of substances occurring as the result of a single process (*e.g.*, evaporation), or sometimes, less satisfyingly, as the net result of a set of processes (*e.g.*, cellulose formation), are expressed with fractionation factors (eq. 2). A fractionation factor is defined as (Flanagan & Ehleringer, 1991; Hobbie & Werner, 2004; O'Leary *et al*., 1992):

$$\alpha = R_s/R_p \qquad \text{Equation 2}$$

where R_s and R_p are the isotope ratios of the substrate and product, respectively. Isotope fractionation occurs during a chemical reaction or during diffusion of a substance along a concentration gradient. There are some basic rules of thumb that help understand how isotope fractionations occur (O'Leary *et al.*, 1992): (a) the heavier isotope tends to concentrate in phases with stronger chemical bonds, usually in the starting state of a reaction (the 'ground state'), rather than in the 'transition state' (the highest energy structure that occurs during the reaction), and thus, the heavier isotope is transformed more slowly, (b) fractionations in chemical processes are generally larger than those in physical processes, (c) fractionations with enzymes are often smaller than those for the corresponding chemical reactions, and (d) changes in temperature and other reaction conditions may cause large changes in isotope fractionations in enzymatic reactions. As a result, the abundance of the heavy isotopes in the *substrate* is greater than the abundance of the heavy isotopes in the *product* (Dawson *et al.*, 2007; Marshall *et al.*, 2007). And for most isotopic fractionation processes, we can distinguish between those that occur in one direction (no back reactions), or 'kinetic' fractionation (*e.g.* Rubisco

carboxylation), and those that are reversible, or 'equilibrium' fractionation (*e.g.* diffusion or dissociation). An example of 'equilibrium' isotope effects is the equilibrium between CO_2 in air and in solution. For biological systems, kinetic fractionation is generally associated with enzyme-mediated processes (*e.g.* photosynthesis) and is commonly referred to as *isotope discrimination* (eq. 3) (Dawson *et al.*, 2007). The reason for this is that, in the case of enzyme-mediated processes, the isotope fractionation can be related to δ-values of the substrate and of the product by:

$$\Delta = \frac{\delta^{XX}E_s - \delta^{XX}E_p}{1+\delta^{XX}E_p/1000} \qquad \text{Equation 3}$$

where the subscripts s and p refer to substrate and product, respectively. The second term in the denominator ($\delta^{XX}E_p/1000$) is usually small and can be ignored, in which case (eq. 4):

$$\Delta = \delta^{XX}E_s - \delta^{XX}E_p \quad \text{Equation 4}$$

The kinetic or equilibrium characteristics of different isotopes involved in physicochemical or biologically mediated (enzymatic discrimination) reactions are what lead to the measured changes in the isotope abundances. And while in absolute terms such changes are only on the order of a few percent, in relative, or 'delta' terms, some of these changes are very specific and quite large and can therefore be used to track processes, determine sources, and therefore record change (Dawson *et al.*, 2007; Flanagan, 2005; Marshall *et al.*, 2007).

1.8.2. Variation in the $\delta^{13}C$ in organic matter

From the early-to-mid 1950s, scientists began to grasp the underlying reasons for how and why $\delta^{13}C$ of organic and gas samples varies during the processing of carbon in the biogeosphere. The basis for much of the observed variation rests on the two major metabolic processes, photosynthesis and respiration (Brugnoli & Farquhar, 2000; Farquhar *et al.*, 1989) with additional variation being expressed during biosynthetic, anabolic, or catabolic reactions that rely on carbon-based substrates (Schmidt *et al.*, 2005; Tcherkez *et al.*, 2003). Major differences in the $\delta^{13}C$ of plant carbon are observed when comparing marine and terrestrial plants as well as among terrestrial plants that possess different photosynthetic pathways [*e.g.* C3, C4, and crassulacean acid metabolism (CAM)]. Plants contain less ^{13}C than the atmospheric

CO_2 on which they rely for photosynthesis. They are therefore 'depleted' of ^{13}C relative to the atmosphere. This depletion is caused by enzymatic and physical processes that discriminate against ^{13}C in favor of ^{12}C. The basis for the characteristic carbon isotope ratios observed among these groups is largely explained by the different ways they assimilate carbon and their associated fractionations (Brugnoli *et al.*, 2000; Farquhar *et al.*, 1989) as well as the responses different plant taxa show in relation to ecological changes in resource availability (figure 9). Accordingly, C_3 plants (as in the case of the coffee plant) can vary in their $\delta^{13}C$ from -20 ‰ to -35 ‰ in response to water, light, and nutrient availability (Dawson *et al.*, 2002). Water availability in particular can be especially important in inducing changes in stomatal physiology and/or biochemical discrimination that in turn are expressed in the $\delta^{13}C$ of photosynthetic products as well as tissues and compounds synthesized from these products (Gleixner *et al.*, 1993). On other hand, plants such as tropical grasses including agricultural species like corn and sugar cane possess what is known as the C_4 photosynthetic pathway, assimilating carbon dioxide in a two-stage process that involves two different cell types within the leaf and two carboxylating enzymes. The initial step in C_4 photosynthesis is the same as in C_3 plants: the diffusion of CO_2 from the atmosphere into the leaf via stomata. However, C_4 photosynthesis is catalyzed by an additional enzyme, phosphoenolpyruvate (PEP) carboxylase, which discriminates carbon atoms differently (Marshall *et al.*, 2007). The C_4 carbon assimilation process leads to carbon products that are 'heavier' in ^{13}C, compared to C_3 plants, with values that range from near -10 ‰ to near -19 ‰.

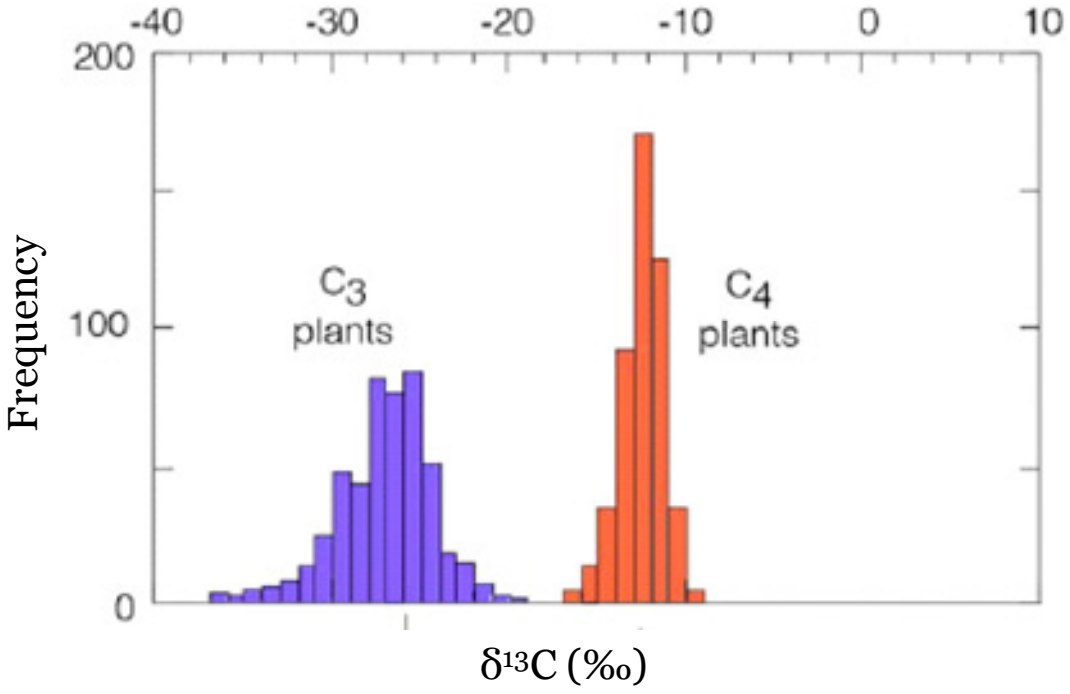

Figure 9. Histogram of the carbon isotope ratios of modern grasses (*in* Ehleringer *et al.*, 2002).

This difference allows for the distinction between these photosynthetic groups using the $\delta^{13}C$ values from leaf tissues (Máguas & Griffiths, 2003). Because of different opportunities for isotopic fractionation in the initial fixation of CO_2 in the two pathways, C_3 and C_4, the $^{13}C/^{12}C$ also differ, with C_3 plants depleted in ^{13}C relative to C_4 plants (figure 9) (Hobbie *et al.*, 2004). If these leaf tissues become soil organic matter, one can use the $\delta^{13}C$ values of soil cores to document land-use or vegetation changes over time (Dawson *et al.*, 2007). Particularly in the case of C_3 plants, CO_2 is assimilated from atmosphere, which enters and diffuses out of the leaf through stomata. During diffusion into the intercellular space within the leaf, the CO_2 is fractionated against ^{13}C in favor of the light isotope ^{12}C by ~ 4.4 ‰. This effect relates to the differential mobility of the isotopically heavy and light CO_2 and is largely dependent of factors such as temperature or vapor pressure (Farquhar & Lloyd, 1993). During photosynthesis, the internal CO_2 (c_i) is combined enzymatically with leaf water to produce sugars via carboxylation. This results in a biochemical fractionation against the heavy isotope, the net effect of which is a further isotopic depletion by ~ 27 ‰ (Barbour & Farquhar, 2000a). An increase or decrease in stomatal conductance will affect the rate at which this internal CO_2 can be replenished. In this manner, where external factors exert a direct influence on either of these controls then it will be integrated by the plant during photosynthesis and expressed as a change in the *intrinsic water use efficiency* ($_i$WUE) (figure 10) of the plant and the $\delta^{13}C$ of the resulting product (Loader *et al.*, 2007). However, care should be taken in a direct relationship between $\delta^{13}C$ and WUE in particularly under field conditions (Werner & Máguas, 2010). When the sugars are converted to form the different components of the plant, there are additional fractionations such that cellulose and lignin exhibit lower $\delta^{13}C$ than the sugars formed in the leaf (Barbour *et al.*, 2001). The nature of these fractionation processes, which have been modeled at leaf level (Farquhar *et al.*, 1989) are not yet precisely characterized for other plant tissues. The wide range of $\delta^{13}C$ values within biological and geological materials suggests that multiple and very different types of processes can lead to the observed variation (Lakatos *et al.*, 2007; Máguas *et al.*, 2003). As environments change in space and time, it is therefore no surprise that we would expect the $\delta^{13}C$ of many different types of materials to also occur. As such, $\delta^{13}C$ can serve as an important indicator of change (Dawson *et al.*, 2007).

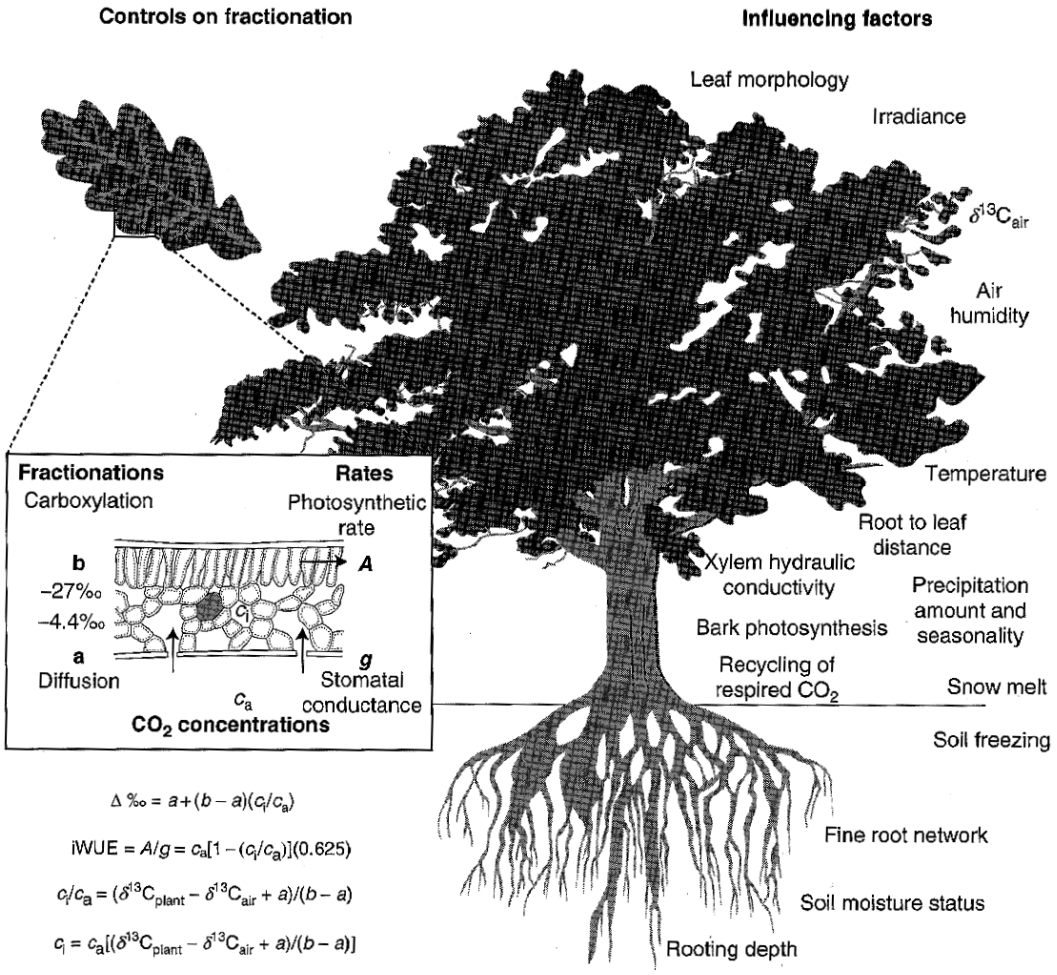

Figure 10. Diagram of a tree showing the main controls on the fractionation of carbon isotopes and the environmental factors that influence them (*in* Loader *et al*., 2007). Legend: a, fractionation due to CO_2 diffusion (~ 4.4 ‰), b, biochemical fractionation (~ 27 ‰), c_i, CO_2 pressure in leaf intercellular space, c_a, atmospheric CO_2 pressure, A, photosynthetic activity, g, stomatal conductance, Δ ‰, discrimination, $_i$WUE, plant intrinsic water use efficiency.

1.8.3. The influence of the variation in the $\delta^{18}O$ and $\delta^{2}H$ in hydrologic processes on the $\delta^{18}O$ and $\delta^{2}H$ of organic matter

Perhaps the best-understood cycle from an isotope perspective is the cycling (and recycling) of water on planet Earth. Environmental isotopes in water and other substances have been extensively used for almost five decades to improve our understanding of hydrologic, climatologic and oceanographic processes as well as other environmental processes involving several geochemical cycles. A vast literature exists on the diversity of ways in which meteoric waters can vary in their $\delta^{2}H$ and $\delta^{18}O$ as they move through the hydrological cycle (Bowen & Revenaugh, 2003a; Bowen &

Wilkinson, 2003b) (figure 11). The water evaporates from the ocean forming vapor with a more negative (lighter) δ^2H or $\delta^{18}O$ value than the source (ocean) water. As the vapor moves inland it will condensate forming rain with a more positive (heavier) δ^2H and $\delta^{18}O$ value than the cloud (vapor) water. The remaining cloud vapor becomes more negative (with a lower δ^2H and $\delta^{18}O$ value). Due to the process of Rayleigh distillation[2], rainfall values become more negative (depleted) as the storm moves across the landscape.

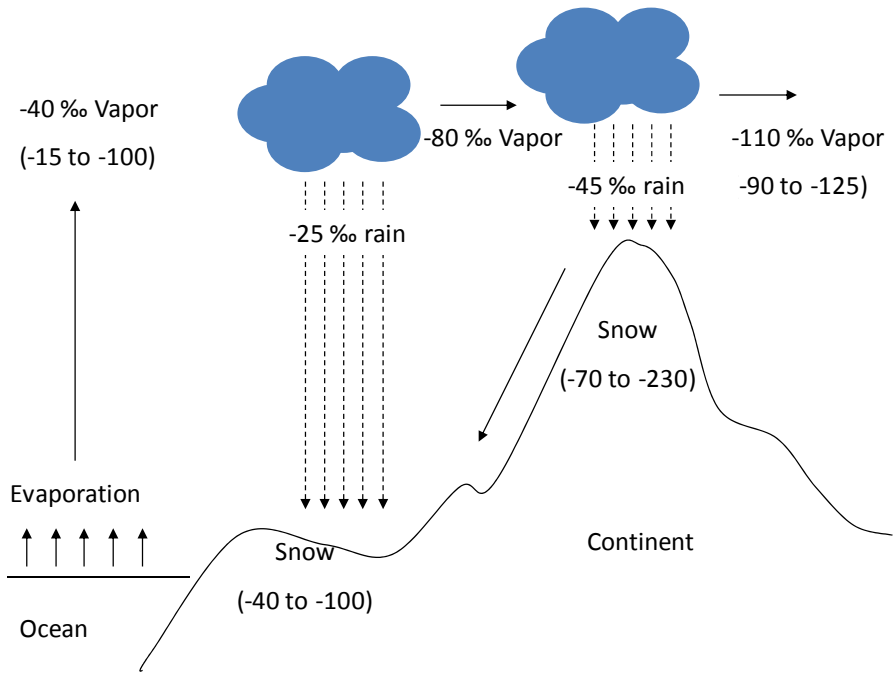

Figure 11. Isotope effects on precipitation (adapted from Dawson & Ehleringer, 1998).

Among the most important effects that have been shown to influence the δ^2H and $\delta^{18}O$ of meteoric waters are seasonality - and, therefore, the changes in condensation temperatures of precipitation - latitude, and altitude which, like seasonality, impact condensation temperature as well as the orographic/topographic lapse rates at which air masses that contain water move across the Earth (Ehleringer *et al.*, 1992). Another known effect that influences the isotope composition of meteoric waters is 'continentality', or the isotope effect caused by the distance the air mass containing water has traveled over land from coastal zones where most rain storms have their origin (Ingraham & Taylor, 1991). As moisture-laden air masses move and interact with topographic features below, along their pathways, water condenses from them and the isotope composition of the remaining vapor within the air mass becomes more

[2] The progressive depletion of ^{18}O and ^{2}H is typically described using a Rayleigh distillation. Gibson, J. J., Fekete, B., & Bowen, G. (2009). Stable isotopes in large scale hydrological applications. In: J. West, & G. Bowen, *Isoscapes: Understanding movement, pattern, and process on Earth through isotope mapping*: Springer.

depleted in ^{2}H and ^{18}O. This leads to the general finding that water collected in continental interiors is more negative in $\delta^{2}H$ and $\delta^{18}O$ (figure 12). In addition, during heavy rainfall events there is a so-called 'amount effect' that is known to influence the $\delta^{2}H$ and $\delta^{18}O$ of precipitation in storm systems; as greater quantities of precipitation are lost from an air mass during one of these heavy rain storms, the precipitation becomes progressively more negative in both $\delta^{2}H$ and $\delta^{18}O$ (Bowen *et al.*, 2003b) (figure 12).

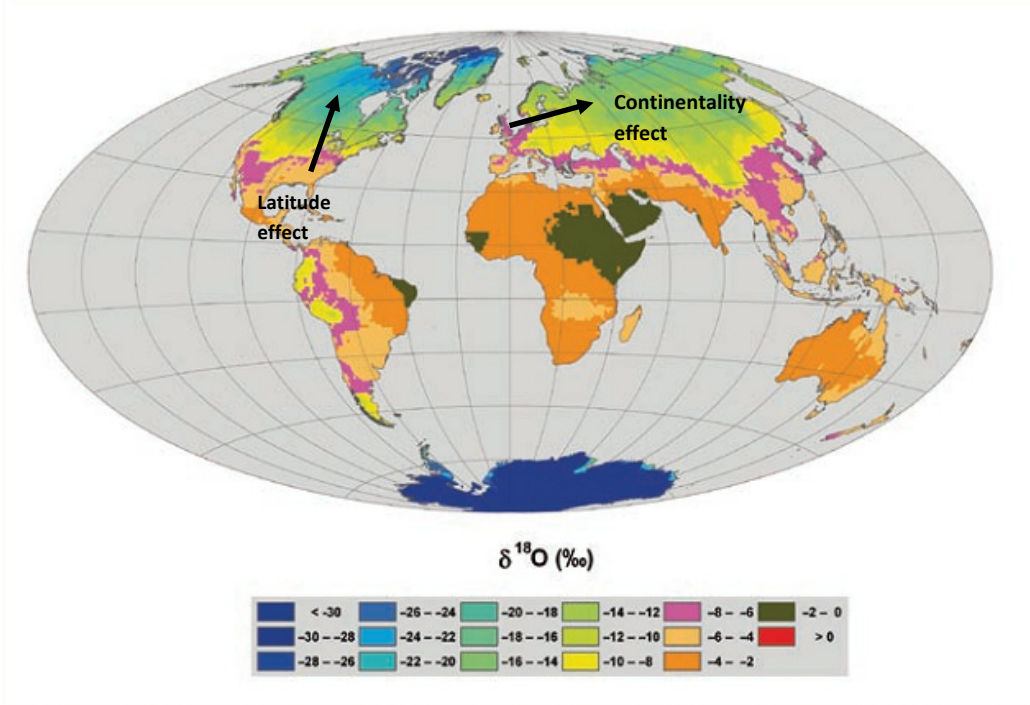

Figure 12. Global interpolation map of oxygen-18 composition of precipitation (*in* Ággarwal *et al.*, 2010).

There is no fractionation of isotopes during water uptake by plant roots (Barbour, 2007; Dawson *et al.*, 1998; White *et al.*, 1985). The isotopic composition of water in roots and stems, therefore, reflects the isotopic composition of water available to the plant. There are two potential sources of water for plant roots. Water may be taken up from the deep, ground-water reservoir, or water may be obtained from recent precipitation. However, the isotopic composition of ground water represents a long-term average of the isotopic composition of precipitation that falls in an area (Flanagan *et al.*, 1991). While there is no fractionation of isotopes during water uptake by plants, fractionation does occur during transpiration. The isotopic composition of the source (meteoric) water is overprinted by the evaporative-transpirative signal in the leaf dominated by vapor pressure deficit (relative humidity) (Loader *et al.*, 2007). Figure 13 resumes the main controls of the fractionation of the water isotopes in plants. Also, biosynthetic compounds that incorporate H or O may or may not also have associated fractionations that are 'recorded' in the organic molecules that contain these elements (Dawson *et al.*, 2007).

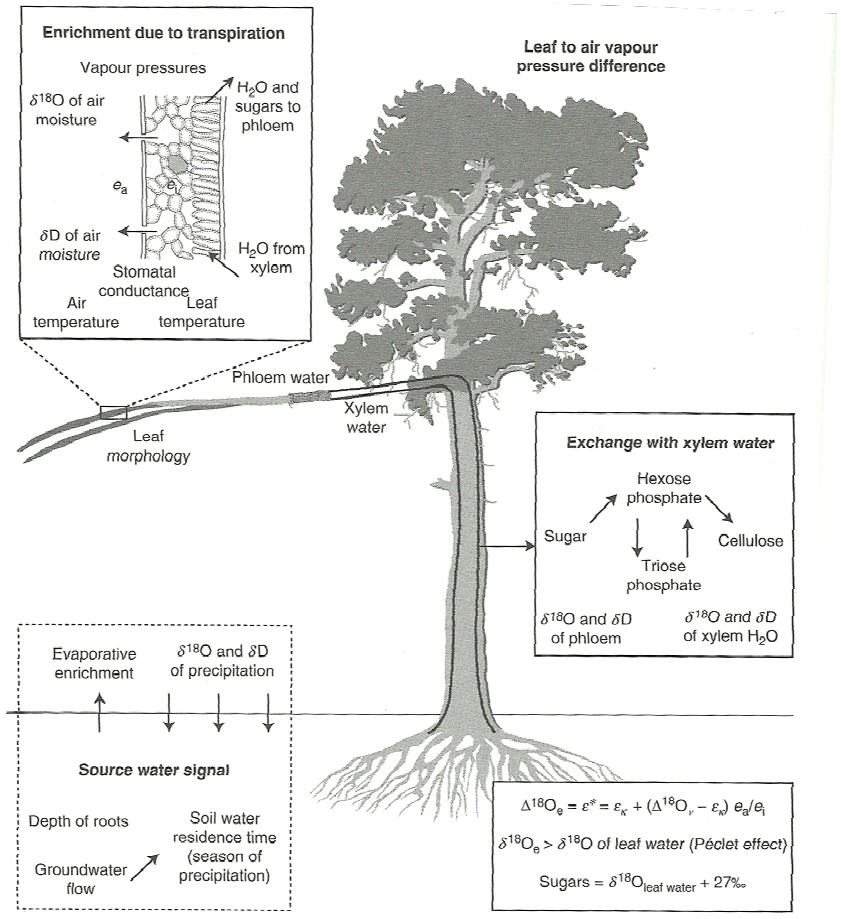

Figure 13. Diagram of a needle-leaf tree showing the main controls on the fractionation of the water isotopes and the environmental factors that influence them (*in* Loader *et al*., 2007). Legend: $\Delta^{18}O_e$, oxygen enrichment at the sites of evaporation in the leaf, ε^*, proportional depression of vapour pressure by the heavier molecule (temperature dependent), ε^k, kinetic fractionation relative to stomatal and boundary layer resistances, $\Delta^{18}O_v$, isotopic composition of water vapour in the air, and e_a and e_i are the ambient and intercellular vapour pressures.

Many of these fractionation effects are among the largest known in biological systems, leading to highly enriched organic matter. In recent years the processes that lead to enrichment in O and H of organic matter are becoming better understood and such these materials are becoming increasingly more valuable as 'biomarkers' of ecological change largely because they are known to record temperatures, water sources, and even levels of relative humidity that were present at the time these tissues were synthesized. Therefore, the H and O stable isotope analysis of this broad suite of organic molecules is now providing one of the most useful archives of ecological change (Borella & Sauer, 1999; Yakir, 1992).

1.8.4. Variations in the $\delta^{15}N$ in plant and animal tissues

One of the most intensively studied, yet poorly understood, biogeochemical cycle from a stable isotope perspective is the nitrogen cycle (Dawson *et al.*, 2002). Nitrogen is the element that most often limits plant growth in many terrestrial ecosystems (Evans, 2001). As natural abundance studies that have used $\delta^{15}N$ data increased in the areas of physiology, ecology, and biogeochemistry, it became clear that new challenges had to be faced in applying N isotopes to trace, integrate, or record a particular process (Dawson *et al.*, 2002). Of particular importance is the challenge of characterizing the many and varied fractionation factors associated with the transformation, utilization, and immobilization of N substances as they move through the N cycle. Other authors state that plant $\delta^{15}N$ is not a tracer of nitrogen source; instead, it provides a synthesis of the $\delta^{15}N$ of the nitrogen source, fractionation events that occur during nitrogen absorption and by different mycorrhizal associations and during assimilation, allocation and loss of nitrogen from the plant (Robinson, 2001) (figure 14).

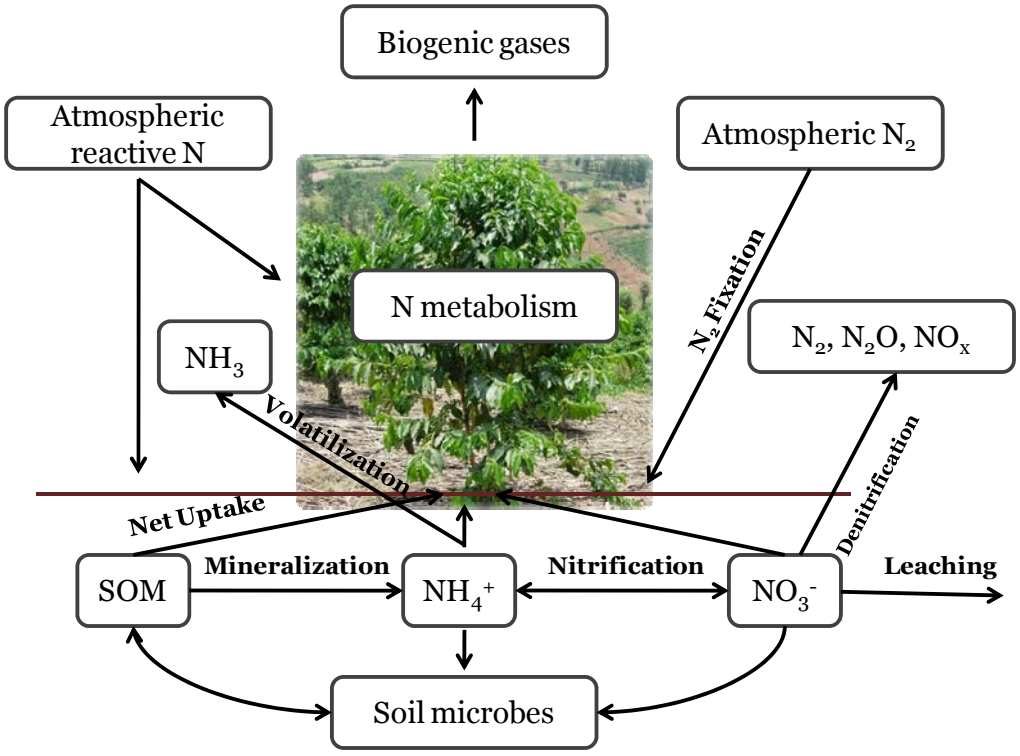

Figure 14. Primary source pools and uptake pathways in the N cycle. Boxes represent pools and arrows represent fluxes. Various N transformations in the soil and atmosphere lead to varying amounts of ^{15}N enrichment or depletion in natural ecosystems, which can vary greatly with geographical location and environmental conditions. SOM represents soil organic matter derived from pant, microbial, and faunal organic tissues (adapted from Vallano & Sparks, 2007).

Using $\delta^{15}N$ has gained popularity as knowledge of how the isotopes of N fractionate during catabolic reactions (Macko *et al.*, 1986), in soils and plants in relation to N utilization, transformation, and N fixation (Evans, 2001), and in food web and trophic interactions studies aimed at elucidating the pathways and interactions among producers and consumers as well as predators and their prey in a diversity of marine, aquatic, and terrestrial ecosystems. In general, animals are more enriched in 15-N than plants and at each trophic level the consumers are commonly 3-4‰ more enriched than the foods they consume (West *et al.*, 2010). Some key applications using $\delta^{15}N$ in plant tissues include assessing contributions of various N sources to the plant N uptake in the field, including symbiotic nitrogen fixation and atmospheric deposition, the role of mycorrhizal infection, uptake of dissolved N, and the interpretation of $\delta^{15}N$ profiles in soils. Because N demand frequently exceeds N supply in natural systems, this suggests that plant $\delta^{15}N$ is a good approximation of $\delta^{15}N$ of the available N source(s), under most filed conditions (Marshall *et al.*, 2007).

1.8.5. Variation in the $\delta^{34}S$ and $^{87}Sr/^{86}Sr$ in mineral cycle processes

Recently, it has become more apparent that the use of both S and Sr isotopes show great potential for detecting and therefore understanding the nature and magnitude of ecological change. Organisms exposed to sulfur-based pollutants are commonly more enriched (and more variable) in their $\delta^{34}S$ and this allowed early investigators to use S isotopes to trace pollutants from their anthropogenic sources into and through various ecosystems as well as to characterize the degree of impacts experienced by the biota (Trust & Fry, 1992). The $\delta^{34}S$ values of major contributors to the atmosphere can be broadly subdivided into marine and continental source regions having both anthropogenic and natural components (Wadleigh & Blake, 1999). Sulfur is not just an atmospheric pollutant but also an essential nutrient for all vegetation. For most plants, the normal source of sulfur is the sulfate taken up by the soil fine roots. The largest part (90%) of the 'organic-S' in plants is concentrated (via proteins) in the two amino acids cysteine and methionine (Krouse *et al.*, 1991) which are also the sulfur sources for the most other S-containing molecules. The plant's assimilatory sulfate reduction, providing 'organic sulfur' from sulfate, proceeds without important sulfur isotope fractionations (Tanz & Schmidt, 2010). According to the general experience, the bulk plant sulfur is depleted by only 1-2‰ relative to its primary sources, soil and sea spray sulfate or SO_2 from the atmosphere (Trust *et al*., 1992), due to the partition of individual biosynthesis steps to different plant compartments, where they can proceed without branching and with quantitative turnover (Tanz *et al.*, 2010). However, further S transfers from cysteine to secondary products may imply S-isotope fractionations and thus provide ^{34}S-differences between the amino acid and secondary products (Tanz *et al.*, 2010). This element exhibits natural variations in the abundance of its stable isotopes due to

fractionations that occur during chemical, physical, and biological processes. Those variations impart a characteristic 'isotopic signature' that can be used to trace the origins of sulfur-bearing compounds (Moire & Wadleigh, 2003).

With regards to Sr isotope ratios, they are not commonly expressed in standard 'delta notation' but instead as the ratio of ^{87}Sr to ^{86}Sr in a sample. For all Sr isotope research, it is important to understand that the $^{87}Sr/^{86}Sr$ ratio depends on what the parent-daughter Rb to Sr (specifically, $^{87}Rb/^{86}Sr$) ratio in the source is, and how long ago in time it fractionated. For example, Himalayan rocks have very high $^{87}Sr/^{86}Sr$ mainly because they are old and were formed from crustal material with high $^{87}Rb/^{86}Sr$ ratios. Unlike continental crust, oceanic crust is very young being basalt the primary constituent. For this reason oceanic basalt reflects the isotopic compositions of the present-day mantle (Allègre, 2008) (figure 15).

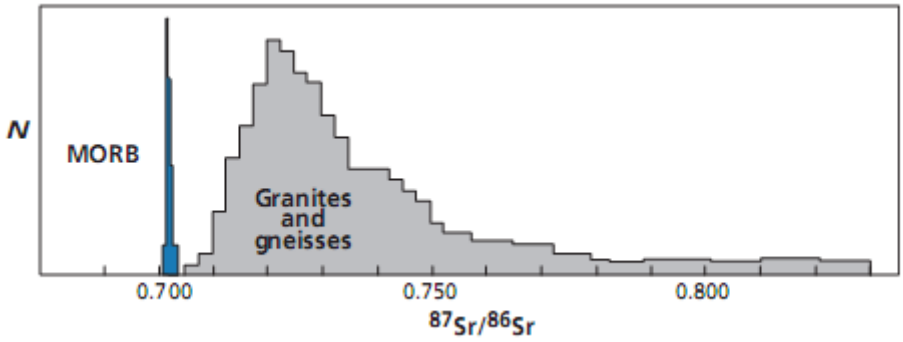

Figure 15. Histogram of $^{87}Sr/^{86}Sr$ ratios measured in the mid-ocean-ridge basalts (MORBs) and in the granulites of the lower continental crust, and in the granitoids of the upper continental crust. Notice the wide dispersion of values for granite compared with MORB values (*in* Allègre, 2008).

Oceanic basalts such as mid-ocean-ridge basalts (MORBs) are the product of mantle-melting that occur at high temperatures at which isotopic equilibrium is achieved. There is also the ocean-island basalt (OIB) produced very largely by subaerial volcanism and which forms island chains, *e.g.* Hawaii. The $^{87}Sr/^{86}Sr$ isotope ratios of MORBs (0.7025) are statistically lower than the ratios for OIBs (0.7035) (Allègre, 2008). In plants, the uptake of mobile Sr takes place via water and represents therefore the source of isotope information (Swoboda *et al.*, 2008). However, soil depth and the amount of water absorbed by plants result in the differences observed in $^{87}Sr/^{86}Sr$ in plants grown in the same region. Nonetheless, the $^{87}Sr/^{86}Sr$ values are specific functions of the local environment, and therefore precise isotope analysis of Sr isotope ratios constitutes a promising tool for food authentication studies and routine traceability applications (Swoboda *et al.*, 2008; Techer *et al.*, 2011).

1.8.6. Isoscapes

Stable isotopes of H, C, N, O, and heavy elements like Sr, vary in concentration within environmental substrates and depending on spatially and temporal Earth systems process. The resulting geographically patterned variation in isotopic compositions of a substrate is known as an 'isoscape' (Bowen *et al.*, 2009b; West *et al.*, 2010). For example, the global mean annual average leaf water $\delta^{18}O$ isoscape for the sites of evaporation within leaves (West *et al.*, 2008) is shown in figure 16.

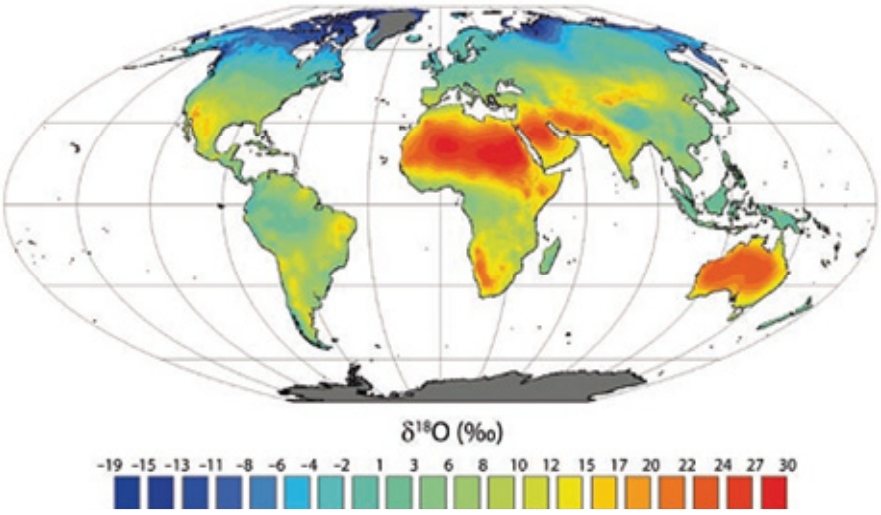

Figure 16. Global mean annual average leaf water $\delta^{18}O$ isoscape for the sites of evaporation within leaves (*in* West *et al*., 2008).

Today scientists are putting great effort in the development of isoscapes. The underlying premise behind isoscapes is that isotopic composition can be predicted as a function of time, location, and spatially explicit variables describing isotope-discrimination processes. Models of isoscapes therefore provide a means of interpreting observed isotopic data in terms of spatial patterns within Earth systems. Well-calibrated models also help predict patterns of environmental isotope variation that can be used to 'fingerprint' the origin of geological and biological materials (Bowen *et al.*, 2009b). Recent and future increases in data availability and the development of user-friendly, geographic information system (GIS)-based spatial modeling tools are opening doors to new uses of isotopes. But this will only be possible through a joint effort of many research groups that will contribute with new data for a final tool that will expand the use of isoscapes in, *e.g.* carbon cycle science and migration ecology and advance new approaches in areas such as water cycle science, biogeochemistry, anthropology and forensic science.

1.9. Roasted coffee aroma profile: a tool to evaluate the industrial roasting process

The coffee processing starts after the coffee cherries are harvested and will ultimately end with the roasting process. Besides its stimulatory effect, coffee is appreciated and consumed for its pleasing aroma, which is the result of roasting. It is not surprising, therefore, that numerous investigations have been carried out to identify the volatile compounds which evoke this pleasing aroma to many people. Different factors such as the geographical origin, the coffee plant species and variety as well as the breeding techniques and processing will determine the aroma quality of the coffee blend. In spite of the coffee plant flower and the green coffee bean being rich in aromatic compounds (Emura *et al.*, 1997; Lee & Shibamoto, 2002) the origin and chemical nature of the compounds responsible for the roasted coffee aroma is very different, resulting from pirolitic reactions occurring during the roasting process. Since the 30's of the XX century that several authors (Grosch, 2001) have put great effort in the study of coffee aroma and in the identification of the large number of volatile aroma compounds responsible for this pleasant aroma. These compounds are produced during roasting when Maillard reactions (Fay & Brevard, 2005) and Strecker additions (Yeretzian *et al.*, 2002) occur. From the technical point of view, the roasting process is complex and several parameters interact (Eggers & Pietsch, 2001). Roasting is induced by energy transfer from the roaster to the green coffee bean (figure 17). The amount of heat to be transferred to the coffee beans is controlled through time and temperature of roasting. In the first phase of the roasting process, the endothermic phase, the coffee bean heats and releases water vapor. As the temperature continues to rise, an exothermic phase begins in which massive amount of CO_2 and volatile compounds are released from the coffee bean. It's due to the formation of gas inside the coffee bean (mostly CO_2 and water vapor) that its internal pressure increases, and causing its expansion. When the proper roasting degree is obtained (depending on the bean color, flavor, and loss of dry weight) the coffee beans are released from the roaster and cooled-down (Buffo & Cardelli-Freire, 2004; Eggers *et al.*, 2001; Hernandéz *et al.*, 2007). Thus, the color of the roasted coffee bean is related with the final roasting temperature. The higher this temperature, the darker will be the coffee bean. The degree of roasting is usually described as 'light', 'medium' or 'heavy' (Buffo *et al.*, 2004). The type and abundance of volatile compounds produced during roasting is related with the presence of certain non-volatile compounds in the green coffee bean, namely proteins, chlorogenic acids and sucrose (Flament, 2002). During the roasting process, mono-, di-, and polyoligosaccharides degrade giving origin to the volatile compounds responsible for the sensorial notes of caramel, sweet and earth.

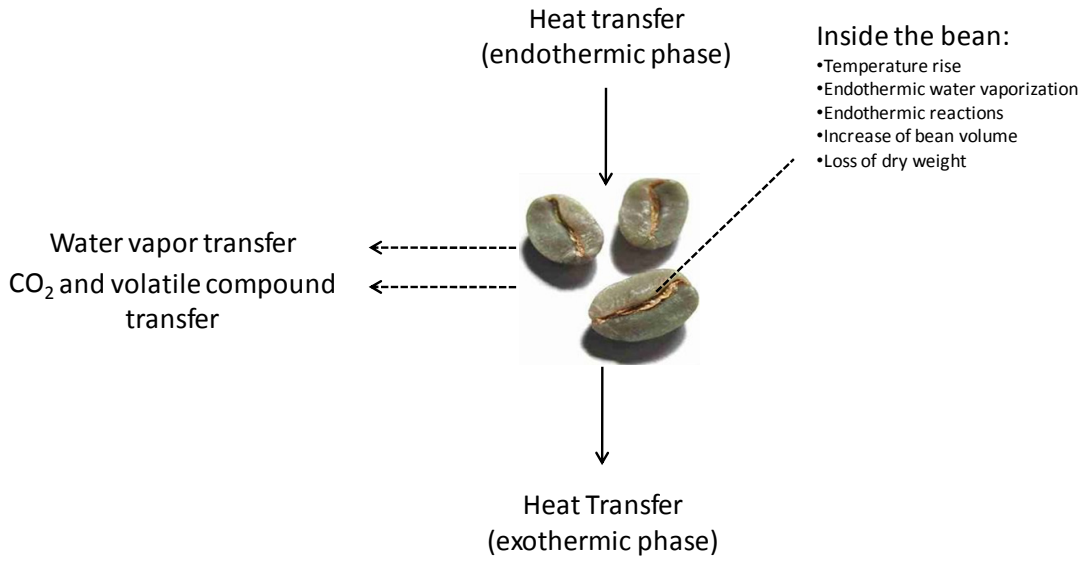

Figure 17. Roasting of coffee beans – main aspects (adapted from Eggers & Pietsch, 2001).

Compounds such as methylpropanal, 2- and 3- methylbutanal (Yeretzian *et al.*, 2002) and methional derive from Strecker degradations, involving the amino acids valine, isoleucine, leucine and methionine (Grosch, 2001). The type and intensity of the compounds resultant from roasting is dependent on the time and temperature selected for roasting. Small variations in the final roasting temperature result in different abundances of the compounds that compose the coffee aroma. As the majority of these compounds are volatile to semi-volatile, the mostly used analytical technique in the coffee aroma analysis is GC-MS. Several chemical classes constitute the coffee aroma *e.g.*, aldehydes, ketones, alcohols, pyrrols, pyrazines, furans, esters, sulfur compounds, pyridines, pyranones, acids, benzenic compounds, alkanes and alkenes, etc. This makes coffee aroma a very complex matrix, rich in volatile compounds with different molecular weight and polarity (Amstalden *et al.*, 2001; Bicchi *et al.*, 1997; Sanz *et al.*, 2002; Zambonin *et al.*, 2005). For this reason, the analysis of the volatile fraction of a coffee blend constitutes a challenge from the analytical point of view, especially in what refers to sampling preparation techniques prior to GC-MS. It is important to select a methodology that allows reflecting the original composition of the sample, in order to evaluate the roasting process and control the quality of the final product. Moreover, the sample preparation approach must allow extracting and concentrating the maximum number of volatile aroma compounds from the original matrix. These compounds may be extracted with solvents, distillation or isolated from the matrix through traps filled with specific sorbents. However, these techniques are time-consuming, may extract impurities or originate chemical artifacts. In alternative, it is possible to make use of the compounds volatility and apply headspace (HS) analytical techniques, in which it is possible to obtain an extracted sample of similar composition to the original matrix, solventless in many cases and with low sample manipulation (Harmon, 2002). HS

techniques are frequently divided in two modes, static and dynamic. In static mode, the sample is kept in a sealed vial for a determined period of time in order to allow the establishment of the sample/HS chemical equilibrium. The most volatile compounds leave the original matrix and migrate to the HS. The advantages of this technique are the possibility to extract low molecular weight compounds avoiding the solvent peak, it is cost-effective and easy to work-up. However, only a part of the original sample is injected in the chromatographic system, depending on the chemical equilibrium that is established. In dynamic mode, the atmosphere around the original sample is constantly removed by a carrier gas that flows through the vial. Several traps filled with specific sorbents and crio conditions are used to extract all the analytes from the sample. This is the reason that this technique is often called 'purge-and-trap'. It has the same advantages of the static HS mode, but an additional increased sensitivity because it allows the analysis of the total volatile fraction of the sample. However, it has a higher cost and may be time-consuming as it implies several steps separated in time, involving the use of valves and heating (Harmon, 2002).

The amount of compound(s) present in the HS will depend on several aspects:

a. Number, chemical nature and amount present in the original matrix
b. Volatility of each compound
c. Solubility of each compound, in the case of liquid samples
d. Equilibration temperature, during the extraction
e. Equilibration time, during the extraction
f. Amount of original sample in the vial
g. Volume of the vial

As already mentioned, in spite of the advantages of static HS mode, only a certain amount of the target compound(s) is extracted and injected in the chromatographic system, which, sometimes, may traduce in low analysis sensitivity, especially in the case of the compounds present at low concentrations in the sample. For roasted coffee, the aroma profile is very complex, constituted by a large number of volatile aroma compounds from different chemical classes and with different chemical characteristics. The different compounds show large differences in their abundances at the HS. Therefore, it is necessary to use an extraction methodology that simultaneously extracts and concentrates the different compounds prior to the chromatographic system allowing better sensitivity of the analysis. In the 1990's, the solid-phase microextraction (SPME) technique was introduced, contributing to a more efficient approach, making possible the extraction and concentration of target compound(s) in only one single step immediatly before the chromatographic analysis. This technique is solventless which reduces the production of chemical artifacts when thermal desorption is used. It was introduced by Janus Pawliszyn mainly for water analysis (Harmon, 2002). Since then, hundreds of applications have been published demonstrating the versatility of this extraction technique whether for HS or liquid samples analysis. SPME makes use of compound sorption to a polymeric phase that covers a silica fiber which is inserted in a

SPME device. The fiber covered by the polymer is exposed to the HS allowing the extraction of the compounds that have chemical affinity to the polymer. Different polymers are available in the market like the nonpolar polydimethylsiloxane (PDMS) and the polar polyacrilate (PA), divinylbenzene (DVB), Carbowax (CW), and Carboxen (CAR). Certain mixtures of these polymers are also available in order to increase the number of applications of this technique *e.g.* PDMS/DVB, CAR/PDMS or CAR/PDMS/DVB. The PDMS polymer with 100 µm of thickness is the most frequently used. However, polymer selection is always dependent on the polarity of the solutes or the target compounds in the HS. The diffusion coefficient of organic molecules in PDMS is close to those verified with organic solvents (Górecki & Pawliszyn, 1999). The diffusion is relatively rapid and occurs via absorption (figure 18). The diffusion coefficients in PA are very low but still allow the sorption of the analytes. As for DVB and Carboxen, the diffusion coefficients are much lower and the analytes remain at the surface of the polymer. In this case, the only mechanism of extraction with these polymers is the adsorption (Górecki *et al.*, 1999) (figure 18).

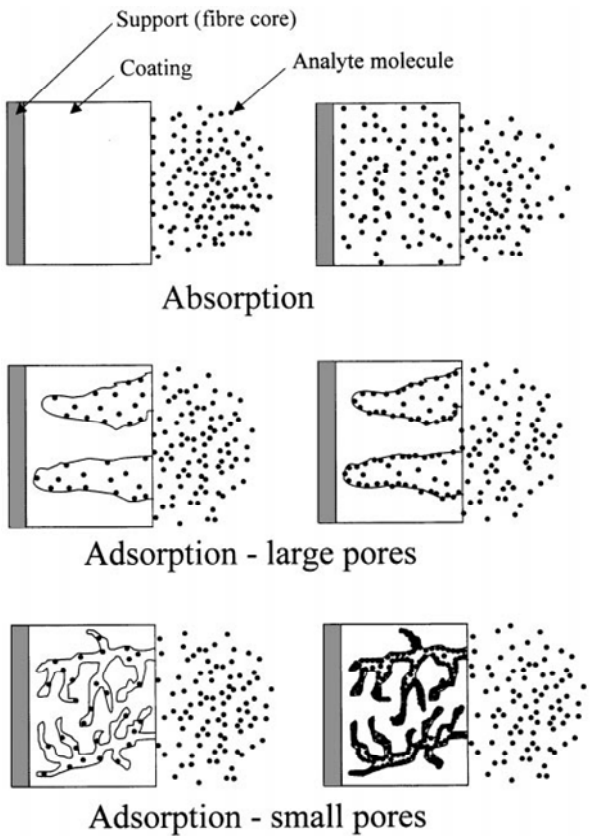

Figure 18. Initial and equilibrium states of the extraction process with SPME polymers of absorption and adsorption type (*in* Górecki *et al*., 1999).

Because it is an equilibrium technique, the SPME requires that the extraction conditions must be carefully controlled. Each analyte will behave differently depending on its polarity, volatility and partition coefficient usually estimated by the octanol/water (K_{ow}) system, the sample and HS volumes, equilibration's time and temperature. In SPME, the sample is kept in a vial closed with a cap with septum. The SPME needle is inserted through the septum into the vial that contains the sample. The polymer that covers the fiber is exposed in the sample HS. After the equilibration period of time, the fiber is withdrawn and the SPME needle is inserted in the GC injector port (figure 19). The SPME is frequently used combined with GC-MS which has been the analytical tool most frequently used in coffee aroma analysis (Akiyama *et al.*, 2005; Franca *et al.*, 2009; Gonzalez-Rios *et al.*, 2007; Roberts *et al.*, 2000; Sanz *et al.*, 2001; Sanz *et al.*, 2002; Zambonin *et al.*, 2005). With MS, it is possible to obtain total ion chromatograms (TIC) of the compounds present in the coffee aroma, and their respective identification is possible by comparing each compound mass spectra with reference spectral databases.

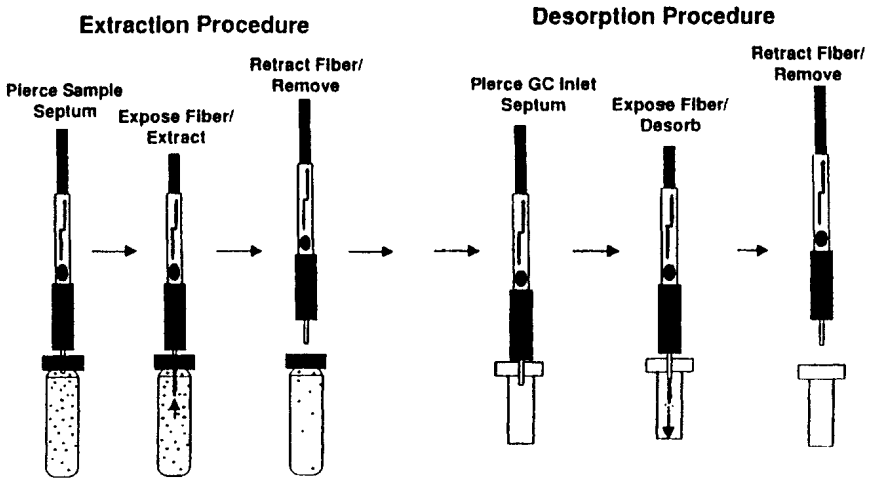

Figure 19. SPME extraction and desorption steps (*in* Harmon, 2002).

Recently, SPME has been applied to the evaluation of the impact of coffee post-harvest processing on coffee quality (Gonzalez-Rios *et al.*, 2007) and in the determination of the effect of roasting temperature in the coffee aroma (Franca *et al.*, 2009). However, it has not been applied in a systematized way, in order to define the best polymeric phase for coffee aroma profile determination independently of the origin of the coffee bean, coffee processing method, roasting profile and final composition of the coffee blend. In addition, the SPME sensitivity may be limited by the reduced amount of polymer fiber (usually less than 0.5 μL) which may result in lower extraction

efficiency. To improve the analytes extraction efficiency, it becomes evident that the amount of SPME polymer must be higher. For this reason, SPME has been the precursor of other sorptive extraction techniques, in particular the stir bar sorptive extraction (SBSE). SBSE basic principles are the sorption of the target compounds towards a polymer film (PDMS) coated on a magnetic stir bar and incorporated into a protector glass cylinder. The analytical sensitivity of SBSE is 50 to 250 times higher comparing to SPME, due to the higher volume of PDMS used (Neng *et al.*, 2007; Serôdio *et al*., 2004). Although this approach is frequently used with liquid samples it may also be applied in the HS mode. After extraction, the analytes may be back extracted via thermal (TD) or liquid desorption (LD) prior to chromatographic analysis. LD offers several advantages such as the possibility of re-analysis, good reproducibility and avoiding the production of artifacts during TD at high temperatures. Commercially available SBSE bars with 24 to 126 μL of PDMS make possible the use of a substantial higher amount of polymer in relation to SPME fibers. This technique has been applied for aroma analysis of wine (Coelho *et al.*, 2008), vinegar (Callejón *et al.*, 2009), pasta sauce (Zunin *et al.*, 2009) and mushrooms (Wihlborg *et al.*, 2008). However, SBSE shows some limitations when used in the HS mode in what respects to the more polar compounds due to the nonpolar characteristics of the PDMS. To overcome these limitations, several authors have proposed new polymeric phases as alternatives to SPME and SBSE. Recently, polyurethane (PU) foams have been used a novel polymeric phase (Neng *et al.*, 2007; Silva *et al.*, 2008b). These polymers are synthesized from polyisocianate, polyols and water in the presence of a specific catalyst (Hatchett *et al.*, 2005; Oka *et al.*, 2006). Depending on the type of isocianates, polyols and catalysts used, it is possible to obtain PU foams with different physical and chemical characteristics. PU foams are a very versatile material whose degree of rigidity may vary depending on the application (Hatchett *et al.*, 2005) making this polymer very attractive for SBSE. This polymeric phase has demonstrated excellent capacity to retain compounds in liquid phase (Portugal *et al.*, 2008), showing good efficiency in the extraction of more polar compounds (Portugal *et al.*, 2008; Silva & Nogueira, 2008a; Silva et al., 2008b). However, this polymeric phase has never been applied in HS phase mode for volatile analysis.

2. Stable isotope analysis of green coffee beans from different geographical origins[3]

Based on Rodrigues, C., Maia, R., Miranda, M., Ribeirinho, M., Nogueira, J.M.F., Máguas, C., 2009, *Stable isotope analysis for green coffee bean: A possible method for geographic origin discrimination.* Journal of Food Composition and Analysis, 22 (5), 463-471

2.1. Introduction

Nowadays, a considerably effort is being made to find reliable analytical methods for food origin discrimination and authentication. The UK Food Standards Agency (FSA) displays an interesting report on labelling research, showing that consumers strongly support Country of Origin Labelling and that consumers think it is important that labelling of food always clearly identifies the country of origin of the ingredients (Food Standards Agency, 2007).The importance of the coffee market and its globalization arise increased concern about its origin and producers respond by offering products with origin labelling to the consumer. The quality of coffee has a high variation according to its geographic origin and several attempts have been made to discriminate analytically the origin of green and roasted coffees. Analytical methods such as gas chromatography-mass spectrometry (Bicchi *et al.*, 1997; Costa Freitas *et al.*, 2001), near infrared spectroscopy (Bertrand *et al.*, 2005), determination of organic compounds such as chlorogenic acids (Bicchi *et al.*, 1995), fatty acid profiles (Martín *et al.*, 2001), tocopherols and triglycerides (González *et al.*, 2001) and stable isotope analysis of specific compounds extracted from the green coffee bean (Weckerle *et al.*, 2002) have been studied extensively with promising results. The stable carbon, nitrogen and oxygen isotope ratios are related to the plants' climatic conditions during growth, mainly water and nutrient availability along with light intensity and temperature (Evans, 2001; Farquhar *et al.*, 1989; Flanagan, 2005), and can be useful as indicatives of their origin, providing tools to delimit their potential cultivation areas if the conditions are significantly different. Carbon isotope fractionation occurs in C_3 plants via two processes; $^{13}CO_2$ diffuses more slowly across the stomatal pathway, resulting in fractionation of ~ 4.4 ‰ (Barbour & Farquahr, 2000a). The second fractionation occurs during carboxylation by Rubisco, where ^{13}C is effectively discriminated against by

[3] This chapter encompasses data on nitrogen percentage of green coffee beans, that were also used to determine the Crude Protein Content of coffee beans from different geographical origins (Rodrigues, C., Maia, R., Máguas, C., 2010, *Applying Elemental Analysis for Total Nitrogen and Crude Protein Content Determination in Green Coffee*, Coffee Science (*accepted*)).

about ~ 27 ‰ (Barbour *et al.*, 2000a). The fractionations are weighted by the CO_2 partial pressure imposed at the step involved. The total carbon isotope discrimination caused by photosynthesis in C_3 plants leaf material is defined by eq. 5 (Farquhar *et al*., 1982 *in* Barbour *et al.*, 2000a):

$$\Delta^{13}C = R_a/R_l - 1 \qquad \text{Equation 5}$$

where R_a and R_l are the $^{13}C/^{12}C$ ratios of CO_2 in the air and in the leaf, respectively. The model explaining carbon isotope discrimination is shown by eq. 6 (Farquahr *et* al., 1982 in Barbou *et al.*, 2000a):

$$\Delta^{13}C = a + (b-a)\,(c_i/c_a) \qquad \text{Equation 6}$$

where c_a and c_i are CO_2 partial pressures in ambient and intercellular air, respectively; a is the value for fractionation due to CO_2 diffusion through stomata (~ 4.4 ‰) and b is the value for fractionation related with Rubisco carboxylation (~ 27 ‰) (as above mentioned). Equation 6 predicts a positive linear relationship between c_i/c_a and $\Delta^{13}C$ in C_3 plants. To predict $\Delta^{13}C$ from eq. 6, c_i/c_a must be known, and is dependent on the stomatal conductance (g_s), meaning that any environmental factors influencing stomatal conductance will affect plant's leaf c_i/c_a thus, contributing to variations in $\Delta^{13}C$. Several factors, such as the growth rate for C_3 plants, inter-species variation, environmental effects *e.g.* latitudinal, seasonal and photoperiodic effects on plant carbon assimilation, altitude related variations of CO_2 pressure, ground water salinity, water availability, and leaf morphology and plant water use influence the $\delta^{13}C$ values of plant organic matter (Murray *et al.*, 1998). Consequently, all C_3 plants adjust stomatal conductance to balance water loss though the stomata while simultaneously optimizing CO_2 assimilation rate (Farquhar *et al.*, 1989). It is also important to consider isotopic variability among different biochemical components: changes in $\delta^{13}C$ accompany the biosynthesis of biochemically distinct constituents such as cellulose, lignin and lipids (Murray *et al.*, 1998). For instance, a plant seed like the green coffee bean is very rich in high molecular weight polysaccharides such as arabinogalactan, mannan and cellulose, and in lipids (Bradbury, 2001). Other authors have previously reported that $\delta^{13}C$ is determined primarily by stomatal behavior in the case of assimilating plant organs (*e.g.* the plant leaf) but in what relates to other plant organs (*e.g.* seeds) this is more complex due to secondary discrimination as a result of various environmental or metabolic factors (Saranga *et al.*, 1999). In what respects to N, physiological mechanisms influence plant nitrogen isotope composition. The forms of nitrogen absorbed by plants can have different isotope compositions. Plants derive N primarily from the soil in the

form of ammonium (NH_4^+), nitrate (NO_3^-), and, secondarily, from organic N. Plant-available soil N originates from decomposition of organic matter, biological N fixation, additions of N in organic or inorganic fertilizers, and deposition originating from fossil fuel combustion and animal production (Evans, 2001). Due to this, there is a large variability in the isotopic composition of the soil N pool available to plants. Differential uptake of multiple N sources with different $\delta^{15}N$ values, differences in fractionation during uptake and assimilation, and physiological differences between plants and mycorrhizal symbionts will influence the $\delta^{15}N$ value of plant organic matter (Evans, 2001; Robinson, 2001). Nonetheless, variability in substrate supply, abiotic conditions, organism assemblages, and their demand for N influence foliar $\delta^{15}N$ values to a degree beyond that of pollution additions to the soil surface or foliage and make most field-based studies challenging (Evans, 2001; Vallano *et al.*, 2007).

The oxygen stable isotope composition of organic molecules and of plant tissues is now providing one of the most useful archives of ecological change (Dawson et al., 2007; Yakir, 1992). In what refers to water isotopes, there is no fractionation of water upon uptake into the plant (Barbour, 2007), except perhaps under exceedingly unusual conditions. Furthermore, there is no evaporation, and therefore no fractionation, of water until it reaches the leaves (Lajtha & Marshall, 1994). Therefore, the isotope ratio of xylem water can be used as a measure of the isotopic signature of the water being utilized by the plant. However, evaporation enriches water at the sites of evaporation in the leafs because the heavier $H_2{}^{18}O$ vapour has a lower vapour pressure than $H_2{}^{16}O$ and because $H_2{}^{18}O$ diffuses more slowly than $H_2{}^{16}O$. The heavier molecule diffuses 1.028 times more slowly than the lighter molecule in air and through stomata, but 1.019 times more slowly through the laminar boundary layer (Barbour *et al.*, 2000a). These are two different resistances to water flux in plant leaves. Following the notation developed for carbon isotope discrimination, oxygen isotope enrichment at the sites of evaporation ($\Delta^{18}O_e$) is presented in relation to the isotope ratio of source water as (eq. 7):

$$\Delta^{18}O_e = R_e/R_s - 1 \qquad \text{Equation 7}$$

where R_e and R_s are the $^{18}O/^{16}O$ ratios at the sites of evaporation and for source water, respectively. In steady-state conditions, $\Delta^{18}O_e$ is related to kinetic and vapour pressure fractionation factors and the leaf evaporative environment (Farquhar *et al.*, 1993) by:

$$\Delta^{18}O_{ss} = \varepsilon^* + \varepsilon_k + (\Delta^{18}O_v - \varepsilon_k)e_a - e_i, \qquad \text{Equation 8}$$

where $\Delta^{18}O_v$ is the isotopic composition of water vapour in the air, relative to source water, and e_a and e_i are ambient and intercellular vapour pressures, respectively. ε_k is the

kinetic fractionation factor relative to stomatal and boundary layer resistances and ε^* is the proportional depression of vapour pressure by the heavier molecule that is dependent on temperature (ε^* is 9.2 ‰ at 25 ºC). Equation 8 suggests that at constant e_a, increasing stomatal conductance will result in less enrichment at the sites of evaporation within leaves, owing to the reduction in both leaf temperature and e_i caused by increased transpiration. As a result the oxygen enrichment in plant material ($\Delta^{18}O_p$) should be negatively related to relative humidity (Barbour *et al.*, 2000a; Roden *et al.*, 2000). The model in eq. 8 shows that, the isotopic composition of oxygen of plant leaf water is a function of isotopic composition of source water and of atmospheric water vapour and also of the ratio of air and leaf vapour pressure (Flanagan, 1993). Differences in altitude, annual precipitation, water stress, and processes like evaporation and transpiration and also on the kinetics of the exchange of CO_2 with leaves will affect leaf-water isotopic composition. Also, evaporative enrichment of water in the leaf is passed on to organic material due to exchange of carbonyl oxygen with water, resulting in a mean 27 ‰ enrichment of the organic oxygen compared to water at equilibrium (Barbour *et al*., 2000a). Due to these relations between isotopes in plant organic matter and environmental factors, isotopes are often used for fingerprinting food as they integrate the isotopic signature of its provenance.

In this chapter, isotope ratios of carbon, nitrogen and oxygen were determined in green coffee beans from different geographical origins. The coffee bean's carbon (C) and nitrogen (N) elemental percentage was also addressed. Discriminant analysis and analysis of variance (ANOVA) data were performed in order to confirm the differences between different green coffees. Correlations between environmental factors and analytical data were calculated to evaluate which factors were most relevant for the green coffee bean geographical origin discrimination.

2.2. Experimental

2.2.1. Samples

Green coffee beans from 33 different countries in a total of 224 samples were provided from Novadelta, Comércio e Indústria de Cafés, S.A. (Campo Maior, Portugal), University of Hawai'i (Honolulu, US), Coffea Consulting (Hawai'i, US), University of Lavras (Lavras, Brazil) and Evolve, Consulting for Sustainable Development (Kirchzarten, Germany). The coffee samples were of *Arabica* (*Coffea arabica*) and *Robusta* (*Coffea canephora*) type of coffee. Whenever possible, the geographical coordinates of each coffee sample were used to access altitude and to predict the oxygen isotopic composition of precipitation. Altitude data were searched in the Google Earth software, version 5.0 (Google, UK) and precipitation $\delta^{18}O$ values were acquired from the Online Isotopes in Precipitation Calculator (OIPC) (Bowen, 2010).

2.2.2. Elemental analysis

2.2.2.1. Reagents and Materials

For C and N elemental analysis, grinded coffee was weighted in folded tin capsules 5 × 9 (EuroVector, Milano). The combustion was done in excess oxygen (H_2O < 3 ppm, C_nH_m < 0.5 ppm) (AirLiquide, Portugal) and gas chromatography carrier was helium (He) (H_2O < 3 ppm, O_2 < 2 ppm, CnHm < 0.5 ppm) (AirLiquide, Portugal). Chromium oxide (20 – 50 mesh) (EuroVector, Milano) and silvered cobalt (II, III) oxide (20 – 50 mesh) (EuroVector, Milano) were used a oxidation catalysts. Water was removed with a magnesium perchlorate water trap (6 – 18 mesh) (EuroVector, Milano). Reduction of NO_x and removal of excess O_2 was achieved with copper reduced (fine wire ∅ 0.7 mm) (EuroVector, Milano). The calibration was performed with Wheat Flour standard OAS (certified value for carbon: 39.53% w/w (+/- 0.26 %); certified value for nitrogen: 1.47% w/w (+/- 0.07 %)) from Elemental Microanalysis Ltd, United Kingdom.

2.2.2.2. Apparatus

Elemental analysis was performed in a EuroEA 3000 Elemental Analyser (EuroVector, Milano) with a TCD detector. Separation was done on gas chromatography column EVR 8 × 6 mm, 2.0 m (EuroVector (Milano). Carrier gas (He) pressure was set to 70 KPa. Sample combustion was carried at 1025 ºC with an oxygen pressure of 20 Kpa and a sample delay time of 15.7 sec. NO_x reduction was achieved at 650 ºC. GC oven temperature was set to 120 ºC. The detector signal was acquired and processed on Callidus 4.1.21 software (EuroVector, Milano).

2.2.2.3. Assay procedure

Green coffee beans were grinded in a Retsch mill, 3 times 5 minutes to reach a particle size of less than 1 mm. After grinding, samples were dried overnight at 60 °C and weighted in tin capsules, folded and weighted again. The folded capsule weight was registered and used for C and N percentage calculation. The elemental analysis was performed in triplicates and the average and standard deviation was calculated. Certified Reference Material (CRM) for method validation was Wheat Flour Standard OAS. The certified values for C and N of the CRM were determined with an elemental analyser

calibrated to acetanilide 141d from National Institute of Standards and Technology (NIST), Maryland, USA.

2.2.2.4. Carbon and nitrogen determination

Chromatographic peak areas (µV.sec) allow C and N weight (µg) determination from linear calibration function directly calculated by Calidus 4.1.21 (EuroVector, Milano). C and N percentage (w/w) are calculated based on the initial weight (mg) of the sample.

2.2.3. Isotope ratio mass spectrometry (IRMS)

2.2.3.1. Combustion (EA-C) mode

Carbon stable isotope ratio was determined on a Sira II (VG ISOGAS, UK) stable isotope ratio mass spectrometer coupled to an EuroEA elemental analyser (EuroVector, Italy) for sample preparation by combustion-reduction. Nitrogen stable isotope ratio was determined on an Isoprime (Micromass, UK) isotope ratio mass spectrometer coupled to an EuroEA elemental analyser (EuroVector, Italy). Coupling of the elemental analysers and isotope ratio mass spectrometers is via open-split. Samples' isotope ratio was corrected against international standards (IAEA CH6 and IAEA CH7 for carbon isotope ratio and IAEA N1 for nitrogen isotope ratio). Analytical performance was checked by inserting laboratory standards between samples to check for stability and to allow drift correction when necessary. Precision was 0.06 ‰ for carbon isotope ratio determination and 0.08 ‰ for nitrogen isotope ratio determination.

2.2.3.2. Pyrolysis (EA-P) mode

Oxygen isotope ratio was determined on an Isoprime (Micromass, UK) isotope ratio mass spectrometer coupled to an EuroEA elemental analyser (EuroVector, Italy) by high temperature pyrolysis. Pyrolysis occurred at 1300ºC on a glassy carbon reactor with glassy carbon chips and nickel plated carbon as catalysts, mounted co-axially on a ceramic tube. Coupling of the elemental analyser and isotope ratio mass spectrometer is via open-split. Samples' isotope ratio was corrected against international standards (IAEA 601 and IAEA 602). Analytical performance was checked by inserting laboratory standards between samples to check for stability and to allow drift correction when necessary. Precision was 0.14 ‰.

2.2.4. Statistics

Statistical analysis of data was performed with Statistica 9.0 software (StatSoft, Inc., US).

2.3. Results

The results obtained allowed the characterization of the green coffee bean at global scale in what respects to C, N and O isotopic composition as well as to C and N percentages. Mean and standard deviation values of $\delta^{13}C$, $\delta^{15}N$ and $\delta^{18}O$ and of C and N percentage of green coffees per continent are shown in table 5. The C percentage of coffee beans varied from 39.5 to 52.5 % with a global mean of 45.9 ± 1.7 %. In relation to N, values ranged from 1.2 to 3.3 % with a mean value of 2.2 ± 0.3 % (table 5). The $\delta^{13}C$ values of the green coffee beans showed a global mean of -27.4 ± 1.4 ‰, which is approximate to the value of 26 ‰ reported by Yakir and co-authors (Yakir & Sternberg, 2000) for $\delta^{13}C$ in plant tissues. Nonetheless, coffee bean $\delta^{13}C$ values ranged globally from -31.4 to -22.1 ‰ (table 5), and this range encompasses the reported by Serra and co-authors (-23.8 to -28.1 ‰) (Serra *et al.*, 2005). The mean $\delta^{13}C$ value reported by these authors for 46 coffees from the three continents was -25.8 ± 1 ‰, slightly below the mean value of -27.4 ± 1.4 ‰ obtained in this work. Variations in the $\delta^{15}N$ of the green coffee beans were also observed ranging from -0.4 to 6.5 ‰, with a global average 2.9 ± 1.4 ‰ (table 5). This range of values was also in agreement to the reported by Serra and co-authors for the range of $\delta^{15}N$ values (~ 5 ‰) and for the mean value of 3.5 ± 1.2 ‰. As for oxygen isotope ratios, green coffee bean $\delta^{18}O$ varied from a minimum of 18.3 ‰ to a maximum of 39.8 ‰ with global mean value of 27.7 ± 3.5 ‰ (table 5), which is approximate to the value reported by Yakir and co-authos (Yakir & DeNiro, 1990) for $\delta^{18}O$ values of leaf cellulose (27 ‰). At continental level, there were no differences concerning coffee bean N percentage and isotopic composition (table 5). In relation to C, mean values of C percentage and $\delta^{13}C$ were approximate between continents although the more negative (enriched) $\delta^{13}C$ values were measured in the green coffee beans from Africa. The most relevant difference was observed in relation to the coffee bean $\delta^{18}O$ values, particularly in the case of Africa in comparison to Asia. The difference between coffee bean $\delta^{18}O$ values obtained for the two continents allowed the discrimination of the coffees from the two continents (figure 20). In Africa, higher values for coffee bean $\delta^{18}O$ (mean 30.4 ± 3 ‰) were observed comparing to a mean value of 24.3 ± 3 ‰ in Asia (table 5).

Table 5. Mean, standard deviation and range of values of C and N% and of $\delta^{13}C$, $\delta^{15}N$ and $\delta^{18}O$ of green coffee beans from America, Africa and Asia continents.

Continent	**C%**			**$\delta^{13}C$**		
	mean	std. dev.	range	mean	std.dev.	range
America	45.9	1.5	41.5 to 52.5	-27.4	1.5	-22.1 to -31.4
Africa	46.4	1.8	42.7 to 51.9	-27.1	1.4	-24.5 to -29.9
Asia	44.7	1.7	39.5 to 49.3	-28	0.9	-25.4 to -29.5
All groups	45.9	1.7	39.5-52.5	-27.4	1.4	-22.1 to -31.4
Continent	**N%**			**$\delta^{15}N$**		
	mean	std. dev.	range	mean	std.dev.	range
America	2.2	0.3	1.2 to 2.8	2.7	1.3	0.2 to 5.8
Africa	2.2	0.3	1.2 to 3.3	3.5	1.5	-0.4 to 6.5
Asia	2.3	0.3	1.4 to 3	2.7	1.1	0.4 to 5.7
All groups	2.2	0.3	1.2 to 3.3	2.9	1.4	-0.4 to 6.5
Continent				**$\delta^{18}O$**		
				mean	std. dev.	range
America				27.2	2.9	18.7 to 33.2
Africa				30.4	3	23.9 to 39.8
Asia				24.3	2.5	18.3 to 29.4
All groups				27.7	3.5	18.3 to 39.8

Figure 21 shows the variation of coffee bean $\delta^{13}C$, $\delta^{15}N$ and $\delta^{18}O$ values per country. Differences between the geographical origins were observed particularly in relation to $\delta^{18}O$. In general, there was a decrease in coffee bean $\delta^{18}O$ values from Africa to Asia. The African countries Uganda (UG), Kenya (KE), Ethiopia (ET), Rwanda (RW) and Zambia (ZA) had the highest mean coffee bean $\delta^{18}O$ values ($\geq$ 30 ‰) (figure 21). Coffees with lowest $\delta^{18}O$ values originated from Papua New Guinea (20.6 ± 2.9 ‰) and Vietnam (22.8 ± 0.7 ‰) in Asia, and from Costa Rica (22 ± 1.6 ‰), Peru (21 ± 0.6 ‰) and Nicaragua (22.9 ‰) in America.

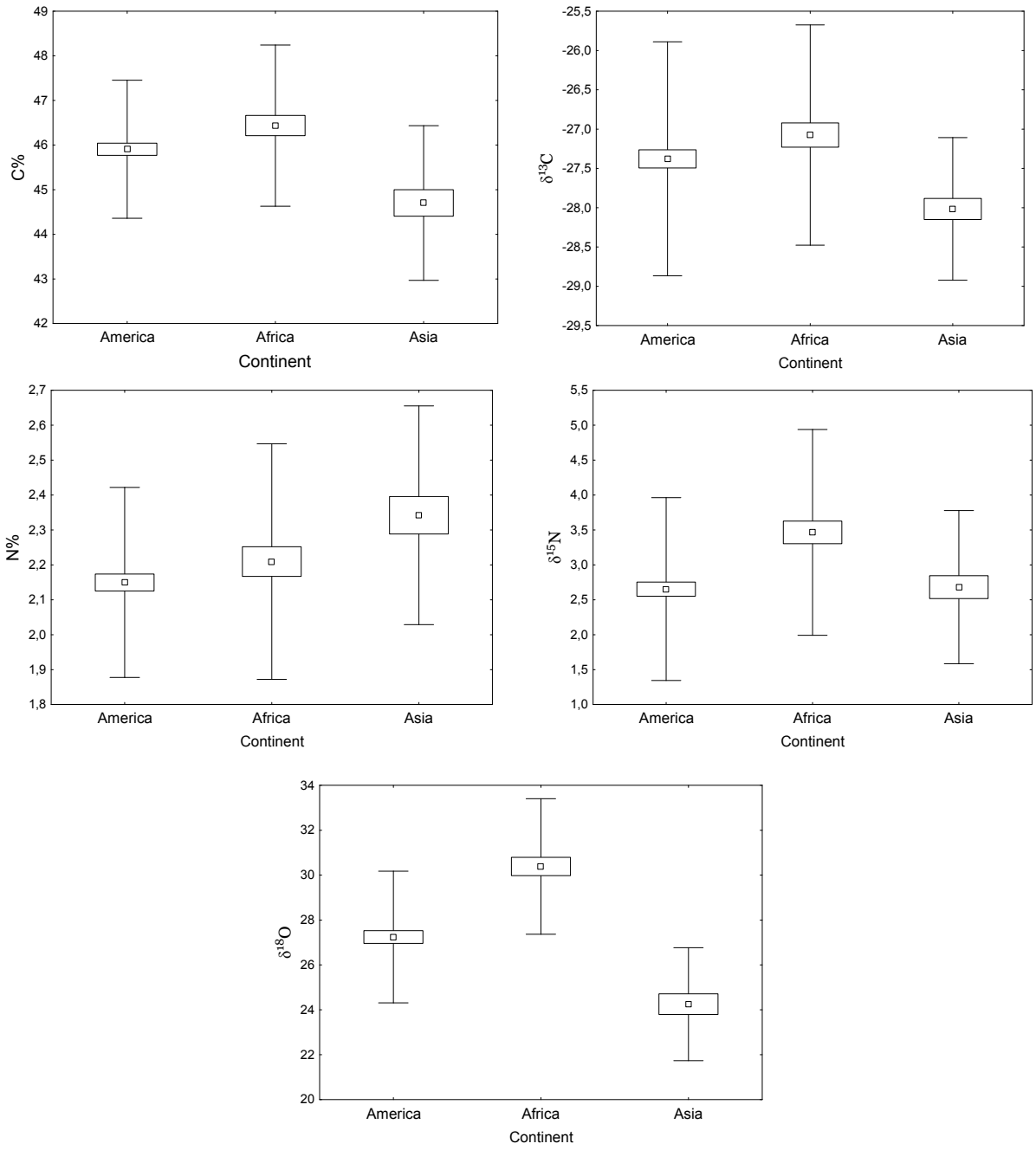

Figure 20. Mean, standard error and standard deviation of C and N % and of $\delta^{13}C$, $\delta^{15}N$ and $\delta^{18}O$ of green coffee beans in America (n=127), Africa (n=63) and Asia (n=34) (legend: □ – mean; □ - mean ± SE; bar – mean ± SD).

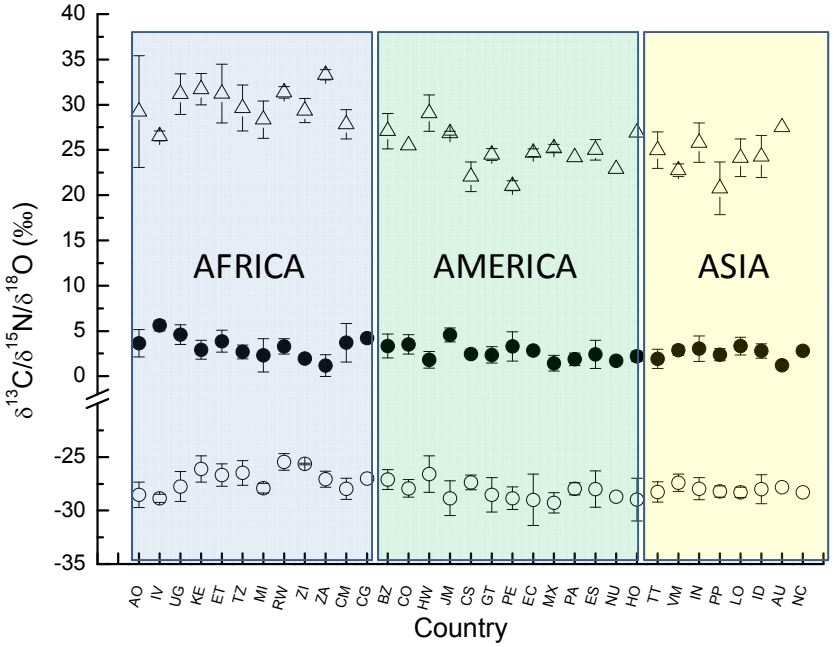

Figure 21. $\delta^{13}C$, $\delta^{15}N$ and $\delta^{18}O$ of green coffee beans from different geographical origins (countries). Legend: (Δ)$\delta^{18}O$; (●)$\delta^{15}N$; (○)$\delta^{13}C$. Country code: AO, Angola, IV, Ivory Coast, UG, Uganda, KE, Kenya, ET, Ethiopia, TZ, UR Tanzania, MI, Malawi, RW, Rwanda, ZI, Zimbabwe, ZA, Zambia, CM, Camaroon, CG, Congo, BZ, Brazil, CO, Colombia, HW, Hawai'i (US), JM, Jamaica, CS, Costa Rica, GT, Guatemala, PE, Peru, EC, Ecuador, MX, Mexico, PA, Panama, ES, El Salvador, NU, Nicaragua, HO, Honduras, TT, East Timor, VM, Vietnam, IN, India, PP, Papua New Guinea, LO, Laos, AU, Australia, NC, New Caledonia.

ANOVA analysis showed significant differences ($p < 0.001$) in what refers to C percentage and $\delta^{13}C$, $\delta^{15}N$ and $\delta^{18}O$ of the different green coffee beans from different geographical origins. However, in the case of N percentage this was confirmed with a lower level of significance ($p = 0.002$). In spite of this, it did not contribute to geographical origin (country) discrimination through multivariate analysis of data performed at global scale or even at continental level. Clear origin discrimination between coffee-producing countries was not achieved based on the series of elemental and isotope ratio analysis performed. Nonetheless, canonical analysis of data was performed at the continental level. The result is shown in figure 22. Coffees from Africa were differentiated from coffees from Asia. This differentiation was achieved mainly on the basis of the coffee bean $\delta^{18}O$ value. Two significant ($p < 0.05$) canonical components were obtained with canonical coefficients of 0.65 and 0.34, respectively. These were significantly correlated with the classification variable (the continent of origin).

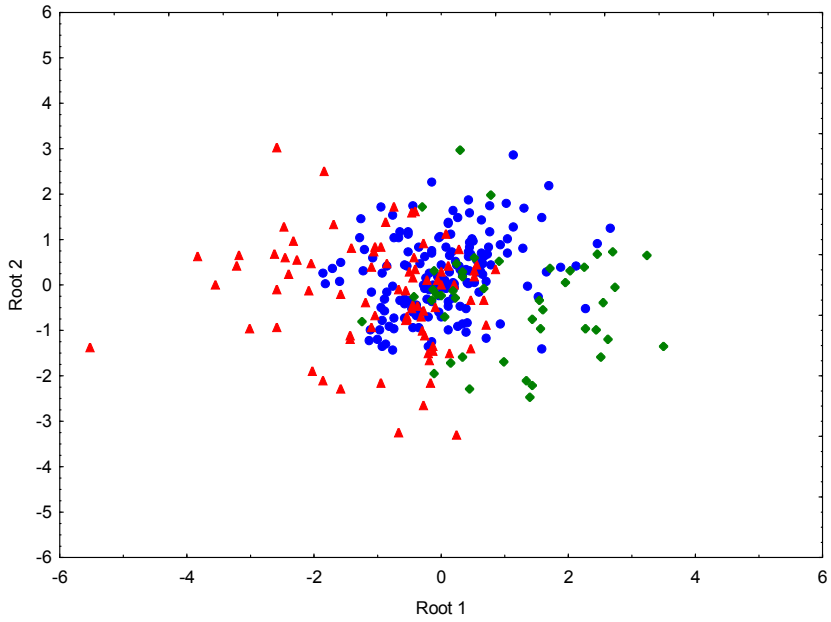

Figure 22. Canonical analysis of C and N percentage and $\delta^{13}C$, $\delta^{15}N$ and $\delta^{18}O$ of green coffee beans from America, Asia and Africa. Legend: (▲) Africa; (●) America; (♦) Asia.

In order to evaluate possible relationships between the isotopic composition of the coffee bean and certain environmental factors, Spearman's rank correlation between the analytical results and values of altitude, latitude and mean annual $\delta^{18}O$ of precipitation ($\delta^{18}O_{prec}$) was evaluated. Spearman's rank correlation was used as a non-parametric alternative to correlation as the number of samples per country and per continent varied and in most cases did not allow to test for normality, homoscedasticity and linearity, the assumptions of regression and correlation. The analysis was done at global scale and at continental level as well (tables 6 to 9). A significant positive correlation between coffee bean $\delta^{13}C$ ($\delta^{13}C_{bean}$) and $\delta^{18}O$ ($\delta^{18}O_{bean}$) was obtained at global scale ($r = 0.38$) (table 6) and in Africa ($r = 0.52$) (table 7). Also, coffee bean $\delta^{13}C$ showed a positive correlation with latitude in Africa. Also, in the same continent, $\delta^{18}O_{bean}$ and latitude was positively correlated (table 7).

Table 6. Correlation coefficient matrix for analysis at global scale (bold values correspond to significant correlations; $p<0.05$;

	Altitude	Latitude	C%	N%	$\delta^{13}C$	$\delta^{15}N$	$\delta^{18}O_{bean}$	$\delta^{18}O_{prec}$
Altitude	1	**-0.54**	**0.24**	**-0.22**	0.08	**0.31**	0.01	**-0.75**
Latitude	**-0.54**	1	**-0.19**	0.08	0.05	-0.16	**0.18**	**0.5**
C%	**0.24**	**-0.19**	1	-0.11	0.12	0.07	**0.2**	**-0.18**
N%	**-0.22**	0.08	-0.11	1	-0.02	**0.18**	-0.02	**0.2**
$\delta^{13}C$	0.08	0.05	0.12	-0.02	1	0.02	**0.38**	0.09
$\delta^{15}N$	**0.32**	-0.15	0.07	**0.18**	0.02	1	-0.07	**-0.17**
$\delta^{18}O_{bean}$	0.01	**0.18**	**0.2**	-0.02	**0.38**	-0.07	1	**0.33**
$\delta^{18}O_{prec}$	**-0.75**	**0.49**	**-0.18**	**0.19**	0.09	**-0.17**	**0.33**	1

Table 7. Correlation coefficient matrix for African continent (bold values correspond to significant correlations; $p<0.05$).

	Altitude	Latitude	C%	N%	$\delta^{13}C$	$\delta^{15}N$	$\delta^{18}O_{bean}$	$\delta^{18}O_{prec}$
Altitude	1	**0.77**	**0.33**	-0.28	**0.52**	0.29	**0.42**	**-0.73**
Latitude	**0.77**	1	**0.35**	-0.11	**0.47**	**0.34**	0.21	-0.21
C%	**0.33**	**0.35**	1	-0.24	0.16	-0.05	0.13	-0.04
N%	-0.28	-0.11	-0.23	1	-0.17	0.24	**-0.35**	0.22
$\delta^{13}C$	**0.52**	**0.47**	0.16	-0.17	1	-0.12	**0.52**	-0.27
$\delta^{15}N$	0.29	**0.34**	-0.05	0.25	-0.12	1	0.1	0.05
$\delta^{18}O_{bean}$	**0.42**	0.21	0.13	**-0.35**	**0.52**	0.1	1	-0.33
$\delta^{18}O_{prec}$	**-0.73**	-0.21	-0.04	0.22	-0.27	0.05	-0.32	1

Table 8. Correlation coefficient matrix for American continent (bold values correspond to significant correlations; $p<0.05$).

	Altitude	Latitude	C%	N%	$\delta^{13}C$	$\delta^{15}N$	$\delta^{18}O_{bean}$	$\delta^{18}O_{prec}$
Altitude	1	**-0.6**	0.16	-0.16	-0.13	**0.26**	**-0.66**	**-0.92**
Latitude	**-0.6**	1	-0.1	0.1	0.02	-0.02	**0.58**	**0.65**
C%	0.16	-0.1	1	0.16	-0.11	0.13	-0.01	-0.21
N%	-0.16	0.1	0.16	1	0.15	0.05	**0.26**	0.17
$\delta^{13}C$	-0.13	0.02	-0.11	0.15	1	-0.12	0.16	0.17
$\delta^{15}N$	**0.26**	-0.03	0.13	0.05	-0.12	1	**-0.36**	**-0.3**
$\delta^{18}O_{bean}$	**-0.66**	**0.58**	-0.01	**0.26**	0.16	**-0.36**	1	**0.74**
$\delta^{18}O_{prec}$	**-0.92**	**0.66**	-0.21	0.17	0.17	**-0.29**	**0.74**	1

Table 9. Correlation coefficient matrix for Asian continent (bold values correspond to significant correlations; $p<0.05$).

Spearmans' R	Altitude	Latitude	C%	N%	$\delta^{13}C$	$\delta^{15}N$	$\delta^{18}O_{bean}$	$\delta^{18}O_{prec}$
Altitude	1	-0.25	0.22	0.35	0.09	-0.05	-0.15	**-1**
Latitude	-0.25	1	0.06	0.01	-0.09	0.11	-0.58	0.26
C%	0.22	0.06	1	**-0.38**	**0.34**	-0.16	0.15	-0.32
N%	0.35	0.01	**-0.38**	1	0.04	**0.35**	0.06	-0.38
$\delta^{13}C$	0.09	-0.09	**0.34**	0.04	1	**0.42**	0.12	-0.16
$\delta^{15}N$	-0.05	0.11	-0.16	**0.35**	**0.42**	1	0.15	-0.02
$\delta^{18}O_{bean}$	-0.15	-0.58	0.15	0.06	0.12	0.15	1	0.35
$\delta^{18}O_{prec}$	**-1**	0.26	-0.32	-0.38	-0.16	-0.03	0.35	1

In the American continent, a different scenario was observed, with a strong positive correlation between $\delta^{18}O_{bean}$ and $\delta^{18}O_{prec}$ (r = 0.74) (figure 23a, table 8) and a negative correlation between altitude and $\delta^{18}O_{bean}$ (r = - 0.66, figure 23b) (table 8). These correlations were not obtained with the coffees from the Asian continent (table 9).

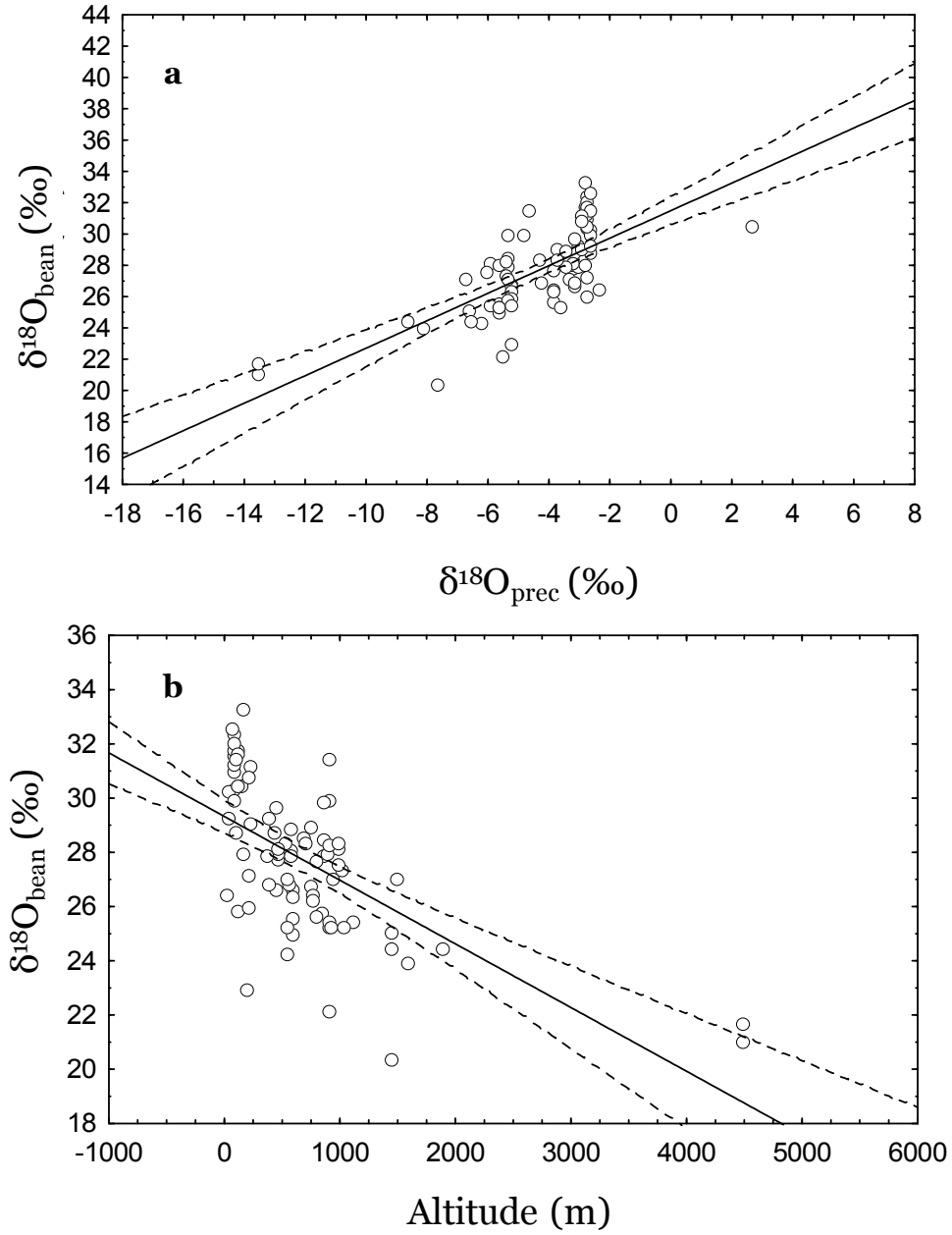

Figure 23. (a) $\delta^{18}O_{bean}$ *versus* $\delta^{18}O_{prec}$, and (b) *versus* altitude.

2.4. Discussion

It is generally accepted that, $\delta^{13}C$ of plant organic matter will be a resultant of equilibrium and kinetic fractionations associated to the metabolic pathways involved in carbon fixation (Barbour *et al.*, 2000a; Farquhar *et al.*, 1989). Factors changing stomatal conductance (g_s) and/or photosynthetic capacity (*e.g.* water deficit, light, vapor pressure deficit), thus changing the ratio of CO_2 partial pressure in the leaf interior sub-stomatal cavities and air surrounding the leaf, will change the values of $\delta^{13}C$ found for plant tissues. Also, other authors (Saranga *et al.*, 1999) reported significant differences in $\delta^{13}C$ for different plant organs in a study conducted with cotton plants, although plant organ effect did not interact with either cultivars or irrigation regimes. Thus, the variation observed in coffee bean $\delta^{13}C$ values (-31.4 to -22.1 ‰; table 5) may be related to differences in water availability, precipitation amount, temperature, and air relative humidity (RH) among the different regions considered in this study. A decrease in air RH and/or higher temperatures during the developmental period of the coffee bean would influence its $\delta^{13}C$ value. Enriched (less negative) values of $\delta^{13}C$ would be expected in these conditions, indicating stomatal regulation to avoid transpiration. In fact, the less negative values of coffee bean $\delta^{13}C$ were obtained with coffees from Africa (figure 21), characterized by lower precipitable water and higher surface temperatures (IAEA, 2001). Even without knowing the absolute of additional fractionation, the observed 10‰ variation in coffee bean $\delta^{13}C$ should be related to the occurrence of factors changing stomatal conductance during the coffee bean developmental period. The lack of knowledge on *how* these factors interacted with coffee plants at each location difficults the understanding of the data obtained. Ecophysiology studies under field conditions would be necessary to yield understanding on the processes that determine carbon fractionation in the coffee plant, fruit and seed. On the other hand, additional information can be taken if combining the results on coffee bean $\delta^{13}C$ and $\delta^{18}O$. The $\delta^{18}O$ of rainwater directly translates to the $\delta^{18}O$ of soil water (West *et al.*, 2008; Yakir *et al.*, 2000). After soil water has been uptake through plant roots, plant stem water remains virtually with the same $\delta^{18}O$ value as for soil water. Oxygen isotopes fractionation will occur in leafs during photosynthesis (Yakir *et al.*, 2000) and the newly synthesized plant organic compounds $\delta^{18}O$ will not only be dependent on fractionation occurring during this process but also on the specific biosynthetic pathways involved in their synthesis (their enzymes and regulation). Also, the leaf water oxygen isotope signal is dampened in organic material formed from exported sucrose in other plant parts. As a consequence, organic molecules may reflect or not the water in which they are formed. In addition, the oxygen isotopes are known to fractionate in plant leaves (Barbour, 2007) but less is known concerning fractionation in seeds (*e.g.* the coffee bean). In spite of this, several authors report that oxygen isotope composition of plant organic material is known to reflect that of source water and leaf evaporative conditions at the time the material was formed (Barbour, 2007; Barbour *et*

al., 2000b; West *et al.*, 2008). The extent to which the $\delta^{18}O$ of plant organic material reflects the $\delta^{18}O$ of local precipitation *and/or* the leaf evaporative conditions will be dependent on local climate, particularly in what refers to temperature and air RH. This may explain the different correlations observed among different continents in what respects to coffee bean $\delta^{13}C$ and $\delta^{18}O$. In Africa, where lower precipitable water and higher surface temperatures have been reported (IAEA, 2001), a correlation between $\delta^{13}C$ and $\delta^{18}O$ was observed (table 7) which, in turn, influenced the result at global scale (table 6). According to the conceptual model linking stable oxygen and carbon isotopes with stomatal conductance and photosynthetic capacity proposed by Scheidegger and co-authors (Scheidegger *et al.*, 2000) this type of correlation is related with changes in g_s due to reduced air RH, which has also been reported by other authors (Roden et al., 2000). In that scenario, from an increase in $\delta^{18}O$ it is expected a decrease in RH, whereas from increasing $\delta^{13}C$ it is possible to infer a decreasing of CO_2 partial pressure at intercellular spaces (c_i) (Scheidegger *et al.*, 2000). When c_i decreases *and* RH decreases, it is unlikely that g_s would increase because *two* factors suggest stomata would tend to close. Higher values of $\delta^{18}O$ for the sites of evaporation within plant leaves were predicted in certain regions of Africa (North of Africa) in comparison to America and Asia as can be seen in the isoscape developed by West and co-authors (West *et al.*, 2008) (figure 16, section 1.9). This is in accordance to the higher values of coffee bean $\delta^{18}O$ observed in Africa (figures 20 and 21), and also with the significant positive correlation between latitude and $\delta^{18}O_{bean}$ (table 7). In Africa, leaf evapotranspiration conditions must have a more prominent role in the determination of $\delta^{18}O$ of leaf water and, consequently, in the $\delta^{18}O$ of the plant tissues (leafs, fruits, seeds). It is also probable that, in Africa, soil water evaporation occurs to a greater extent as well as evaporation of rain as droplet fall due to lower air RH, influencing the oxygen isotopic composition of the water taken up by the plants. In this sense, $\delta^{18}O_{prec}$ should also be important in the interpretation of variations of $\delta^{18}O_{bean}$. If this is true, it is possible to call on the amount-weighted annual precipitation $\delta^{18}O$ maps of Africa, Central and South America and South Pacific regions are shown in figure 24 to aid in the interpretation of the results obtained. Although the range of $\delta^{18}O$ values of precipitation may overlap, more depleted values are observed in Asia in comparison to America and Africa. This may explain the coffee differentiation obtained at continental level based on the $\delta^{18}O_{bean}$ values (figure 22). In the American continent, plant source water isotopic composition seems to have a higher contribution the $\delta^{18}O_{bean}$, which would explain the altitude isotope effect in the $\delta^{18}O_{prec}$ and, hence, in the $\delta^{18}O_{bean}$ revealed by a negative correlation between $\delta^{18}O_{bean}$ and altitude ($r = -0.66$; table 8; figure 23b). Rain at higher altitudes (characterized by lower temperatures) becomes more depleted in ^{18}O (Bowen *et al.*, 2003) consequently having lower $\delta^{18}O$. However, in spite of the results obtained, it is important to caveat that, a solid interpretation of the ^{18}O abundance in the green coffee bean is complicated by a combination of environmental, climatic and physiological processes that occur during the green coffee bean development period in each geographical origin. For instance, the correlations between $\delta^{18}O$ and $\delta^{13}C$ and environmental factors were not observed in Asia (table 9). This continent is characterized by a highly humid climate (high air relative humidity)

and by its typical monsoons. The very strong tropical rainfalls at times of the passage of the Intertropical Convergence Zone (ITCZ) are characterized by strong downdrafts and may be extremely depleted in ^{18}O. This 'amount isotope effect' (Dansgaard, 1964) may be responsible by the lower $\delta^{18}O_{prec}$ in Asia (figure 24) and consequently by the lower $\delta^{18}O_{bean}$ values (figures 21 and 22). In addition, storms difficult predicting of $\delta^{18}O_{prec}$ by available models (Bowen, 2010; Gibson *et al.*, 2008 and 2009) which may compromise a correlation between $\delta^{18}O_{bean}$ with $\delta^{18}O_{prec}$ in the coffee-producing regions where storms are frequent (*e.g.* in the Asian continent).

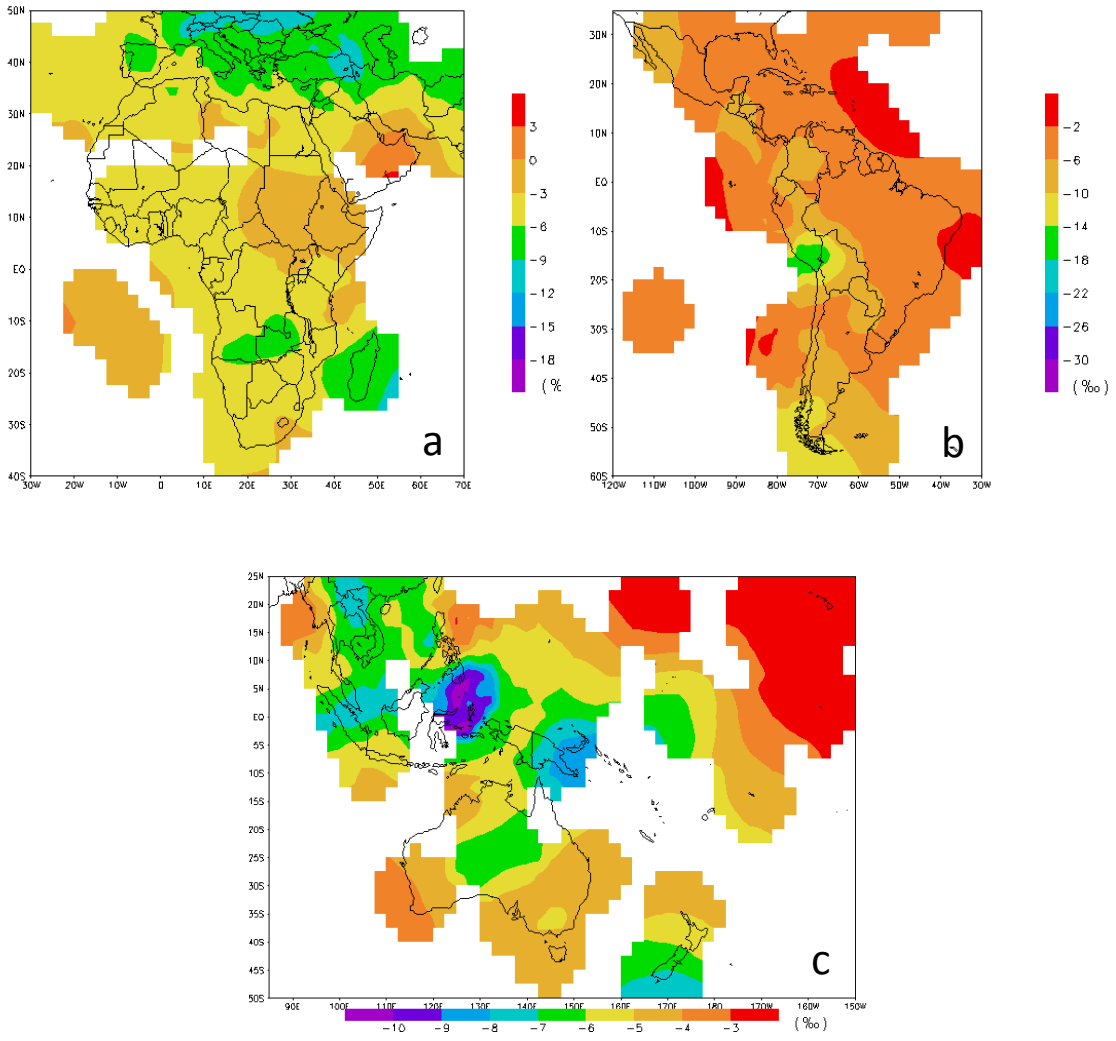

Figure 24. GNIP map of amount-weighted annual precipitation $\delta^{18}O$ in (a) Africa, (b) South and Central America and (c) South Pacific (*in* IAEA, 2001).

As for N, the $\delta^{15}N$ values of green coffee beans had a global variation of ~ 8 ‰. The reported variation in plant $\delta^{15}N$ is between -10‰ and 10‰ (Evans, 2001a) which is in agreement with the range of values obtained for green coffee beans (-0.4 to 6.5 ‰).

The global mean value of coffee bean $\delta^{15}N$ was 2.9 ‰ (table 5), which was approximate to mean values obtained per country with two exceptions, *e.g.* Ivory Coast 6.3 ± 1.2 ‰ and Jamaica 4.5 ± 0.6 ‰. Differences in $\delta^{15}N$ of the green coffee beans depend on $\delta^{15}N$ of the nitrogen source and fractionations associated with nitrogen metabolism in the coffee plant. Other authors report that the global $\delta^{15}N$-value of any plant biomass is primarily determined by that of the actual nitrogen source (Werner & Schmidt, 2002). Nitrate (NO_3^-) is the main inorganic nitrogen compound available to most cultivated coffee plants grown under field conditions (Carelli *et al.*, 2006). The reduced forms of N applied as fertilizers in coffee plantations undergo rapid nitrification under normal conditions of soil management (Carelli *et al.*, 2006). Significant discrimination has been observed for plants grown on NO_3^-. A general pattern is that the discrimination increases with external NO_3^- concentration and decreases with plant age (Evans, 2001). Carelli and co-authors (Carelli *et al.*, 2006) refer that light, tissue age, the physiology of root NO_3^- assimilation and its seasonality peaks influence the nitrogen metabolism of coffee plants. The rate of NO_3^- assimilation decreases with coffee plants age and for that lower ^{15}N discrimination is expected. However, coffee plants have nitrogen assimilation peaks particularly during the development stages of flowers and fruits (Carelli *et al.*, 2006). Organ-specific loss of nitrogen, different patterns of nitrogen assimilation, and reallocation of nitrogen can cause intra-plant variation in $\delta^{15}N$ (Evans, 2001; Werner *et al.*, 2002). As already reported by other authors (Robinson, 2001), plant $\delta^{15}N$ is not a tracer of nitrogen source; instead, it provides a synthesis of the $\delta^{15}N$ of the nitrogen source, fractionation events that occur during nitrogen absorption and by different mycorrhizal associations (if present) and during assimilation, allocation and loss of nitrogen from the plant. The data obtained in this study does not allow evaluating the relationship between nitrogen availability and demand in controlling ^{15}N discrimination at the time the green coffee beans were formed. It is difficult to interpret the impact of these factors on the resultant $\delta^{15}N$ of green coffee beans. Further research should be directed at quantifying the $\delta^{15}N$ of coffee plant available nitrogen under field conditions and at understanding how environmental factors influence the nitrogen isotopic composition of the green coffee bean.

2.5. Conclusions

In this chapter, it was demonstrated that isotope ratio analysis may yield understanding on how coffee plants respond to environmental factors that influence C, N and O assimilation. From the three elements studied, oxygen was the most relevant for coffee bean differentiation, with significant correlations observed between $\delta^{18}O_{bean}$ and $\delta^{13}C_{bean}$ values, and also between $\delta^{18}O_{bean}$ and the $\delta^{18}O_{prec}$. The $\delta^{18}O_{bean}$ values allowed the discrimination of the coffees from Africa in relation to Asia. Nonetheless, the series of analysis performed did not lead to the geographical origin (country)

discrimination at global scale or at continental level, suggesting the isotope analysis of additional chemical elements may be necessary. However, O should the element selected for continuing the study of coffee bean isotopes geographical patterned distribution to achieve a better differentiation, and of the relations with environmental factors.

3. Strontium and oxygen isotope fingerprinting of green coffee beans and its potential to proof authenticity of coffee

Rodrigues, C., Máguas, C., Prohaska, T., 2011, *Strontium and oxygen isotope fingerprint of green coffee beans and its potential to proof authenticity of coffee,* European Food Research and Technology, 232 (2), 361-373

3.1. Introduction

The coffee market and its various elements (consumption, exportation, and importation) have a major impact on the coffee industry. Many coffee companies sell 'coffee specialities' according to their geographical origin like the Ethiopian Yirgacheffe or the Hawaiian Kona Fancy among numerous others. Coffee, after roasting, is an important food product as well commercialized through *fair trading* commerce which reinforces the importance of assurance of geographical origin to the final consumer. Several attempts have been made to determine the origin of green and roasted coffee beans. Analytical methods such as gas chromatography mass spectrometry (Costa Freitas *et al.*, 2001) and near infrared spectroscopy (Bertrand *et al.*, 2005) were applied for the determination of organic compounds such as fatty acid profiles (Martín *et al.*, 2001), tocopherols and triglycerides (González *et al.*, 2001). Stable isotope ratios of carbon, nitrogen and oxygen of specific compounds extracted from green coffee beans (Weckerle *et al.*, 2002) were studied with promising results. Isotope ratios are frequently used for fingerprinting of food because they can indicate, integrate, record and trace fundamental chemical and physical processes. The so called 'light elements' or 'bio elements' such as O, H, C, N and S are of great interest since they are ubiquitously present in food matrices and show significant natural variation due to thermodynamic or kinetic fractionation processes. These isotopes have been analysed mainly by isotope ratio mass spectrometry (IRMS) (Camin *et al.*, 2010; Suzuki *et al.*, 2008). Seasonal variations in humidity, agricultural practices and experimental or human impacts influence the isotopic signature of these elements in food. These effects make data interpretation more challenging but may enable the discrimination of curtailed small regions. $\delta^{18}O$ values of precipitation vary systematically with latitude and altitude, largely as a result of temperature-driven enrichment of the heavier isotope from humid air masses as they move to the cooler, higher latitudes or over orographic barriers (Bowen & Wilkinson, 2002). As the $\delta^{18}O$ of plants reflects the $\delta^{18}O$ of the water, plant material can be used to identify the geographical origin of samples, processing techniques or adulteration (Barbour, 2007). However, 'light' elements showed some limitations in their information content due to their seasonal variation.

Additional isotopes are gaining increasing interest including so called 'heavy elements' (*e.g.* Sr, Pb) which show a natural variation due to radioactive processes with very long half time (Ággarwal *et al.*, 2008). Other authors have underlined the amendatory importance of combining isotope ratios of 'light' elements (H, C, O, N, and S) and 'heavy' elements (such as lead (Pb) and strontium (Sr)) in supplying essential information for the discrimination of origin of food and beverage (Critteren *et al.*, 2007; Rummel *et al.*, 2008). Sr isotope ratios reflect directly the geological background as biological processes involved in plant and/or animal metabolism do not fractionate strontium isotopes significantly. A significant correlation between the value of $^{87}Sr/^{86}Sr$ of products and soils has been demonstrated in wine (Almeida *et al.*, 2004), asparagus (Swoboda *et al.*, 2008) and paprika (Brunner *et al.*, 2010). Krivan *et al.* (1993) demonstrated the potential of measuring elemental fingerprints in *Coffea arabica* beans and used Mn along with C, Co, Cs, Na and Rb to discriminate between green coffees from 8 different origins. The study was complemented by Anderson and Smith (2002) with the determination of the multi element composition of roasted coffee beans from 8 different origins from Central and South America, Indonesia and East Africa. Other authors studied variations in the boron isotope composition of *Coffea arabica* beans, showing that the measured variation in $\delta^{11}B$ values among different coffee beans is significant due to different local growing conditions (Wieser *et al.*, 2001). Based on previous studies, Serra *et al.* (2005) determined the isotopic composition of carbon, nitrogen and boron in green coffees from 19 different countries, showing that the isotopic composition of these three elements is a good indicator of geographical-dependent parameters, and therefore a useful tool to infer the region of production of green coffee. They suggested that the use of stable isotope ratios might be improved by the use of climatic data as an additional variable for the construction of a statistical model.

In this work, isotope analysis of oxygen (analysed by IRMS) and strontium (analysed by MC-ICP-MS) have combined, for the first time, with environmental parameters in order to discriminate between green coffees and to understand how climate and geological factors influence the discrimination through isotopes. This is of major importance in order to be able to establish a valid and time-invariant database for authentication. In this sense, the relation of experimental data with environmental factors was used to define relevant factors influencing the isotopic composition of green coffee. The origin of each green coffee included in this study was exactly known to access information on environmental factors such as *e.g.* altitude, precipitation amount and latitude and oxygen isotopic composition of mean annual precipitation.

3.2. Experimental

3.2.1. Samples

Green coffee beans (60 samples) from 20 different geographic origins (table 10) were provided from Novadelta, Comércio e Indústria de Cafés, S.A. (Campo Maior, Portugal). The location of origin of the green coffee samples was known and, whenever possible, was used to access latitude, longitude, and local altitude as well as the annual mean precipitation, the annual mean $\delta\ ^{18}O$ of precipitation, the strontium amount and isotope ratio of parent rock, as well as the distance from coast (tables 10 and 12). Altitude data were tracked in the Global Gazetteer version 2.1 (Global Gazetter, 2006). $\delta^{18}O$ values were acquired from the OIPC (Bowen, 2010). Soil type and geological information were obtained from the European Digital Archive on Soil Maps of the World (EuDASM, 2005). Data on Sr amount and $^{87}Sr/^{86}Sr$ isotope ratios of parent rock of geographical locations included in this study were obtained from Advanced Data Management in Solid Earth Geochemistry (EarthChem, 2003).

3.2.2. Oxygen isotope ratio measurement by isotope ratio mass spectrometry (IRMS)

3.2.2.1. Sample preparation

Green coffee beans were grinded in a mill Retsch mill Type MM2 (Retsch, Germany), 3 times 5 minutes to obtain particle sizes of less than 1 mm. After grinding, samples were dried overnight at 60 ºC, weighted in tin capsules and folded.

3.2.2.2. Pyrolysis (EA-P) mode

Oxygen isotope ratios were determined on an Isoprime (Micromass, UK) isotope ratio mass spectrometer coupled to an EuroEA elemental analyser (EuroVector, Italy) by high temperature pyrolysis. Pyrolysis was accomplished at 1300ºC on a glassy carbon reactor with glassy carbon chips and nickel plated carbon as catalysts, mounted co-axially on a ceramic tube. Coupling of the elemental analyser and isotope ratio mass spectrometer is performed via open-split. The isotope ratio data was corrected against international standards (IAEA 601 and IAEA 602). Analytical performance was checked by inserting laboratory standards between samples to control stability and to allow drift correction when necessary. Precision was 0.14 ‰.

3.2.3. Strontium isotope ratio measurement by multicollector inductively plasma mass spectrometry (MC-ICP-MS)

3.2.3.1. Reagents

Pro analysi (*p.a.*) grade 65% HNO_3 (Merck, Darmstadt, Germany) was subboiled doubly in an ultrapure quartz apparatus (MLS DuoPur, MLS, Leutkirch im Allgäu, Germany). Deionised water (18 MΩ.cm; REWA HQ5 Austria Wasseraufbereitung, Guntramsdorf, Austria) was subboiled prior to usage as well. Subboiled HNO_3 and 31 % H_2O_2 (p.a., Merck) were used for digestion. Polyethylene flasks and cartridges as well as polypropylene tubes and lids were cleaned sequentially with HNO_3 (10 % w/w) and HNO_3 (1 % w/w) and rinsed with deionised water before use. Dilution of standards and samples was performed gravimetrically with HNO_3 (1 % w/w), prepared from subboiled water and doubly subboiled HNO_3. Mass bias correction was performed by analysing a 20 ng g^{-1} solution of SRM 987 $SrCO_3$ (NIST, Gaithersburg, MD, USA). The certified $^{87}Sr/^{86}Sr$ ratio is 0.71034 ± 0.00026 whereas a generally 'accepted value' of the $^{87}Sr/^{86}Sr$ ratio for this reference material is reported in the literature as 0.710263 ± 0.000016 (the error represents a standard deviation of 2σ from the external reproducibility) (Stein *et al.*, 1997).

3.2.3.2. Sample Preparation

Four to six beans (amounting to about 1.0 g) were grinded in a Retsch mill Type MM2, 3 times for 5 minutes to obtain particle sizes of less than 1 mm. Approximately 0.5 g of the grinded material was directly weighed into Teflon bombs for subsequent microwave-assisted digestion (MLS 1200mega, MLS, Leutkirch im Allgäu, Germany). Concentrated double-subboiled HNO_3 (6 mL) and H_2O_2 (1 mL) were used as digestion reagents. Details are presented elsewhere (Swoboda *et al.*, 2008). The samples were finally transferred into 20-mL flasks, filled with HNO_3 (1% w/w) to 20g and stored at 4 ºC for further analysis. A digestion blank was prepared with each digestion batch.

Table 10. Geographical origin of the 60 green coffees included in this study and correspondent distance to the sea, altitude and average annual precipitation values.

Region	Country	Location	Coordinates[1] (latitude/ longitude)	Sample	Distance to the sea (Km)	Altitude (m)	Mean annual precipitation (mm)
Eastern Africa	Rwanda	Gataré	-2.3/ 29.2	1	1350	1533	1310
				2	1350	1533	1310
	Ethiopia	Yirga Ch´efe	6.17/ 38.2	3	860	1918	1494
				4	860	1918	1494
				5	860	1918	1494
	UR Tanzania	Lunji	-7.17/31.33	6	215	1300	560
		Mount Kilimanjaro	-3.12/37.21	7	254	700	880
				8	254	700	880
				9	254	700	880
				10	254	700	880
	Kenya	Mount Kenya	-0.15/37.30	11	481	4750	1180
				12	481	4750	1180
				13	481	4750	1180
				14	481	4750	1180
				15	481	4750	1180
				16	481	4750	1180
				17	481	4750	1180
				18	481	4750	1180
				19	481	4750	1180
				20	481	4750	1180
		Kirimiri	-0.91/37.30	21	427	1500	1230
				22	427	1500	1230

Table 10 (continued).

	Malawi	Ludwing-Mzuzu	-11.43/33.92	23	712	1327	1293
				24	712	1327	1293
	Zambia	Mubuyu Estate	-15.87/27.77	25	901	1101	-
	Zimbabwe	Peruzu	-	26	-	-	-
Pacific	Hawaii (Hawaii Island)	Greenwell estate	19.58/-155.10	27	14	400	2770
				28	14	400	2770
		Kona	19.06/-155.80	29	7	400	620
Central America	Mexico	Santa Rita	-	30	-	-	-
		Tuxtla (Chiapas)	16.75/-93.12	31	486	750	690
	Costa Rica	San Marcos de Tarrazu	9.7/-84.1	32	33	1450	1790
				33	33	1450	1790
	Guatemala	Huehuetenango	15.32/-91.97	34	99	1908	1021
		Acatenango	14.55/-90.93	35	71	1586	1218
	El Salvador	San Antonio	14/-89	36	93	1100	2278
		San Miguel	14.20/-89.21	37	93	1100	2278
	Nicaragua	Santa Rita	14.28/-85.18	38	156	200	-
South America	Brazil	Fazenda da Terra	-20.52/-47.38	39	899	700	1580
		Fazenda S. Benedito	-22.12/-45.12	40	317	900	1580
		Fazenda Muzambo	-	41	-	-	-
		Mogiana	-22.37/-46.95	42	188	607	1580
		Zona da Mata	-20.25/-42.33	43	429	877	1580
		Unknown	-	44	-	-	-
		Fazenda Nossa	-20.47/-45.97	45	752	857	1580
	Peru	Yanesha	-10.57/-75.40	46	294	4500	594
				47	294	4500	594

Table 10 (continued).

	Ecuador	San Cristobal Island	-0.38/-89.72	48	5	1492	-
				49	5	1492	-
Caribbean	Jamaica	Sierra del Centro	18.2/-76.83	50	17	750	2439
				51	17	750	2439
South-East Asia	Indonesia	Mandeling	0/102	52	231	30	2304
	East Timor	Ermera	-8.75/125.40	53	19	1195	1987
				54	19	1195	1987
				55	19	1195	1987
				56	19	1195	1987
				57	19	1195	1987
				58	19	1195	1987
Malenesia	Papua New Guinea	Western Highlands	-5.23/144.33	59	118	2000	2970
				60	118	2000	2970

[1]Negative latitude values correspond to South latitudes and negative longitude values correspond to West longitudes.

3.2.3.3. Strontium/matrix separation

The obtained digestion solutions of green coffee bean samples were separated according to Swoboda and co-authors (Swoboda *et al.*, 2008), using Eichrom Sr resin (Eichrom Industries, Darien, IL, USA). The solutions were diluted after separation to a final Sr concentration of about 20 ng g-1 to obtain optimum signal intensities of ^{88}Sr from 3 to 5 Volts. Fractionation effect of the column extraction procedure on the Sr isotopic ratio was checked according to Schultheis (Schultheis, 2003) and proved to be insignificant.

3.2.3.4. Instrumentation

Screening of the solutions for Rb and Sr prior and after separation was performed by using a quadrupole based inductively coupled plasma mass spectrometer ICP-MS (Elan DRCe, Perkin Elmer, Waltham, MC, USA). Sr isotope ratio measurements of the final solutions were accomplished using a double-focusing multicollector inductively coupled plasma mass spectrometer (MC-ICP-MS) (Nu Plasma, Nu Instruments, Wrexham, UK) coupled to a membrane desolvating system (DSN-100, Nu Instruments). The DSN-100 instrument was equipped with a PFA nebuliser (MicroFlow nebuliser, Elemental Scientific, Omaha, NE, USA) and a spray chamber with additional hot gas flow to eliminate condensation and droplet formation. The multicollector inductively coupled plasma mass spectrometer is equipped with a collector configuration consisting of 12 Faraday cups and three ion counters. All isotopes in this work (^{82}Kr, ^{83}Kr, ^{84}Sr, ^{85}Rb, ^{86}Sr, ^{87}Sr, ^{88}Sr) were measured simultaneously using Faraday cups. Experimental parameters of the MC-ICP-MS including nebuliser gas, rf power and ion transfer lens potentials, were optimised to achieve the maximum ion intensity for ^{88}Sr, using NIST SRM 987 solution with a content of 20 ng^{-1}.g. The operation parameters are given in table 11. Blank correction and mass bias correction was performed according to previous measurements (Swoboda *et al.*, 2008). The 20 ng^{-1}.g solution of NIST SRM 987 is certified for its Sr isotopic composition and is also used for strontium ratio measurement as quality control. The absolute abundance ratios in SRM 987 are $^{86}Sr/^{88}Sr$ (0.11935 ± 0.00325 SD), $^{87}Sr/^{86}Sr$ (0.71034 ± 0.0026 SD) and $^{84}Sr/^{86}Sr$ (0.05655 ± 0.00014 SD). The strontium isotope ratio uncertainty was calculated with Excell software (Microsoft Office, 1994). For more detailed information on this approach, please refer to the EURACHEM/CITAC Guide Quantifying Uncertainty in Analytical Measurement (EURACHEM/CITAC, 2000).

Table 11. Operating parameters and scheme of the monitored isotopes for the Sr measurements.

Nu Plasma settings										
Rf power	1,300 W									
Auxiliary gas flow rate/cooling gas flow rate	0.75 mL min^{-1}/13.0 mL min^{-1}									
Sample uptake rate	100 µL min^{-1}									
Sample/skimmer cone	Ni									
Nebuliser	Perfluoroalkoxy nebuliser									
Sampling mode	6 blocks of 10 measurements									
Measurement time	10 min per sample									
Mass analyser pressure	< 10^{-8} mbar									
Background/baseline determination	HNO_3 (1% w/w)									
Washout time	3 min									
Axial mass/mass separation	86.05/0.5									
Detection system	12 Faraday collectors									
Cups	L5	L4	L3	L2	L1	Ax	H1	H2	H3	H4	H5	H6
Isotope	^{82}Kr	^{83}Kr	^{84}Sr	^{85}Rb		^{86}Sr		^{87}Sr		^{88}Sr		
DSN-100 nebuliser settings												
Nebuliser pressure	2 bar (30 psi)											
Hot gas flow	0.7 – 0.9 L min^{-1}											
Membrane gas flow	4 L min^{-1}											
Spray chamber temperature	112 ºC											
Membrane temperature	122 ºC											

3.2.4. Data analysis

Statistical analysis of data (Principal Component Analysis and Spearman's correlation) was performed with Statistica 8.0 software (Statsoft Inc., USA) and MatLab software (version R2007b) (The MathWorks, Inc., USA). Spearman's rank correlation coefficient was calculated between analytical measurements and available climatic and geographical data. A level of significance of $p < 0.05$ for Spearman's correlation was the criteria for selecting climatic and geographical factors that were included as variables in principal component analysis.

3.3. Results and discussion

3.3.1. Strontium isotope abundance ratios of green coffee

$^{87}Sr/^{86}Sr$ isotope abundance ratios along with Sr concentration determined for 60 green coffee bean samples are shown in table 12. Coffees from Rwanda, Malawi, Zambia, Peru, East Timor and a part of the samples from Brazil showed $^{87}Sr/^{86}Sr$ values higher than 0.710 (table 12). All other coffee samples had lower $^{87}Sr/^{86}Sr$ isotopes abundance ratios. American coffees had variable $^{87}Sr/^{86}Sr$ values in the range of 0.7041

to 0.7155. Asian coffee from Papua New Guinea and Indonesia revealed significantly different $^{87}Sr/^{86}Sr$ values from East Timor coffee. African green coffee beans had $^{87}Sr/^{86}Sr$ range of 0.7047 – 0.7148. The latter allowed a clear discrimination between the group of coffees from Rwanda, Malawi and Zambia and the other three geographical origins, UR Tanzania, Kenya and Ethiopia. Samples from Kenya showed $^{87}Sr/^{86}Sr$ range from 0.7061 to 0.7075 (table 12). Kenyan samples (except samples 21 and 22; table 12) originated from Mount Kenya and had been cultivated in soils with moderate to high fertility. Kenyan coffee from Kirimiri (samples 21 and 22; table 12) came from an area of deep, red, strongly weathered acid soil with low fertility common in wet (sub) tropical climates (Exploratory Soil Map of Kenya, (EuDASM, 2005)). Both regions are rich in mugearites (basalts) which have an expected $^{87}Sr/^{86}Sr$ range from 0.702 to 0.707. $^{87}Sr/^{86}Sr$ values determined in Kenyan coffees (table 12) overlap with this range. $^{87}Sr/^{86}Sr$ values found for all Kenyan coffees are in the same range of values reported for parent rock at the same locations (table 12). Green coffee from UR Tanzania had $^{87}Sr/^{86}Sr$ values from 0.7047 to 0.7072 (table 12). UR Tanzania sample 6 came from a region classified as Eutric Cambisol (Provisional Soils Map of Tanzania, (EuDASM, 2005)) and had a higher $^{87}Sr/^{86}Sr$ ratio (0.7072) compared to the other Tanzanian coffees that stem from Mount Kilimanjaro, where Eutric Nitisols prevail (Provisional Soils Map of Tanzania, (EuDASM, 2005)). In this region, EarthChem (EuDASM, 2005) reports the existence of basalts (absarokite; GEOROC 118466, table 12) with higher $^{87}Sr/^{86}Sr$ values (0.7063) comparing with Mount Kilimanjaro. Basalts in locations at Mount Kilimajaro show lower values of $^{87}Sr/^{86}Sr$. This is in agreement with the values determined for coffee from Kilimanjaro and with a $^{87}Sr/^{86}Sr$ range from 0.702 – 0.707 which is reported for basaltic rocks, specifically ocean basalts (Capo *et al.*, 1998). Coffee from Ethiopia had an $^{87}Sr/^{86}Sr$ ratio ranging from 0.7073 to 0.7077 which is higher than the $^{87}Sr/^{86}Sr$ ratio of parent rock at that location (table 12). The difference may be explained by the fact that the Sr in the mobile phase can differ from the composition of the total rock (Prohaska *et al.*, 2005). This hypothesis is taken into account in the case of coffee plants and beans from certain locations (*e.g.* coffee from Ethiopia and Zambia and some of the coffees from Brazil, table 12). Green coffees from Zambia, Malawi and Rwanda show the highest $^{87}Sr/^{86}Sr$ values among African coffees (table 12). Malawi samples 23 and 24 came from a location with soil characterized as Lithosol, (Soil Map of Malawi, (EuDASM, 2005)) with clay minerals formed from silicate bearing rocks. This may explain $^{87}Sr/^{86}Sr$ ratios found in coffee that are similar to values for silicate rocks (≥ 0.710). Rwanda samples 1 and 2 came from a location rich in silicate rocks ($^{87}Sr/^{86}Sr \geq 0.710$) like paragneiss and orthogneiss (Carte Lithologique du Rwanda, (EuDASM, 2005)). $^{87}Sr/^{86}Sr$ ratios (0.7140 and 0.7144, table 12) of Rwandese coffees match the range of values reported for this type of parent rock. $^{87}Sr/^{86}Sr$ values allow the discrimination between the different American coffees (Ecuador, Jamaica, Nicaragua, El Salvador, Brazil and Hawaii), as well, with the exception of samples from Mexico which show overlapping isotope ratios with coffees from Hawaii, part of the Brazilian coffees. Coffee from Hawai'i was produced in a region of soil over pahoehoe lava bedrock at the Island of Hawaii (General Soil Map of Island of Hawaii, (EuDASM, 2005)). Values of $^{87}Sr/^{86}Sr$ found for Hawaiian coffee

(table 12) are in accordance to the values of $^{87}Sr/^{86}Sr$ reported for ocean basalts (0.702 to 0.707). We could not obtain further information about parent rock nature at the Mexican locations included in this study, neither by the analysis of soil or geological maps or by consulting database GEOROC. For this reason, Sr isotopic composition of Mexican coffees could not be included in the comparison with $^{87}Sr/^{86}Sr$ of local parent rock. Moreover, we could not access soil maps or geological maps of Jamaica, Costa Rica, Guatemala and Nicaragua. However, GEOROC samples of these locations (table 12) reported in EarthChem (EuDASM, 2005) allowed us to compare $^{87}Sr/^{86}Sr$ values of rock samples and green coffee beans. Coffees from Jamaica and Guatemala showed $^{87}Sr/^{86}Sr$ values equivalent to those reported for parent rock whereas coffees from Costa Rica and Nicaragua had values of $^{87}Sr/^{86}Sr$ above those reported to corresponding rock samples (table 12). Brazilian coffee beans revealed a wide variation in Sr isotopes abundance ratios although these samples were distinguishable from coffees obtained from Ecuador, Jamaica, Nicaragua and El Salvador (table 12). We were unable to find information on Sr isotopic composition of parent rock for each Brazilian geographical location. Nevertheless, it was possible to compare $^{87}Sr/^{86}Sr$ of green coffee to $^{87}Sr/^{86}Sr$ of the parent rock for samples 39, 40, 42 and 45 (table 12). With the exception of sample 45, these Brazilian green coffees had higher $^{87}Sr/^{86}Sr$ ratios than values reported for parent rock. We were not able to obtain information on soil and parent rock for Peruvian coffee, making it difficult to relate $^{87}Sr/^{86}Sr$ of the coffee bean to the geology. Coffee from Ecuador came from a region rich in clays, metamorphic rocks derived from volcanic rocks and also granites (Mapa General de Suelos del Ecuador, (EuDASM, 2005)). Values of $^{87}Sr/^{86}Sr$ for the Ecuadorian coffees are close to the range of values referenced for basalts which is the type of rock reported for GEOROC samples (EuDASM, 2005) used to compare $^{87}Sr/^{86}Sr$ values in our work (table 12). East Timor green coffee could be distinguished from all other origins included in this study solely on the basis of the $^{87}Sr/^{86}Sr$ isotopes abundance ratio. In spite of this, East Timor coffees showed high scattering of $^{87}Sr/^{86}Sr$ ranging from 0.7159 to 0.7296 (table 12). Coffees from Papua New Guinea had different $^{87}Sr/^{86}Sr$ ratio compared to coffee from Indonesia and lower $^{87}Sr/^{86}Sr$ ratio compared to East Timor coffee, where parent rock had higher $^{87}Sr/^{86}Sr$ values compared to the other geographical origins included in this study (table 12). A correlation was found between the $^{87}Sr/^{86}Sr$ ratios of African green coffee and the distance from coast of each geographical location (with a Spearman's correlation coefficient (r) of 0.74; significant at $p<0.05$). Positive correlations between $^{87}Sr/^{86}Sr$ of the African green coffees and the mean annual precipitation ($r = 0.76$) and between precipitation and distance from coast ($r = 0.87$) were obtained, as well. This indicates an influence from ocean and precipitation Sr inputs in Africa, and consequently in the coffee plants and their seeds developed in these regions. We cannot fully exclude that Sr isotopic composition is influenced by dry deposition. Sr atmospheric signature can be estimated by direct measurement on bulk precipitation. Unfortunately, to our knowledge, there are no available databases with this information. Precipitation samples from each location and harvest time were not available to our study.

Table 12. $\delta^{18}O$ and $^{87}Sr/^{86}Sr$ of the 60 green coffees included in this study and strontium concentration and isotope ratio of parent rock reported at the geographical coordinates (whenever available).

Region	Country	Location	Sample	$\delta^{18}O_{bean}$ (‰)	Mean annual $\delta^{18}O_{prec}$ (‰)[1]	$^{87}Sr/^{86}Sr_{bean}$[2] (mean)	Sr_{bean}[3] (µg g^{-1})	Mean $^{87}Sr/^{86}Sr$ in parent rock[4] (range)	Mean Sr in parent rock[4] (ppm)	*EarthChem* Reference[4]
Eastern Africa	Rwanda	Gataré	1	30.9	-4.0	0.7144	7.6	0.7067	941	GEOROC 85572, 85576/7/9, 85592/7,
			2	31.5	-4.0	0.7140	7.7	(0.7054-0.7080)		85607, 85629, 85636/7, 85641
	Ethiopia	Yirga Ch´efe	3	34.8	-1.8	0.7077	3.1	0.7035	625	GEOROC 73614, 73622, 73621
			4	30.8	-1.8	0.7074	3.1	(0.7034–0.7035)		
			5	30.3	-1.8	0.7073	4.2			
	UR Tanzania	Lunji	6	27.2	-4.6	0.7072	9.2	0.7063	1034	GEOROC 118466
		Mount Kilimanjaro	7	31.2	-2.7	0.7047	21.8	0.7035	470	GEOROC 113112
			8	29.5	-2.7	0.7047	25.0			
			9	25.6	-2.7	0.7058	2.6			
			10	28.2	-2.7	0.7047	26.5			
	Kenya	Mount Kenya	11	31.7	-10.2	0.7061	7.6	0.7068	793	GEOROC
			12	31.6	-10.2	0.7074	6.4	(0.7061-0.7073)		89749, 118458, 118400
			13	29.6	-10.2	0.7074	6.0			
			14	33.8	-10.2	0.7062	7.8			
			15	30.9	-10.2	0.7065	6.1			
			16	31.7	-10.2	0.7067	6.3			
			17	33.6	-10.2	0.7072	8.1			
			18	34.1	-10.2	0.7066	5.2			
			19	34.1	-10.2	0.7075	8.1			
			20	28.1	-10.2	0.7063	7.1			
		Kirimiri	21	29.6	-3.9	0.7073	7.6	0.7068	793	GEOROC
			22	31.8	-3.9	0.7072	6.7	(0.7061-0.7073)		89749, 118458, 118400
	Malawi	Ludwing-Mzuzu	23	29.9	-5.4	0.7131	5.4	-	-	-
			24	26.8	-5.4	0.7148	6.2			
	Zambia	Mubuyu Estate	25	33.4	-5.3	0.7121	6.0	-	-	-
	Zimbabwe	Peruzu	26	30.3	-	0.7169	3.4	-	-	-
Pacific	Hawaii	Greenwell estate	27	26.6	-3.1	0.7059	3.1	0.7041	25	GEOROC
	(Hawaii island)		28	29.2	-3.1	0.7067	4.8	(0.7038-0.7047)		28810/12/13/14
		Kona	29	29.7	-3.1	0.7063	2.8			
Central America	Mexico	Santa Rita	30	25.2	-6.4	0.7076	7.7	-	-	-
		Tuxtla (Chiapas)	31	24.7	-5.8	0.7064	4.0			
	Costa Rica	San Marcos	32	19.2	-7.6	0.7064	6.8	0.7039	362	GEOROC
		de Tarrazu	33	21.1	-7.6	0.7051	9.7	(0.7035-0.7049)		8838,10339,10342,38652
	Guatemala	Huehuetenango	34	24.3	-8.4	0.7067	4.4	-	-	-
		Acatenango	35	23.8	-8.1	0.7045	3.8	0.7055	169	GEOROC
								(0.7039-0.7066)		6277, 6278

Table 12 (continued).

	El Salvador	San Antonio	36	25.7	-7.3	0.7041	5.4	0.7032	482	GEOROC
		San Miguel	37	24.0	-7.3	0.7041	5.8			135763
	Nicaragua	Santa Rita	38	22.7	-5.2	0.7047	4.7	0.7037	-	GEOROC 16708
South America	Brazil	Fazenda da Terra	39	30.1	-5.1	0.7068	4.2	0.7057	452	GEOROC 145808/9/27
		Fazenda S. Benedito	40	28.2	-5.8	0.7155	9.0	0.7060 (0.7059-0.7061)	357	GEOROC 43474, 43541
		Fazenda Muzambo	41	27.0	-	0.7139	6.6	-	-	-
		Mogiana	42	26.7	-5.2	0.7077	4.2	0.7055 (0.7055-0.7056)	377	GEOROC 43567
		Zona da Mata	43	27.9	-5.3	0.7126	2.9	-	-	-
		-	44	27.6	-	0.7077	4.4	-	-	-
		Fazenda Nossa	45	25.6	-5.4	0.7154	5.6	0.7125 (0.7057-0.7288)	363	GEOROC 114909/14
	Peru	Yanesha	46	21.6	-13.5	0.7127	3.7	-	-	-
			47	21.1	-13.5	0.7112	3.6			
	Ecuador	San Cristobal Island	48	24.2	-6.4	0.7049	2.5	0.7030 (0.7024-0.7038)	334	GEOROC 78680/8
			49	25.0	-6.4	0.7052	2.2			111071/2/3/4/5/6/7/8/9 112983
Caribbean	Jamaica	Sierra del Centro	50	26.6	-5.2	0.7057	-	0.7055	523	GEOROC
			51	26.8	-5.2	0.7053	6.7	(0.7035-0.7088)		100921/2/4
South-East Asia	Indonesia	Mandeling	52	24.9	-7.0	0.7062	8.9	0.7047 (0.7045-0.7047)	375	GEOROC 146992/3/4
	East Timor	Ermera	53	26.7	-7.5	0.7270	5.2	0.7109	268	GEOROC
			54	26.2	-7.5	0.7159	3.2			45581
			55	21.3	-7.5	0.7227	3.7			15143/4/5/6/8/9
			56	23.7	-7.5	0.7285	4.9			15150/1/2
			57	25.4	-7.5	0.7296	5.1			
			58	25.8	-7.5	0.7259	4.0			
Malenesia	Papua New Guinea	Western Highlands	59	18.7	-11.1	0.7042	5.9	0.7044 (0.7036-0.7054)	759	GEOROC 82070/1/2/3/4/5/7/8/9
			60	20.0	-11.1	0.7044	5.0			82081/2/3/4/5

[1]From OIPC (Bowen *et al*., 2010).
[2]Relative standard deviation of results from independent prepared samples.RSD values varied from 0 to 0.0006 with the exception of samples 32 and 54 with RSD of 0.0012 and 0.0147, respectively.
[3]In digested solution.
[4]From EarthChem – Advanced Data Management in Solid Earth Geochemistry. The values in this table are means of values of $^{87}Sr/^{86}Sr$ of parent rock/s found in the same or very approximate geographical coordinates from were green coffee samples were obtained (the range of values is also indicated, whenever there was more than one parent rock sample per location).

The effect of dry deposition in combination with wet deposition has to be further evaluated depending on the geographical region (*e.g.* geology, climate). Sea-salt aerosols show constant marine $^{87}Sr/^{86}Sr$ but continental dust sources may impart spatial and temporal variations on this value on certain locations (Drouet *et al.*, 2007). Whereas the isotopic signature of the atmospheric inputs and the plant materials are relatively easy to determine, the estimation of the weathering end-member remains more problematic. Nonetheless, natural weathering can be simulated by extraction of soil samples with acidic solutions. The soil exchangeable fraction, which corresponds to the plant-available pool, can be leached from soil by salt solution (Swoboda *et al.*, 2008). Future steps of our study will involve strontium isotopes analysis not only of the bulk coffee bean but of corresponding precipitation water and soil. These observations cannot be verified in the case of Latin American, Caribbean coffees and Asian coffees due to the limited number of samples.

3.3.2. Oxygen isotope abundance ratios of green coffees

Oxygen isotopic ratios ($\delta^{18}O$ values) of green coffee beans varied globally from 18.7 to 34.8 ‰ (table 12). In Africa, we found values ranging from 25.6 to 34.8 ‰. Pacific (Hawai'i), Central American and Caribbean (Jamaica) origins as well as South American coffee displayed a lower range of values for $\delta^{18}O$ (19.2 to 30.1 ‰). The same was observed in South Asia and Melanesia (Papua New Guinea) with values for $\delta^{18}O$ of the coffee bean between 18.7 and 26.7 ‰. A solid interpretation of the ^{18}O abundance in the green coffee bean is complicated by the combination of environmental, climatic and physiological processes. Moreover, oxygen isotopes are known to fractionate in plant leaves (Barbour, 2007) but less is known concerning fractionation in seeds (*e.g.* the coffee bean). However, most of seed organic matter should derive from leaf photosynthesis, probably with minor contribution of seed photosynthesis. $\delta^{18}O$ of rainwater directly translates to the $\delta^{18}O$ of soil water (Yakir *et al.*, 2000). After soil water has been uptake through plant roots, plant stem water remains virtually with the same $\delta^{18}O$ value as for soil water and for plant water lost by transpiration. However, oxygen isotopes fractionation occurs in leafs during photosynthesis (Yakir *et al.*, 2000). Newly synthesized plant organic compounds $\delta^{18}O$ will not only be dependent on fractionation occurring during this process but also on the specific biosynthetic pathways involved in their synthesis (their enzymes and regulation). Also, the leaf water oxygen isotope signal is dampened in organic material formed from exported sucrose in other plant parts. As a consequence, organic molecules may reflect or not the water in which they are formed. In spite of this, several authors report that oxygen isotope composition of plant organic material is known to reflect that of source water and leaf evaporative conditions at the time the material was formed (Barbour *et al.*, 2000b). On this basis, we have tried to correlate green coffee bean $\delta^{18}O$ with environmental factors

known for the correspondent origins included in this study. In fact, Serra and co-authors (Serra *et al.*, 2005) had already indicated the importance of relating isotope analysis with known data on environmental variables in order to build the best model for origin discrimination. We calculated Spearman's rank correlation coefficient (r) between isotopic composition of oxygen and climate and geographical information of each known geographical location. A weak correlation was found between values of $\delta^{18}O$ of green coffees and the distance from coast ($r = 0.27$; significant at $p<0.05$). Several authors reported a continental effect on isotopic fractionation of oxygen in precipitation in which a trend of lighter isotopic composition is seen as a function of the distance from coast. Most water vapour in the atmosphere is derived from evaporation of low-latitude oceans. Precipitation derived from this vapour is always enriched in ^{18}O relative to the vapour. The fractionation between rain and vapour is a function of condensation temperature. Therefore, as clouds move across the continent, progressive rain-out leads to increasingly isotopically lighter rain (Augusti & Schleucher, 2007; Barbour, 2007). However, our results do not show this continentality effect on $\delta^{18}O$ of green coffee beans. This suggests that a variety of processes are influencing the $\delta^{18}O$ values of the bulk bean, *e.g.* variations in $\delta^{18}O$ of water taken up by plants and leaf water enrichment in ^{18}O during plant transpiration, depending on the atmospheric conditions (relative humidity, and ^{18}O of water vapour in the atmosphere). As seen for the distance to the sea, weak correlations between $\delta^{18}O$ of the coffee bean and mean annual precipitation and latitude were observed ($r = -0.34$ for both correlations; significant at $p<0.05$). Isotopically lighter (depleted; with less ^{18}O) rain is observed with increasing latitude (Bowen *et al.*, 2002). This effect is known as latitude effect on isotopic fractionation of ^{18}O in precipitation and is well described in literature (Augusti *et al.*, 2007). The correlations found between $\delta^{18}O$ of the coffee bean and values of latitude and mean annual precipitation could be an indication that variations in the isotopic composition of oxygen of the green coffee bean were related to these factors. However, this was not found on the analysis at global scale. Additionally, we have not found any correlation between oxygen isotopic composition of the coffee bean and values of altitude. The statistical analysis was repeated for smaller regions. Oxygen isotopic composition of green coffees from islands correlated with values of altitude ($r = -0.91$; significant at $p<0.05$). Lower values of altitude correspond to enriched values of $\delta^{18}O$ of green coffees. In this system, the altitude effect on oxygen isotopic composition seems clear (this pattern is often not observed in interior mountains or on the leeward side of mountains). Due to Rayleigh distillation (Augusti *et al.*, 2007), rainfall values become more depleted in ^{18}O as a storm moves across the landscape. Rain at higher altitudes (where lower temperatures are also verified) becomes more depleted in ^{18}O. This leaves a plausible explanation of the variation on the $\delta^{18}O$ of the green coffees originating from islands. The same approach was applied to the case of South American coffee beans (Peru, Ecuador and Brazil), and the oxygen composition of the mean annual precipitation as well as the corresponding values for latitude and altitude seemed to be relevant to the $\delta^{18}O$ values of green coffee ($r_{\delta 18O \text{ bean versus } \delta 18O \text{ mean annual precipitation}} = 0.84$, $r_{\delta 18O \text{bean versus latitude}} = 0.68$ and $r_{\delta 18O \text{bean versus altitude}} = -0.89$). An altitude effect on the

isotopic composition of oxygen was observed as well as a strong correlation with precipitation. As verified in plant leaf organic material (Barbour, 2007), we assume that the oxygen isotope composition of a seed (*i.e.* the green coffee bean) reflects that of source water and coffee plant leaf evaporative conditions at the time the seed was formed. Lack of studies and experimental data still limit the understanding of the fractionation of oxygen isotopes of the green coffee bean during its formation. Seeds are very complex matrices, rich in a large number of compounds originating from primary and secondary metabolism leading to possible divergence to models that have been described for other plants and/or plant tissues.

3.3.3. Multivariate analysis

The variable reduction method of principal component analysis (PCA) was used for exploratory data visualization to determine to what extent we could discern differentiation of the samples according to geographic origin. Data on Sr amount and isotope ratio of coffees and correspondent parent rock (whenever available) (table 12) were used to determine principal components and green coffee samples scores on principal components (figure not shown). The first two principal components (PCs) selected to plot samples scores had eigenvalues of 1.9792 and 0.9877 and together explained > 74 % of the total variance of the data. PC1 explains 49.48 % of the total variance and correlates negatively with $^{87}Sr/^{86}Sr$ of green coffees and $^{87}Sr/^{86}Sr$ of parent rock (the two variables have loading values approximate or higher than |0.65|). PC2 explains 24.69 % of the remaining variance with Sr (ppm) of parent rock having the major loading (0.7900). In PC3, explaining 21.39 % of variance, the loading of Sr (ppm) in green coffees was higher than |0.65| (0.8793). Spearman's correlation *r* (significant at $p<.05$) between $^{87}Sr/^{86}Sr$ of green coffees and $^{87}Sr/^{86}Sr$ of rock was 0.698907 and between Sr ($\mu g\ g^{-1}$) in green coffees and Sr ($\mu g\ g^{-1}$) in rock was 0.522956, showing that these parameters are related to each other. There was evidence that most $^{87}Sr/^{86}Sr$ ratios of the green coffee bean are related to Sr isotope abundance ratio of the parent rock and/or soil. Reserves of bioavailable cations in the soil are mainly in exchangeable form, adsorbed on the mineral and organic matter surface (exchange complex). The advantage of the use of the Sr isotope technique is that soil $^{87}Sr/^{86}Sr$ remains a robust signature, although concentrations in major elements released by weathering can be modified by the formation of secondary minerals or exchange processes on the adsorbing complex. Lacking agreement of isotope ratios of total rock and soil with bioavailable Sr can be interpreted that Sr fractions in soil have different solubility (Swoboda *et al.*, 2008). Thus the isotopic composition of all sources of Sr such as soil, soil extracts, wet and dry precipitates; surface and groundwater as well as water used for watering have to be subject to broader investigations for further interpretation. The final combination of the isotopic composition of both oxygen and strontium did not allow total discrimination between all 20 different countries in one single analysis. However, it is possible to achieve a separation between selected origins

and groups of provenances. East Timor discriminated significantly from all other origins. The samples from Peru separated from the group of Costa Rica and some coffees from Brazil as well as from Papua New Guinea and from the group enclosing coffee from Malawi, Rwanda, Zambia and finally from a major group of origins including samples from UR Tanzania, Kenya, Ethiopia, Hawaii, Jamaica, Nicaragua, El Salvador, Guatemala, Ecuador, Mexico, Indonesia (figure not shown). We have furthermore applied the same multivariate analysis to smaller regions (Africa, Islands and South America). A strong competitive market is observed within these regions. PCA of the isotopic composition of oxygen and strontium of the African green coffees is shown in figure 25a. The first two PCs selected to plot samples scores had eigenvalues of 1.038 and 0.962. Coffees from Ethiopia, UR Tanzania and Kenya discriminate significantly from coffees from Rwanda, Malawi and Zambia. $^{87}Sr/^{86}Sr$ of the samples originating from Rwanda, Malawi and Zambia show $^{87}Sr/^{86}Sr$ values higher than 0.710 while Ethiopian, Tanzanian and Kenyan coffees have significantly lower values (table 12). A positive correlation between $\delta^{18}O$ values of African green bean samples and higher altitudes ($r = 0.56$ (significant at $p<0.05$)) as well as between mean annual precipitation and distance from coast with strontium isotopic composition of the African green coffees ($r = 0.76$ and 0.74, respectively; significant at $p<0.05$) was observed. When PCA was repeated including these factors as variables the result was the distinction between the African origins (figure 25b). The two first PCs had eigenvalues of 2.378 and 1.666, respectively and explained 80% of the variability observed. $^{87}Sr/^{86}Sr$ and the distance to the sea were positive in the two PCs, whereas mean annual precipitation, altitude and $\delta^{18}O$ of the green coffee beans were negative on the first PC but positive on the second. The same approach was applied to coffees originating from islands (Hawaii, Jamaica, East Timor, Indonesia, and Papua New Guinea) (figure 26). East Timor coffees discriminated from coffees from Papua New Guinea and from a third group enclosing Indonesian, Hawaiian and Jamaican coffees. In this analysis, the eigenvalues of the two PCs were 1.021 and 0.979, respectively. Figure 27 shows the result of PCA of isotopic composition of oxygen and strontium of green coffees from South America. The two PCs had eigenvalues of 1.028 and 0.972, respectively. Green coffee samples from Ecuador discriminate from coffees from Peru and from Brazilian coffees.

3.4. Conclusions

We proved evident that a combination of the isotopic systems of oxygen and strontium is a good approach to discriminate coffees according to their geographical origin in smaller competitive regions (such as South America or Africa). The results indicate that the isotopic composition of oxygen and strontium of the green coffee bean is related with the isotopic composition of oxygen of wet precipitation and with the isotopic composition of bioavailable strontium in soil.

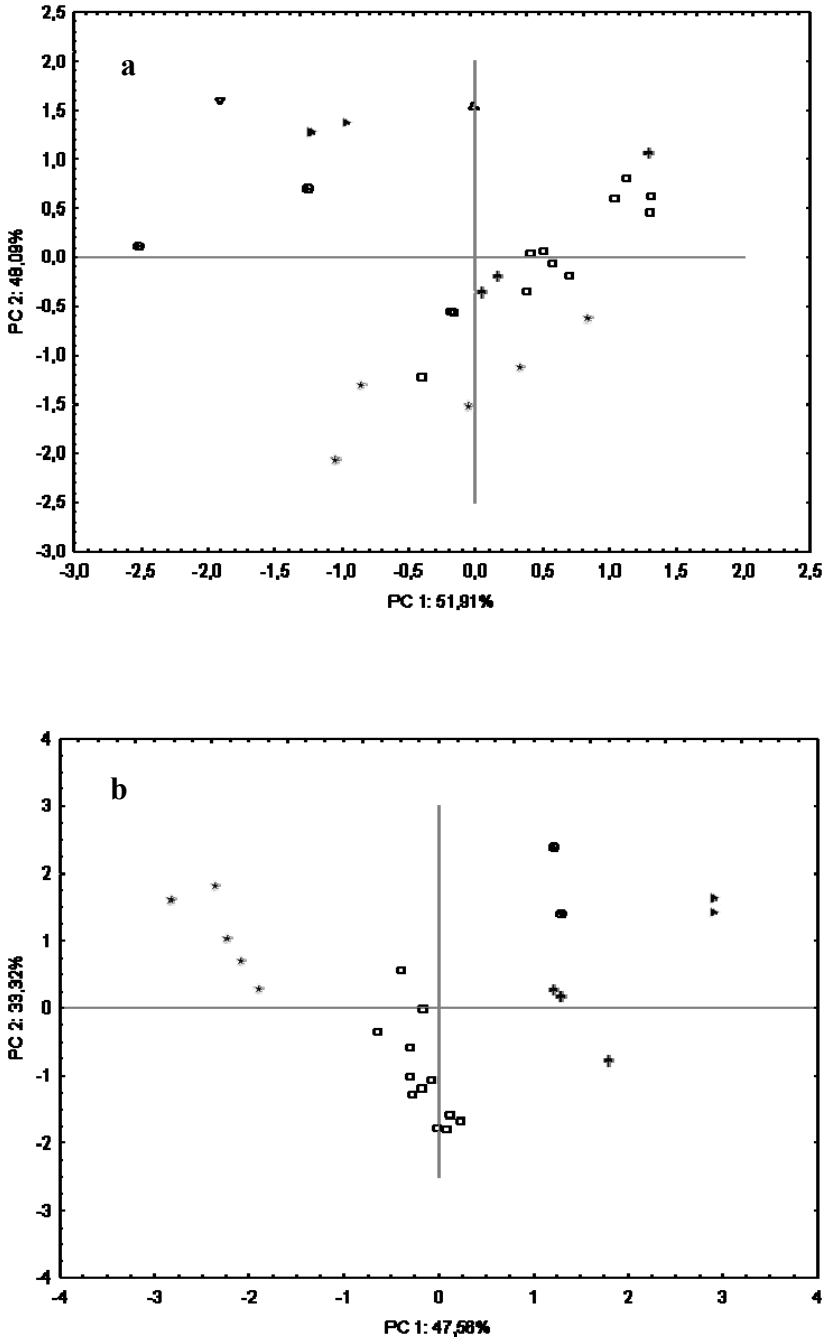

Figure 25. Principal component analysis of oxygen and strontium isotopic composition of African green coffees (a) and with values of annual mean precipitation, distance from coast and altitude (b) (Legend: + – Ethiopia; □ – Kenya; ⊕ – Malawi; ► –Rwanda; ★ – UR Tanzania; △ – Zambia; ▽ - Zimbabwe).

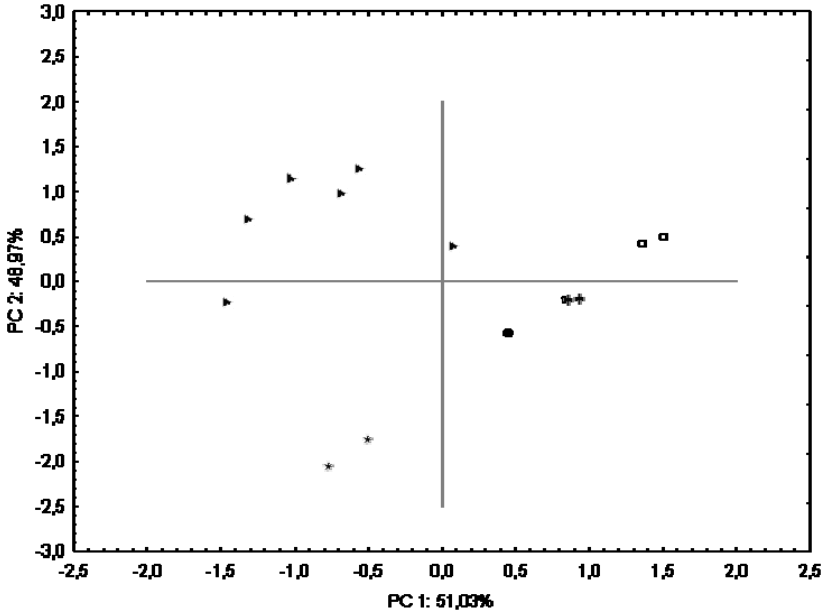

Figure 26. Principal component analysis of oxygen and strontium isotopic composition of green coffees from islands (Legend: ☐ – Hawaii; ⊕ – Indonesia; + – Jamaica; ★ – Papua New Guinea; ► – East Timor).

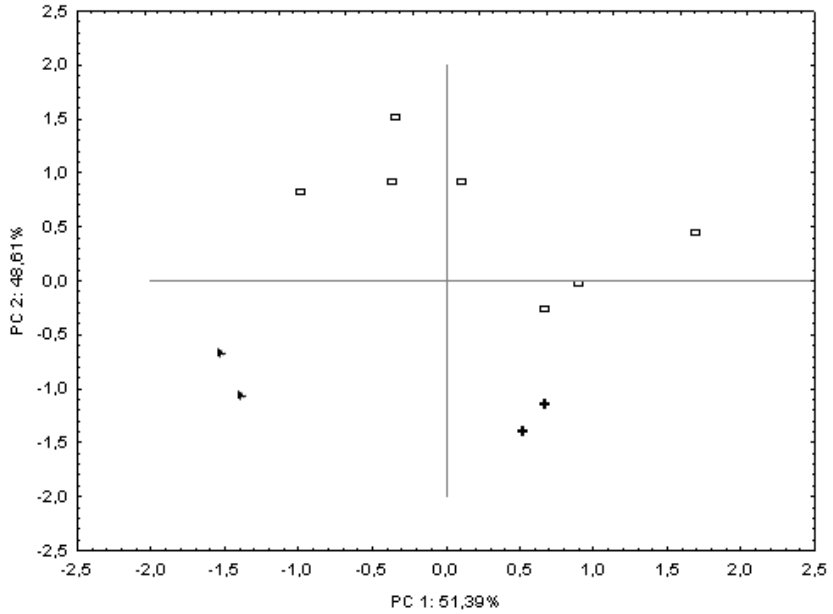

Figure 27. Principal component analysis of oxygen and strontium isotopic composition of green coffees from South America (Legend: ☐ – Brazil; + – Ecuador; ► – Peru).

We still have to consider additional influences such as e.g. CO_2 sources, variations in temperature, the time of the year when rain and plant irrigation occur as well as coffee plant metabolism (primary and secondary). Further research on Sr isotopic composition variation during coffee bean phenology leaves room for investigations (similar to considerations for the interpretation of the variation of the oxygen isotopic composition) even though Sr fractionation caused by metabolic processes is expected to be far less pronounced (if even measurable).The use of isotope ratios for origin determination can be further improved by establishing a sampling network allowing the use of additional climatic and geological data as variables. Additional information on the stability of environmental parameters that influence isotopic signature of foods is fundamental. This will bring an innovative approach in which it may be possible to relate environment with food isotopes and so, explain 'why' it is possible to get a discrimination based on isotope analysis of the food.

A conclusive *Coffee Geographical Origin Discrimination Model* requires an increased number of samples besides fundamental studies of influencing parameters and on how these are stable with time. The work is a key for using both strontium isotopes abundance ratios and $\delta^{18}O$ for origin discrimination of coffee as well as it proves that the combination with additional parameter enhances the validity of a discrimination model.

4. Isotopes as tracers of the main environmental factors that contribute to the specificity of Hawaiian green coffee (a case-study)

Rodrigues, C., Brunner, M., Steimann, S., Bowen, G., Nogueira, J.M.F., Gautz, L., Prohaska, T., Máguas, C. (*submitted*)

4.1. Introduction

Several studies have shown that green coffee beans from different geographical origins have different elemental and isotopic compositions (Anderson *et al.*, 2002a; Krivan *et al.*, 1993; Serra *et al.*, 2005; Wieser *et al.*, 2001). Krivan and collaborators (Krivan *et al*., 1993) demonstrated the potential of measuring elemental fingerprints of coffee beans to discriminate between different origins. The study was complemented by Anderson and Smith (Anderson *et al.*, 2002) with the determination of the multi element composition of roasted coffee beans from Central and South America, Indonesia and East Africa. Other authors studied variations in the boron isotope composition of *Coffea arabica* beans, showing that the measured variation in $\delta^{11}B$ values among different coffee beans is significant due to different local growing conditions (Wieser *et al.*, 2001). Serra and co-authors (Serra *et al.*, 2005) determined the isotopic composition of carbon, nitrogen and boron in green coffees from 19 different countries, showing that the isotopic composition of these three elements is a good indicator of geographical-dependent parameters, and therefore a useful tool to infer the region of production of green coffee. However, the study of the relations between isotopes of the coffee plant seed and environmental factors is still recent (Rodrigues *et al.*, 2011; Rodrigues *et al.*, 2009). Rodrigues and co-authors (Rodrigues *et al.*, 2011; Rodrigues *et al.*, 2009) have determined isotope ratios of carbon, nitrogen, oxygen and strontium of green coffee beans and have searched for relationships between the measured isotope ratios and available information on environmental factors. Furthermore, stable isotope ratios of specific compounds extracted from the green coffee beans have also been used for origin discrimination with promising results (Weckerle *et al.*, 2002). Such studies are important in order to understand how the seed integrates isotope fractionations occurring during its development, associated to change of local climate and geology. This may ultimately lead to the discrimination of coffee producing regions. Currently, stable isotope analysis is a powerful tool in ecological studies to trace, record, source, and integrate ecological parameters of interest (West *et al.*, 2006) and has been extensively used in food authentication studies. Moreover, the impacts and variations that result in changes to modern environments are also seen as changes to the H, C, N, O, S and Sr isotope ratios of atmospheric gases, animal and plant tissues, soil organic

matter and its diverse chemical substrates, as well as water sources in the hydrosphere and the atmosphere (Dawson & Siegwolf, 2007). The H, C, N, O, S, and Sr isotopes are the elements that vary the most on Earth, constitute the bulk of all living matter, and are used most effectively to track changes in the Earth's biogeochemical cycles. In what refers to carbon isotopes, the basis for much of the observed variation in $\delta^{13}C$ of organic samples derives from two metabolic processes, photosynthesis and respiration (Farquhar *et al.*, 1989). The major differences in the $\delta^{13}C$ of plant carbon are observed when comparing marine and terrestrial plants as well as among terrestrial plants that possess different photosynthetic pathways (*e.g.* C3, C4, and CAM) due to the different ways carbon is assimilated and their associated fractionations (Farquhar *et al.*, 1989). Also, as environment changes, a wide range of $\delta^{13}C$ values within biological materials suggest multiple and very different processes leading to this observation, such as stomatal control (Scheidegger *et al.*, 2000) and plant hydraulics properties (Dawson, 1993). In relation to oxygen, meteoric waters can vary in their $\delta^{2}H$ and $\delta^{18}O$ as they move through the hydrological cycle (Bowen *et al.*, 2005). Many important factors influence the $\delta^{2}H$ and $\delta^{18}O$ of meteoric waters *e.g.* seasonality and therefore the changes in condensation temperatures of precipitation (Craig, 1961), latitude, altitude, and orographic barriers (Ehleringer *et al.*, 1992). Once water is taken up by plants, the $\delta^{2}H$ and $\delta^{18}O$ of 'body/source' water and biosynthetic compounds that incorporate H or O may or may not also have associated fractionations that are 'recorded' in the organic molecules that contain these elements (Barbour, 2007; Barbour *et al.*, 2001; Dawson *et al.*, 2007; Roden *et al.*, 2000). As the processes involved in these fractionations become better understood, plant materials present themselves as valuable 'biomarkers' of ecological processes because when tissues are formed they are known to record temperatures, water sources, and levels of relative humidity prevailing at that time (Anderson *et al.*, 2002b; Williams *et al.*, 2005). In the case of nitrogen, variation in the $\delta^{15}N$ in its cycle processes has been increasingly studied. Knowledge of how the isotopes of N fractionate during catabolic reactions in soils and in plants in relation to N utilization, transformation, and N fixation (Evans, 2001) elucidate the pathways and interactions that are many times resultant from land-use and agricultural practices. In addition, it has become apparent that the use of both sulphur (S) and strontium (Sr) isotopes holds great promise for detecting and therefore understanding the nature and magnitude of ecological change. Sulphur stable isotopes have been useful in pollution studies (Trust *et al.*, 1992; Wadleigh, 2003; Wadleigh *et al.*, 1999). For all Sr isotope research, it is important to understand that the $^{87}Sr/^{86}Sr$ ratio depends on what the parent-daughter rubidium (Rb) to strontium ratio (specifically, $^{87}Rb/^{86}Sr$) in the source is, and how long ago in time it fractionated. Although isotope fractionation in seeds (*e.g.* coffee beans) is yet poorly understood, previous work suggests that the coffee bean may be a valuable indicator of ecological processes and geology (Rodrigues *et al.*, 2011). Nonetheless, a solid interpretation of isotope abundance in the green coffee bean is complicated by the combination of environmental, climatic, and physiological processes. The results obtained so far suggest that there is not a unique interpretation for the distribution of isotopic composition of green coffee beans at global scale. Seasonal

variations in humidity, temperature and precipitation as well as geology, and experimental or human impacts influence the isotopic signatures (ratios) of elements in coffee. These effects make data interpretation more challenging but may enable the discrimination of easily delineated small regions. For this reason, a scale-down was done in this study to coffees produced in the state of Hawai‘i, whose gourmet quality is known worldwide.

In this chapter, isotopic composition of C, N, O, S and Sr and multi-element concentrations were measured in green coffees originating from 5 Hawai‘i coffee producing regions. In order to interpret isotope variations in the Hawaiian green coffee beans, relationships of the results obtained with available information on altitude, volcanic activity, and annual mean ^{18}O values of precipitation were determined. The results demonstrate that, by combining isotope and multi-element analysis, it is possible to discriminate Hawai'i coffee producing regions.

4.2. Experimental

4.2.1. Samples and climate

Arabica green coffee beans (47 samples) from 5 different Hawai'i coffee producing regions were provided by Coffea Consulting and the University of Hawai‘i (Hawai‘i, US). The Hawai'i state regions included in this study were Hawai'i, Kaua'i, Maui, Moloka'i and O'ahu (figure 28). Hawai'i was the only region where it was possible to collect samples from two different harvest years, 2007 and 2008. All other green coffee bean samples included in this study dated from 2007. The samples from Hawai'i were obtained from 3 districts: Ka'u, Puna, and Kona (figure 28), where farms are characterized for being just a few acres. The harvest period in Hawai'i region starts in June/August (depending on altitude) and will extend until February/March, being the middle point September/October. Each sample from Ka'u district was collected at a different farm. The 13 coffee samples from Kona district were obtained from 8 farms. In 5 of these 8 farms, it was possible to obtain one sample from 2007 and one from 2008. The 2 samples from Puna were obtained from 2 different farms, during the harvest period of 2007. Samples from 'Ele'ele at Kaua'i (figure 28) originated from one single estate farm considered the largest in Hawai'i State, with more than 12 000 m^2 of coffee in production. One sample was obtained also at this region but from another farm at Kapahi. In Kaua'i, the coffee harvest period is shorter comparing to the other regions, beginning in late August and ending in late November. In the case of Maui, Moloka'i and O'ahu, coffee is harvested from July/August until February. Samples from Maui were obtained from a farm located in Ka'anapali, and from another farm in Kula (figure 28). The two samples from Moloka'i region were produced from the same farm. In O'ahu region, samples were collected in a farm at Waialua, and at Waiahole and Kunia (figure 28).

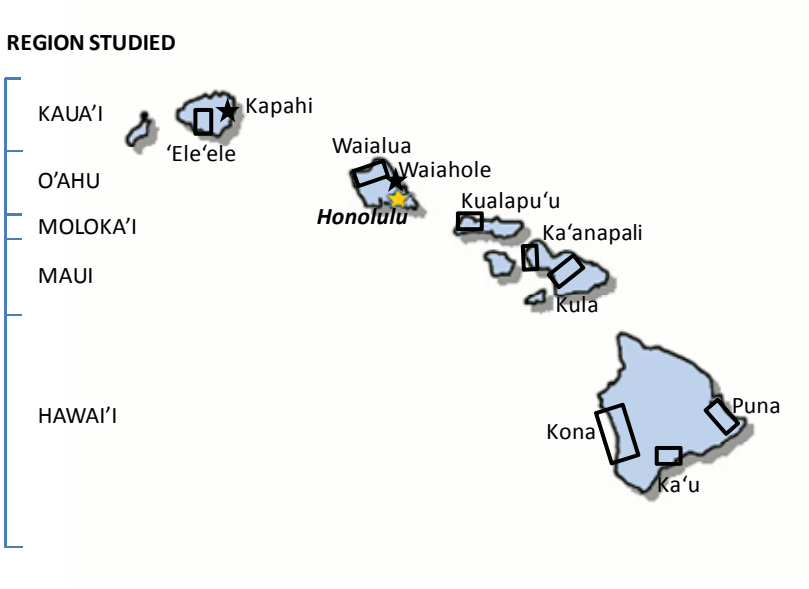

Figure 28. Different Hawai'i regions and correspondent districts/sites from where green coffee bean samples were obtained.

Each green coffee bean sample consisted in 100g of green coffee beans. The samples were packed under vacuum and transferred to the laboratory for further analysis. Whenever possible, latitude and longitude data were obtained with Google Earth software, Version 5.0 (Google, UK), and annual mean $\delta^{18}O_{prec}$ was acquired from the Online Isotopes in Precipitation Calculator (OIPC 2.2) (Bowen, 2010). Information on temperature was acquired from the Hawaii Natural Resource Information System (HNRIS) (Meng & Liang, 2007).

4.2.2. Isotope ratio mass spectrometry (IRMS)

4.2.2.1. Sample preparation

Each green coffee bean sample (100g) was ground in a mill (Type MM2, Retsch, Germany), 3 times for 5 minutes each time, to obtain particle sizes of less than 1 mm, in order to get an homogeneous sample. After grinding, samples were dried overnight at 45 ºC, weighed in tin capsules that were then folded close. Moreover, from one of the samples (chosen randomly), 30 green coffee beans were separated and grinded individually. The goal was to analyze the 30 green coffee beans separately for C, N, S, and O isotopic composition to have an indication of the standard deviation of the isotopic composition of each element within each coffee.

4.2.2.2. Combustion (EA-C) mode

Carbon stable isotope ratio was determined on a SIRA II (VG ISOGAS, UK) stable isotope ratio mass spectrometer coupled to an elemental analyser (EuroVector, Italy) for sample preparation by combustion-reduction. Nitrogen and sulfur stable isotope ratios were determined on an Isoprime (Micromass, UK) isotope ratio mass spectrometer coupled to an elemental analyser (EuroVector, Italy). Coupling of the elemental analysers and isotope ratio mass spectrometers was via open-split. Sulfur isotope ratios were determined by Dumas combustion/reduction at 1025 ºC on a quartz reactor with tungsten oxide on alumina as oxidation catalyst and pure reduced copper wires as reduction agent for removal of excess oxygen. Water resulting from combustion was removed with a magnesium perchlorate trap, and gas separation was achieved on a gas chromatography column for S (EuroVector, Italy), maintained at 95ºC. Isotope ratios were calibrated against international standards, namely IAEA CH6 (sucrose) and IAEA CH7 (polyethylene) for carbon isotope ratio, IAEA N1 (ammonium sulphate) for nitrogen isotope ratio, and IAEA S1 (silver sulfide) and NBS 127 (barium sulfate) for sulfur isotope ratio. Analytical performance, stability and drift, was checked by inserting laboratory standards between samples, *i.e.* sorghum flour standard OAS (B2158, Elemental Microanalysis) for carbon and nitrogen, and grinded green coffee bean for sulphur. Correction was made when necessary. Precision (standard deviation of the set of standards analysed in each batch, n=6) was 0.06 ‰ for carbon, 0.08 ‰ for nitrogen, and 0.3 ‰ for sulphur isotope ratio determinations. Carbon, nitrogen, and sulfur isotopic composition of 30 individual coffee beans from a single site were determined in order to estimate the possible variation of $\delta^{13}C$, $\delta^{15}N$, and $\delta^{34}S$ within each coffee sample. The standard deviations obtained for $\delta^{13}C$, $\delta^{15}N$, and $\delta^{34}S$ of the 30 individual beans were of 1.4, 0.8, and 0.5 ‰, respectively.

4.2.2.3. Pyrolysis (EA-P) mode

Oxygen isotope ratios were determined on an Isoprime (Micromass, UK) isotope ratio mass spectrometer coupled to an elemental analyser (EuroVector, Italy) by high temperature pyrolysis. Pyrolysis was accomplished at 1300ºC on a glassy carbon reactor with glassy carbon chips and nickel-plated carbon as catalysts, mounted co-axially on a ceramic tube. Coupling of the elemental analyser and isotope ratio mass spectrometer was performed via open-split. The isotope ratio data was corrected against international standards (IAEA 601 and IAEA 602). Analytical performance, stability and drift, was checked by inserting laboratory standards between samples. Correction was made when necessary. Precision was 0.14‰. Oxygen isotopic composition of 30 individual coffee beans yielded a standard deviation for $\delta^{18}O$ of 0.4‰.

4.2.3. Strontium isotope ratio measurement by multicollector inductively coupled plasma sector field mass spectrometry (MC-ICP-SFMS)

4.2.3.1. Reagents

Pro analysis (p.a.) grade 65% HNO_3 (Merck, Darmstadt, Germany) was subboiled doubly in an ultrapure quartz apparatus (MLS DuoPur, MLS, Leutkirch im Allgäu, Germany). Deionised water (18 MΩ cm; SG, Wasseraufbereitung und Regenierstation GmbH, Barsbuttel, Germany) was subboiled prior to usage as well. Subboiled HNO_3 and 31% H_2O_2 (p.a. grade, Merck, Darmstadt, Germany) were used for microwave assisted digestion. Polyethylene flasks and cartridges as well as polypropylene tubes and lids were cleaned sequentially with HNO_3 (10 % (v/v)) and HNO_3 (1 % (v/v)) and rinsed with deionised water before use. Dilution of standards and samples was performed gravimetrically with HNO_3 (1 % (v/v)), prepared from subboiled water and doubly subboiled HNO_3. A 20 ng g^{-1} solution of SRM 987 $SrCO_3$ (NIST, Gaithersburg, MD, USA) was used for quality control of the Sr isotope ratio measurements. The certified $^{87}Sr/^{86}Sr$ ratio is 0.71034 ± 0.00026 whereas a generally 'accepted value' of the $^{87}Sr/^{86}Sr$ ratio for this reference material is reported in the literature as 0.710263 ± 0.000016 (the error represents a range of two standard deviations determined from the external reproducibility) (Shultheiss, 1993).

4.2.3.2. Sample preparation

Four to six beans (amounting to about 1.0 g) were ground in a Retsch mill Type MM2, 3 times for 5 minutes each time to obtain particle sizes of less than 1 mm. Approximately 0.5g of the ground material was directly weighed into Teflon bombs for subsequent microwave-assisted digestion (MLS 1200mega, MLS, Leutkirch im Allgäu, Germany). Concentrated double-subboiled HNO_3 (6 mL) and H_2O_2 (1 mL) were used as digestion reagents. Details are presented elsewhere [29]. The samples were finally transferred into 50-mL flasks, filled with HNO_3 (1% v/v to 20g, filtered using a 5 mL syringe through 0.45 µm filters (Minisart RC 25) and stored at room temperature for future analysis. A digestion blank was prepared with each digestion batch.

4.2.3.3. Strontium/matrix separation

The obtained digestion solutions of green coffee bean samples were separated according to Swoboda et al. (2008), using Eichrom Sr resin (Eichrom Industries, Darien, IL, USA). The solutions were diluted after separation to a final Sr concentration of about 20 ng g^{-1} to obtain optimum signal intensities of ^{88}Sr from 3 to 5 Volts. Fractionation effect of the column extraction procedure on the Sr isotopic ratio was checked according to (Swoboda *et al.*, 2008) and proved to be insignificant.

4.2.3.4. Instrumentation

Screening of the solutions for Rb and Sr prior and after separation was performed by using a quadrupole based inductively coupled plasma mass spectrometer ICP-MS (Elan DRCe, Perkin Elmer, Waltham, MA, USA). Sr isotope ratio measurements of the final solutions were accomplished using a double-focusing multicollector inductively coupled plasma mass spectrometer (MC-ICP-MS) (Nu Plasma HR, Nu Instruments Ltd., Wrexham, UK) coupled to a membrane desolvating system (DSN 100, Nu Instruments Ltd. Wrexham, UK). The DSN 100 instrument was equipped with a PFA nebuliser (MicroFlow nebuliser, Elemental Scientific, Omaha, NE, USA) and a spray chamber with additional hot gas flow to eliminate condensation and droplet formation. The multicollector inductively coupled plasma mass spectrometer is equipped with a collector configuration consisting of 12 Faraday cups and three ion counters. The latter ones were not used throughout this study. All isotopes in this work (^{82}Kr, ^{83}Kr, ^{84}Sr, ^{85}Rb, ^{86}Sr, ^{87}Sr, ^{88}Sr) were measured simultaneously using Faraday cups. Experimental parameters of the MC-ICP-MS including nebuliser gas, rf power, and ion transfer lens potentials were optimised to achieve the maximum ion intensity for ^{88}Sr, using NIST SRM 987 solution with a concentration of 20 ng g^{-1}. The operation parameters are given in table 11 (section 3.2.3.). Blank correction and mass bias correction were performed according to previous measurements (Swoboda *et al.*, 2008).

4.2.3.5. Multi element analysis by ICP-MS

All digestion solutions obtained for Sr isotope analysis were screened for different elements and their total concentration was calculated through external calibration performed with a multi-element standard solution VI (MERCK KGaA, Damrstadt, Germany). For internal normalization, an Indium standard was added to a final content of 10 ng g^{-1}. HNO_3 (1 % (v/v)) was used for blank correction. The

determination of the element concentrations was accomplished with a quadrupole mass spectrometer ELAN DRC-e (PerkinElmer, Ontario, Canada), and in the case of rare earth elements (REE), with a high resolution sector field mass spectrometer ELEMENT 2 (Thermo Scientific, Bremen, Germany) under the operational conditions described in table 13. The concentration of the elements B, Na, Mg, Al, Cr, Mn, Fe, Co, Ni, Cu, Zn, Ga, Rb, Sr, Mo, Ba, Pb, Bi, Y, La, Ce, Pr, Sm, Nd, Eu, Dy, Th, Sc, Ho and Gd was determined in all green coffee bean samples. The uncertainty of the multi element measurements was calculated using GUM Workbench Pro (version 1.2, Metrodata GmbH, Germany). The Guide to the Expression of Uncertainty in Measurement (GUM) was published by ISO and establishes the general rules for evaluating and expressing uncertainty (Barwick *et al.*, 2001).

Table 13. Operating parameters for multi-element measurements.

Instrument settings	**ELAN DRCe**	**ELEMENT 2**
RF Power	1350 W	1300 W
Cool gas flow rate	13 L min^{-1}	16 L min^{-1}
Auxiliary gas flow rate	0.75 L min^{-1}	0.85 L min^{-1}
Nebulizer gas flow rate	0.98 – 1.02 L min^{-1}	1.1 – 1.2 L min^{-1}
Lens settings	optimised for optimal sensitivity and peak shape	
Sample cone	Nickel	Aluminium
Skimmer cone	Nickel	Aluminium
Typical sensitivity on In	750,000 cps per 10 ng g^{-1}	1,000,000 cps per 1 ng g^{-1}
Detection system	Secondary electron multiplier	
Measurement statistics	10 sweeps, 1 reading, 5 replicates	3 runs, 3 passes
Resolution mode	-	LR ($m/\Delta m$ = 300); MR ($m/\Delta m$ = 4,000); HR ($m/\Delta m$ = 10,000)
Mass window	-	LR: 20%, MR: 120%, HR: 150 %
Sample time	-	LR: 0.01, MR: 0.02, HR: 0.02
Samples per peak	-	LR: 100, MR: 20, HR: 20
Sample introduction system	Cyclonic spray chamber with Micromist glass nebulizer	Cooled PC^3 spray chamber (+2°C) with PFA nebulizer
Sample uptake rate	500 µl min^{-1}	100 µl min^{-1}
Pump velocity	20 rpm	Self aspirating mode

4.2.4. Statistical analysis

Canonical analysis (CA) was performed in SPSS, version 15.0, and ANOVA analysis was performed using Statistica software (version 9.0) (Statsoft, US).

4.3. Results

4.3.1. Coffee bean isotopic composition

The stable isotopic composition of the green coffee bean samples varied by approximately 20 ‰ for sulphur, and 8.5, 7, and 5 ‰ for, C, O and N, respectively. In the case of $^{87}Sr/^{86}Sr$ there was a variation of approximately 0.005. The mean values of $\delta^{18}O$, $\delta^{34}S$, $\delta^{13}C$, $\delta^{15}N$, and $^{87}Sr/^{86}Sr$ of the green coffee beans per region are shown in table 14. Analysis of variance of the results obtained revealed significant differences between the different Hawai'i coffee producing regions (ANOVA; $p < 0.05$). It is also important to refer that the determination of the isotopic composition of O, S, C, and N of 30 individual coffee beans of one sample (data not shown) resulted in standard deviations of 0.4, 0.5, 1.4, and 0.8 ‰, respectively. These values were assumed to indicate variations in the isotopic composition of the respective elements within each sample from each region and were taken in consideration when assuming differences among the coffee producing regions. In the case of oxygen isotopic composition, green coffees varied from 25.9 ‰ (Hawai'i) to 32.5 ‰ (O'ahu; table 14). Higher values of mean $\delta^{18}O$ were obtained for coffees produced at lower altitude. All coffees with $\delta^{18}O$ higher than 29 ‰ were produced at less than 300 m of altitude (figure 29a). Coffees from 'Ele'ele and Kapahi (Kaua'i), from Kunia, Waialua, and Waiahole (O'ahu), from Kualapu'u (Moloka'i), and from Ka'anapali (Maui), produced under 250 m of altitude, had a mean $\delta^{18}O$ value from 29 to 32.5 ‰ (table 14). In comparison to these sites, coffees from Hawai'i region, and Kula in Maui, had lower mean $\delta^{18}O$ values, ranging from 25.9 to 28.9 ‰ (table 14). The mean normalized $\delta^{18}O$ values per region, and respective standard deviations, are shown in figure 30a. The mean $\delta^{18}O \pm$ standard deviation (SD) obtained in each region allows the separation of two groups: Hawai'i and the other regions. For each coffee, known values of latitude and longitude, and of altitude allowed the calculation of the correspondent values of $\delta^{18}O$ of local precipitation with the OIPC (The Online Isotopes in Precipitation Calculator) (Bowen, 2010). A positive correlation was obtained between the $\delta^{18}O$ of coffee beans and of precipitation ($r = 0.56$; $p < 0.05$). In what respects to the sulfur isotopic composition of the green coffee bean samples ranged from -1.5 to 21.3 ‰ (table 14). In spite of this wide range of variation, sulfur isotopic composition allowed the separation of the Hawai'i Island in relation to the other islands (figure 30b). Coffees from Hawai'i region had $\delta^{34}S$ values from -1.5 to 7.7 ‰, with the exception of a sample from Kona (11.9 ‰), and one from Puna (12.7 ‰) (table 14).

Table 14. Origin, daily mean temperature, annual mean $\delta^{18}O$ of precipitation, and isotopic composition of C, N, O, S and Sr of Hawaiian green coffees (whenever $n \geq 3$, average and standard deviation are shown).

Island	Specific Location	Altitude[1] (m)	Temperature[2] (daily mean; °C)	Annual mean $\delta^{18}O$ of precipitation[3] (‰)	$\delta^{18}O$ (‰)	$\delta^{34}S$ (‰)	$^{87}Sr/^{86}Sr$	$\delta^{13}C$ (‰)	$\delta^{15}N$ (‰)
Hawai'i	Kau	< 400	22.2	-3.0	27.8	0.4	0.7051	-27.4	2.3
		400 to 500 (n=3)	21.9	-3.2	27.9 (0.2)	3.3 (3.0)	0.705 (0.0002)	-24.4 (2.0)	0.8 (0.5)
		500 to 600	22.2	-3.4	28.3	3.5	0.7051	-24	4.4
					28.8	0.8	0.7051	-26.4	1.2
		700 to 750	17.9	-3.7	28.5	1.6	0.7052	-25.7	0.7
					28.9	-1.5	0.705	-25.2	1.2
	Kona	300 to 400	23.4	-2.7	25.9	3.5	0.7062	-26.9	1.3
					27.1	6.4	0.7070	-25	1.5
		400 to 600 (n =5)	22.6 (1.4)	-3.3 (0.1)	28.1 (0.7)	7.7 (2.7)	0.7057 (0.0008)	-25.4 (0.9)	1.9 (0.7)
		700 to 800 (n=6)	21 (1.5)	-3.8 (0.1)	26.6 (1.2)	3.8 (1.4)	0.7067 (0.001)	-26.5 (2.5)	1.9 (0.3)
	Puna	30	22.6	-2.3	26.4	5.7	0.7084	-27.6	3.3
		400	20.6	-3.1	26.8	12.7	0.7073	-24.3	1.3
Kaua'i	'Ele'ele	< 150 (n=8)	-[4]	-2.7 (0.04)	31.5 (0.6)	18 (1.8)	0.7057 (0.0006)	-27.1 (1.1)	1.9 (0.3)
	Kapahi	50	23.2	-2.6	30.2	10.5	0.7067	-26.2	2
Maui	Kã'anapali	100 to 150 (n=6)	22.5 (0.3)	-2.7 (0.1)	30.4 (1.1)	16.8 (3.8)	0.7071 (0.0002)	-27.6 (0.6)	1.3 (0.1)
	Kula	1000	17.2	-4.3	28.3	11.1	0.7063	-30.6	0.9
Moloka'i	Kualapu'u	250	22.6	-2.9	29	9.8	0.7086	-28.7	5.4
					31.1	9.7	0.7082	-29.3	2.1
O'ahu	Waialua	< 250 (n=4)	22.7 (0.3)	-2.8 (0.1)	30.6 (2.2)	10.4 (2.7)	0.7087 (0.0002)	-27.2 (1.8)	1.9 (0.7)
	Waiahole	50	23.6	-2.6	29.2	15.2	0.7091	-25.2	3.8
	Kuna	80	-[4]	-2.6	32.5	14.4	0.7056	-27.5	1.2

[1]Latitude and longitude values are not shown to maintain grower or farm anonymous; [2]From HNRIS (Meng et al., 2007); [3]From OIPC (Bowen, 2010a); [4] data is unavailable for the selected location.

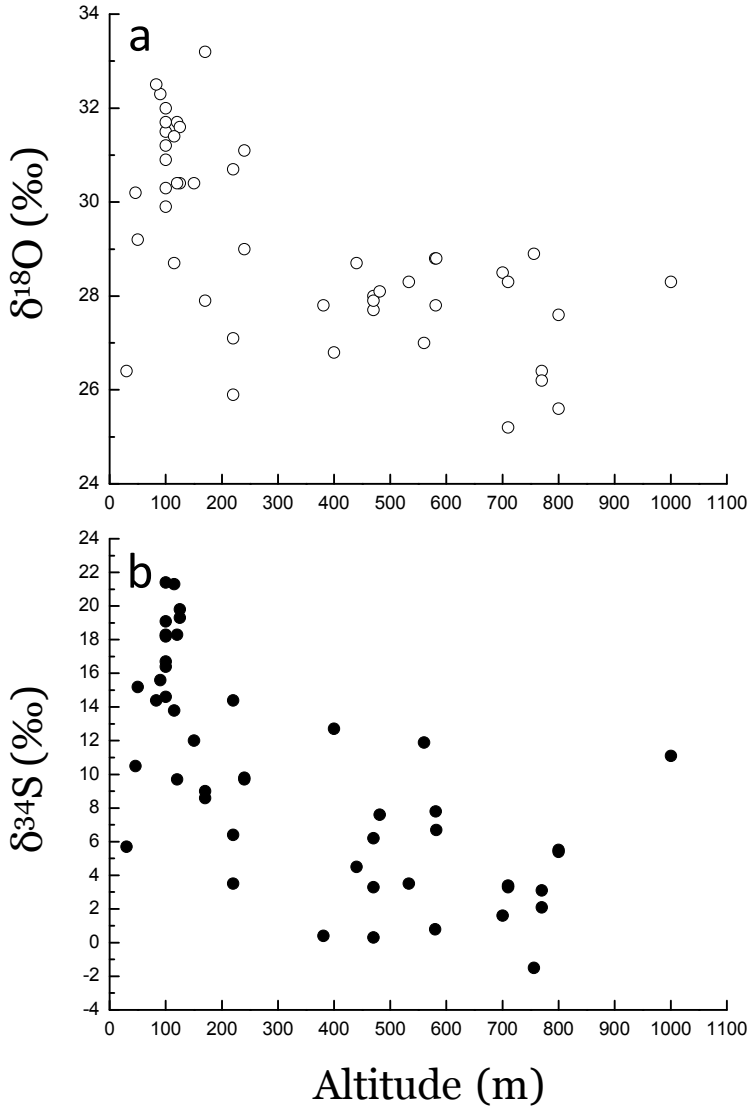

Figure 29. $\delta^{18}O$ (a) and $\delta^{34}S$ (b) of the green coffee beans in relation to altitude.

The $\delta^{34}S$ values of Hawai'i coffees were lower than those from Kaua'i, especially in the case of 'Ele'ele that showed a $\delta^{34}S$ average of 18 ± 1.8 ‰ (table 14). Also in Kaua'i in Kapahi, the observed $\delta^{34}S$ value was 10.5 ‰. Coffees from Maui showed $\delta^{34}S$ values of 11.1 ‰ (Kula) and a mean $\delta^{34}S$ of 16.8 ± 3.8 ‰ in Ka'anapali (table 14). In the case of Moloka'i, the observed $\delta^{34}S$ of the two coffee bean samples was 9.8 and 9.7 ‰ (table 14). In O'ahu, $\delta^{34}S$ varied from an average of 10.4 ± 2.7 ‰ (Waialua) to values of 14.4 and 15.2 ‰ at Kuna and Waiahole, respectively (table 14). Figure 29b shows the variation of $\delta^{34}S$ values in the different coffee bean samples in relation to altitude. The higher $\delta^{34}S$ values (>15 ‰) were observed at altitudes under 200 m, where coffee is produced closer to the ocean.

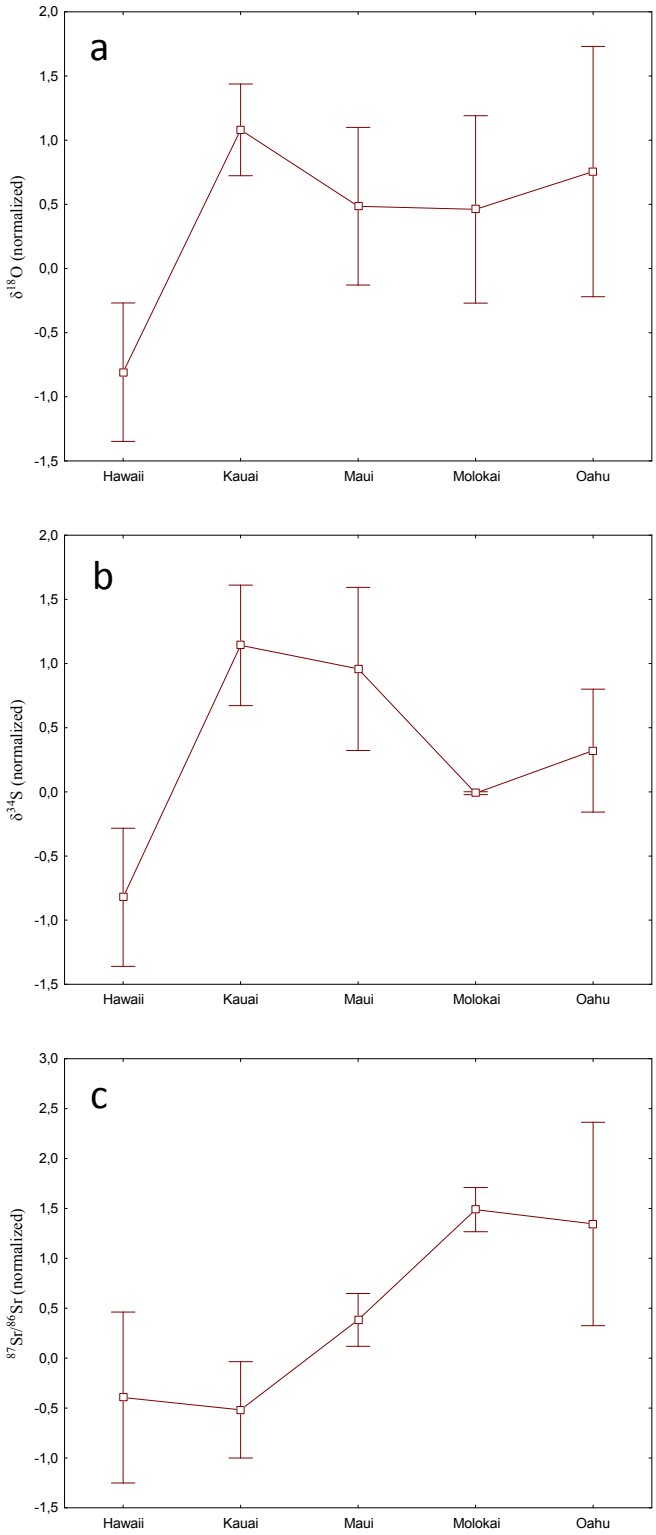

Figure 30. Normalized $\delta^{18}O$ (a), $\delta^{34}S$ (b) and $^{87}Sr/^{86}Sr$ (c) mean ± SD values of green coffee bean samples from Hawai'i, Kaua'i, Maui and O'ahu (Moloka'i not included as n = 2). Legend: ⊥ Mean ± SD; Mean.

As for Sr, the $^{87}Sr/^{86}Sr$ values for the green coffee beans of the different coffee-producing regions are shown in figure 31. The highest values were observed in coffees from Kualapu'u at Molokai, Waialua and Waiahole at O'ahu, with the exception of one coffee from Puna and from Kona produced at lower altitude or closer to the ocean (figure 31). Coffees from Ka'u district, grown under a greater influence of the Kilauea volcano, showed lower mean values of $^{87}Sr/^{86}Sr$ ranging from 0.705 to 0.7052 (table 14). These values are closer to the reported values for Hawaiian lava (figure 31). In the case of the coffees from Kualapu'u (Moloka'i), Waiahole and Waialua (O'ahu) the $^{87}Sr/^{86}S$ values are approximate to the value reported for the Sr isotopic composition of sea salt aerosol (figure 31).

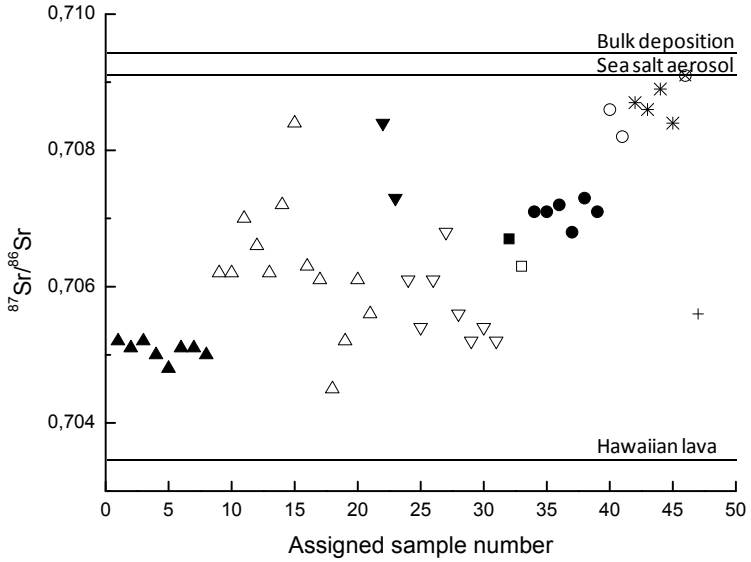

Figure 31. Sr isotope ratio of green coffees from Hawai'i. Legend: (▲) Ka'u (Hawai'i), (△) Kona (Hawai'i), (▼) Puna (Hawai'i), (▽) 'Ele'ele (Kaua'i), (■) Kapahi (Kaua'i), , (□) Kula (Maui), (●) Ka'anapali (Maui), (○) Kualapu'u (Moloka'i), (✱) Waialua (O'ahu), (⊗) Waiahole (O'ahu), (+) Kunia (O'ahu),. Bulk deposition: 0.7095 (Kennedy *et al*., 1998), sea salt aerosol: 0.70917 (Capo *et al*., 1998), Hawaiian lava: 0.7035 (Whipkey *et al*., 2000).

The mean $^{87}Sr/^{86}Sr$ and standard deviation values observed for each region is shown in figure 30c differentiating O'ahu from Kaua'i and also from Hawai'i regions. In what refers to C, $\delta^{13}C$ values of green coffee beans are shown in table 14. For the overall coffees analyzed, the minimum and maximum $\delta^{13}C$ values were -22.1 ‰ (Kona, Hawai'i) and -30.6 ‰ (Kula, Maui), representing a total variation of 8.5 ‰. The ranges of $\delta^{13}C$ values observed for each region are overlapping although the maximum and minimum values are different. The less negative (enriched) $\delta^{13}C$ values were observed in coffees from Hawai'i region. The more negative (depleted) values were determined in coffees from Maui, Moloka'i and O'ahu (table 14). ANOVA did not reveal

significant differences between the different regions in what respects to coffee bean $\delta^{13}C$ values. As in the case of $\delta^{13}C$, there were no significant differences among $\delta^{15}N$ of the green coffee bean samples (ANOVA). The $\delta^{15}N$ values of coffee beans are shown in table 14. Values of $\delta^{15}N$ varied from 0.7 to 5.4 ‰ (a variation of 4.7 ‰) with lower values measured in Hawai‘i and Maui (table 14).

4.3.2. Multi-element composition and canonical analysis

The green coffee beans from Hawai‘i regions were analyzed for 30 different elements. The results are shown in table 15. Significant differences (ANOVA; $p<0.05$) were observed in the concentration of the elements Na, Mg, Al, Mn, Ga, Rb, Ba, Pb, Y, La, Ce, Pr, Sm, Nd, Eu, Dy and Gd between the different coffee producing regions. Coffees from Moloka‘i showed the most differentiated multi-element fingerprint. The concentrations of Al, Fe, Cu, Rb, Sr and Ce differentiate Moloka’i from other regions (ANOVA). Similarly, for Kaui region, Ba, Na and Ga concentrations were significant for the differentiation from the other regions. O’ahu coffees were different in what respects to the Ni concentration and Hawai’i showed similar results but for Nd, La, Y, Co and Mn (table 15). Nonetheless, high standard deviations in the different element concentrations per region were observed. A combination of the isotope ratio analysis with data from multi element analysis through canonical analysis allowed the discrimination of the coffee-producing regions. The result of the CDA is shown in figure 32. Three canonical components with coefficients higher than 0.9 were obtained ($p < 0.05$). The analysis showed that the values of $\delta^{34}S$ as well as the concentrations of the elements B, Al, Fe, Ni, Cu, Rb, Sr, Mo and Ba were the variables contributing to the coffee producing regions discrimination.

4.4. Discussion

The results obtained from isotope ratio analysis of the Hawaiian green coffee bean samples indicate that the isotopic composition of the elements studied varies according to several environmental factors, such as the altitude at which the coffee is produced, the isotopic composition of local precipitation, and influences from the ocean, anthropogenic emissions, and volcanic activity. The isotope fractionation processes occurring during the coffee plant fruit and seed development are still poorly understood. However, the isotopic composition of O, S, C, N and Sr of green coffee beans is expected to be a result of the fractionations associated with several metabolic pathways of the plant and of the specific organ that is the fruit (coffee cherry), occurring during the seed development period (8 months on average in the case of *Arabica* coffee).

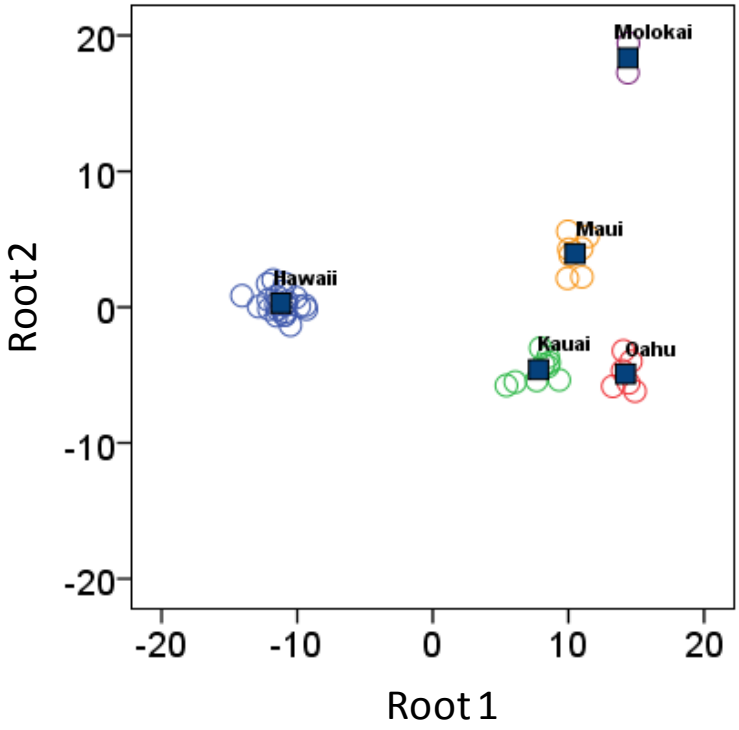

Figure 32. Canonical analysis of isotopic and multi-element composition of the 47 green coffee bean samples (squares indicate group centroids).

Plants can actively control different metabolic and diffusion processes dependent on environmental conditions, *e.g.* temperature, radiation, and water availability, and in conjunction with variation in the isotope ratios of elemental sources available to the plant these regulated processes should govern the isotopic composition of organic compounds in the coffee bean. Several authors have shown that the $\delta^{18}O$ of water in plants changes as a result of variations in $\delta^{18}O$ of water taken up by the plants and leaf water enrichment of ^{18}O during transpiration, the latter of which is dependent on atmospheric conditions (relative humidity and $\delta^{18}O$ of water vapor in the atmosphere) and stomatal regulation of water loss, and the variation in $\delta^{18}O$ of water in cells forming organic material (Barbour *et al.*, 2005a and b; Roden *et al.*, 2000; Scheidegger *et al.*, 2000). It is important to refer that due to uneven ripening a coffee tree will have fruits with different degrees of ripeness. It is quite common to see immature, mature and overripe fruits simultaneously on the same branch. Hence, environmental conditions (*e.g.* temperature, humidity, water availability, radiation) will influence the metabolism of such fruits at distinct developmental stages. The beans analyzed in this study derive from the same origin, and in some cases from the same plantation, but most probably from different coffee plants.

Table 15. Mean ± SD (w/w) for the 30 elements determined in Hawaiian green coffees[1].

Growing island		Mean, ng.g^{-1}																			
		B	Na	Mg	Al	Cr	Mn	Fe	Co	Ni	Cu	Zn	Ga	Rb	Sr	Mo	Ba	Pb	Bi	Y	La
Hawaii	Mean	7009	25276	1904396	1617	10315	26319	83391	106	1241	15099	8412	56	10684	4263	127	1191	33	26	< LOD	2
(n=23)	SD	2332	15604	789083	812	29135	11678	39743	61	891	6465	5510	71	5719	2089	204	1428	66	12	1	7
Kauai	Mean	8765	129435	2174746	1156	5236	36259	84690	328	1405	15613	6212	406	6818	6642	99	9355	6	30	19	53
(n=9)	SD	2598	62448	880194	595	10294	16817	35199	122	906	2480	1051	221	1342	1512	72	5072	16	19	17	32
Maui	Mean	10008	47223	1641182	4187	2691	47085	95118	252	1027	15375	5875	166	10991	7897	115	3571	10	22	93	68
(n=7)	SD	3651	46272	1161311	2121	2488	14509	34817	153	388	3322	1324	54	4083	1519	21	904	13	1	48	34
Molokai	Mean	14618	< LOD	< LOD	16045	1204	79030	154536	201	1298	21348	7970	87	22844	10438	156	2376	14	21	83	72
(n=2)	SD	968	< LOD	< LOD	10302	6	8189	3559	46	83	988	771	30	1729	314	1	843	7	< LOD	46	43
Oahu	Mean	13276	< LOD	< LOD	3832	1795	83955	116319	228	2749	13541	9019	159	13446	6328	72	4203	5	23	60	95
(n=6)	SD	3608	< LOD	< LOD	925	1148	64835	13783	136	1531	1859	4929	106	5371	1867	68	2712	4	5	66	94

Table 15 (continuation).

Growing island		Mean, ng.g^{-1}									
		Ce	Pr	Sm	Nd	Eu	Dy	Th	Sc	Ho	Gd
Hawaii	Mean	7	< LOD	< LOD	< LOD	40	< LOD	7009	3	4	25276
(n=23)	SD	16	< LOD	< LOD	1	62	< LOD	2332	7	15	15604
Kauai	Mean	11	< LOD	< LOD	21	371	< LOD	8765	2	< LOD	129435
(n=9)	SD	10	< LOD	< LOD	18	207	< LOD	2598	4	< LOD	62448
Maui	Mean	26	< LOD	4	53	155	1	10008	7	< LOD	47223
(n=7)	SD	14	1	4	26	52	2	3651	4	1	46272
Molokai	Mean	180	5	6	75	74	1	14618	8	< LOD	< LOD
(n=2)	SD	103	7	9	47	27	2	968	2	< LOD	< LOD
Oahu	Mean	21	2	3	44	180	1	< LOD	3	< LOD	10
(n=6)	SD	18	4	6	46	150	2	< LOD	6	< LOD	11

This may affect the isotope values measured in the green coffee samples. However, our results indicate that the $\delta^{18}O$ of the green coffee beans reflects the $\delta^{18}O$ of local precipitation with variations possibly associated with each region characteristic climate and plant ecophysiology. Two groups were distinguished based on $\delta^{18}O$ of coffee beans: Hawai'i and the other regions (figure 29a). Coffees from Hawai'i region are produced at higher altitudes in relation to the other regions, which, in turn, can be associated with more negative values of $\delta^{18}O$ of precipitation (table 14). In this island, high values of green coffee bean $\delta^{18}O$ were only observed at low elevations, where high $\delta^{18}O$ water is expected. However, some of the lightest coffees come from low elevations (Kona region; table 14). Precipitation patterns on islands with appreciable topography can be complex. The climate in Hawai'i island is dominated by trade winds from the east-northeast that flow down slope past the summit of Kilauea (1225 m elevation) causing a rain shadow on its southwest flank. This area receives rainfall from storm systems unrelated to trade winds which can be accentuated by frontal systems and 'Kona storms' (Scholl *et al.*, 1996). A more depleted isotopic content of rainfall in the rain shadow of Kilauea volcano is observed and is likely due to the fact that the area receives only storm rainfall. Scholl and co-authors report a value of $\delta^{18}O$ of precipitation for a tropical storm in Puna, Hawai'i Island, of -5 ‰, different from the long-term volume-weighted average for that area which is -3.2 ‰. This difference in the $\delta^{18}O$ of storm precipitation may explain the lower values of $\delta^{18}O$ of the green coffee beans from Kona and Puna districts, in spite of the lower altitudes. The differences in $\delta^{18}O$ of precipitation in relation to trade wind and rain shadow sites and also resulting from storms occurrence are difficult to predict using the OIPC (table 14). This is because the existence of a rain shadow makes the prediction of precipitation $\delta^{18}O$ of more difficult. In the case of S, the $\delta^{34}S$ of green coffee beans was higher at lower elevations and, in most cases, in regions other than Hawai'i. The $\delta^{34}S$ values seem related with altitude (related with the distance to the sea) (figure 29b) but the interpretation for this observation is different from what has been discussed in relation to the $\delta^{18}O$ of coffee beans. For most plants, the normal source of sulfur is the sulfate taken up by the soil fine roots. The largest part (90 %) of the 'organic-S' in plants is concentrated (via proteins) in the two amino acids cysteine and methionine which are also the sulfur sources for the most other S-containing molecules. The plant's assimilatory sulfate reduction that provides 'organic sulfur' from sulfate, proceeds without important sulfur isotope fractionations (Tanz *et al.*, 2010). In general, bulk plant sulfur is depleted by only 1-2 ‰ relative to its primary sources, soil and sea spray sulfate or SO_2 from the atmosphere (Trust *et al.*, 1992), due to the partitioning of individual biosynthesis steps to different plant compartments, where they can proceed without branching and with quantitative turnover (Tanz *et al.*, 2010). Further S transfers from cysteine to secondary products may introduce S-isotope fractionations and thus provide ^{34}S-differences between the amino acid and secondary products (Tanz *et al.*, 2010). Although the details of sulfur isotope biochemistry in coffee plant seeds are unknown, it is not unreasonable to hypothesize that green coffee beans record the

isotopic signature of the sulfur source(s). One possibility could be the use of fertilizers, which also influence $\delta^{34}S$ of sulfates in soil and plants. The sulfur isotope composition of commercial fertilizers available in Hawai'i reported in the literature is 0.8 ‰ (ammonium sulfate) and 10.4 ‰ (monoammonum polyphosphate) (Mizota & Sasaki, 1996). Several coffees included in this study were produced with organic fertilizers, while others were grown applying synthetic fertilizers. However, differences between organic and synthetically fertilized coffees in what respects to $\delta^{34}S$ of coffee beans have not been observed. The presence of active volcanoes in some of the regions included in this study is also expected to influence the $\delta^{34}S$ values of several coffee bean samples. According to literature, the $\delta^{34}S$ of sulfates from volcanic ash and basalt derived soils in Hawai'i islands range from 6.3 to 18.1 ‰, with higher values corresponding to shorter distances to the sea (Mizota *et al.*, 1996). Atmospheric deposition is an important sulphur source to the Hawaiian coast, but its contribution decreases with increasing distance to the sea (Hue *et al.*, 1990). This could explain the results obtained as there seems to be a relation between $\delta^{34}S$ values of coffee beans and altitude (therefore, increased distances to the sea) (figure 29b). A lower island area/shorter distance to the sea, and consequently, a higher marine influence, may be responsible for the differences observed in $\delta^{34}S$ values of coffee beans from different regions, *e.g.* higher values of $\delta^{34}S$ in coffees from Kaua'i, Maui, and O'ahu in comparison to Hawai'i, where a greater influence from volcanic activity is expected (table 14, figure 30b). Volcanoes Kilauea and Mauna Loa located at the Hawai'i Island are active with eruptions from 1974 to 2010 and in 1984, respectively. Previous studies report $\delta^{34}S$ values of 0.8 and 0.9 ‰ in the volcanic sulfur gases, predominantly SO_2, from the 1971 and 1974 fissures in Kilauea Crater (Sakai *et al.*, 1982). As coffee plantations from Ka'u, Kona and, Puna receive the influence from these volcanoes, lower values of $\delta^{34}S$ of coffee beans from these regions are expected in comparison to other regions. Coffees from Ka'u receive a greater influence from Kilauea emissions as the trade winds blow the volcanic smog from its main source on the volcano to the southwest, where Ka'u is located. It is possible that this volcanic activity is the main reason explaining the lower values of $\delta^{34}S$ in the coffee beans produced on Hawai'i region (table 14). Coffees from O'ahu and Moloka'i show intermediate values of $\delta^{34}S$ (table 14). O'ahu is the most populated region of Hawai'i with 96% of the energy produced from fossil fuels. In this case, the influence from anthropogenic sources of sulphur may be important in the interpretation of $\delta^{34}S$ of coffee beans. In the Moloka'i region, the reduced number of samples difficult the interpretation of data. In short, results indicate that the coffee bean records sulfur isotopic composition of the marine and volcanic sources of sulfate existent in Hawai'i regions. Monitoring atmospheric, volcanic ash, soil, and precipitation sulfate isotopes will be important in order to understand how sulfur isotopes of coffee beans reflect these important environmental impacts. Further research on S-isotopes fractionation processes during coffee seed development is also necessary to evaluate the differences in S-assimilation and isotope fractionation. Similarly, the differences observed in $^{87}Sr/^{86}Sr$ values of green coffee bean samples seem to be related with environmental factors, *e.g.* volcanic activity, sea aerosol and Sr bulk deposition (figure 31). It is known

that Sr isotope ratio in plant material is related to local geology, in particular with soil bioavailable Sr isotopic composition (Swoboda *et al.*, 2008). In the case of coffee beans, Sr isotope ratio analysis has previously proved to be an important tool when accessing coffee bean geographical origin (Rodrigues *et al.*, 2011) because it reflects the sources of strontium available during plant growth (Techer *et al.*, 2011). The Hawai'i islands are ideally suited for Sr isotopic studies because there are relatively few sources of Sr to the island ecosystems and these sources have distinct values that do not vary spatially or temporally (Vitousek *et al.*, 1999) and are relatively well defined (Chadwick, 2009). Atmospheric Sr is derived mainly from marine aerosol, and the atmospheric end member can be considered equivalent to sea water with a minimal contribution of dust from Central Asia ($^{87}Sr/^{86}Sr = 0.7093$) (Kennedy *et al.*, 1998; Vitousek *et al.*, 1999). The young basaltic substrate has accumulated minimal amounts of radiogenic ^{87}Sr since eruption, providing a weathering end-member of 0.7035 from all mineral phases (Vitousek *et al.*, 1999). The Hawaiian Islands are constructed of plume basalts with relatively minor compositional variation (compared to typical continental settings) (Chadwick, 2009), meaning that rock-derived Sr isotope ratios are relatively homogeneous within and among the islands. The sites correspondent to coffee beans with higher $^{87}Sr/^{86}Sr$ values (Kona, Puna, Kualapu'u, Waialua and O'ahu; figure 31) have in common the proximity of the ocean (less than 3 km). In contrast, the coffees from Ka'u region, under a closer influence from Kilauea volcano, showed lower values of $^{87}Sr/^{86}Sr$ (table 14, figure 31). Ka'u's coffees had $^{87}Sr/^{86}Sr$ values close to what is reported to Hawaiian lavas (Whipkey *et al.*, 2000) whereas coffees from O'ahu show $^{87}Sr/^{86}Sr$ values approximate what is referred for bulk deposition (dust) and sea salt aerosols (Capo *et al.*, 1998; Kennedy *et al.*, 1998; Whipkey *et al.*, 2000) (figure 31). However, the Sr isotopic composition of local meteoric water has not been determined in order to confirm if the Sr in the coffee plant derives from the atmosphere. Nonetheless, studies with other Hawaiian plant species indicate that Sr isotopic signature of plant leaves is a resultant of the contribution from the 3 main sources of Sr: Hawaiian lavas, mineral aerosol and seasalt aerosol (Chadwick, 2009; Whipkey *et al.*, 2000). Other authors reported that leaves from dominant canopy species in Hawaii islands have $^{87}Sr/^{86}Sr$ values that closely reflect the isotopic composition of ammonium acetate (NH_4Ac) extractable soil Sr (Kennedy *et al.*, 1998). Concomitantly, in a study reported by Vitousek *et al* (1999) variations in annual precipitation, distance from the ocean and lava flow texture were the best predictors of foliar Sr isotopes. The same authors refer that basalt weathering is still the dominant source of Sr in young ecosystems like in the southernmost part of Ka'u region. It is not possible to evaluate to what extension this is valid for coffee plants, specifically in the case of fruits and seeds, but the results of this work indicate that main sources of Sr in these seeds may be the Hawaiian lavas and the seasalt aerosols. Fertilizers that provide high Sr contents and high $^{87}Sr/^{86}Sr$ ratios (0.7093-0.7135) could also constitute the source of the ^{87}Sr enrichment in soils (Techer *et al.*, 2011). But, in the case of the Hawaiian coffee beans, the Sr isotopic composition is clearly lower than the range of values reported for fertilizers, suggesting that this should not be the main source of Sr. As for C and N, the results did not show significant differences among the coffee producing regions.

Although these elements seem not to contribute to the main objective of this work, which is to achieve coffee producing region discrimination, it is important to underline that carbon and nitrogen isotopes are important indicators of ecological change. Carbon fractionations can occur during plant metabolism, transport, and due to differences in chemical composition among plant parts (Badek *et al*, 2005; Brugnoli & Farquhar, 2000). Imposition of stresses and the timing of organ development (*e.g.* leaf emission and expansion, fruit formation, and source-sink relationships) may influence isotope composition of the different plant parts. In relation to nitrogen, the forms absorbed by plants can have different isotope combinations. In general, $\delta^{15}N$ of composted manures (> 8 ‰) are higher than those of synthetic fertilizer (-3 to 2 ‰). This $\delta^{15}N$ difference between N inputs may lead to a difference in N isotope signatures of plants and/or soils dependent upon fertilizer type. Because inorganic-N is directly available for plant uptake, the differences in $\delta^{15}N$ of the inorganic-N in soil treated with compost and fertilizer would provide some information on the variation of $\delta^{15}N$ of plants as affected by N application (Choi *et al.*, 2003). Although some of the coffee samples were produced with organic fertilizers, N isotopes did not distinguish between coffees grown with organic and conventional fertilization methods in our study. Probably due to the complexity of N isotope fractionation during N transformations and uptake by the coffee plants, it was very difficult to relate the $\delta^{15}N$ values found for the coffee beans with any differences in N fertilization methods. Further research on carbon and nitrogen isotopic composition variations during the coffee bean developmental period is necessary to understand how carbon and nitrogen isotopes are integrated in the coffee plant, fruit and seed tissues. As already demonstrated, multi-element and isotopic composition of O, S, Sr, C and N of the Hawaiian coffees does not lead to the discrimination of the Hawai'i coffee producing region when considered separately. Nonetheless, the relations between the isotopic composition of the coffee bean and several environmental factors were very important as may reveal how the plants and their seeds reflect ecological change. It has already been demonstrated that a combination of 'light' and 'heavy' elements isotope ratio analysis constituted a good approach to the discrimination between green coffees from different provenances (Rodrigues *et al.*, 2011). However, in order to achieve discrimination of the Hawaiian coffee producing regions it was fundamental to combine the all information available in the same multivariate analysis. The canonical analysis with all variables available allowed the discrimination of these coffee producing regions (figure 32). It is, however, important to state that the significant group discrimination obtained in this study must be interpreted with caution. As with all multivariate analyses, the ratio of samples to variables should be high. Few samples were available in some of the groups. Because the data analysis was based on more variables than groups in the current dataset, new data may not be correctly classified into the groups because of differences not reflected in the current dataset. In addition, this study does not include data addressing multi-year variation. The most important next step is to build a model using many more samples including multiple years of harvest. Despite these limitations, our work demonstrates that multi-element and isotopic ratio analysis can reveal robust patterns of variation

among coffees grown on the Hawaiian Islands. Moreover, the characterization of discriminating patterns, elements and types of analysis in this study presents researchers with information on how the chemistry of the coffee plant responds to specific changes in the environment. Ultimately, this can help illustrate the physiological responses of the coffee plant and seed to agronomic conditions.

4.5. Conclusions

In this chapter it was shown that the combination of 'light' (S, O, C and N) and 'heavy' (Sr) isotopes with multi-element analysis allowed the discrimination of Hawaiian coffee producing regions. Moreover, it demonstrates relationships between environmental variables and the green coffee bean isotopic composition. Although additional work is needed to clarify the mechanisms underlying many of these relationships, the results presented in this chapter suggest that the isotopic composition of coffees from different regions may to some degree be predictable. If so, this would support the use of stable isotopes as a tool for the verification of coffee origin. In addition, the coffee plant seeds' isotopes may contribute to tracing environmental impacts occurring in Hawai'i in particular if related with volcanic activity, distance to the ocean, anthropogenic emissions and altitude.

5. Global variation of green coffee beans caffeine $\delta^{18}O$: a possible proxy for coffee plants water relations

Rodrigues, C., Pimpão, M., Maia, R., Lauteri, M., Brugnoli, E., Bowen, G., Máguas, C. (*submitted*)

5.1. Introduction

Until now, the physiological processes of crop water consumption haven't been detailed completely. However, it is known that hydrogen and oxygen isotopes participate in all the physiological processes related with water, *e.g.* heat-resistance in hot weather (Farquhar *et al*., 2007; Zhang *et al*., 2009). For this reason, they can be used as a tool to disclose the quantificational correlation of water and crop physiological processes (Farquhar *et al*., 2007; Zhang *et al*., 2009). In general, δD and $\delta^{18}O$ found in the stems of crops can indicate the isotope composition of water source in the environment (Flanagan *et al.*, 1991). Water sources for crops generally are precipitation, soil water, runoff (including snowmelt), and groundwater (Dawson, 1993). On the other hand, δD and $\delta^{18}O$ of different water sources are quite different, mainly due to some physical transport processes (such as precipitation) (Bowen *et al*., 2003a) and phase changes (Bowen *et al*., 2003a; Dawson, 1993; Gibson *et al*., 2008; West *et al*., 2008). Therefore, the values of δD and $\delta^{18}O$ in crops can be used to investigate the water source used by crops at different growth stages and help to understand the relative contribution of an individual water source to crop growth. δD and $\delta^{18}O$ have been widely applied to study the plants water use which includes plant water competition, plant interaction, and plant spatial and temporal distribution (Drake & Franks, 2003; Rose *et al*., 200; Sekiya & Yano, 2002; Smith *et al*., 1997; Snyder & Williams, 2000; Stratton *et al*., 2000; Weltzin & McPherson, 1997). Water relations research is important in the studies of water saving agriculture, breeding program, and energy and material cycles in soil plant atmosphere continuum (Zhang *et al*., 2009). There is no discrimination to ^{18}O during water uptake by roots from soils (Yakir, 1998) and during water transportation from roots to leaves through stems. However, the ^{18}O enrichment of plant leaf water was obvious during transpiration (Lin & Sternberg, 1992). In general, there are two isotope effects during transpiration, which are equilibrium fractionation of phase change from liquid to vapor and kinetic fractionation in different diffusivities of the light and heavy isotopes from vapor into air, which alter the isotope composition of leaf water (Flanagan, 1993). In this sense, besides using δD and $\delta^{18}O$ for determination of water source used by a crop it is possible to apply hydrogen and oxygen isotope composition to evaluate the degree of ^{18}O enrichment during plant leaf

transpiration (Barbour, 2007; Zhang *et al*., 2009). Experiments conducted by Yakir *et al*. (1990) using two cotton species under wet (irrigated) and dry (non-irrigated) conditions in the same field showed that $\delta^{18}O$ of leaf cellulose could reflect the isotope composition of the actual water pool involved in cellulose synthesis which is a resultant of isotope fractionations occurring due to the above mentioned factors. This was also confirmed by other authors, *e.g.* Barbour *et al.* (2000b). The ^{18}O-cellulose model requires a number of parameter inputs for estimation of leaf water enrichment and ^{18}O exchange of photosynthates with medium water during cellulose formation (Williams *et al*., 2005). The biochemical pathway of cellulose formation is the same for all parts of a plant. The difference isotopically between cellulose synthesis in leaves and other parts of the plant is that medium water at the site of cellulose formation where precursors are allowed to exchange oxygen isotopes differs and the fraction of O atoms in the photosynthate that re-equilibrate with medium water (carbonyl-water interaction) before cellulose formation (Williams *et al*., 2005). This results in $\delta^{18}O$ values of leaf cellulose 27 ‰ elevated above leaf water (Yakir *et al.*, 1990). This value is considered the isotope biological fractionation factor for autotrophic carbohydrate metabolism. For instance, Barbour *et al.* (2000b) were able to subtract 27 ‰ from the enrichment of sucrose in castor bean plant leaves, obtaining the $\delta^{18}O$ correspondent to the effective substrate water enrichment due to plant transpiration. In this sense, the isotopic composition of synthesized cellulose (δ_{cell}) can be predicted according to equation 9 (Roden *et al*., 2000):

$$\delta_{cell} = f.(\delta_w + \varepsilon) + (1\text{-}f).\delta_{non\text{-}exchangeable} \qquad \text{Equation 9}$$

where δ_w refers to the isotopic composition of medium water, ε is the fractionation factor for the enzyme-mediated exchange or addition of either H or O, f is the proportion of the C-bound H or O that undergoes exchange with medium water and $\delta_{non\text{-}exchangeable}$ accounts for the non-exchanged stable isotopes of the substrate. Thus, the non-exchangeable H and O atoms in sucrose leaving the leaf and being transported in the phloem to the developing plant cells are predicted to be depleted by -171 ‰ and enriched by 27 ‰ as compared to leaf water for H and O isotope ratios, respectively (Roden *et al*., 1990). This has made cellulose a preferred material for plant ecophysiological studies. However, the presence of oxygen-containing chemical bonds between cellulose and lignin, and the isotope effects on the apparent composition of cellulose raises questions regarding the fidelity of cellulose oxygen isotopic analysis. No matter what extraction method is used the chemical bond between cellulose and lignin will be cleaved before pure cellulose can be obtained (Zhou *et al*., 2010). This is even more complex when measuring O isotope ratios of 'bulk' plant material, *e.g.* the coffee bean. In the case of coffee, the bean is a complex matrix, including cellulose and other carbohydrates, lipids, and products of secondary metabolism, *e.g.* the caffeine. The pattern of caffeine synthesis in the coffee plant has been extensively studied (Ashihara *et al*., 1996, 2006, 2008). It occurs during the fruit development and is similar in *Coffea arabica* and *Coffea canephora*, although its content in these two species is 0.6-1.5 and 2.2-2.7, respectively (Ashihara *et al.*, 2008; Wintgens, 2004b). Caffeine is

present in the seed (coffee bean) but is neither degraded nor additionally formed during the development of cotyledons (Baumann, 2006). However, as soon as leaflets develop and push apart the stipules, caffeine concentration sharply increases. During further expansion, caffeine easily permeates through all kinds of biological barriers and will be present in young leaves, internodes, and young fruits (Ashihara *et al.*, 2008; Baumann, 2006). Active caffeine biosynthesis occurs from pericarp expansion to endosperm formation, from juvenile seeds through to maturation (figure 33). During the seed development, the endosperm (bean) resorbes the perisperm and displays its own caffeine biosynthetic capacity (Baumann, 2006; De Castro & Marraccini, 2006). In ripened coffee seeds, accumulated caffeine appears to be synthesized within the developing seeds (Koshiro *et al.*, 2006). In short, the final amount and concentration of caffeine in the coffee bean is a result of (1) acquisition from the perisperm, (2) import from the pericarp, and (3) intrinsic biosynthesis. The first two depend on the allocation of chlorogenic acids in the plant whereas the intrinsic biosynthesis is higher during the time of endosperm expansion (Baumann, 2006; De Castro *et al.*, 2006; Koshiro *et al.*, 2006).

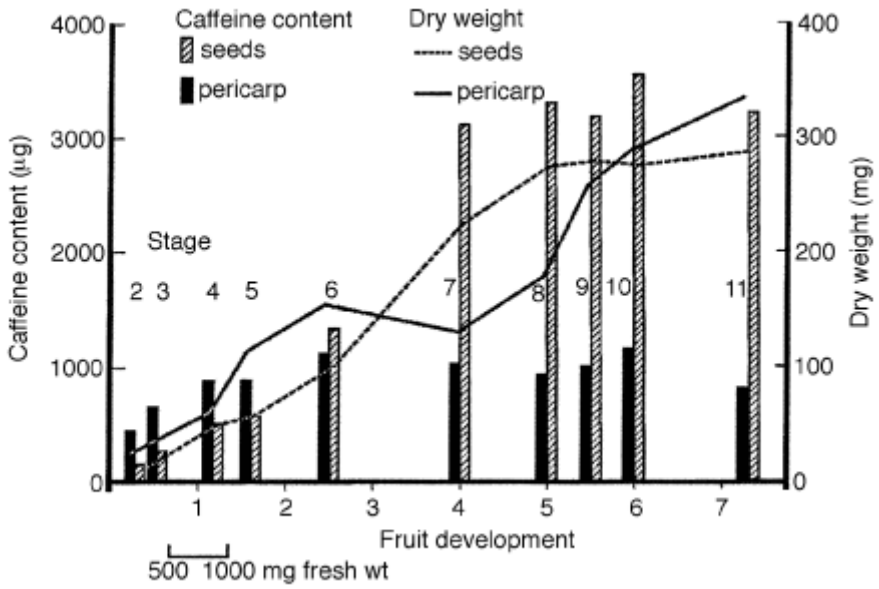

Figure 33. Absolute caffeine contents and dry weights during fruit development of *C. arabica* (*in* Sondahl and Baumann, 2001). Stages 1 to 11 (fresh wt in mg) are characterized as follows: 1 (38), separation into pericarp and seed tissue not possible, 1 to 2 weeks; 2 (240) green, 2 to 3 weeks; 3 (400) green, 3 weeks; 4 (800) green, 4 weeks; 5 (1200) green, 5 weeks; 6 (1180) green, endocarp hard, 2 to 3 months; 7 (1080) green, 4 months; 8 (1600) light-green/olive, mesocarp slightly fleshy, endosperm tough, 5 to 6 months; 9 (2180) exocarp partially reddish, mesocarp very fleshy, endosperm very tough, 5 to 6 months; 10 (2160) exocarp bright red, mesocarp very fleshy, endosperm very tough, 6 months; 11 (1800) exocarp dark red, mesocarp slightly dry, endosperm very tough, 7 to 8 months.

There is strong evidence that the biosynthesis of caffeine is initiated by the degradation of purine nucleotides (Ashihara *et al.*, 1996). The carbon and nitrogen skeletons of the caffeine molecule derive from purine nucleotides (Ashihara *et al.*, 1996; Ashihara *et al.*, 2006; Ashihara *et al.*, 2008; Koshiro *et al.*, 2006; Shulthess & Baumann, 1995). The main metabolic steps involved in the purine alkaloids biosynthesis are shown in figure 34. The adenosine monophosphate (AMP) route is the predominant route in the coffee plants (Ashihara *et al*. 2008). O atoms are introduced in the course of the incorporation of HCO_3^- into the purine nucleus, and by the addition of H_2O (Dunbar *et* al., 1982; Schmidt *et al.*, 2001) to form xanthosine, the initial substrate of purine alkaloid synthesis (Ashihara *et al.*, 2008) (figure 34). The biosynthetic pathway leading from primary metabolism to caffeine involves three methylation reactions and a de-ribosylation, which does not involve the oxygen atoms of the xanthosine purine nucleus (figure 39), but secondary partial oxygen atoms exchange with water is possible (Schmidt *et al.*, 2001). Nonetheless, it is expected a correlation between $\delta^{18}O$ value of caffeine to the leaf water, sensitive to the individual conditions of plant cultivation and climate (Dunbar *et al.*, 1982; Schmidt *et al.*, 2001). For this reason, it was hypothesized, in this work, that the caffeine molecule should constitute a better alternative to cellulose/'bulk' organic material oxygen isotope ratio analysis to study plant-atmosphere interactions.

The aim of this chapter was to unravel how the coffee bean and caffeine $\delta^{18}O$ records important aspects of coffee plant's growth environment and physiological activity and may yield understanding on water cycle processes at regional and global scales.

5.2. Experimental

5.2.1. Green coffee bean samples

Samples of green coffee beans (n = 106) from 21 different countries were provided by Novadelta, Comércio e Indústria de Café, S.A. (Campo Maior, Portugal), by Coffea Consulting and the University of Hawai'i (Hawai'i, US), by University of Lavras in Minas Gerais, Brazil, and Evolve Consulting (Germany). All samples were of *Arabica* coffee (*Coffea arabica*) except one *Robusta* from Angola (*Coffea canephora*). Each green coffee sample consisted in 100g of green coffee beans. Whenever possible, latitude and longitude data as well as altitude were tracked with Google Earth software, Version 5.0 (Google, UK). Annual and monthly mean $\delta^{18}O$ values of precipitation were acquired from the Online Isotopes in Precipitation Calculator (OIPC) (Bowen, 2010; Bowen *et al.*, 2005).

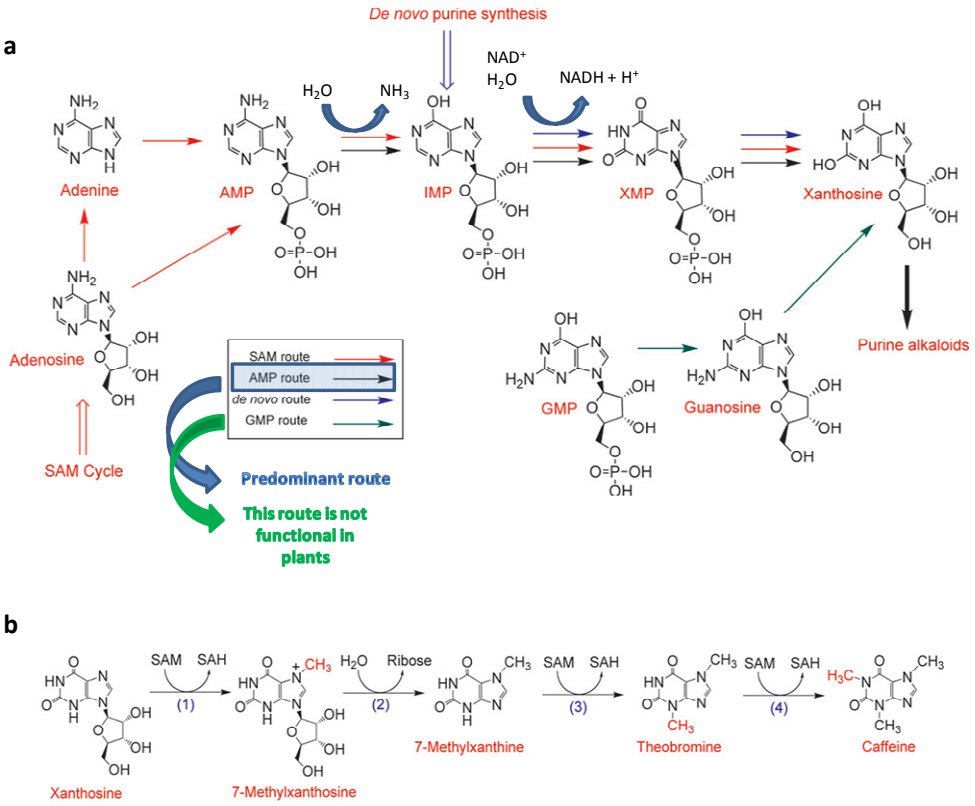

Figure 34. **(a)** Purine alkaloids are synthesized from xanthosine which is produced via at least four routes: from adenosine released from the SAM cycle (SAM route); from IMP originating from *de novo* purine synthesis (*de novo* route), from the cellular adenine nucleotide pool (AMP route) and from the guanine nucleotide pool (GMP route) (adapted from Ashihara *et al*., 2008). Abbreviations: SAM – *S*-adenosyl-L-methionine; AMP – Adenosine monophosphate; IMP – Inosine monophosphate; XMP – Xanthosine monophosphate; GMP – Guanosine monophosphate; **(b)** The major biosynthetic pathway of caffeine from xanthosine: (1) 7-methylxanthosine synthase (xanthosine *N*-methyltransferase); (2) *N*-methylnucleosidade; (3) theobromine synthase (monomethylxanthine *N*-methyltransferase); (4) caffeine synthase (dimethylxanthine *N*-methyltransferase); (3-4) dual-functional caffeine synthase (EC 2.1.1.160). Several *N*-methyltransferase with different substrate specificities contribute to the conversion of xanthosine to caffeine (*in* Ashihara *et al*., 2008).

5.2.2. Caffeine extraction

5.2.2.1. Sample preparation

Green coffee bean samples were grinded to fine powder in a laboratory mill (Type MM2, Retsch, Germany).

5.2.2.2. Caffeine extraction

Caffeine was extracted according to (Weckerle *et al.*, 2002) with some modifications in order to facilitate filtration steps. 50 g of finely grounded beans of green coffee were boiled in Milli-Q water (Millipore, US) in microwave, for 10 minutes. After cooling down, samples were filtrated with gauze. The solution was centrifuged at 5 000 rpm for 10 minutes in order to remove remaining plant tissues and mucilage. Then, it was filtered with GFC 0.45 µm filters (Macherey-Nagel, Germany). The filtered solution was subjected to continuous liquid-liquid extraction (5 h) with chloroform (Carlo Erba, Italy) (100 mL). The organic phase was dried over anhydrous Na_2SO_4 (Panreac, Spain), filtered, and concentrated under reduced pressure to approximately 5 mL. The caffeine, precipitated by addition of 10 mL petroleum ether (Sigma-Aldrich, Germany), was isolated by filtration and recrystallised from methanol (Sigma-Aldrich, Germany). After separation from the solvent and drying in the oven (45 ºC) overnight, its purity was checked by HPLC. Extractions with synthetic caffeine (with $\delta^{18}O$ = 18.3 ± 0.6 ‰) as a surrogate were performed with different amounts of caffeine to check the extraction procedure for potential oxygen isotope discrimination. The $\delta^{18}O$ values of 18.5 ± 0.4 ‰, 18.7 ± 0.2 ‰, and 17.9 ± 0.4 ‰ were obtained for n=5 extractions performed with 10, 50, and 100 mg of synthetic caffeine, respectively.

5.2.3. Isotope ratio mass spectrometry (IRMS)

5.2.3.1. Sample preparation

After grinding, samples were dried overnight at 60 ºC, weighed in tin capsules that were then folded close.

5.2.3.2. Pyrolysis (EA-P) mode

Oxygen isotope ratios were determined on an Isoprime (Micromass, UK) isotope ratio mass spectrometer coupled to an EuroEA elemental analyser (EuroVector, Italy) by high temperature pyrolysis. Pyrolysis was accomplished at 1300ºC on a glassy carbon reactor with glassy carbon chips and nickel plated carbon as catalysts, mounted co-axially on a ceramic tube. Coupling of the elemental analyser and isotope ratio mass spectrometer is performed via open-split. The isotope ratio data was corrected against international standards (IAEA 601 and IAEA 602). Analytical performance was checked by inserting laboratory standards between samples to control stability and to allow drift correction when necessary. Precision was 0.14 ‰.

5.2.4. Statistical analysis

Spearman's correlation coefficients were calculated with Statistica software, version 9.0 (StatSoft, Inc., US). ANOVA analysis was also performed with this software.

5.3. Results

The oxygen isotopic composition of coffee beans ($\delta^{18}O_{bean}$), caffeine ($\delta^{18}O_{caff}$) and of precipitation ($\delta^{18}O_{prec}$) obtained for each geographical origin is shown in table 16. Values for global scale and for Hawai'i are indicated in separate to facilitate a comparison between results at global scale and when a smaller region is addressed. The mean global $\delta^{18}O_{bean}$ value (28.1 ± 3.5 ‰) obtained was in agreement with the reported value for the global mean ^{18}O enrichment of + 27 ‰ ± 4 ‰ of carbohydrate relative to the water from the same source (Barbour, 2007; Schmidt *et al.*, 2001; Yakir *et al.*, 1990; Zhou *et al.*, 2010). In what refers to caffeine, the global mean $\delta^{18}O_{caff}$ was 2.9 ± 3.3 ‰ (table 16). This value was in agreement with values reported by other authors for the caffeine molecule oxygen isotopic composition (Dunbar *et al.*, 1982; Schmidt *et al.*, 2001; Weckerle *et al.*, 2002). The $\delta^{18}O_{caff}$ and correspondent $\delta^{18}O_{prec}$ were of approximate magnitude (table 16). Results for each geographical origin, per continent, are shown in figure 35. In particular, higher values of $\delta^{18}O_{bean}$ and $\delta^{18}O_{caff}$ were observed in Africa (23.9 ‰ ≤ mean $\delta^{18}O_{bean}$ ≤ 33.7 ‰; 0.1 ‰ ≤ mean $\delta^{18}O_{caff}$ ≤ 7.9 ± 1 ‰) (table 16, figure 35) comparing to the other continent, particularly in relation to Asia. The differences $\delta^{18}O_{bean}$ - $\delta^{18}O_{prec}$ and $\delta^{18}O_{caff}$ - $\delta^{18}O_{prec}$ were also calculated as an approximation to the $\delta^{18}O$ resultant of fractionations related to plant metabolism and physiology (table 16). Global mean values of $\delta^{18}O_{bean}$ - $\delta^{18}O_{prec}$ and $\delta^{18}O_{caff}$ - $\delta^{18}O_{prec}$ were 32 ± 3.1 ‰ and 6.9 ± 3.1 ‰, respectively. The same was verified at smaller scale (with coffees from Hawai'i) (table 16).

Table 16. Geographical origin and $\delta^{18}O$ of coffee beans, extracted caffeine and of correspondent local precipitation (when n ≥ 3, average and standard deviation are indicated).

.

Origin	**Country**	**Number of Samples**	**$\delta^{18}O_{bean}$ (‰)**	**$\delta^{18}O_{caffeine}$ (‰)**	**$\delta^{18}O_{prec}$[1] (‰)**	**$\delta^{18}O_{bean}$ - $\delta^{18}O_{prec}$ (‰)**	**$\delta^{18}O_{caff}$- $\delta^{18}O_{prec}$ (‰)**
Africa	Angola	1	23.9	3.7	- 1.6	25.5	5.3
	Ethiopia	6	31.9 (±3.4)	5.4 (±1.9)	- 1.3 (± 0.5)	33.2 (±3.4)	6.7 (±2.2)
	Kenya	11	31.7 (±1.9)	7.9 (±1.0)	- 4.7 (±0.7)	36.4 (±2.2)	12.6 (±1.1)
	Malawi	1	26.9	0.1	- 4	30.9	4.1
	Rwanda	1	31.8	6.6	- 7.1	38.9	13.7
	UR Tanzania	3	31 (±2.8)	6 (±3.3)	- 2.3 (±1)	33.3 (±2.6)	8.3 (±3)
	Zambia	2	33.7	6.1	- 3.2	36.9	9.3
			32.9	5.5	- 3.2	36.1	8.7
	Zimbabwe	1	30.3	3.2	-	30.3	3.2
Central and South America	Brazil	22	27.1 (±2.3)	1.2 (±1.7)	- 5.3 (±0.9)	31.1 (±3.3)	5.3 (±2.7)
	Costa Rica	2	20.3	- 4.6	- 7	27.3	2.4
			21.5	0.7	- 7.5	29	6.8
	Ecuador	1	25	0.8	- 6.7	31.7	7.5
	El Salvador	2	25.8	- 0.4	- 4.9	30.7	4.5
			24.2	- 2.7	- 5.5	29.7	2.8
	Guatemala	2	24.4	0	- 7.5	31.9	7.5
			23.9	2.9	- 7	30.9	9.9
	Jamaica	2	26.7	2.6	- 4.2	30.9	6.8
			27	3	- 5.6	32.6	8.6
	Mexico	2	25.5	0	- 4.8	30.3	4.8
			24.9	0	- 4.8	29.7	4.8
	Nicaragua	1	22.9	- 2	- 4.2	27.1	2.2
Asia	East Timor	4	24.2 (±2.1)	- 1.2 (±1.1)	- 7.6 (0)	31.7 (±2.1)	6.3 (±1.1)
	India	1	29.4	- 0.5	- 6.3	35.7	5.8
	Indonesia	2	24.8	- 4	- 6.9	31.7	2.9
			20.6	- 5.5	- 5.5	26.1	0
	Papua New Guinea	2	18.7	3.9	- 7.3	26	11.2
			20	-2	- 10.7	30.7	8.7
Others (Hawaii)	Hawaii (US)	37	28.8 (±1.9)	3.4 (±2.3)	- 3.1 (±0.5)	31.9 (±1.7)	6.6 (±2)
Global mean (± SD)			**28.1 (±3.5)**	**2.9 (±3.3)**	**- 4.3 (±1.8)**	**32.1 (±3.1)**	**6.9 (±3.1)**

[1] correspondent to the average of $\delta^{18}O$ of precipitation for the 8 month period prior to the reported harvest period for each geographical origin. Monthly $\delta^{18}O_{prec}$ values obtained at the OIPC (Bowen *et al.*, 2010).

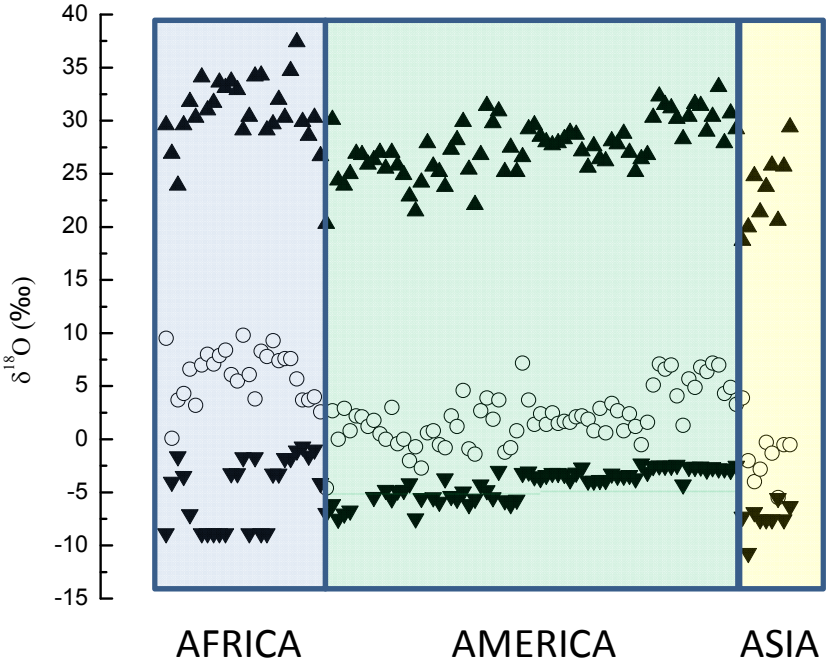

Figure 35. Global variation of (▲) $\delta^{18}O_{bean}$, of (○) $\delta^{18}O_{caff}$, and correspondent $\delta^{18}O_{prec}$ (for the period of fruit development) of the green coffee bean samples.

Spearman's rank correlation coefficients (r) between $\delta^{18}O_{bean}$ and $\delta^{18}O_{caff}$, and $\delta^{18}O_{prec}$ were calculated at global scale and also for the region of Hawai'i (table 17).

Table 17. Spearman's correlation coefficients of significant correlations ($p < 0.05$) obtained between the different values of $\delta^{18}O$, at two different spatial scales (global scale and Hawai'i).

		$\delta^{18}O_{bean}$	$\delta^{18}O_{caff}$	$\delta^{18}O_{PREC}$ [1]	$\delta^{18}O_{prec}$ [2]
Global	$\delta^{18}O_{bean}$	1	0.8	0.5	0.52
	$\delta^{18}O_{caff}$	0.8	1	0.44	0.52
	$\delta^{18}O_{prec}$	0.5	0.44	1	0.87
	$\delta^{18}O_{prec}$	0.52	0.52	0.87	1
Hawai'i	$\delta^{18}O_{bean}$	1	0.76	0.55	0.73
	$\delta^{18}O_{caff}$	0.76	1	0.61	0.79
	$\delta^{18}O_{prec}$	0.55	0.61	1	0.93
	$\delta^{18}O_{prec}$	0.73	0.79	0.93	1

[1] mean annual $\delta^{18}O$ of local precipitation (from OIPC); [2] $\delta^{18}O_{prec}$ correspondent to the mean value for the 8 month period of coffee bean development at each geographical origin. Monthly $\delta^{18}O_{prec}$ values obtained at OIPC (Bowen *et al*., 2010).

In search for the most adequate temporal scale to study the relationship between coffee bean and caffeine oxygen isotopic composition and environmental factors, two different local $\delta^{18}O_{prec}$ mean values were calculated, one referring to the annual mean $\delta^{18}O_{prec}$ at each location, and the other to the period of the fruit development, which was defined as the 8 month period prior to harvest for each geographical location.

In table 17, it can be seen that, at the global scale, a positive correlation between $\delta^{18}O_{bean}$ and $\delta^{18}O_{caff}$ was also obtained (r=0.8; $p < 0.05$) (shown in figure 36). The $\delta^{18}O_{prec}$ also correlated with $\delta^{18}O_{bean}$ and with $\delta^{18}O_{caff}$ (r = 0.52, for both correlations) ($p < 0.05$) (figure 37a and b). However, at a smaller scale (Hawai'i), stronger correlations were obtained (table 17). A positive correlation between $\delta^{18}O_{bean}$ and $\delta^{18}O_{caff}$ (r = 0.76; $p < 0.05$), between $\delta^{18}O_{bean}$ and $\delta^{18}O_{prec}$ (r = 0.73; $p < 0.05$) and between $\delta^{18}O_{caff}$ and $\delta^{18}O_{prec}$ (r = 0.79, $p < 0.05$) were observed. Higher correlation coefficients were also obtained with $\delta^{18}O_{prec}$ then when considering the annual mean value $\delta^{18}O$ of local precipitation ($\delta^{18}O_{PREC}$) (table 17).

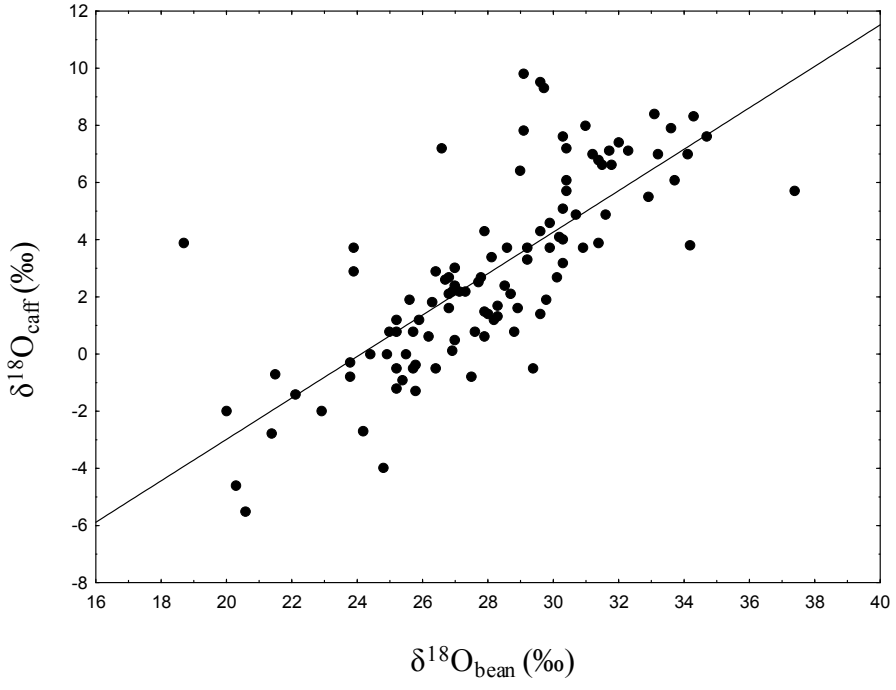

Figure 36. $\delta^{18}O_{caff}$ versus $\delta^{18}O_{bean}$ scatterplot.

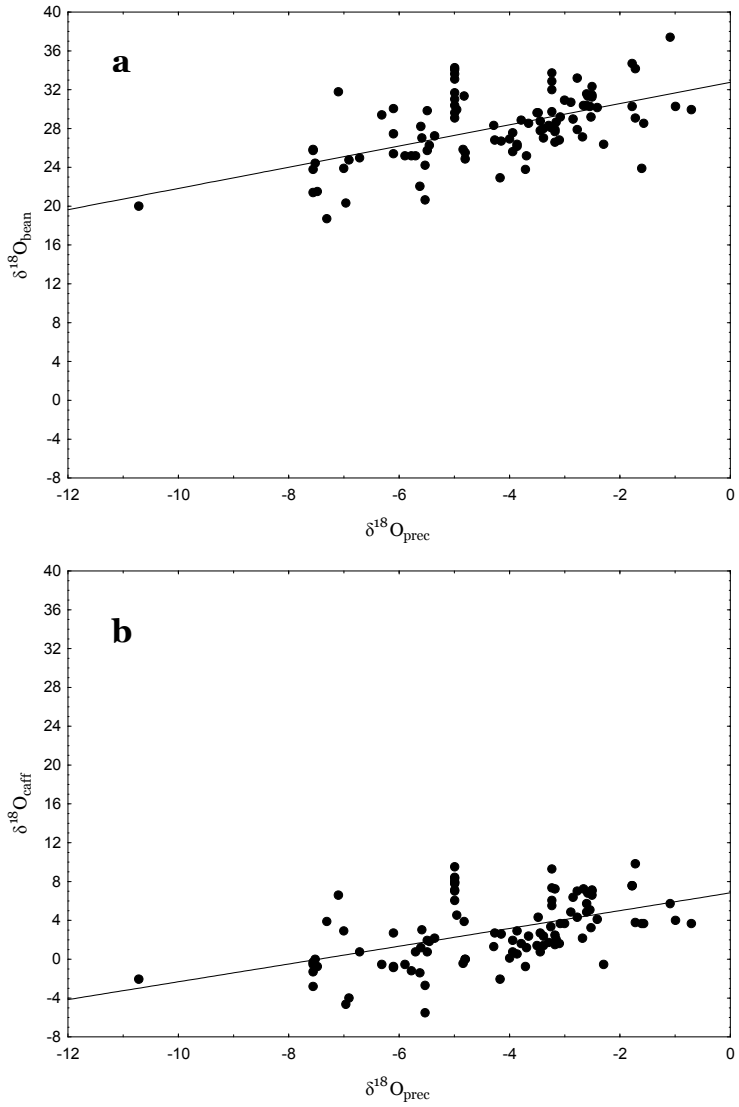

Figure 37. (a) $\delta^{18}O_{bean}$ and (b) $\delta^{18}O_{caff}$ in relation to local $\delta^{18}O_{prec}$.

5.4. Discussion

Several factors influence the oxygen isotope ratio of plant organic material, *e.g.* variations in $\delta^{18}O$ of water taken up by the plants, the leaf enrichment in ^{18}O that occurs during transpiration, and variation in $\delta^{18}O$ of water in cells synthesizing organic material (*e.g.* cellulose) (Barbour *et al.*, 2005a; Farquhar *et al.*, 2007). The main plant's source water component is the soil water which represents an integrated signal of local precipitation (Anderson *et al.*, 2002b; West *et al.*, 2008). However, the value of leaf water $\delta^{18}O$ is moderately sensitive to variations in humidity and stomatal conductance (Williams *et al.*, 2005), particularly at the sites of leaf evaporation (Farquhar *et al.*, 2007) and, additionally, organic molecules' biosynthesis can also lead to $\delta^{18}O$ variations in plant organic material (Barbour *et al.*, 2005a). In the case of caffeine, the fractionation due to metabolic factors should not influence its $\delta^{18}O$ as the O isotopes derive from water and no exchange of O seems to occur in its biosynthetic pathway. According to Smith *et al.* (2001) caffeine $\delta^{18}O$ should only reflect individual conditions of plant cultivation and climate ($\delta^{18}O_{caff} \approx \delta^{18}O_{leaf\ water}$). The kinetic discrimination against $H_2{}^{18}O$ during transpiration leads to the following relationship (Powers *et al.*, 2008):

$$\delta^{18}O_{leaf\ water} = \delta^{18}O_{source\ water} + \varepsilon^{*} + \varepsilon_k + (\delta^{18}O_v - \delta^{18}O_{source\ water} - \varepsilon_k)(e_a/e_i) \quad \text{Equation 10}$$

where ε^{*} is the fractionation that occurs during the change from liquid water to vapor, ε_k is the kinetic fractionation that occurs as water diffuses across the stomata and leaf's boundary layer and $\delta^{18}O_v$ is the oxygen isotope ratio of atmospheric water vapor. e_a and e_i are the atmospheric and leaf water vapor pressure, respectively. This may explain the approximate magnitude between values of $\delta^{18}O_{caff}$ and of $\delta^{18}O_{prec}$ (figures 35 and 37b). Also, eq. 10 suggests that leaf water enrichment should be negatively related to RH and negatively related to g_s when RH is similar among leaves (Powers *et al.*, 2008). If $\delta^{18}O_{source\ water} \approx \delta^{18}O_{prec}$ (Gibson *et al.*, 2008; West *et al.*, 2008) then eq. 10 can be abbreviated to:

$$\delta^{18}O_{leaf\ water} \approx \delta^{18}O_{prec} + \delta^{18}O_{evaporative\ enrichment} \quad \text{Equation 11}$$

thus, showing the factors influencing the $\delta^{18}O_{caff}$ (if considering $\delta^{18}O_{caff} \approx \delta^{18}O_{leaf\ water}$). This supports the correlation found between $\delta^{18}O_{caff}$ and the mean values of local $\delta^{18}O_{prec}$ occurring during the coffee bean developmental period (figure 37b). However, fractionations leading to ^{18}O enrichment as a result of plant evapotranspiration (dependent on temperature and air RH) must be considered, which may account for the differences observed at continental level (figure 35). In Africa, were less precipitation and higher temperatures are reported (IAEA, 2001), and so, low RH values are expected, there was a $\delta^{18}O$ lag between $\delta^{18}O_{bean}$ and $\delta^{18}O_{caff}$ in relation to $\delta^{18}O_{prec}$ which, in general, is not observed in the other continents (figure 35). In the case of African coffees, it is possible that plant cultivation conditions (correspondent to a higher

evaporative demand) play a more relevant role in the determination of the $\delta^{18}O$ values of the 'bulk' coffee bean and caffeine. In the present work, the $\delta^{18}O_{caff}$ - $\delta^{18}O_{prec}$ values (table 16) were given as an indication of ^{18}O enrichment occurring locally due to plant evapotranspiration. A global mean value of $\delta^{18}O_{caff}$ - $\delta^{18}O_{prec}$ of 6.9 ‰ (table 16) was in agreement with the global mean leaf water $\delta^{18}O$ at evaporation sites predicted by the isoscape presented by West and co-authors (2008). This is assumed as an indication that $\delta^{18}O_{caff}$ reflects plant cultivation climate conditions, during the coffee bean development period. Beyond this, the higher correlation coefficients obtained when using mean $\delta^{18}O_{prec}$ instead of the annual mean values ($\delta^{18}O_{PREC}$; table 17), shows that it is important to consider the period of coffee bean development, corresponding to the caffeine biosynthesis period in the fruit and seed (Ashihara *et al*., 2008), in order to interpret the results obtained for $\delta^{18}O_{bean}$ and $\delta^{18}O_{caff}$. This is verified whether at global scale or when a smaller region is considered (Hawai'i) (tables 16 and 17). The lower correlation coefficients obtained at global scale in comparison to the smaller region of Hawai'i (table 17) suggest that more detailed information on local climate is necessary to understand $\delta^{18}O_{caff}$ and $\delta^{18}O_{bean}$ variations at larger spatial scales. At global scale, different coffee plant populations are considered, as well as different climate systems and geography encompassing nonseasonal to sites with pronounced seasonality. Also, the absence of field experiments did not allow addressing the degree to which seasonality influenced the evaporative enrichment and how this may influence $\delta^{18}O_{bean}$ and $\delta^{18}O_{caff}$ values. Under changing environmental conditions, such as changes in relative humidity and available moisture, a plant will react with a change in physiological processes, resulting in different proportions of leaf water that is subjected to evaporative isotopic enrichment (Anderson *et al.*, 2002e). Also, coffee is cultivated over a wide range of altitudes (from ~ 100 to 2500 m) and high altitudes can have also a more pronounced impact on the estimation of $\delta^{18}O_{prec}$ (Gibson *et al.*, 2008). Applying stable isotope to trace the coffee plant-atmosphere interactions and related ecosystem processes at the local, regional, and global scale will require baseline information on isotopic signatures of precipitation and atmospheric moisture, as well as general climatic factors such as relative humidity and temperature that control the degree of equilibrium and kinetic isotopic fractionation. In the present work, it is also regretted the lack of information on $\delta^{18}O$ of local soil water and the effect of soil type and soil evaporation on ^{18}O enrichment. These processes involve oxygen isotope fractionation of water molecules. It would be important to distinguish plant transpiration from soil evaporation in relation to water O isotopic composition. Results show a significant positive correlation between values of $\delta^{18}O_{bean}$ and $\delta^{18}O_{caff}$ (figure 36, table 17). This was expected as both reflect to a certain extent the $\delta^{18}O_{prec}$ (figure 37a) (Rodrigues *et al*., 2009, 2011). Nevertheless, caffeine is a good alternative to 'bulk' coffee bean analysis from the biochemical point of view because more input parameters (due to biochemical fractionations associated with other metabolic pathways) are necessary to interpret the measured $\delta^{18}O_{bean}$. In addition, the caffeine extraction method is less time-consuming and does not raises the problems related with isotope fractionation from chemical bond break between cellulose and lignin during the extraction procedure (Zhou *et al*., 2010). But there are other advantages concerning the analysis of caffeine

extracted from the green coffee bean, which are related to the pattern of global distribution of these plant species. As being a seed, the coffee bean is a very stable matrix, from 'farm to fork', allowing sampling all over the world in a systematic way, as coffees are imported. This allows obtaining a material for study plant-atmosphere interactions from globe regions where, many times, it is difficult to access data and experimental samples, compromising the development and consequently, the application of models for studying water cycles (*e.g.* in Africa). It is likely that detailed general circulation models of the water cycle will increasingly involve isotopic considerations, and plant leaves and/or seeds are relevant here also (Farquhar *et al*., 2007). Eventually, the approach presented in this work may be expanded to other plant species, growing in specific regions of the globe. Caffeine is widespread among several plant species that grow all over the globe. It is not only present in the coffee bean but also in other commercially important species, *e.g. Teobroma cacao* (cocoa) and *Paullinia cupana* (guarana).

5.5. Conclusions

In this chapter it was shown that the $\delta^{18}O$ of caffeine extracted from green coffee beans may be a powerful tool to study coffee plant's growth environment and physiological activity during the period of coffee bean development. The $\delta^{18}O_{caff}$ of green coffee beans reflects the local $\delta^{18}O_{prec}$, particularly during the coffee bean developmental period, and the ^{18}O enrichment due to plant cultivation conditions. Caffeine constitutes a good alternative to the isotope ratio analysis of 'bulk' coffee bean or even of extracted cellulose as the oxygen isotopes in this molecule are known to derive from metabolic water.

6. Discrimination of green *Arabica* and *Robusta* coffee beans by Raman spectroscopy[4]

Keidel, A., von Stetten, D., Rodrigues, C., Máguas, C., Hildebrandt, P., 2010, *Discrimination of green arabica and robusta coffee beans by Raman spectroscopy.* Journal of Agricultural and Food Chemistry, 58, 11187-11192

6.1. Introduction

Coffee is a major foodstuff with an annual global consumption of about 7 million tons (ICO, 2009). Commercially available coffee roasts consist of two main variants in pure or blended forms: *Coffea arabica* and *Coffea canephora* var. *robusta*, commonly referred to as *Arabica* and *Robusta*, respectively. *Arabica* coffees are considered to be of higher quality and of finer taste than *Robusta* coffees, which is reflected by distinctly higher prices by 20 % at average and more than 200 % when compared to the cheapest and most expensive *Arabica* coffees (ICO, 2009). The price also depends on the geographic origin (ICO, 2009). Furthermore, there are substantial variations of the price over time with 10 % short-term fluctuations within days and mid-term changes by more than 100 % over years, often related with crop yield variations. In addition, the continuous splitting of large coffee estates, the excessive expansion of new plantations and the growing number of intermediaries in the marketing chains has resulted in a deterioration of coffee quality and its price. In a situation of overproduction a higher quality coffee is likely to command premium prices. Farmers will have to pay more attention to quality which may be, in turn, associated with lower yields (Wintgens, 2004b). Thus, there is a strong economic interest in safely distinguishing coffee beans of different species (*Arabica* vs. *Robusta*) and different geographical origins to verify the purity of batches and, specifically, to detect possible admixtures of cheaper (*Robusta*) to more precious (*Arabica*) beans. Currently, the main procedure to distinguish green *Arabica* and *Robusta* beans is based on visual inspection of the size, color, and shape of the beans. This approach does not only depend on the skills and experience of the inspector but its reliability may also be reduced by natural variations of the appearance of the beans from different species. Among different types of coffee,

[4] Rodrigues, C. initially applied NIR spectroscopy for the differentiation between *Arabica* and *Robusta* green coffee beans in the Center for Biological and Chemical Engineering at IST/UTL, Portugal. The results were presented in the international conference ASIC 2008, in Campinas, Brazil. In the beginning of 2009, a collaboration with the Technical University of Berlin was initiated to apply Raman spectroscopy for the discrimination of *Arabica versus Robusta* coffee based on kahweol content of the green coffee bean. For this, green coffee bean samples were selected and prepared in SIIAF laboratory at F.C.U.L. and Raman spectra were taken in Berlin. The results obtained were published and constitute this chapter of the thesis.

there are considerable variations in size, shape and density as a result of both genotype and environmental factors. Furthermore, visual inspection does not allow the safe detection of "contaminations" of *Arabica* beans by small amounts of *Robusta* beans. Consequently, developments of more objective methods that can be certified are desirable. Analytical approaches which are employed to green (Alves *et al.*, 2003; Alves *et al*., 2009; Andrade *et al*, 1998; Bertrand *et al.*, 2005; Carrera *et al*., 1998; Casal *et al*., 2003; Downey *et al.*, 1994; Fischer *et al.*, 2001; González et al., 2001; Martín et al., 2001; Martín *et al.*, 1998; Mendonca *et al.*, 2009 ; Mendonca *et al.*, 2008; Rodrigues *et al.*, 2009; Rubayiza *et al.*, 2005; Suchanek *et al.*, 1996) as well as to roasted coffees (Alves *et al.*, 2003; Alves *et al.*, 2009; Casal *et al.*, 2003; Casal *et al.*, 2000; Downey *et al.*, 1997; Esteban-Diez *et al.*, 2004; Esteban-Diez *et al.*, 2007; González *et al.*, 2001; Kemsley *et al.*, 1995; Martín *et al*., 2001; Martin *et al.*, 1999; Mendonca *et al*., 2009 ; Pizarro *et al.*, 2007; Rubayiza *et al*., 2005) may be grouped in two classes depending on the processing of the coffee. The first class (chemical methods) is based on traditional analytical methods in which coffee beans are mechanically and chemically processed for applying chromatographic techniques to distinguish between the two coffee species on the basis of different compositions of hydroxycinnamic acids (Andrade *et al*., 1998), sterols (Carrera *et al*., 1998), chlorogenic acid, caffeine, trigonelline (Casal *et al*., 2000; Martín *et al*., 1998), amino acids (Casal *et al*., 2003; Martín *et al*., 1998), metals (Martin *et al*., 1999), fatty acids (Alves *et al*., 2003; Martín *et al*., 2001), polysaccharides (Fischer *et al.*, 2001), tocopherols (Alves *et al*., 2009; González *et al*., 2001), and diterpernoids (de Roos *et al.*, 1997; Kölling-Speer *et al.*, 1999; Rubayiza *et al*., 2005). The second class is based on spectroscopic techniques, mainly using mid-IR (Downey *et al*., 1997; Kemsley *et al*., 1995) and near-IR (Downey *et al*., 1997; Esteban-Diez *et al*., 2004; Esteban-Diez *et al*., 2007; Pizarro *et al*., 2007) spectroscopy which have been proven to be useful for discrimination between roasted *Arabica* and *Robusta* coffees. In particular in combination with spectral pattern recognition methods, a reliable distinction between *Arabica* and *Robusta* coffees was achieved. In addition, IR spectroscopy in combination with principal component analysis has been shown to distinguish between *Arabica* and *Robusta* instant coffees (Briandet, Kemsley & Wilson, 1996), and even "Timor Hybrid" (Híbrido de Timor - HdT), which is a crossbreed of *Arabica* and *Robusta* coffees, was correctly identified by this method (Bertrand *et al*., 2005). The two classes of analytical approaches are associated with specific advantages and disadvantages. Chemical methods rely upon different chemical compositions in *Arabica* and *Robusta* coffees but the quantitative analysis requires a time-consuming and costly sample processing in an adequately equipped chemical laboratory. On the other hand, the previously employed spectroscopic methods were applied to ground roasted or green beans without further chemical extraction procedures. However, the spectra analysis relies upon statistical evaluation procedures which sensitively depend on the calibration model. Moreover, sample preparation has to follow a precise protocol since, for instance, water content and grain size may affect the spectra and thus the principal component analysis (Downey *et al*., 1994; Suchanek *et al.*, 1996). The present Fourier-transform (FT) Raman spectroscopic approach is capable to overcome the drawbacks associated with

the chemical and IR-spectroscopic techniques since it represents a fast procedure applicable to ground as well as to whole beans. High quality Raman spectra are obtained which allow identifying the characteristic vibrational bands of kahweol which in a previous study were detected in chemical extracts of processed green and roasted beans (Rubayiza *et al*., 2005). Due to the different content of this diterpenoid in *Arabica* and *Robusta* (Briandet *et al*., 1996; Cavin *et al.*, 2002; de Roos *et al*., 1997; Kölling-Speer *et al*., 1999), these two coffee species can readily be distinguished on the basis of the kahweol Raman bands without sophisticated spectra analysis. Using Fourier-transform Raman spectroscopy with 1064-nm excitation it is possible to monitor the characteristic Raman bands of kahweol in green coffee beans without chemical and physical processing of the beans. The procedure was optimized on the basis of 83 and 125 measurements of whole and ground beans, respectively, using coffee samples of different type (*Arabica*, *Robusta*) and different origins. The relative contribution of the kahweol in individual beans can be determined quantitatively by means of a component analysis of the spectra, yielding a spectral kahweol index σ_{ka} that is proportional to the relative content of kahweol in a coffee bean. The reproducibility of the spectroscopic measurement and analysis was found to be 3.5 %. Individual beans of the same type and origin reveal a scattering of the σ_{ka} values. Nevertheless, an unambiguous distinction between *Arabica* and *Robusta* samples is possible on the basis of single bean measurements as the σ_{ka} values are larger and lower than 10 for *Arabica* and *Robusta*, respectively. Measurements of whole and ground beans afford very similar results, despite the heterogeneous distribution of kahweol within a bean. Unlike to conventional analytical techniques, the single-bean sensitivity of the present approach may also allow for a rapid detection of unwanted admixtures of low-value *Robusta* coffee to high-quality and more expensive *Arabica* coffee.

6.2. Experimental

6.2.1. Samples

Green coffee beans from different origins were obtained through the University of Lavras in Minas Gerais, Brazil, and University of Hawaii in Manoa, Novadelta, S. A. (Portugal) and from a local contact in Dili, East Timor, as described in detail in table 18. The country of origin of all samples is known. Exact geographical location coordinates are indicated whenever available.

Table 18. Data on the origin of the various coffee samples.[1]

Country	Sample	State	Region	Latitude	Longitude	Type
Brazil	1	Minas Gerais	Cerrado, Coromandel	18º 28' 26" S	47º 12' 01" W	*Arabica*
	2		Cerrado, Patrocínio	18º 56' 27" S	46º 59' 22" W	*Arabica*
	3		Cerrado, Carmo do Paranaíba	19º 02' 23" S	46º 26' 18" W	*Arabica*
	4		Cerrado, Araxá	19º 35' 34" S	46º 56' 26" W	*Arabica*
	5		Cerrado, Patrocínio	20º 31' S	47º 23' W	*Arabica*
Hawai'i	6	Hawaii	Big Island, Kona	19º 4' 20" N	155º 48' 28" W	*Arabica*
	7		Maui island, Kã'anapali	20º 56' 0" N	156º 42' 0" W	*Arabica*
	8		Kaua'i island, Ele'ele	21º 54' 37" N	159º 35' 14" W	*Arabica*
	9		Big Island, Kona	19º 4' 20" N	155º 48' 28"	*Arabica*
	10		Kaua'i island, Ele'ele	21º 54' 37" N	159º 35' 14" W	*Arabica*
Kenya	11	-	Mount Kenya	0º 9' S	37º 18' E	*Arabica*
	12	-	Mount Kenya	0º 9' S	37º 18' E	*Arabica*
	13	-	Mount Kenya	0º 9' S	37º 18' E	*Arabica*
	14	-	Kirimiri	0º 55' S	37º 15' E	*Arabica*
	15	-	Mount Kenya	0º 9' S	37º 18' E	*Arabica*
East Timor	16	-	Ermera	8º 45' S	125º 23' E	*Arabica*
	17	-	Ermera	8º 45' S	125º 23' E	*Arabica*
	18	-	Dili	8º 33' 31" S	125º 34' 25"	*Arabica*
	19	-	Dili	8º 33' 31" S	125º 34' 25"	*Arabica*
	20	-	Ermera	8º 45' S	125º 23' E	*Arabica*
India	21	-	-	-	-	*Robusta*
	22	-	-	-	-	*Robusta*
	23	-	-	-	-	*Robusta*
	24	-	-	-	-	*Robusta*
	25	-	-	-	-	*Robusta*

Table 18 (Continued).

Papua New Guinea	26	-	-	-	-	*Arabica*
Peru	27	-	-	-	-	*Arabica*
Panama	28	-	-	-	-	*Arabica*
Honduras	29	-	-	-	-	*Arabica*
Camaroon	30	-	-	-	-	*Robusta*
Camaroon	31	-	-	-	-	*Robusta*
Papua New Guinea	32	-	-	-	-	*Robusta*
Laos	33	-	-	-	-	*Robusta*

[1] For coffee samples #21 to #33 which were kindly provided by Novadelta, SA, only the type of coffee (*Arabica*, *Robusta*) and the origin country is know.

The beans were either used directly for FT Raman spectroscopic characterization or after grinding to a fine powder in a mill (Restch, Germany) with a grain size of less than 1 mm as described previously (Rodrigues *et al.*, 2009). Kahweol acetate (CAS 81760-47-6) was purchased from LGC Standards (Wesel, Germany) and used without further purification.

6.2.2. Fourier-transform Raman spectroscopy

Raman spectra were recorded with a Bruker RFS 100/S Fourier-transform spectrometer with 1064-nm excitation and a spectral resolution of 4 cm^{-1} (Brandt *et al.*, 2008). The accumulation for each spectrum was ca. 6 minutes. All experiments were carried out at ambient temperature using a laser power of 300 mW which did not cause any damage of the sample as checked by repetitive measurements and measurements as a function of the laser power. No background correction was applied to the spectra prior to spectra analysis.

6.3. Results and discussion

The Raman spectra of all whole and ground coffee beans display a quite similar overall vibrational band pattern. A characteristic example (*Arabica* sample #28) is shown in figure 38A. In the region between 1400 to 1700 cm^{-1}, the spectrum is dominated by a prominent band pair at 1604 and 1630 cm^{-1}, originating from the aromatic and C=C stretchings of polyphenols and phenolic (chlorogenic) acids which are important constituents of coffee beans with up to 10 % w/w of the dry mass (Andrade *et al.*, 1998; Martin *et al.*, 1998). The high intensities of these bands which are evidently not proportional to the relative concentrations of these constituents result from the relatively large Raman cross sections of these modes and a pre-resonance enhancement even at 1064-nm excitation. Conversely, Raman bands of proteins are relatively weak and give rise to a weak peak at 1690 cm^{-1} and a shoulder at 1656 cm^{-1}, originating from the amide I bands of β-sheet and α-helix structures, respectively. The overall spectral similarity holds for the Raman spectra of typical *Arabica* (figure 38A) and *Robusta* (figure 38B) beans. However, a closer inspection reveals differences related to two weak peaks at 1479 and 1567 cm^{-1} in the spectra of *Arabica* samples. These two peaks, which can be more clearly identified in the difference spectrum "*Arabica*" minus "*Robusta*" (figure 38C), are at the positions of the most prominent bands of kahweol as demonstrated by the comparison with a spectrum of neat kahweol (figure 38D), in agreement with the previous study by Rubayiza and Meurens (Rubayiza *et al.*, 2005). These findings reflect the ca. 10 times higher kahweol content in *Arabica* (0.11 – 0.35 %) as compared to Robusta (< 0.01 %) (de Roos *et al.*, 1997; Kurzrock & Speer, 2001;

Rubayiza *et al.*, 2005). Again, the detectability of the kahweol bands benefits from the relatively large Raman cross section of these modes at 1064-nm excitation.

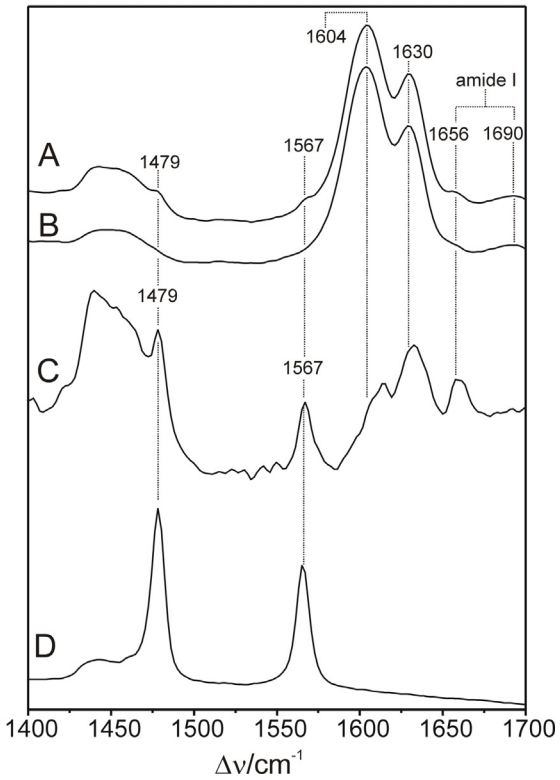

Figure 38. Raman spectra of a whole green bean from *Arabica* (sample no. 28; A) and from *Robusta* (sample no. 21; B). Spectrum C represents the difference "A" minus "B" to show more clearly the Raman bands of kahweol. The experimental Raman spectrum of neat kahweol is shown in trace D. All spectra were obtained with 1064-nm excitation.

6.3.1. Analysis of the Raman spectra

For a quantitative analysis, we have employed a component analysis in which the experimental Raman spectra are simulated by the superposition of the spectra of individual components (Döpner *et al.*, 1996). In this approach, we first used component spectra of kahweol and of the remaining spectral contribution, denoted as "background" (figure 39A-C). These component spectra were constructed by combining several individual bands with Lorentz and Voigt profiles obtained from a band fitting to the experimental spectra of neat kahweol and of a typical *Robusta* sample lacking the kahweol bands.

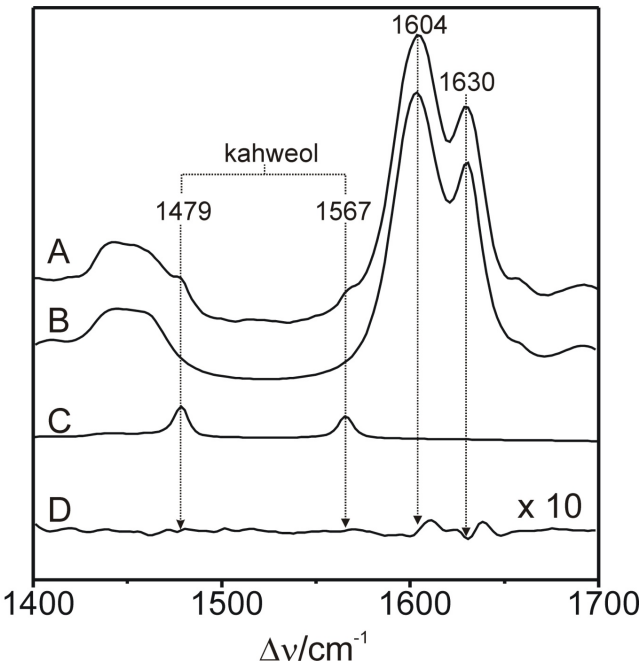

Figure 39. Raman spectra of a whole green bean from Arabica (sample no. 28; A) and the synthetic component spectra of the coffee "background" (B) and kahweol (C). Trace D represents the residuals of a fit of the component spectra B and C to the experimental spectrum A (*see* text for further details).

On the basis of these two "synthetic" component spectra, it was possible to achieve a satisfactory description of the experimental Raman spectra obtained from various coffee samples. However, such highly constraint fits in which the amplitudes of the two component spectra were the only two adjustable parameters afforded relatively high residuals in the region between 1590 and 1650 cm^{-1}, reflecting slight differences of the polyphenol and chlorogenic acid content in the various samples as compared to the reference to which the "background" component spectrum refers to. In the second step, the intensity of the prominent 1604-cm^{-1} band of the background as well as the relative intensities of the two kahweol bands was taken as additional independent variable. In this way, the overall quality of the fits was improved (figure 39D). On the basis of these fits, the relative spectral contribution of kahweol in coffee samples was expressed in terms of the amplitude ratio of the kahweol (1479 cm^{-1}) and "background" (1630 cm^{-1}) component spectra, denoted as the spectral kahweol index σ_{ka}. The results were essential the same for the pure component analysis (first step, *vide supra*) and the mixed component/band fitting analysis (second step).

6.3.2. Raman spectroscopy analysis of ground beans

The Raman spectroscopic determination of σ_{ka} was found to be highly reproducible as demonstrated by repetitive measurements of the same powder samples from various batches. The average mean standard deviation of these measurements was determined to

be 3.5 %. We have then applied the analysis first to 125 ground samples, taken from 25 different origins of both *Arabica* and *Robusta* type (table 19).

Table 19. Average spectral kahweol indices σ_{ka} of ground coffee beans.[a]

Origin	Sample	type	σ_{ka}
Brazil	1	*Arabica*	18 ± 5
	2	*Arabica*	33 ± 5
	3	*Arabica*	30 ± 6
	4	*Arabica*	28 ± 8
	5	*Arabica*	23 ± 8
Hawai'i	6	*Arabica*	20 ± 5
	7	*Arabica*	27 ± 2
	8	*Arabica*	19 ± 2
	9	*Arabica*	31 ± 4
	10	*Arabica*	23 ± 9
Kenya	11	*Arabica*	19 ± 4
	12	*Arabica*	19 ± 1
	13	*Arabica*	19 ± 2
	14	*Arabica*	24 ± 6
	15	*Arabica*	19 ± 4
East Timor	16	*Arabica*	27 ± 4
	17	*Arabica*	26 ± 4
	18	*Arabica*	24 ± 4
	19	*Arabica*	1 ± 1
	20	*Arabica*	20 ± 4
India	21	*Robusta*	2 ± 2
	22	*Robusta*	1 ± 1
	23	*Robusta*	1 ± 2
	24	*Robusta*	1 ± 2
	25	*Robusta*	3 ± 2

[a] The σ_{ka} values were obtained from various beans of ground green coffee beans of the same type and origin as described in the text. Standard deviations typically refer to measurements of five different ground beans. Details of the origin of the coffee are given in the table 18.

From each origin, five samples from different beans were prepared. The individual σ_{ka} values are plotted in figure 40 (top), demonstrating that *Arabica* and *Robusta* samples can unambiguously be distinguished. All *Arabica* samples exhibit σ_{ka} values higher than 10, whereas in the case of *Robusta* values between 0 and 5 are determined. The only deviation refers to the 5 beans assigned to sample no. 19, *i.e.* to an *Arabica* type coffee. However, the very low σ_{ka} values determined for these beans clearly show that this classification is not correct and that they must originate from a *Robusta* coffee.

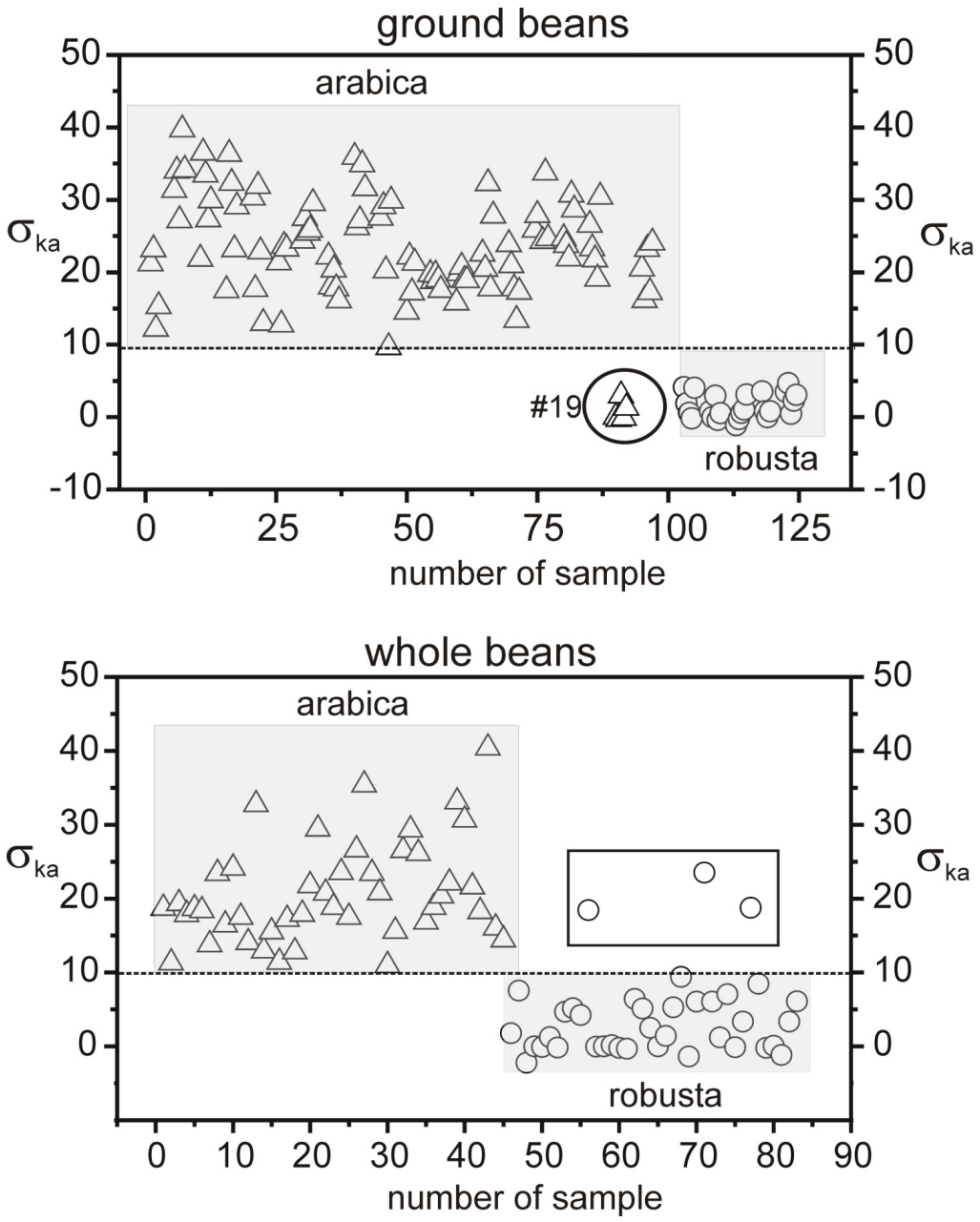

Figure 40. Spectral kahweol index σ_{ka} determined from the Raman spectra of various coffee samples. Samples originally classified as *Arabica* and *Robusta* are represented by triangles and circles, respectively. Top: σ_{ka} values obtained from 125 powder samples (table 19), including 25 different types and origins, 5 different beans of each. Bottom: σ_{ka} values obtained from 83 whole bean samples (table 20), including 12 different types and origins, 5 - 10 different beans of each. Values which fall outside the expected range are indicated by the circular and rectangular frame. Sample numbers are indicated by "#" (see tables 19 and 20).

In contrast to the other samples, coffees no. 18 and 19 were obtained directly from a local roasting facility in Dili, East Timor, with little information about their type. Considering that HdT (Híbrido de Timor) coffee has begun to replace the local *Arabica* in Timor, and that crosses between *C. arabica* var. *caturra* and HdT generated a population called Caturra highly cultivated in that region, the hypothesis that no. 19 is a misidentified *Arabica* coffee has to be considered. For all other samples, the original classification is confirmed by the present analysis. The σ_{ka} values of the individual *Arabica* samples reveal a remarkable scattering ranging from 10 to 40. These variations do not only refer to *Arabica* samples from different origins. Also samples prepared from beans of the same origin exhibit σ_{ka} values in a relatively wide range as expressed by the standard deviations listed in table 19. These standard deviations are larger by nearly factor of 10 than the reproducibility of the spectroscopic analysis for an individual sample (3.5 %; *vide supra*). Thus, these findings indicate a considerable bean-to-bean heterogeneity of the kahweol content. Coffee fruits take several months to ripen. Fruits of the same coffee plant do not necessarily ripen at the same time. Due to uneven ripening, a tree will have fruits with different degrees of ripeness. It is quite common to see immature, mature and overripe fruits simultaneously on the same branch. Hence, environmental conditions (*e.g.* temperature, humidity, water availability, light exposure) will influence the metabolism of such fruits at distinct developmental stages. It is also important to note that the beans analyzed in this study were obtained from the same origin, and in some cases from the same plantation, but most probably from different coffee plants. This heterogeneity might account for the differences observed in chemical composition of various beans, *e.g.* the kahweol content determined here.

6.3.3. Raman spectroscopic analysis of whole beans

In the second step we have applied the Raman spectroscopic analysis to 83 whole beans, including samples of four different origins for which also ground beans have been analyzed (table 20; figure 40, bottom; figure 41, top). Here we note a good agreement when comparing the average σ_{ka} values determined for four ground and four non-ground (whole) beans of the same type and origin. For the *Arabica* coffees no. 20 and 15 the average σ_{ka} values of the ground (whole) beans were determined to be 20 ± 4 (25 ± 6) and 19 ± 4 (18 ± 5), respectively. Values for the *Robusta* coffees no. 21 and 23 were found to be 2 ± 2 (3 ± 2) and 1 ± 2 (3 ± 4), respectively. However, we note that the standard deviation is systematically larger for whole beans as compared to ground beans. In the case of *Arabica* coffee, the average standard deviation for individual beans of coffee from the same origin was determined to be 27 % and 31 % for ground beans and whole beans, respectively.

Table 20. Average spectral kahweol indices σ_{ka} of whole coffee beans.[a]

Origin	Sample	Type	σ_{ka}
Kenya	15	*Arabica*	18 ± 5
East Timor	20	*Arabica*	25 ± 6
Papua New Guinea	26	*Arabica*	22 ± 5
Peru	27	*Arabica*	23 ± 9
Panama	28	*Arabica*	23 ± 6
Honduras	29	*Arabica*	22 ± 11
India	21	*Robusta*	3 ± 2
India	23	*Robusta*	3 ± 4
Cameroon	30	*Robusta*	1 ± 4
Cameroon	31	*Robusta*	4 ± 6
Papua New Guinea	32	*Robusta*	4 ± 8
Laos	33	*Robusta*	7 ± 8

[a] The σ_{ka} values were obtained from various beans of whole green coffee beans of the same type and origin as described in the text. Standard deviations typically refer to measurements of five to ten different beans. Details of the origin of the coffee are given in the table 18.

To identify the origin of the larger standard deviation for whole-bean measurements, we have analyzed for four different samples, *i.e.* the *Arabica* samples no. 28, 15, and 29, and the *Robusta* sample no. 21, a single bean using ten measurements upon refocusing the laser on different spots of the bean. Figure 41 (bottom) displays the respective spectral kahweol indices σ_{ka} of 22 ± 4, 15 ± 5, and 17 ± 2 for the Arabica beans #28, #15, and #29, respectively, whereas for the *Robusta* bean #21 σ_{ka} is determined to be 1 ± 1. Again, the standard deviations are nearly one order of magnitude larger (22%) than that of the reproducibility of the spectroscopic analysis (3.5%, *vide supra*).

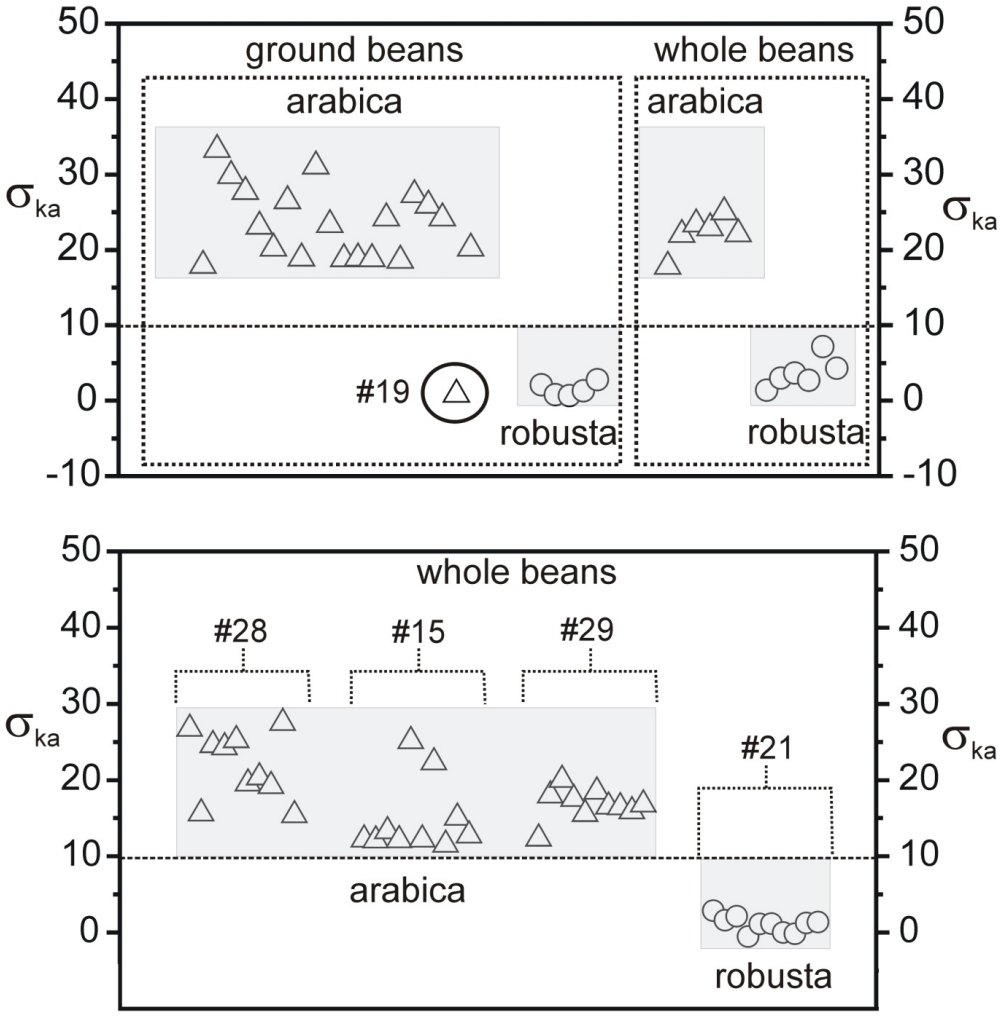

Figure 41. Top: average spectral kahweol index σ_{ka} obtained from the data in figure 40 upon averaging over the values of the various beans of the same type and origin; data referring to powder and whole bean samples are shown in the left and right dotted frame, respectively. The value for sample no. 19 unambiguously points to a *Robusta* coffee although it was classified as *Arabica*. Bottom: σ_{ka} values obtained for 10 measurements from a single bean. The data refer to three *Arabica* and one *Robusta* sample. Sample numbers are indicated by "#" (see tables 19 and 20).

This finding implies that the scattering of σ_{ka} noted for a whole bean at (randomly chosen) different spots cannot be attributed to intrinsic error of the measurements and the data analysis but instead points to a heterogeneity of the kahweol distribution in the bean. This heterogeneity has an impact on the Raman spectroscopic distinction between *Arabica* and *Robusta* coffees using whole-bean measurements. In general, the data allow for a correct classification in terms of *Arabica* and *Robusta* on the basis of the σ_{ka} values of single beans (figure 40, bottom; figure 41, top). However, there are remarkable exceptions referring to three beans of three different *Robusta*

batches (# 31, #32, and #33). In these cases, the σ_{ka} values are outside the "normal" variations of *Robusta* coffee (*vide supra*) and fall into the range indicative for *Arabica* (figure 40, bottom). These unexpected values were found to be reproducible in independent measurements from the same beans. Since in these specific cases erroneous classification by the supplier are not very likely, the data indicate that individual beans of *Robusta* batches may possess unusually high kahweol contents. This finding is quite surprising and has, to our knowledge, not yet reported before since classical analytic approaches usually sample of a large number of beans. The observed heterogeneity could be related to differences in fruit maturation in time and to the impact of the biochemosphere. Further studies are necessary to evaluate the influence of environmental factors in green coffee bean kahweol content. In this respect, the present Raman spectroscopic approach offers the opportunity to explore those parameters controlling the production of kahweol in coffee beans of the same type and origin. Comparing ground and whole beans in a systematic manner, one may clarify whether unusually high σ_{ka} values specifically for *Robusta* beans (*vide supra*; Figure 40, bottom) are partially or entirely the result of the (accidental) match of the laser spot with a region of high kahweol concentrations.

6.3.4. The potential of the approach for routine analysis of coffee

The spectral kahweol index introduced in this work to characterize the various samples and to distinguish between *Arabica* and *Robusta* is proportional to the actual kahweol content (*e.g.* in w/w of dry mass). The determination of the proportional factor requires calibration of the spectral index on the basis of samples of known kahweol content via chemical analyses. Such a calibration is a prerequisite for developing the present Raman spectroscopic approach towards a highly accurate and rapid analytical tool for coffee quality control. However, already the spectral kahweol index that is readily derived from the Raman spectra represents a sound criterion to classify green coffee beans if the kahweol content is considered to be an adequate marker. In fact, previous chromatographic analyses have demonstrated that the kahweol content in green coffee beans varies between 0.11 and 0.35 % of the dry mass for *Arabica* whereas kahweol could only be detected as traces in *Robusta* (de Roos *et al.*, 1997; Dias et al., 2010; Kurzrock *et al.*, 2001; Rubayiza *et al.*, 2005). Particularly high kahweol contents have been determined for *Arabica* coffee from Brazil with ca. 0.6% in fresh fruits (Dias *et al*., 2010). These data are in qualitative agreement with the average kahweol indices for *Arabica* of 23 ± 5 and *Robusta* of 3 ± 3, as derived from all samples studied in this work (tables 19 and 2o). Among them, the *Arabica* coffees from Brazil exhibit a mean kahweol index that is higher than average value of 23. On the basis of the present results, one may estimate the detection limit for *Robusta* contaminations in ground and whole bean measurements. For powder measurements, the detection limit critically depends on the knowledge of the expected kahweol content for the pure *Arabica* batch. Assuming a ten-time higher kahweol content in *Arabica* than in *Robusta* and taking into

account the accuracy of an individual measurement of 3.5 %, the theoretical detection limit of *Robusta* in a sample of coffee powder is evaluated to ca. 4 %. However, particularly in view of the quite substantial bean-to-bean variation of the kahweol content in coffee even of the same origin, an accurate reference value for the kahweol content of a specific *Arabica* sample will usually not be available. Then the accuracy of this procedure is determined by the variations of the kahweol content in *Arabica* coffees in general and thus will not be better than 10 %. In this respect, analytical procedures that rely upon more than just one marker are more accurate (Kölling-Speer *et al*., 1999; Kurzrock *et al*., 2001). The situation is different for the analysis on the basis of whole beans since the distinction between *Arabica* and *Robusta* is possible for individual beans given that a few measurements are carried out for the same bean to account for the heterogeneous intra-bean kahweol distribution. Here the average kahweol indices for *Arabica* of 23 ± 5 and *Robusta* of 3 ± 3 can be considered as sound criteria. Then, the detection limit for *Robusta* contaminations in a batch of *Arabica* coffee solely depends on the number of beans investigated and thus may well compete with certified chromatographic procedures associated with a detection limit of 1 % (Kölling-Speer *et al*., 1999; Kurzrock *et al*., 2001). Moreover, in contrast to the present approach, conventional analytical techniques, which lack this single-bean sensitivity and, instead, average over many beans, cannot distinguish between contaminations of coffee samples by Robusta beans and samples of pure Arabica coffee with somewhat lower kahweol content. The intriguing advantage of the present spectroscopic approach is that it can be performed without any time-consuming chemical processing of the coffee beans, and in the case of whole-bean measurements even without mechanical pre-treatment. Furthermore, this approach does not rely on pattern-matching spectral techniques which depend upon spectral differences regardless of the molecular origin, or are sensitive to the sample (pre-) treatment (*e.g*., water content). Instead, it is based on the relative contribution of a specific chemical ingredient of the coffee beans (*i.e.* kahweol) and thus may be applied as an accurate tool in all cases where the kahweol content is a classification criterion, *i.e.* distinction between *Arabica* and *Robusta*, detection of admixtures of *Robusta* to *Arabica*, and possibly also the identification of different origins (de Roos *et al*., 1997). A single Raman spectroscopic measurement of a coffee sample (powder or bean) does not require more than six minutes. Thus, the technique is much less time-consuming and less costly compared to chemical methods such that a reliable analysis of a given coffee sample can be obtained within less than an hour for powder samples and for whole beans within a few hours depending on the desired accuracy. Improved technical adaptation of the equipment to the needs of these specific experiments and optimization of the evaluation software are expected to further reduce the times required for the spectroscopic analysis. Fields of applications are, for example, quality control by coffee roasting companies and coffee dealers, or monitoring of the growth and development of beans at coffee plants.

7. New analytical strategies for the characterization and discrimination of roasted coffee aroma

7.1. Aroma profile discrimination of coffees and industrial blends according to the chromatic value

Rodrigues, C., Máguas, C., Nogueira, J.M.F. (*submitted*)

7.1.1. Introduction

Different mixtures of roasted coffee originate different blends whose aroma and flavour can be quite distinct and exquisite (Mendes *et al.*, 2001). *Arabica* coffee is usually used in blends for the aroma effect whereas *Robusta* is used for taste and body (Correia, 1990). Nevertheless, if the type of coffee is an important factor determining blend quality, other characteristics such as origin and roasting conditions may also affect the final product quality. To obtain a good cup of coffee, the step of roasting is a very important task in order to develop specific organoleptic properties, *i.e.* flavour, aroma and colour (Hernandéz *et al.*, 2007). During this process, pyrolitic reactions take place leading to the formation of volatile and semi-volatile aroma compounds responsible for the sensory qualities of roasted coffee (Grosch, 2001; Hernandéz *et al.*, 2007). Therefore, roasting temperature affects the volatiles profile by favouring different reactions and product removal pathways at different processing conditions (Franca *et al.*, 2009). Industrially, the degree of roast is evaluated by measuring roasted ground beans light reflectance and by visual inspection of the colour of the beans. The value obtained by light reflectance is often designated as the "chromatic value" of the roasted coffee, as it is related to the degree of roast and ultimately with the final colour of the roasted beans (Mendoza *et al.*, 2006). The offer of commercial *gourmet* blends has increased largely over the last years since the greater quality of these products demands a higher degree of quality control. There is a major concern in maintaining the aroma characteristics of those blends over time. To manage this, coffee industry has to rely on analytical methods that are reproducible and more efficient on general aroma compounds profile determination. Solid-phase microextraction in the static headspace mode combined with gas chromatography coupled to mass spectrometry (HS-SPME/GC-MS) has been largely accepted for the determination of aroma compounds in many food stuffs such as fruits (Ferreira *et al.*, 2009), beverages (Alves *et al.*, 2005; Câmara *et al.*, 2007), sauces (Harmon, 2002) and coffee (Akiyama *et al.*, 2003; Akiyama *et al.*, 2005; Roberts *et al.*, 2000; Rocha *et al.*, 2003; Sanz *et al.*, 2001). HS-SPME is a reproducible and precise methodology although the optimization concerning

the selection of the most suitable fibre coating polarity as well as the most important experimental parameters, which are known to influence the sampling performance of the system under study are required (Pawliszyn, 1997). In the case of HS-SPME application on roasted coffee samples, several methodologies are reported in literature that demonstrate the best conditions for the enrichment of the aroma compounds (Akiyama *et al.*, 2003; Akiyama *et al.*, 2005; Franca *et al.*, 2009; Roberts *et al.*, 2000; Rocha *et al.*, 2003; Sanz *et al.*, 2001). Important coffee aroma compounds have been identified by the former authors by applying this methodology, *e.g.* pyridine, the pyrazines 2-methylpyrazine, 2,5-dimethylpyrazine, 2,6-dimethylpyrazine, 2-ethyl-6-methylpyrazine and 2-ethyl-5-methylpyrazine, the furans 2-furancarboxaldehyde, 2-furanmethanol and 5-methyl-furfural, the phenolics 2-methoxyphenol (guaiacol), 2-methoxy-4-vinylphenol (vinylguaicol) and 4-ethyl-2-methoxyphenol, the pyrroles 1H-pyrrole-2-carboxaldehyde and 1-(1-H-pyrrol-2-il)-ethanone, as well as maltol and acetic acid. Nonetheless, few studies have showed how SPME fibres performance may change with the degree of roast and which fibre is more convenient to evaluate the aroma independently of the roasting degree. Recently, Franca *et al.* (Franca *et al.*, 2009) have introduced this concept by assaying at laboratory scale a preliminary evaluation of the effect of roasting temperature on coffee aroma compounds using the HS/GC-MS approach. However, the aroma compounds of roasted coffee obtained at an industrial quality control laboratory, according to in-house quality control methods, were never characterized in relation to different chromatic values. The aim of the work presented in this section was to develop a methodology adapted to quality control on different chromatic values of coffee and blends at industrial laboratories in order to promote the aroma profile characterization and differentiation. The discrimination of the aroma compounds found at different roasting levels has been evaluated through Kruskal-Wallis analysis of variance and multivariate data analysis.

7.1.2. Experimental

7.1.2.1. Samples

Different roasting bean colour samples were prepared with commercial *Arabica* Brazilian green coffee (crude) at Novadelta S.A. industrial installation (Campo Maior, Portugal). The green coffee was roasted in Novadelta's quality control laboratory using a Probat (Germany) roaster and each degree of roast was prepared with 300 g of green coffee. The roaster was allowed to cool between the different roasts. The chromatic values of grinded roasted coffee samples were determined using a Colour Reflectance Meter (Dr. Lange, Germany). The in-house chromatic values practice for the coffee analysed was from 73 to 83. The aroma profiles achieved in the roasted samples were for chromatic values from 64.9 (dark roast), 70.6, 75.3, 86.9 and 89.6 (light roast). Dr. Lange chromatic values are lower when roasting is heavier and higher for lighter

roasting degrees (González-Miret *et al.*, 2007). The roasting degrees and experimental roasting conditions are summarized in table 21. One batch for each treatment was obtained. Samples were grinded in an industrial grinder at a degree of grinding 13 (Mahlkoning, Germany) at Novadelta and immediately transferred to 20 mL vials for transportation and kept at -20 ºC until analysis.

Table 21. Experimental roasting conditions for the different chromatic values.

Chromatic Value	**Roasting Final Temperature (ºC)**	**Roasting Time (min)**
89.6	175	8.8
86.1	185	9.5
75.3	190	10.0
70.6	190	10.5
64.9	195	11.0

7.1.2.2. HS-SPME assays

A manual SPME device and fibres coated with polydimethylsiloxane (PDMS; 100 μm), Carboxen-PDMS (CAR/PDMS; 75 μm) and PDMS-divinylbenzene (PDMS/DVB; 65 μm) polymeric phases were supplied from Supelco Inc. (Bellefonte, PA, USA). 2.0 g of grounded coffee sample were placed into 20 mL vials sealed with caps having PTFE-faced silicone septa (Supelco) using a manual crimper and placed in a water bath maintained at 60 ºC. For sampling, the SPME fibre was inserted into the HS during 60 min at 60 ºC, according to other authors (Chen *et al.*, 2007; Rocha *et al.*, 2003; Zambonin *et al.*, 2005). Subsequently, the SPME device was introduced in the injector port for GC-MS analysis and was allowed to remain in the inlet for 10 minutes. Blank runs using empty vials instead of sample were done in order to control for possible memory effects.

7.1.2.3. GC-MS analysis

GC-MS analysis was performed on an Agilent 6890 series gas chromatograph interfaced to an Agilent 5973 *N* mass selective detector (Agilent Technologies, Little Falls, DE, USA). A vaporization injector was used in the splitless mode (2 min) at 270 ºC using a fused silica capillary column, 30 m × 0.32 mm ID × 0.25 μm film thickness (HP-5MS; 5% diphenyl 95% dimethyl polydimethylsiloxane, Agilent Technologies). The oven temperature program was 40 ºC for 1 min, 40-150 ºC at 3 ºC/min, 150 ºC for 15 min, 150-250 ºC at 5 ºC/min and 250 ºC for 5 min according to Zambonin *et al*., (2005). Helium was used as carrier gas at 35 cm sec^{-1}. Electron ionisation mass spectra in the range 40-400 Da were recorded at 70 eV. The quadrupole, source and transfer line temperatures were maintained at 150, 230 and 280 ºC, respectively, and a turbo molecular pump (10^{-5} torr) was used. All data were recorded using a MS ChemStation (G1701CA; Rev C.00.00; Agilent Technologies). Volatile compounds were tentatively identified by comparing their mass spectra with the Wiley´s library spectral data bank (G1035B; Rev D.02.00; Agilent Technologies) and retention index (RI) using C_{10}-C_{24} *n*-alkanes, as well as by comparison with Adams database (Adams, 2001). All samples having different chromatic values were analysed in triplicate by HS-SPME. For semi-quantification purposes, the average of abundances (n=3) of each identified compound was accepted whenever the standard deviation was lower than 5 %.

7.1.2.4. Statistic analysis

Kruskal-Wallis analysis of variance was performed according to VassarStats (Vassar College, USA). For principal component analysis (PCA), the average abundances of the aroma compounds obtained by HS-SPME(CAR/PDMS)/GC-MS assays were standardized and used as variables for object description (chromatic values), and performed with Statistica 8.0 software (Statsoft, USA).

7.1.3. Results and discussion

7.1.3.1. Aroma characterization according to the chromatic values

From the onset, SPME fibers were selected according to the best response to the volatile aroma compounds expected to be found in the HS of roasted coffee samples. In

a first approach, the PDMS fiber was found to present good sensitivity and stability among the set of the tested fibers, namely under repeated assays. Nevertheless, since aroma compounds in roasted coffee also include targets with a great prominence of polar characteristics, other fibres such as CAR/PDMS and PDMS/DVB were also tested. Therefore, to select the best polymeric coating, HS-SPME assays on *Arabica* coffee samples from Brazil were carried out under a temperature of 60 ºC for 60 minutes (Rocha *et al.*, 2003; Sanz *et al.*, 2001). Figure 42 shows the main differences on the average abundances of several chemical classes observed by using three fibre types (PDMS/DVB (a), PDMS (b) and CAR/PDMS (c)) obtained by HS-SPME/GC-MS analysis on roasting coffee samples having different chromatic values. From the data obtained it is possible to observe that the HS-SPME(CAR/PDMS)/GC-MS assays show a much higher average of abundances in what relates to pyrazines, furans, pyridines, acids and ketones (figure 42c), the most relevant classes of aroma compounds usually founded in roasted coffee aroma. The statistical comparison in between the abundances variance obtained by each fiber for the different chromatic value was performed through *F*-test in order to evaluate if it was possible to apply the parametric single-factor ANOVA. Nevertheless, this was not possible as the data from *F*-test did not allow the rejecting of the null hypothesis (H_0 : there is no difference between variances) (Bröhan *et al.*, 2009). As a consequence, the one-way comparison of abundances variance was done through the Kruskal-Wallis test for the most relevant chemical classes corresponding to each chromatic value, *i.e.* pyrazines, furans, pyridines, acids and ketones. Therefore, for the different chromatic levels assayed, the abundances difference among the three fibres tested were quite significant ($p < 0.05$) and we can prove that CAR/PDMS fiber is the most effective, under similar experimental conditions. Pyridines were identified by Franca *et al.* (Franca *et al.*, 2009), as being characteristic of samples submitted to a dark roast; similarly, these compounds had a higher influence on our sample discrimination, as it will be shown in the subsequent multivariate data analysis. Equivalent results were also obtained by other authors (Akiyama *et al.*, 2003), where CAR/PDMS fibre showed much better response for compounds such as 2-methylfuran, 2- and 3-methylbutanals, 1-methyl-1H-pyrrole and 1H-pyrrole, although with lower level of 2-methoxyphenol, 4-ethenyl-2-methoxyphenol and 4-hydroxy-2,5-dimethyl-3(*2H)*-furanone, in relation to the other two fibre types (PDMS and PDMS/DVB). These authors also state that PDMS is the fibre coating with the lowest sensitivity to analyse typical aroma compounds from coffee matrices, which is also agreement with our data. Table 22 summarizes the aroma compounds and the average composition founded by HS-SPME(CAR/PDMS)/GC-MS methodology in Brazilian roasted coffee samples having different chromatic values. The volatile fraction of roasted coffee can be grouped in the following chemical classes, namely, pyrroles, ketones, pyrazines, furans, phenolics, pyridines, alcohols and acids (table 22), where the compounds achieved in the HS had already been reported in the literature (Akiyama *et al.*, 2003; Akiyama *et al.*, 2005; Amastalden *et al.*, 2001; Bicchi *et al.*, 1997; Buffo *et al.*, 2004; González-Rios *et al.*, 2007; Grosch, 2001; Huang *et al.*, 2007; Ishikawa *et al.*, 2004; Rocha *et al.*, 2003; Sanz *et al.*, 2001; Yeretzian *et al.*, 2002;

Zambonin *et al.*, 2005), which are known to coming from the Maillard reactions and Strecker's degradations.

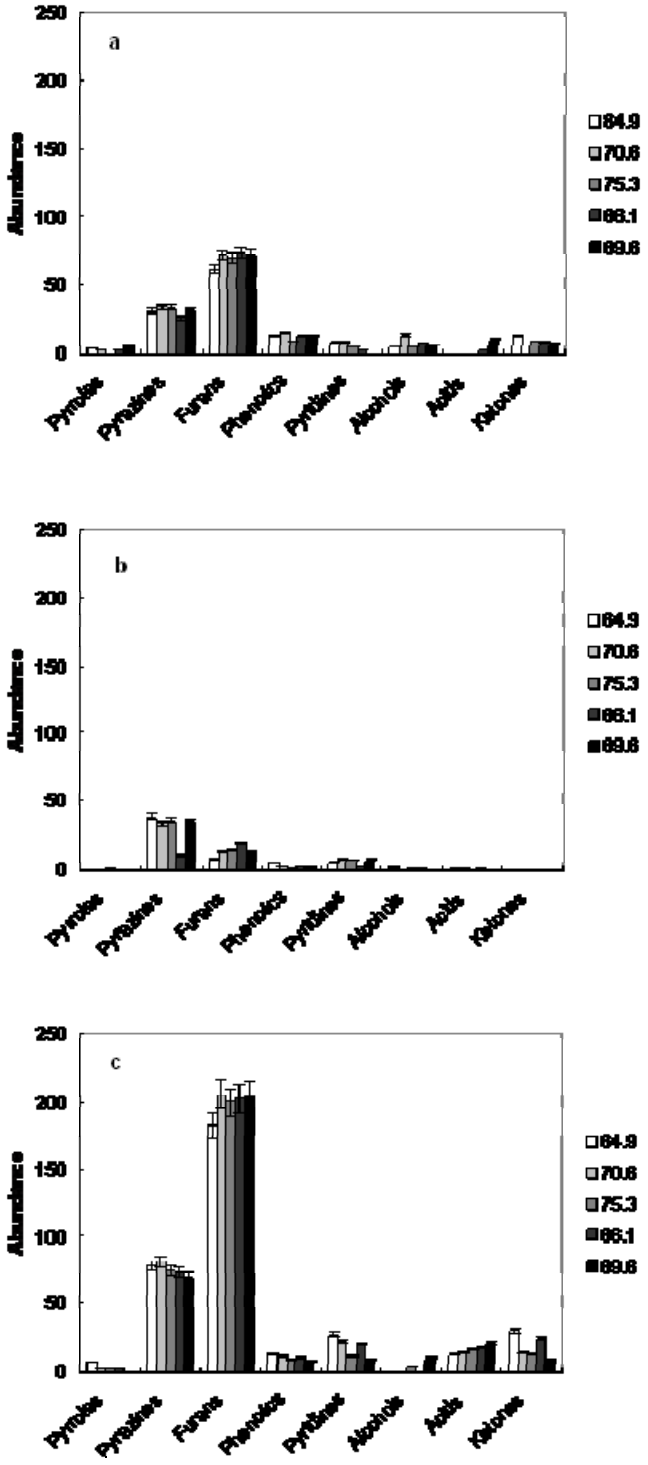

Figure 42. Average abundances ($\times 10^7$) of chemical classes of aroma compounds obtained by HS-SPME/GC-MS using PDMS/DVB (a), PDMS (b) and CAR/PDMS (c) fibres on roasting coffee samples having different chromatic values.

Table 22. Aroma compounds and average composition found in Brazilian coffees with different chromatic values obtained by HS-SPME(CAR/PDMS)/GC-MS.

		%[1]				
		Chromatic Value				
Compound	RI[2]	64.9	70.6	75.3	86.1	89.6
Pyrroles						
1H-pyrrole-2-carboxaldehyde	1166	1.3				
1-(2-furanylmethyl)-1H-pyrrol	1162	1.0	0.8	0.7	0.8	
Total pyrroles		2.3	0.8	0.7	0.8	
Ketones						
1-(1H-pyrrol-2-yl)-ethanone	1047	3.6			2.8	2.8
3-hydroxy-2-methyl-4H-pyran-4-one	1094	5.6	4.1	4.0		
1-(6-methyl-2-pyrazinyl)-1-ethanone	1095				4.5	
Total ketones		9.1	4.1	4.0	7.3	2.8
Pyrazines						
2-methylpyrazine	813	5.4	5.8	5.4	5.5	
2,5-dimethylpyrazine	885	16.5	16.9	15.5	16.5	19.0
3-ethyl-2,5-dimethylpyrazine	1052	1.5	1.7	1.4		1.8
Total pyrazines		23.4	24.4	22.3	22.0	20.8
Furans						
2-furancarboxaldehyde	820	11.4	15.9	15.8	17.2	18.4
2-furanmethanol	848	20.3	19.8	20.5	18.9	18.4
5-methyl-2-furancarboxaldehyde	937	15.6	19.7	18.1	19.2	18.8
2-furanmethanol, acetate	966	8.0	6.9	6.0	6.0	6.2
Total furans		55.3	62.2	60.5	61.3	61.9
Phenolic compounds						
2-methoxyphenol	1063	2.4	2.2	1.5	1.8	1.9
4-ethyl-2-methoxyphenol	1264	0.5		0.4		
2-methoxy-4-vinylphenol	1300	1.1	1.2	1.1	1.5	0.6
Total phenolic compounds		4.0	3.4	2.9	3.3	2.5
Pyridines						
pyridine	772	8.3	6.7	3.4	6.2	2.7
Total pyridines		8.3	6.7	3.4	6.2	2.7
Alcohols						
1,3-butanediol	801			1.2		
maltol	1094					3.0
Total alcohols				1.2		3.0
Acids						
acetic acid	744	3.8	4.4	4.9	5.3	6.3
Total acids		3.8	4.4	4.9	5.3	6.3

[1]Relative to the optimum chromatic value (75.3); [2]Retention index relative to C_{10}-C_{24} *n*-alkenes (for conditions see experimental section).

The flavour development during roasting depends on the time-temperature processing in which the beans are conditioned (Yeretzian *et al.*, 2002). Thus, a chromatic value of 64.9 showed lower peak abundance for furans that are usually associated with caramel and spicy sensory notes (Akiyama *et al.*, 2003; Berlitz *et al.*,

2004; Czerny *et al.*, 1999). In the case of coffee with a chromatic value of 89.6 (the lightest roast degree studied), pyrazines, ketones, pyridine and phenolics appeared in lower abundance (figure 42c). When the degree of roast is lighter some of these aroma compounds are not formed. For higher chromatic values, a lower level of these compounds, which are known to be formed in final roasting stages, combined with a higher abundance of organic acids usually produces a brew with accentuated acidity but with a very poor aroma. With a more intensive roast, pyrazines are formed and the well-known nutty-roast smell of roasted coffee will be developed (Berlitz *et al.*, 2004). The data obtained show that a different aroma profile will developed, depending on the time-temperature of the roasting process. In short, HS-SPME(CAR/PDMS)/GC-MS analytical approach proved to have the best performance for the characterization of aroma profiles from coffee samples independently of the chromatic value they exhibit.

7.1.3.2. Profile discrimination of roasted coffees

As stated in the previous section, HS-SPME(CAR/PDMS)/GC-MS methodology applied to coffee samples having different chromatic values, revealed different aroma profiles. From the data obtained (table 22), the ANOVA (Kruskal-Wallis) test allowed confirming the significance of these differences ($p < 0.005$) for the chemical classes of pyrroles, phenolics, pyridines and acids. Subsequently, PCA was performed to verify the discrimination in between different degrees of roast based on the average abundance of the aroma compounds obtained by HS-SPME(CAR/PDMS)/GC-MS assays. Figure 43 depicts the PCA from the average abundances of 1H-pyrrole-2-carboxaldehyde, 2,5-dimethylpyrazine, 2-furancarboxaldehyde, 2-furanmethanol, 5-methyl-2-furancarboxaldehyde, pyridine, 1,3-butanediol, maltol and acetic acid. All these compounds are known to play a key role in the discrimination of the final aroma of roasted coffee. The first two PCs presenting, respectively, eigenvalues of 5.36 and 2.23, which explain 77.9 % of the variability among the chromatic variance (figure 43). An enough differentiation between the lightest and darkest degrees of roasting was obtained based on the first component, where the light roast (chromatic value 89.6) was negative and the dark roast (chromatic value 64.9) was positive. The variables that influenced PC1 were 2-furancarboxaldehyde, 2-furanmethanol and acetic acid. On the other hand, in the case of PC2, 1H-pyrrole-2-carboxaldehyde, 2,5-dimethylpyrazine and 1,3-butanediol seems to have the greater contribution. The chromatic value 75.3, *i.e*. the optimum roasting degree according to the industrial practice, presents an intermediate behaviour according to PC1 and discriminated from the other roasted samples in relation to PC2. A lower abundance of phenolics and pyridine (table 22) seems to contribute for the discrimination between chromatic value 86.1 and the other roasted samples.

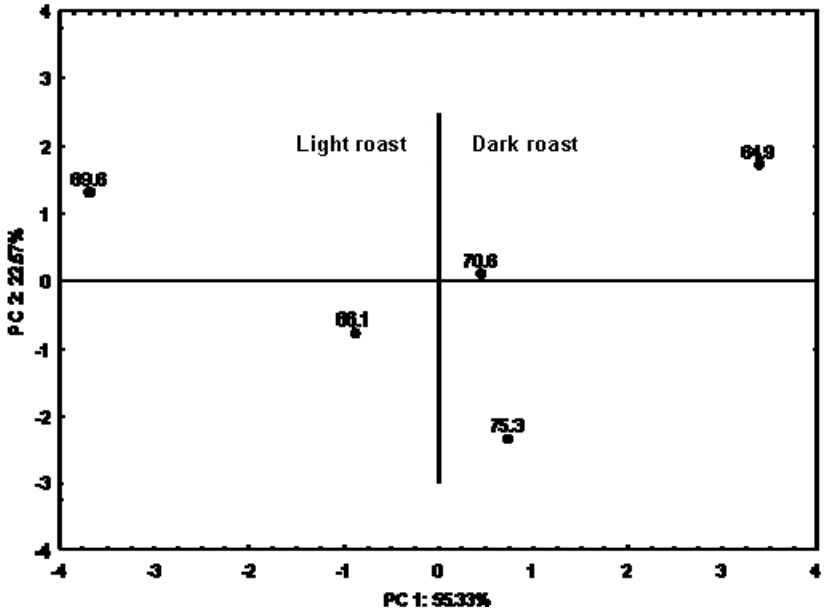

Figure 43. PCA scores scatter plot of the sum of average abundances of the chemical classes from roasted coffees having different chromatic values, obtained by HS-SPME(CAR/PDMS)/GC-MS analysis.

The above mentioned volatile constituents are relevant coffee aroma compounds produced at different stages of the roasting process. To obtain different chromatic values of the same coffee it is necessary to vary the time of the roasting process. In result, we obtain higher chromatic values rich in aroma compounds characteristic of the initial stages of roasting, and with lower concentration of compounds that would be produced it the later stages of the roasting process (*e.g.* pyridines). In the case of the lower chromatic values, the inverse is observed. According to Yeretzian *et al.* (Yeretzian *et al.*, 2002), there are two distinct phases in the roasting process, initially starting with an endothermic drying phase followed by a second exothermic phase with massive formation of volatile compounds. During this stage, a strong change occurs in the aroma composition over time. This author's demonstrated a highest level of 'pyrrol' at dark and very dark degrees of roast, which may explain our data and the importance of this particular chemical class for the discrimination of chromatic values observed. In what relates to our highest chromatic value (89.6), corresponding to the lightest degree of roast, acids and alcohols played a major role discriminating those from other chromatic values. Several authors have also reported a higher abundance of compounds of these chemical families in *Arabica* coffees when the roasting is lighter (Rodrigues *et al.*, 2007; Yeretzian *et al*., 2002). This observation may explain the importance of the total abundance of these types of compounds in the discrimination of our highest chromatic values from all other roasting degree.

7.1.4. Conclusions

Our data shows that different coffees could be discriminated based on HS-SPME(CAR/PDMS)/GC-MS/PCA methodology independently of the roasted degree, which may be used in roasted coffee routine quality control. It may help to build aroma profile databases to a better evaluation of coffee blends quality, development of high quality gourmet blends and in controlling the industrial roasting processes. The described methodology may eventually be applied to other foodstuff matrices in order to develop a narrower control of their production and quality at industry.

7.2. Static headspace analysis using polyurethane phases - application to coffee volatile fraction characterization and discrimination

Rodrigues, C., Portugal, F.C.M., Nogueira, J.M.F. (*submitted*).

7.2.1. Introduction

During the last years, sorptive extraction techniques have played a very important role in trace analysis, especially to monitor many classes of organic compounds in several types of matrices (Smith, 2003). So far, numerous enrichment methods have been proposed prior to chromatographic analysis, such as solid phase extraction, solid phase micro-extraction (SPME) (Arthur *et al.,* 2002) and more recently, stir bar sorptive extraction (SBSE) (Baltussen *et al.*, 1999). The latter one in particular, was introduced as a novel sample preparation methodology based on the same principles of SPME, which has been successfully applied especially to screen traces of priority organic pollutants in water and many other matrices (Almeida *et al*., 2006; Coelho *et al*., 2008; Neng *et al*., 2007; Rosário *et al*., 2006; Serôdio *et al.,* 2004, 2005, 2007; Silva *et al*., 2008a; Sisali *et al*., 2006) SBSE is an environmentally friendly technology since it is a solventless approach, easy to manipulate, presenting remarkable reproducibility and very good sensitivity for trace level analysis. Meanwhile, SBSE is only commercially available with a nonpolar polydimethylsiloxane (PDMS) phase, which cannot retain all types of analytes, in particular, the more polar ones (log $K_{O/W}$ < 3). To overcome this limitation, several authors have recently proposed other strategies, such as the dual-phase stir bar [14], as well as other polymeric phases (Hu *et al*., 2007; Mehdinla *et al*., 2008), but for very specific analytes without embracing the ruggedness and the wide range of applicability demonstrated by the PDMS polymer. Recently, our group has introduced the polyurethane (PU) foams as a novel polymeric phase for SBSE, due the very interesting physical and chemical properties they exhibit (Neng *et al*., 2007). These polymers are easily to produced through the reaction of polyisocyanate with polyols and water in the presence of a specific catalyst (Hatchet *et al*., 2005). Through this synthesis reaction, a very versatile material is obtained, whose degree of rigidity depends on the desired application, in which we proved to have great capacity to retain polar compounds by SBSE, especially to monitor several classes of priority compounds in aqueous media (Portugal *et al*., 2008; Silva *et al*., 2008b; Portugal *et al*., 2010). Besides the remarkable performance attained to monitor organic priority pollutants in liquid phase, PU polymeric phases were never been tested in the HS mode for volatile analysis. A way to evaluate the performance of novel analytical approaches or polymeric phases in the HS mode can be by testing well-known volatile systems (Risticevic *et al*., 2008). For instance, coffee aroma in particular, is highly complex and largely studied by the food chemistry scientific community, mainly to characterize the

volatile aroma compounds, where HS-SPME with carboxen/polydimethylsiloxane (CAR/PDMS) polymeric fibre has demonstrated good analytical performance (Bicchi *et al*., 2002).

In this work we propose, for the first time, the application of static headspace sorptive extraction with PU foams (HSSE(PU)) for volatile analysis followed by gas chromatography-mass spectrometry (GC-MS), using coffee aroma compounds as model system. The advantages and performance achieved for characterization purposes, as well as the comparison in between HS-SPME(CAR/PDMS), HS-SBSE(PDMS) and HSSE(PU) methodologies is also addressed. The applicability and the robustness of the HSSE(PU) approach has also been tested for the discrimination of commercial *gourmet* coffee blends and roasting profiles.

7.2.2. Experimental

7.2.2.1. Chemicals

Certified reagents and standards were used. HPLC-grade methanol (MeOH, 99.9%, Panreac, Spain), acetonitrile (ACN, 99.9%, LabScan, Poland), iso-propanol (99.7% Carlo Erba, Italy), pentane (99%, Riedel-de Haën, Germany), diethyl ether (99.5%, Absolve-José Manuel Gomes dos Santos, Portugal) and acetone (99.8% Panreac, Spain). For the synthesis of the PU phases, the reagents used were a tin catalyst, silicon oil (Dow Corning, Midland, USA), methylene bisphenyl diisocyanate (Lupanat, BSF, Lemförde, Germany), ultra-pure water, glycerol propoxylate (Sigma-Aldrich) and trimethylolpropane ethoxylate (Sigma-Aldrich), PU synthesis and clean-up procedures were performed according to previous report (Wihlborg *et al.*, 2008). Ultra-pure water was obtained from Milli-Q water purification systems (Millipore, Bedford, MA, USA). Commercial stir bars (Twister; Gerstel, Müllheim a/d Ruhr, Germany) coated with PDMS (20 mm length and 1 mm of film thickness; 126 μL) were chosen for HSSE(PDMS). A manual SPME device and fibres coated with CAR/PDMS (75 μm) were supplied from Supelco Inc. (Bellefonte, PA, USA).

7.2.2.2. Samples

Roasted coffee was acquired at the local market and the same blend of coffee was used for the optimisation of the HSSE(PU) method. 2.0 g (Mettler AE 240, Spain) of grounded coffee sample were placed into 20 mL vials sealed with caps having PTFE-faced silicone septa (Supelco). For the applicability studies of the HSSE(PU)-LD/LVI-GC-MS methodology, six *gourmet* coffees were acquired at local market, designated as Classic, Vera Cruz, Kenya, Timor, Mussolo and Colombia. To apply the methodology

for the differentiation of roasting conditions, 200 g of Brazilian green coffee was roasted in laboratory using a domestic roaster. Roasting profile A was composed of three stages: 196 ºC (3 min.), 218 ºC (4 min.) and 235 ºC (2 min.), according to manufacturer. Variations were introduced by reducing (B) or extending (C) the roast time in 2 min. resulting in three different roasting profiles following by HSSE(PU)-LD/LVI-GC-MS analysis, under optimised experimental conditions.

7.2.2.3. HS-SPME assays

For SPME assays, a CAR/PDMS fibre was inserted into the HS of each sample (figure 44a) during 60 min. and the sample was kept in a thermostatised water-bath at 60 ºC, according to several authors (Chen *et al.*, 2007; Rocha *et al.*, 2003; Zambonin *et al.*, 2005). Subsequently, the fiber was introduced in the S/SL injection port of the GC-MS system.

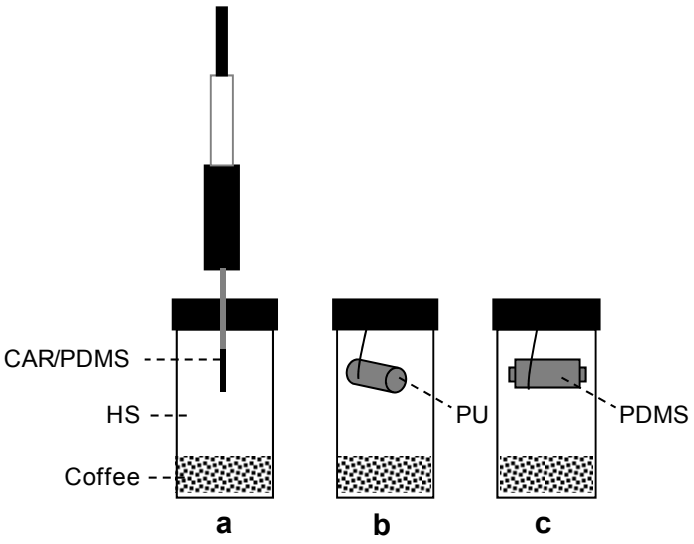

Figure 44. Sampling apparatus applied for the characterization of roasted coffee aroma compounds by HS-SPME(CAR/PDMS) (a), HSSE(PU) (b) and HSSE(PDMS) (c) in the present study.

7.2.2.4. HSSE(PU) and HSSE(PDMS) assays

For HSSE(PU) assays, PU cylinders (1.3 cm length and 0.5 cm diameter) were used having an average volume of 32 µL, according to a previous work (Portugal *et al.*, 2008). For HSSE(PDMS) assays, commercial stir bars were used. Both devices were hold to the silicone septa of each cap by two wires in the middle of the HS (figures 44b and c) and the vials were placed on a thermostatised water-bath, where different

temperatures (30, 60 and 90 ºC) and time (30, 60 and 90 min.) were evaluated. Subsequently, the sampling vials were opened and PU foam cylinders or PDMS stir bars were removed and inserted on 1.5 mL vials, where 1 mL of different back-extraction solvents (acetone, MeOH, iso-propanol, pentane, ACN and diethyl ether) and time (20, 40 and 60 min) were optimised, under ultrasonic treatment, after which they were removed and the extract analysed by LVI-GC-MS. Blank runs using empty vials instead of sample were done in order to control for possible memory effects.

7.2.2.5. GC-MS analysis

For HSSE(PU) and HSSE(PDMS) assays, a programmed temperature vaporization injector (PTV) with a septumless sampling head having a baffled liner (SLH; Gerstel, Mülheim a/d Ruhr, Germany) was used, operating in the solvent vent mode with liquid nitrogen as inlet cooling. For large volume injection (LVI), the solvent vent mode was performed (vent time: 0.30 min; flow rate: 10 mL/min; pressure: 0 psi; purge: 150 mL/min at 2min), in which the inlet temperature was programmed from 45 °C (0.35 min) to 280 °C at a rate of 600 °C/min and, subsequently, decreased to 200 °C (held until end) at a rate of 50 °C/min. The injection volume and speed were 5 µL and 100 µL/min, respectively. For the HS-SPME assays, a split/splitless (S/SL) injector was used, operating in the SL mode. The SPME device was introduced in the injector port (270 ºC) for GC-MS analysis and was allowed to remain in the inlet for 10 min. Blank runs using empty vials instead of sample were done in order to control for possible memory effects. GC-MS analysis were performed on an Agilent 6890 series gas chromatograph equipped with an Agilent 7683 automatic liquid sampler tray (Agilent 7683, Agilent Technologies, Little Falls, DE, USA) and interfaced to an Agilent 5973 *N* mass selective detector (Agilent Technologies, Little Falls, DE, USA). GC analysis was performed on a TRB-5MS (30 m × 0.25 mm i.d., 0.25 mm film thickness) capillary column (5% diphenyl, 95% dimethylpolysiloxane; Teknokroma, Spain). Helium as carrier gas was maintained in the constant pressure mode and the inlet pressure was 9.52 psi with a flow rate of 1.3 mL/min. The oven temperature was programmed from 45 °C (1 min) at 5 °C/min to 200 °C, then at 20 °C/min to 250 °C (5 min) in a 39.50 min running time. The transfer line, ion source, and quadrupole analyzer temperatures were maintained at 280, 230, and 150 ºC, respectively. For HSSE(PU) and HSSE(PDMS) assays a solvent delay of 3 min was selected. The mass spectra were obtained in full-scan mode, with electron ionization mass spectra in the range 35-450 *m*/*z* recorded at 70 eV electron energy, and compared with the Wiley's library reference spectral bank (G1035B; Rev D.02.00; Agilent Technologies, Santa Clara, CA, USA) for aroma compounds identification. Data recording and instrument control were performed by the MSD ChemStation software (G1701CA; version C.00.00; Agilent Technologies, Santa Clara, CA, USA). For semi-quantification purposes, the average of abundances (n = 6) of each identified compound was accepted whenever the standard deviation was lower than 5 %.

7.2.2.6. Statistic analysis

Non-parametric one-way analysis of variance (Kruskal-Wallis) was performed with Statistica software, version 9.0 (StatSoft, US).

7.2.3. Results and discussion

7.2.3.1. HSSE(PU)-LD optimizing conditions

The PU foams had already been proposed as alternative polymeric phase for enrichment purposes with excellent results in what relates to the microextraction of the more polar compounds in aqueous media (Portugal *et al.*, 2008; Silva *et al.*, 2008a; Silva *et al*., 2008b). However, this polymeric phase had never been applied for volatile analysis. Since the volatile fraction of roasted coffee is a very complex matrix constituted by a large number of compounds with very different contents, volatilities and polarities, our intention was to better characterize the aroma through this new analytical approach. So far, HS-SPME(CAR/PDMS) had given very good results on the characterization of roasted coffee aroma and several reports in literature indicate the best experimental conditions to this type of analysis (Franca *et al*., 2009; Zambonin *et al*., 2005). Therefore, to propose and compare different analytical methodologies it is peremptory optimize the experimental conditions for the analysis of coffee aroma compounds. During our study, GC-MS in the full scan mode acquisition is the best choice to identify volatile compounds and we have decided to used liquid desorption (LD) instead of thermal desorption (TD) in order to avoid the formation of possible artifacts. On the other hand, for methodology comparison, *i.e.* HSSE(PU) and HSSE(PDMS), the former just support temperatures as higher as 260 ºC (Portugal *et al*., 2008), which are not the most suitable for the complete back-extraction process, in which "memory effects" can simultaneously occur. Furthermore, to enhance higher sensitivity, LVI were adopted during GC-MS analysis, using an injection of 5 μL, once larger volumes could lead to an increment of solvent background and therefore a lower signal-to-noise ratio is obtained. Since the very beginning, we start to optimize the LD step by selecting different organic solvents (acetone, MeOH, iso-propanol, ACN, pentane and diethyl ether) using standard experimental conditions, *i.e.*, extraction time of 60 min. (60 ºC) and back-extraction of 60 min. under sonification treatment, according to previously reported (Portugal *et al.*, 2008; Portugal *et al.*, 2010; Silva *et al*., 2008b). From the data obtained, MeOH showed to be the best desorption solvent, particularly for the case of ketones, pyrazines, furans, acids and pyridines chemical groups. The LD time (20, 40 and 60 min) was also evaluated and 60 min. was chosen

for further HSSE(PU) assays, corresponding to the minimum period that allowed the best back-extraction of all chemical classes involved. Previous reports (Bicchi *et al.*, 1997), indicating the best equilibration temperature for HS-SPME of volatiles from roasted coffee aroma was the starting point for our study of best temperature for HSSE(PU). Therefore, temperatures of 30, 60 and 90 ºC were tested. From the data achieved, a temperature of 90 ºC allowed the extraction of volatiles in the highest amount, especially in the case of furans, in which were extracted 2 and 10 times more in relation to 30 and 60 ºC, respectively. At 30 ºC, ketones and phenolics were not extracted, whereas the temperature of 60 ºC allowed the extraction of ketones, phenolics, alcohols and pyrazinamides, as well as higher amounts of pyridines, pyrrols, pyrazines, furans and acids. Since the temperature of 60 ºC was easier to control from the experimental point of view, it was selected for further studies. Three equilibration periods of time (30, 60 and 90 min) were also assayed. There was an improvement in the extraction efficiency from 30 to 60 min which was not observed in relation to the equilibration time of 90 min., although acids were the exception, showing a higher level of extraction at 30 min. The data obtained allowed to select an extraction time of 60 min as the best for PU polymeric phases. In short, the results achieved with different HS extraction temperatures, times and different LD conditions (solvent and time) allowed us to establish an optimized HSSE(PU)-LD/LVI-GC-MS methodology (extraction: 60 min. (60 ºC); back-extraction: MeOH (60 min.)), much easier to implement when liquid phases are involved (Portugal *et al*., 2008; Portugal *et al.*, 2010; Silva *et al*., 2008b).

7.2.3.2. Comparison of different methodologies for coffee aroma characterization

HSSE(PU), HSSE(PDMS) and HS-SPME(CAR/PDMS) methodologies were applied under similar optimised conditions, as described in the experimental section, in order to compare the efficiency and selectivity by using different analytical approaches and polymeric phases. Table 23 summarizes the relative average composition of the aroma compounds founded in roasted coffee obtained through the three methodologies, under similar experimental conditions. The aroma compounds achieved in the HS of roasted coffee blends had already been reported by several authors (Akiyama *et al.*, 2003; Buffo *et al.*, 2004; Gonzalez-Rios *et al.*, 2007; Grosch, 2001; Rocha *et al.*, 2003; Sanz *et al.*, 2001; Yeretzian *et al.*, 2002), which are known to be originated from the Maillard reactions in particular due to Strecker's degradations (Yeretzian *et al.*, 2002). A gradient in extraction capacity (in terms of total abundances per chemical class) was observed for HSSE(PU), HS-SPME(CAR/PDMS) and HSSE(PDMS), in which the later showed the lowest efficiency yields, as clearly depict in figure 45. Ketones were better extracted with PU foams as well as pyrroles, pyrazines, furans, alkanes and acids (table 23).

Table 23. Relative average composition of the aroma compounds founded in roasted coffee obtained by HS-SPME(CAR/PDMS), HSSE(PU) and HS-SBSE(PDMS) methodologies followed by GC-MS, under similar experimental conditions.

	%[1]		
Compound	HS-SPME (CAR/PDMS)	HSSE (PU)	HSSE (PDMS)
Ketones			
2-hydroxy-3-methyl-2-cyclopenten-1-one	0.3		
3-hydroxy-2-butanone		0.7	
1-hydroxy-2-propanone		1.6	
1-(acetyloxy)-2-propanone		5.5	1.8
Total ketones	0.3	7.8	1.8
Pyrroles			
1H-pyrrole-2-carboxaldehyde	0.5		
1H-pyrrole-2-carboxaldehyde, 1-methyl-		1.3	
1-(1H-pyrrol-2-yl)-ethanone	1		
1-(1-methyl-1H-pyrrol-2-yl)-ethanone		0.7	0.3
Total pyrroles	1.4	2	0.3
Pyrazines			
2-methylpyrazine	2	4	2.4
2,3-dimethylpyrazine		0.7	0.7
2,5-dimethylpyrazine	5.2	3.7	
(1-methylethenyl)-pyrazine	0.2		
Ethylpyrazine		3	1.9
2-acetyl-3-methylpyrazine		0.6	
2-ethyl-6-methylpyrazine		0.9	
2-ethyl-5-methylpyrazine		1	
2-ethyl-3,5-dimethylpyrazine		0.8	
3-ethyl-5-dimethylpyrazine	0.9		
3-ethyl-2,5-dimethylpyrazine			0.7
1-(6-methyl-2-pyrazinyl)-1-ethanone	1		
2-methyl-5-(1-propenyl)-pyrazine	0.4		
Total pyrazines	9.7	14.7	5.6
Furans			
2-N-butylfuran		0.5	
Furfural	7.3	3.2	1.1
2-furanmethanol	9.4	38.2	6.5
5-methylfurfural	6.2	4	1
2-furanmethanol, acetate	3.7	5.5	2.3
2-furanmethanol, propanoate		0.4	
Furfuryl formate		0.9	
Dihydro-2-methyl-3(2H)-furanone		1.9	
2,5-dimethyl-3(2H)-furanone		0.6	
2,2'-[oxybis(methylene)]bis-furan	0.5		
2,2'-methylene-furan		0.4	
2-methyl-tetrahydrofuran-3-one			0.8
Total furans	27.2	55.7	11.9
Pyridines			
Pyridine	3.2	1.8	3
N-acetyl-4(H)-pyridine		0.7	
Total pyridines	3.2	2.5	3
Alkanes			
Dodecane		0.8	
Tetradecane		0.8	
Total alkanes		1.6	
Phenolics			
2-methoxyphenol (guaiacol)	0.9	0.6	0.1
4-ethyl-2-methoxyphenol	0.8		
2-methoxy-4-vinylphenol	2.8		
1-(2-hydroxy-5-methylphenyl)-ethanone	0.2		
Total phenolics	4.7	0.6	0.1
Benzenic			
3,4-dimethoxy-styrene	0.2		
Total benzenic	0.2		
Acids			
Acetic acid	7.9	10.1	0.6
Total acids	7.9	10.1	0.6
Pyranones			
3-hydroxy-2-methyl-4H-pyran-4-one (maltol)	1		
Total pyranones	1		

[1]Normalized in relation to HSSE(PU) methodology; For conditions see experimental section

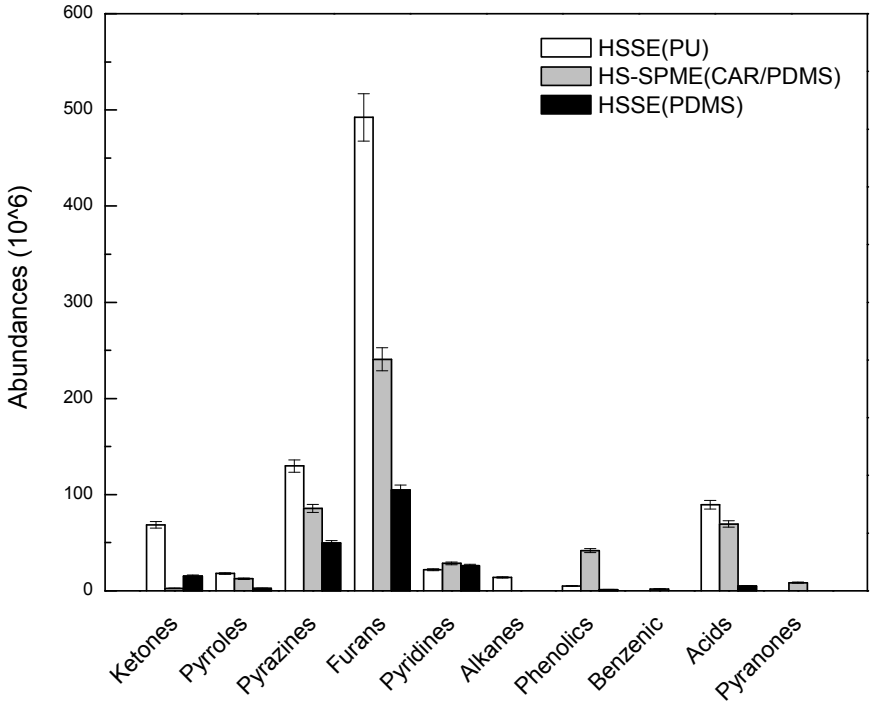

Figure 45. Comparison of the average of total abundances per chemical class from the aroma profile of roasted coffees obtained by HSSE(PU), HS-SPME(CAR/PDMS) and HSSE(PDMS) methodologies followed GC-MS analysis, under similar experimental conditions.

However, phenolic compounds present much higher affinity to CAR/PDMS fiber of the SPME (table 23 and figure 45), although using the thermal desorption mode. Similar behaviours were observed for benzenic compounds and pyranones, which were only extracted by the CAR/PDMS fiber although at very low level (table 23). In the case of pyrazines, ketones, pyridines and furans, which are important coffee aroma compounds, a higher extraction efficiency was due, not only to greater amounts of extracted compounds (figure 45) but also to a larger number of different compounds (table 23) revealed by the HSSE(PU) device in relation to the other two methodologies. For instance, alkanes were exclusively extracted by PU polymeric phases (table 23). Kruskal-Wallis ANOVA of the type of polymeric phase used, as grouping factor, showed that the differences observed in relation to the chemical classes of ketones, pyrazines, furans, phenolics and acids were significant ($p < 0.05$). This evidence proves that HSSE(PU) seems to be very important for the determination of compounds with particular importance for the aroma profile of the different coffee blends, allowing simultaneously the extraction of a wide range of different aroma compounds. The data obtained demonstrates a much higher total abundances per chemical class achieved by the PU foams as the result of the measurable sorptive properties they exhibit, which may be influenced by the residual O-H bonds in the foam matrix (Portugal, 2010; Portugal *et al.*, 2008). When comparing with HS-SPME(CAR/PDMS), the HSSE(PU)

approach seems to be a good alternative for coffee aroma characterization, since a much higher capacity and selectivity seems to be reached in particular for compounds with higher polarity. This methodology shows advantages like being quite affordable and easy to handle, and allowing analytical robustness. Figure 46 compares total ion chromatograms from coffee aroma samples by obtained by HSSE(PU) and HSSE(PDMS) following LD/LVI-GC-MS analysis, where the former methodology demonstrate this evidence, where much higher abundances and number of peaks are notice.

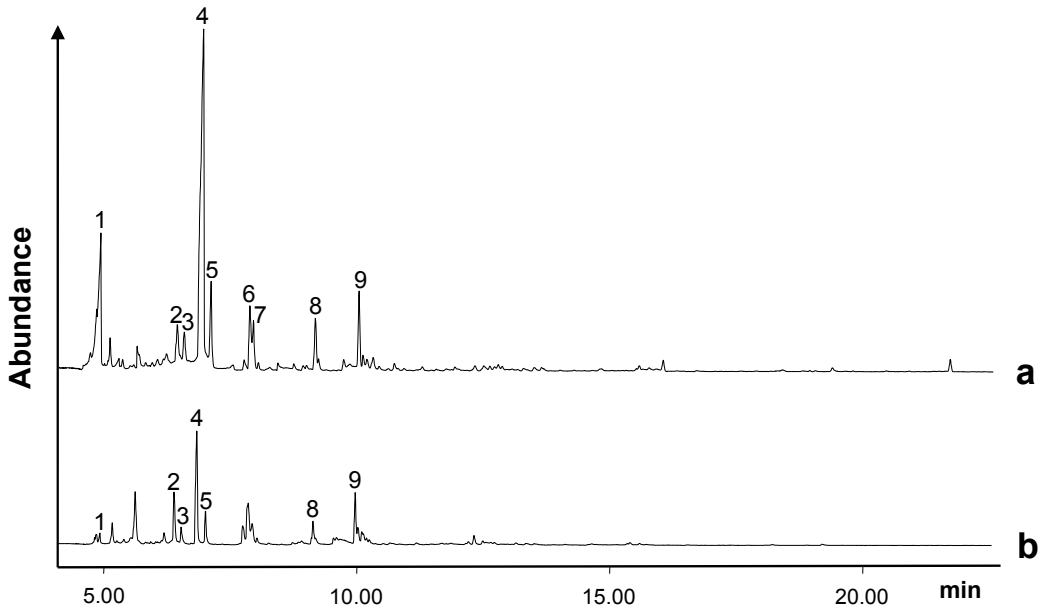

Figure 46. Total ion chromatogram profiles obtained from coffee samples by HSSE(PU) (a) and HSSE(PDMS) (b) following LD/LVI-GC-MS analysis, under optimized experimental conditions. Legend: acetic acid (1); 2-methylpyrazine (2); furfural (3); 2-furanmethanol (4); 1-acetyloxy-2-propanone (5); 2,5 - dimethylpyrazine (6); dihydroxy-2-methyl-3(2H)-furanone (7); 5-methylfurfural (8); 2-furanmethanol, acetate (9).

7.2.3.3. Application of HSSE(PU)-LD/LVI-GC-MS methodology for discrimination gourmet coffee blends

PU foams showed good performance for volatile analysis of complex matrices such as coffee aroma, composed by a large number of volatile organic compounds with great differences in volatility, concentration and polarity. This evidence was demonstrated in the previous section through analysis of the same commercial coffee blend acquired at local market. However, other applications had not been tested by PU polymeric phases in comparison to HS-SPME, which has already been used to discriminate in between different roasted coffee compositions (Sanz *et al.*, 2002) and

roasting degrees (Franca *et al.*, 2009). In the present study, HSSE(PU)-LD/LVI-GC-MS was also applied for the aroma characterization of six different commercial gourmet coffee blends (Classic, Vera Cruz, Kenya, Timor, Mussolo and Colombia). Differences related with type and abundance of compounds has been observed. The Classic blend showed greater overall abundances for pyrroles, pyrazines, furans, phenolics and acids. Additionally, alcohols were only identified in this coffee blend. Furans content was two times higher in Classic, Timor and Kenya blends in relation to Mussolo, Vera Cruz and Colombia. On the other hand, pyrroles were not identified in Mussolo and Colombia blends. Furthermore, phenolic compounds were not extracted from the HS of Kenya and Colombia coffee. Finally, Kenya blend had a greater content in pyridine in relation to the other blends. Therefore, nonparametric (Kruskal-Wallis) ANOVA revealed that the differences observed between each coffee blend in what relates to the total abundance of each chemical class were significant ($p < 0.005$; except for pyrazines, $p < 0.01$). Subsequently, PCA was aplied to the abundances of the identified compounds in order to achieve blend discrimination, as depicted in figure 47a. The five principal components were obtained with eigenvalues of 12.1, 9.6, 6.5, 4.4 and 3.5, respectively. The best blend discrimination was obtained with the two first principal components that explain approximately 60 % of the variability observed, where four groups are defined (figure 47a). Kenya and Mussolo blends are separated from the other coffees. In the case of Kenya blend, pyridine, the ketones (3-hydroxy-butanone, 1-hydroxy-propanone and 1-acetyloxy-propanone), the furans (furfural, furfuryl formate, and furanmethanol), as well as 2,6-dimethylpyrazine, determined its discrimination from other coffees. The pyrazines (2-ethyl-6-methylpyrazine, 2-ethyl-5-methylpyrazine and 3-ethyl-2,5-methylpyrazine) and the furan compound (5-methylfurfural) were the most relevant in the case of Mussolo blend. Acetic and propanoic acids and phenolic compounds (vinylguaiacol and guaiacol), allowed the separation of Classic and Timor blends from the other coffees. These two coffee blends showed differences related with 2-ethyl-3,5-dimethylpyrazine, which was only identified in the HS of Timor blend and, with vinylguaiacol, 2-methyl-tetrahydrofuran-3-one and the alcohols (2-propanol and 1,3-butanediol) found only in the Classic blend volatile fraction. Comparatively to Vera Cruz blend, Colombia does not present compounds from the pyrroles and phenolics chemical groups. This blend had lower number of pyrazine compounds, half of the 5-furanmethanol intensity, no guaiacol and lower pyridine abundance in relation to Vera Cruz. The data obtained through HSSE(PU)-LD/LVI-GC-MS for these six commercial coffee blends, demonstrate that this optimised methodology is a good analytical tool for roasted coffee blend aroma analysis. The results may be combined with information on blend composition, roasting conditions and sensory evaluation to promote better quality control, which facilitate the development of new products. Roasted coffee blends are composed by a mixture of coffee beans from different species and/or varieties that may originate from different locations. The way they are mixed to form the final coffee blend results in its particular aroma characteristics. However, the degree of roast is an important factor determining coffee aroma and flavour (Grosch, 2001).

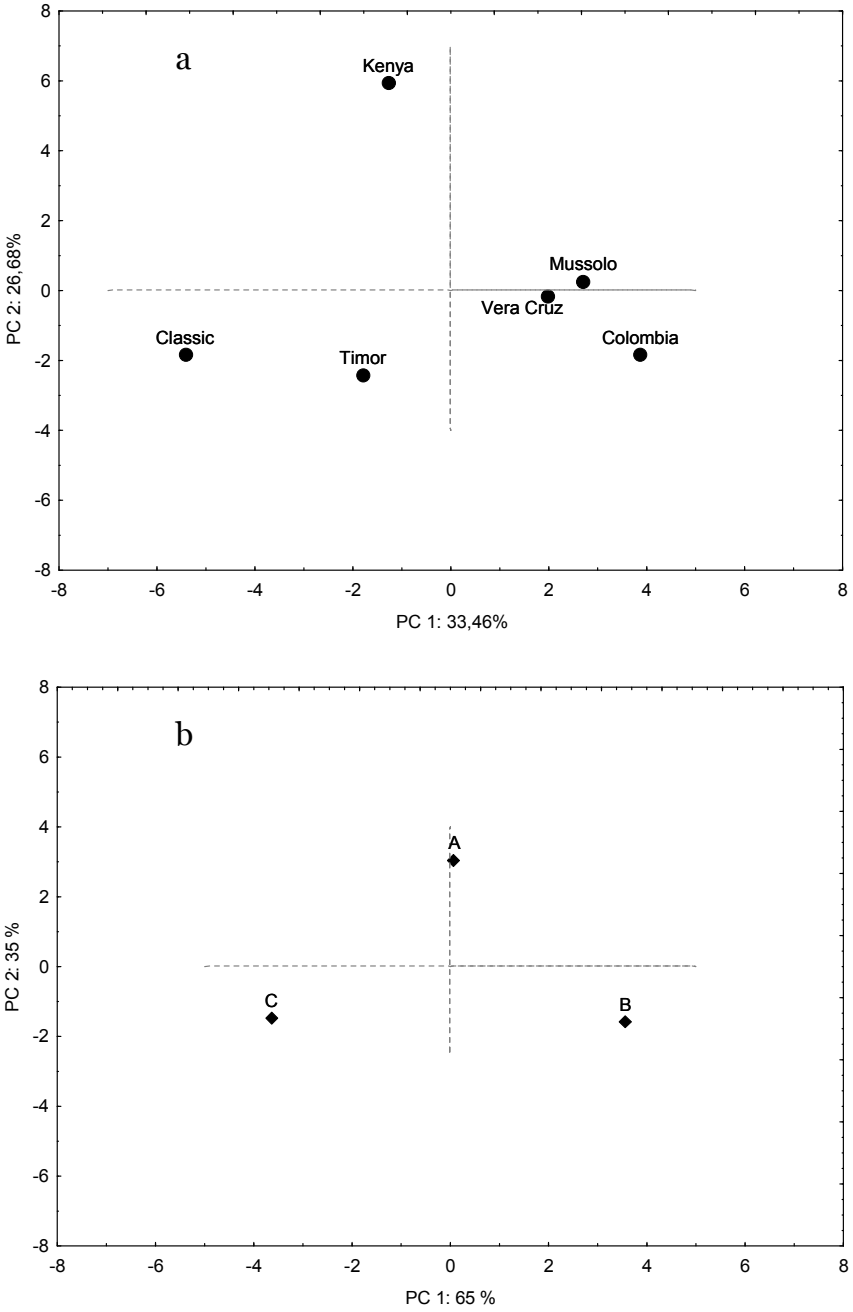

Figure 47. Principal component analysis of abundances of identified aroma compounds in *gourmet* blends (a) and different roasting degree coffees (b) by HSSE(PU)-LD/LVI-GC-MS, under optimised experimental conditions.

Changes in roasting temperature and time profiles may result in major differences in the coffee aroma. This is related to chemical reactions rates that depend on temperature rates and time of roasting to which coffee beans are submitted. In this study, HSSE(PU)-LD/LVI-GC-MS has been also applied to discriminate different

roasting profiles based on the analysis of volatile fraction of coffee. The same Brazilian coffee was submitted to three different roasting profiles, designated as A (light roast), B (- 2 min; the roasting process was stopped 2 min prior to its final) and C (+ 2 min; the roasting process was extended for additional 2 min). There were a lower number of aroma compounds identified in these roasted coffees in comparison with analysis of *gourmet* blends. This is partial due to the fact that only one type of green coffee was used for roasting which results in a less rich aromatic roasted coffee, and also because roasting was conducted at laboratory scale. Nonetheless, more than twenty aroma compounds were identified among the three roasting profiles. Components such as acids and ketones the most abundant in early stages of roasting (Flament, 2002; Rodrigues *et al.*, 2007; Yeretzian *et al.*, 2002). Accordingly, total abundance of these chemical groups was higher for the lighter roasting profile (B). In opposition, pyrroles, some furans (2-furanmethanol) and pyridines are a sign of darker roasts (Flament, 2002; Franca *et al.*, 2009). For this reason, the greater abundance of these aromatics when dark roast profile was applied (C) is observed. Significant differences ($p < 0.05$; ANOVA) were observed in what respects to total abundance of pyridines, acids, ketones and pyrazines. PCA of the abundance of the identified aroma compounds is depicted in figure 47b. HSSE(PU)-LD/LVI-GC-MS allowed the three degrees of roast discrimination based on the correspondent aroma analysis. Two principal components with eigenvalues of 11.1 and 4.9 explained the total variance observed. Compounds such as 1H–pyrrole, 2-furanmethanol, 2-furanmethanol acetate, dihydro-2-methyl-3(2H)-furanone, dihydro-2(3H)-furanone and pyridine were important to discriminate the higher degree of roast (C) from the other two. The ketone 1-acetyloxy-propanone, acetic acid, 2,6-dimethylpyrazine and 2-methyl-tetrahydrofuran-3-one had higher intensities in the lower degree of roast (B). The differences found in the type of identified compounds and correspondent intensities allowed total discrimination in between the different degrees of roast. In short, the proposed methodology (HSSE(PU)-LD/LVI-GC-MS) proved to be a suitable tool to characterize and discriminate variations in the coffee aroma profile according to the degree of roasting.

7.2.4. Conclusions

PU foams have been successfully applied, for the first time, as polymeric phases for static headspace analysis. The application of HSSE(PU) methodology to characterize the aroma profile of coffees and industrial blends revealed remarkable performance, under optimised experimental conditions. From the comparison in between HSSE(PU), HSSE(PDMS) and HS-SPME(CAR/PDMS) analytical methodologies, the former showed much greater capacity and selectivity for coffee aroma characterization, under similar experimental conditions. Furthermore, the HSSE(PU) methodology revealed robustness and good performance for the discrimination in between different commercial *gourmet* coffee blends and roasting profiles, showing to be a suitable tool for coffee aroma quality control.

8. General discussion

Many coffees from different geographical origins and of different types and grades are imported yearly by coffee roasting companies through a commercial chain that usually involves several intermediates. To ensure that coffees had not been adulterated, it is important to develop analytical tools for coffee bean type and geographical origin discrimination. In figure 48 it is shown how the different goals of this work were integrated in the different phases of the global coffee bean pathway, in a tentative to respond to important demands from the coffee industry.

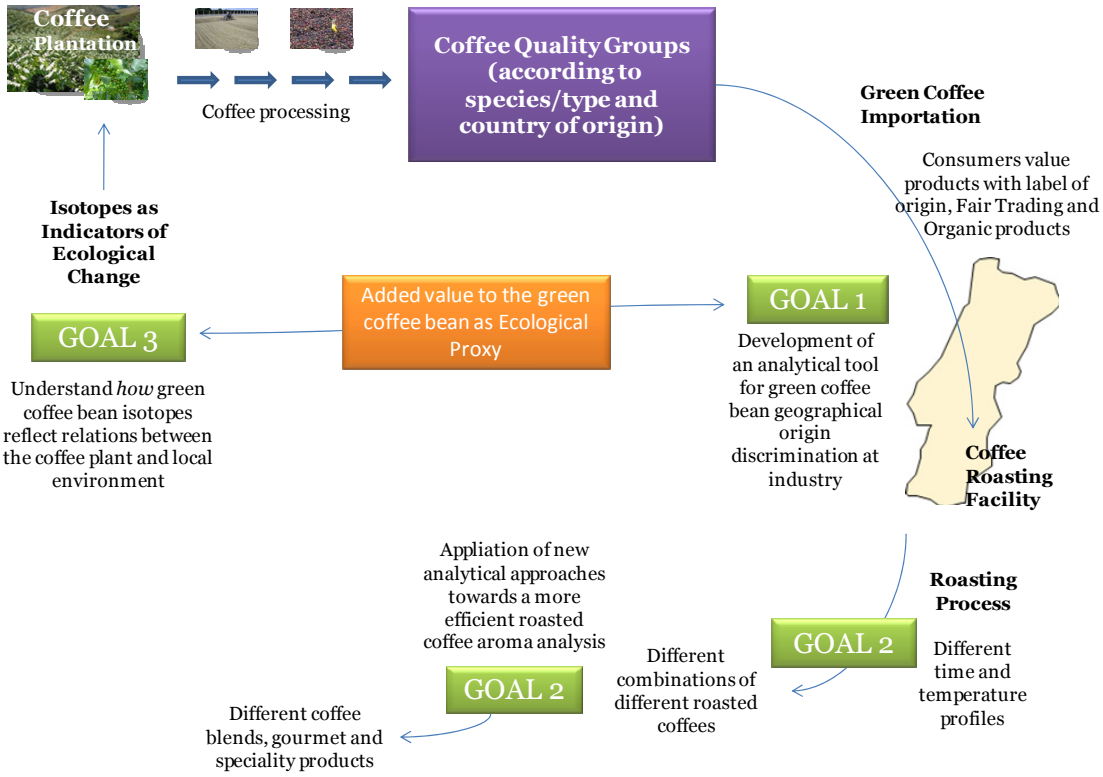

Figure 48. The main goals of this work.

For instance, visual inspection has been common practice to evaluate if a coffee is of *Arabica* or *Robusta* type, but it does not allow the safe detection of "contaminations" of *Arabica* beans by small amounts of *Robusta* beans. Consequently, developments of more objective methods that can be certified are desirable. The Raman spectroscopy approach presented in this work allowed the differentiation between

Arabica and *Robusta* whole green coffee beans based on their kahweol content (chapter 6). A spectral kahweol index (σ_{KA}) proportional to the coffee bean kahweol content represented a good criterion to differentiate *Arabica* versus *Robusta* coffees (figure 49).

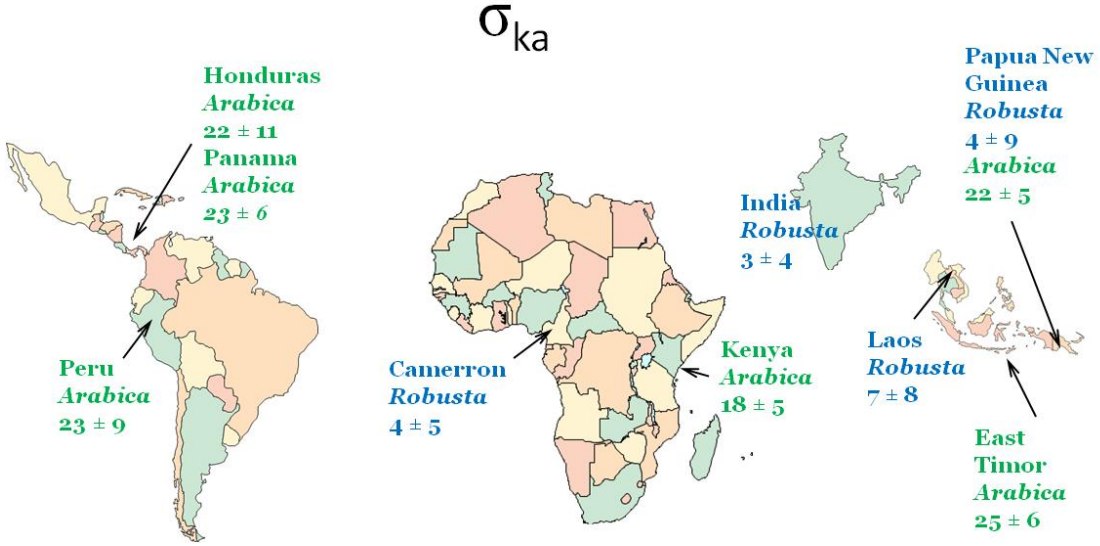

Figure 49. Spectral kahweol index (σ_{ka}) of *Arabica* and *Robusta* whole green coffee beans from different geographical origins (maps are not at scale).

This analytical approach showed several advantages by not relying on pattern-matching spectral techniques dependent on spectral differences between coffee samples, as in the case of NIR spectroscopy (results not shown). Moreover, it was shown that no mechanical or chemical processing of the coffee beans is necessary making this analytical alternative to *Arabica versus Robusta* differentiation less time-consuming and less costly compared to other analytical techniques. Besides the coffee type differentiation, the aim of this work was also to discriminate the geographical origin of the green coffee bean. The measurement of the isotope ratio of different elements in the coffee bean, namely C, N, O, Sr and S was performed in order to achieve this goal (chapters 2 to 4). Applications of stable isotope analysis in fields, *e.g.* chemistry, geochemistry, biogeochemistry and ecology had proven to be an extremely valuable and a powerful tool for indicating (sourcing), tracing, and recording various changes to the Earth's diverse terrestrial, aquatic, marine, and atmospheric systems (Dawson *et al.*, 2007). In this sense, variations in isotopic composition of coffee beans from different geographical origins with their own climate and geology were expected. The isotopic fingerprint of the coffee bean should be a resultant of plant variety, cultivation practices, processing, and, most important, of the relation between plant and local environment. C, N and O were the first elements to be studied in this work at a global scale (chapter 2).

However, an overlapping of the mean coffee bean $\delta^{13}C$, $\delta^{15}N$ and $\delta^{18}O$ values from different countries was observed and compromised the geographical origin discrimination at global scale. Nonetheless, the first results obtained allowed the discrimination between coffees from Africa and Asia (chapter 2, figure 22). The most relevant element to achieve this was the oxygen (chapter 2, figure 20). The values of coffee bean $\delta^{18}O$ clearly separated the coffees originating from these two continents (figure 50), because $\delta^{18}O_{bean}$ reflects the $\delta^{18}O$ of local precipitation, and should also be influenced by plant evapotranspiration.

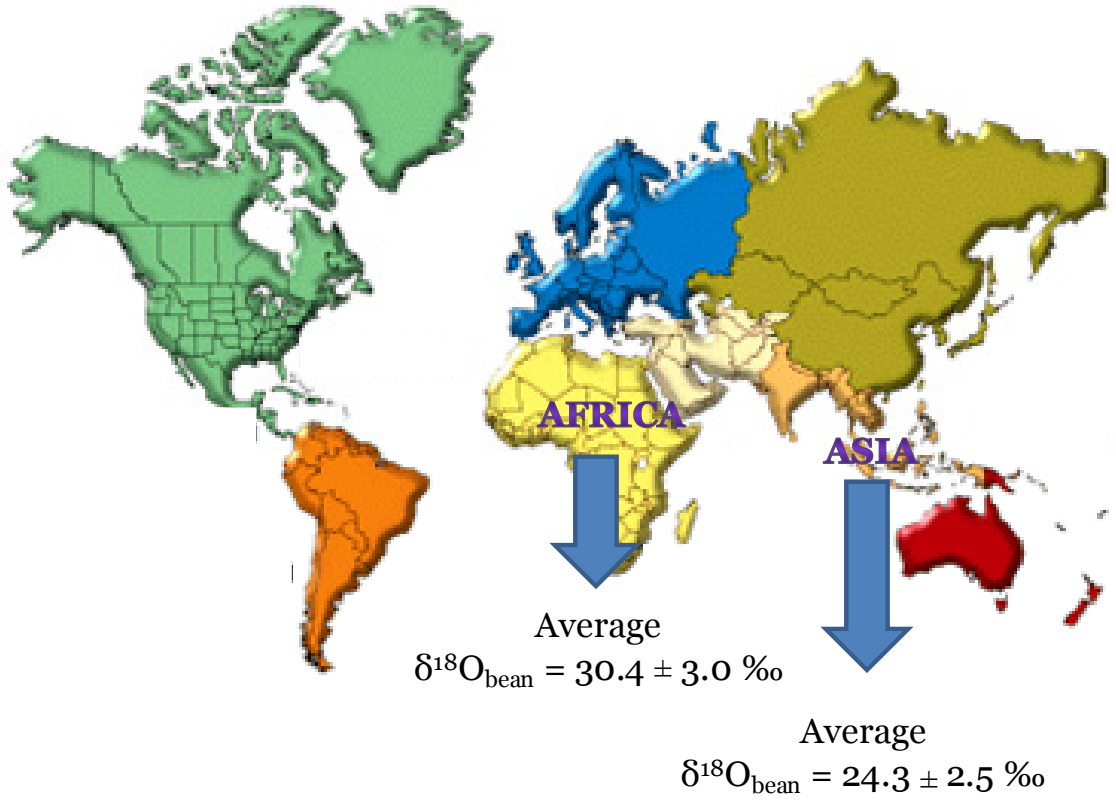

Figure 50. Average $\delta^{18}O$ values of green coffee beans ($\delta^{18}O_{bean}$) originating from Africa and Asia.

At this stage, it was clear that to enhance the degree of geographical origin discrimination it was necessary to measure the isotopic composition of other element(s). Studies with food traceability indicated that the analysis of Sr isotope abundance ratios could improve the development of an analytical tool for coffee authenticity studies. Sr concentration and isotopic composition in plants are closely affected by the soil where they grow, formed by weathering of parent rock and depending on environment (*e.g.* fertilizer and moisture) (Kabata-Pendias, 2001; Techer *et al.*, 2011). By combining O and Sr isotope ratio analysis, it was possible to achieve a separation between selected

origins and groups of provenances (chapter 3). Coffees from East Timor differentiated from all other origins solely based on their $^{87}Sr/^{86}Sr$. In South America, coffees from Brazil, Peru and Ecuador coffees were discriminated based on the principal component analysis of their $\delta^{18}O$ and $^{87}Sr/^{86}Sr$ values (chapter 3, figure 27). Coffees originating from the different islands (Papua New Guinea (PNG), Hawai'i, Indonesia, Jamaica and East Timor) also differentiated on the basis of their $\delta^{18}O$ and $^{87}Sr/^{86}Sr$ values (figure 51). Some of these coffees are considered *gourmet* as is the case of the Hawaiian's and Jamaican's.

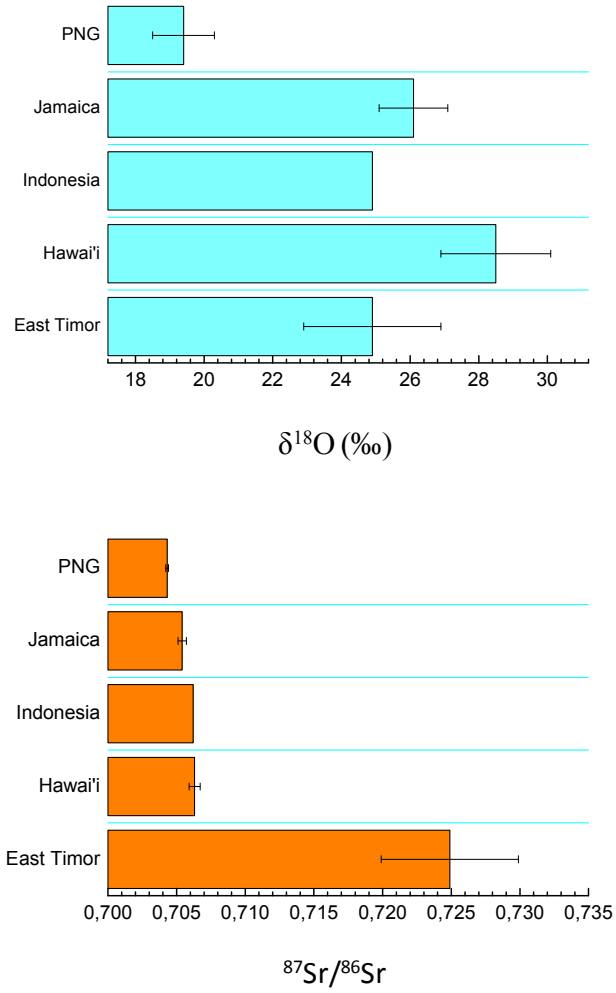

Figure 51. $\delta^{18}O$ and $^{87}Sr/^{86}Sr$ of green coffee beans from different islands. The combination of $\delta^{18}O$ and $^{87}Sr/^{86}Sr$ allows the discrimination of coffees from different islands.

In addition, the $^{87}Sr/^{86}Sr$ values measured in several origins, *e.g.* Hawai'i, Guatemala, Ecuador, Kenya, UR Tanzania, Zambia, Malawi and Rwanda were correspondent to the reported $^{87}Sr/^{86}Sr$ values for local parent rock type. In some cases where it was possible to access information on both Sr amount and isotope abundance ratio of parent rock, principal component analysis allowed the differentiation of coffees from UR Tanzania, Rwanda, Kenya, Hawai'i and East Timor (figure 52). The combined

O and Sr isotope ratio measurement of green coffee bean presented itself as the best approach to discriminate the geographical origin of the green coffee bean. This series of analysis may, however, be reinforced by the measurement of the isotopic composition of other elements depending on the coffee-producing region under study.

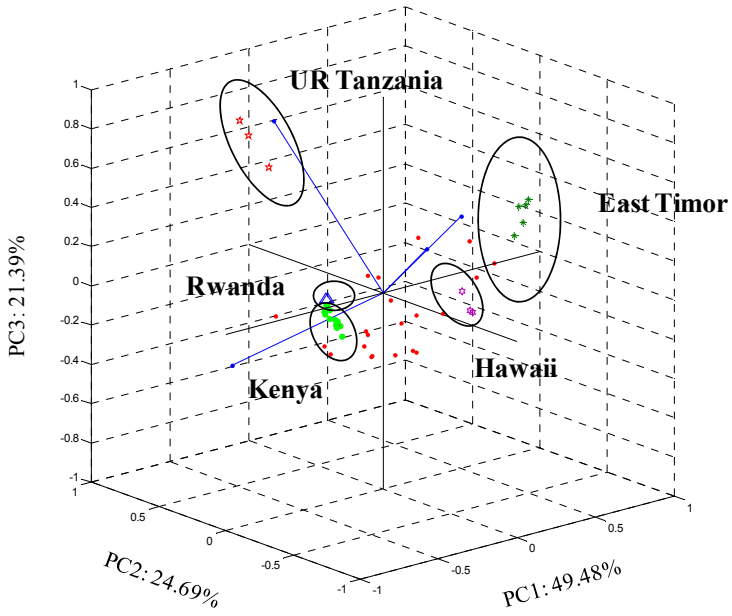

Figure 52. Scores on the three principal components explaining variability in Sr (ppm) and $^{87}Sr/^{86}Sr$ of green coffee beans and correspondent parent rock.

When working at global scale and with the 'bulk' bean isotope analysis, it is as considering a 'black box' where a multitude of climatic, geological and physiological processes are enclosed but not evident. For this reason, a scale-down to a smaller coffee-producing region (Hawai'i) was the next step in this work (chapter 4). In addition, multi element analysis and sulfur isotope ratio analysis complemented the series of analysis performed with the Hawaiian green coffee beans. The results showed that by combining 'light' (S, O, C and N) and 'heavy' (Sr) isotopes with multi element analysis it was possible to discriminate the Hawaiian coffee-producing regions (chapter 4, figure 32). This case-study also constituted an opportunity to improve the understanding of the relationship between environmental variables and the green coffee bean isotopic composition. Again, the results obtained with the Hawaiian coffees confirmed that isotope ratio and multi element analysis constitutes the best analytical tool for coffee authenticity studies. In short, in order to apply this analytical approach, it is important to understand the geographical area under study. A characterization from

the climatic and geological point of view should be performed at first place, and the most extensively possible. Also, information on cultivation methods, species and varieties/cultivars, and processing should be important to build the most extensive database. Next, a series of analyses encompassing a set of chemical elements may then be selected and tested to achieve the highest degree of provenance discrimination. The fact that, for a large number of coffees included in this work, information on exact geographical location and related environmental factors could be accessed, allowed the correlation between experimental results and data available on, *e.g.* altitude, latitude, $\delta^{18}O$ of precipitation, and, in some cases, Sr amount and isotope composition of parent rock (chapters 2 to 4). This represented the innovation of this work in relation to previous studies. It was showed that the $\delta^{18}O_{bean}$ reflects the local precipitation oxygen isotopic signature whether at global scale or, in the case of the Hawai'i. Significant positive correlations between the $\delta^{18}O$ values of coffee bean and of local precipitation were observed. Higher values of $\delta^{18}O_{bean}$ were measured in coffees originated from regions where more enriched weighted annual $\delta^{18}O$ of precipitation are reported (Africa) (figure 53a). The O isotopes of plant water, the organic molecules that make up plant tissues and the gases produced during plant metabolism all record important aspects of a plant's growth environment and physiological activity *at various spatial and temporal scales* (West *et al.*, 2010) (figure 53b). Many isotope effects were observed, *e.g.* altitude effect on $\delta^{18}O_{bean}$ in the American continent (chapter 2, figure 23), and the latitude effect on $\delta^{18}O_{bean}$ in Africa (chapter 2, table 7), and islands (chapter 3). In Hawai'i, the influence of volcanic activity, tropical storms, of the distance to the coast and altitude were inferred from the isotope ratios measured in the Hawaiian coffee beans (chapter 4, figures 29 and 31). These observations were supported by significant correlations between the green coffee bean isotopic composition and the various environmental factors. All this reflects the importance of the seed, the coffee bean, as a 'tool' to study climate and plant primary production spatial and temporal variations. Cellulose, which is an important component of the green coffee bean, has the preferred material for $\delta^{18}O$ analyses for climatic and ecophysiological studies (Zhou *et al.*, 2010). However, its $\delta^{18}O$ has a mean 27 ‰ enrichment resultant of the carbonyl-water interaction during its biosynthesis. This biochemical fractionation may difficult the application of isotopic considerations in plant ecophysiological studies. In the present work, it was demonstrated that oxygen isotope ratio measurement of caffeine constitutes a viable alternative to cellulose or 'bulk' organic matter analysis, not only from the biochemical point of view but also in what refers to extraction method (chapter 5). In caffeine, the origin of the O isotopes is different comparing to plant carbohydrates (figure 54). That consists in the advantage of studying caffeine in comparison to cellulose, as biochemical fractionation does not theoretically determine caffeine's oxygen isotopic composition. This is supported by the observed similar magnitudes of $\delta^{18}O_{caff}$ and $\delta^{18}O_{prec}$ (chapter 5, figure 35), and by correlation between $\delta^{18}O_{bean}$ and $\delta^{18}O_{caff}$ in relation to $\delta^{18}O_{prec}$. Caffeine $\delta^{18}O$ measurement is important because it gives an approximate isotopic signal of plant leaf water, and may eventually aid in the estimation of plant transpiration on the basis of the ^{18}O enrichment at leaf or seed level,

providing additional information is available on local isotopic composition of water vapor and soil water.

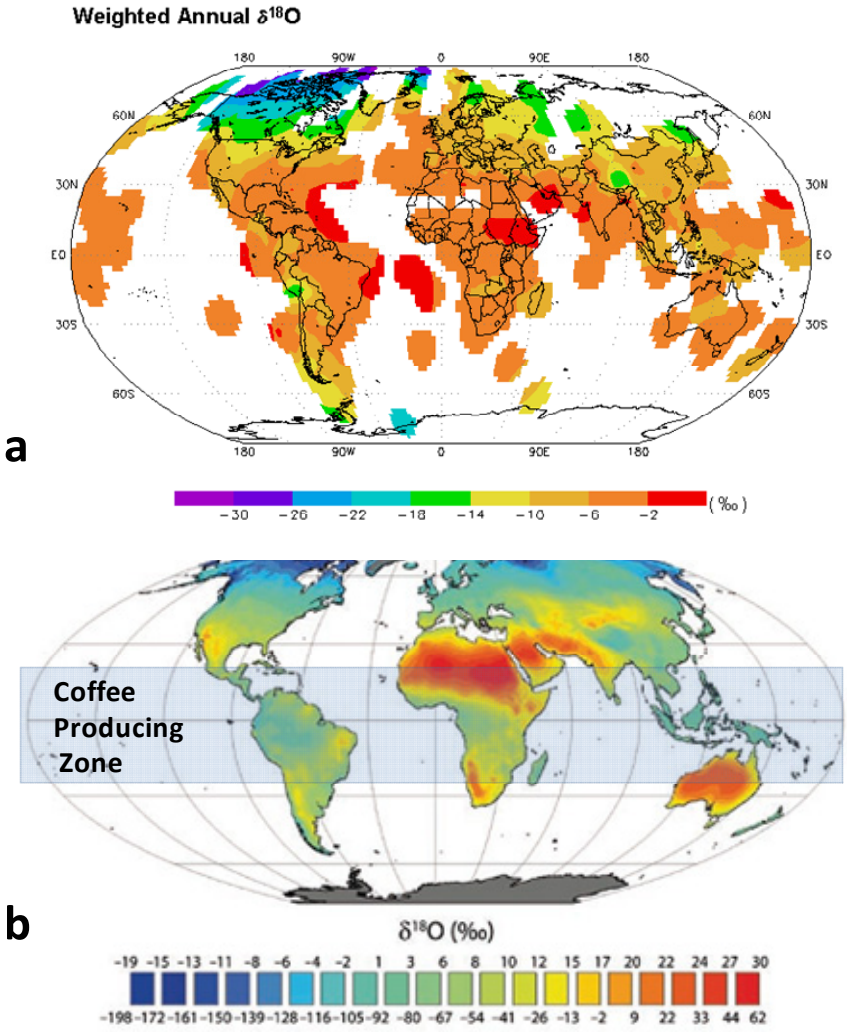

Figure 53. Global map of weighted annual $\delta^{18}O$ of precipitation (a) (IAEA, 2001) and of annual average leaf water $\delta^{18}O$ for the sites of evaporation within leaves (b) (adapted from West *et al.*, 2008).

The caffeine isotope ratio analysis should work as an 'inversion method' to point trends in $\delta^{18}O_{prec}$ and in plant water $\delta^{18}O$, in different globe regions, thus, improving global precipitation and plant water $\delta^{18}O$ isoscapes. It will be fundamental to develop real time field experiments in order to relate the results from the coffee bean isotope ratio analysis with physiological responses from the plant. Additional isotope ratio analysis of hydrogen of the coffee bean and caffeine will be an important complement to this research.

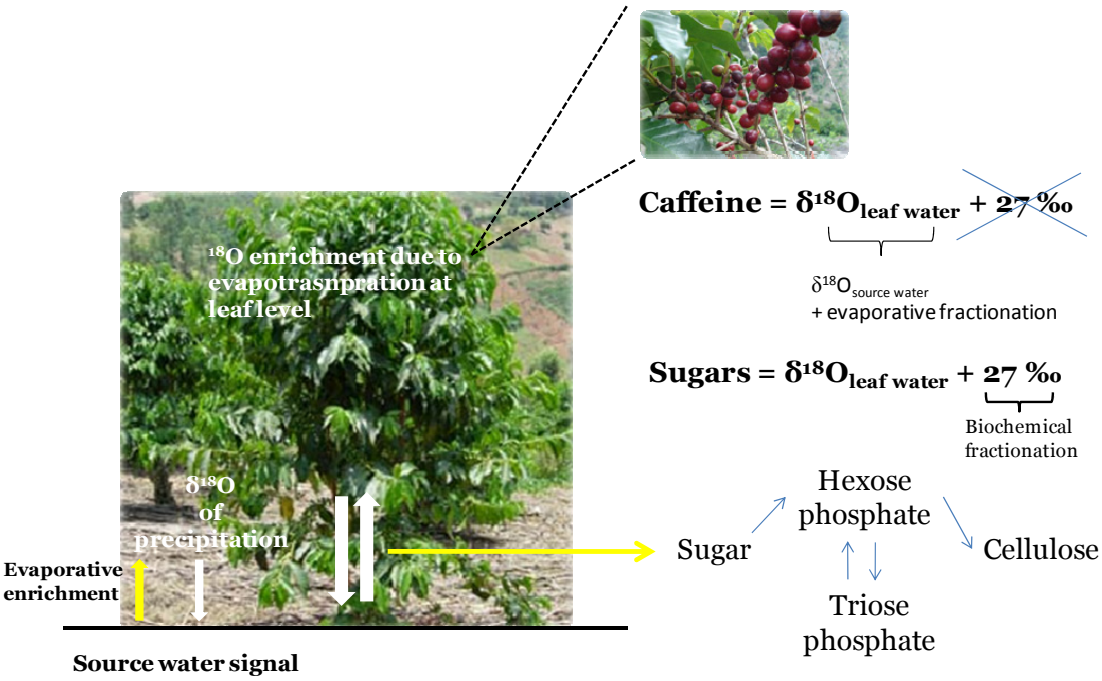

Figure 54. Diagram of a coffee plant and fruit showing the main fractionations of O isotopes determining cellulose and caffeine $\delta^{18}O$.

At the same time, it is well-known that the quality of the coffee blend provided to the final consumer depends not only on the coffee geographical origin, but also on the roasting conditions. The flavor and aroma of a roasted coffee is intrinsically related with roasting time and temperature profile as it has been reported by other authors (Franca *et al.*, 2009b; Rodrigues *et al.*, 2007). Most of these studies of roasted coffee aroma make use of SPME as a solventless, fast and efficient sample preparation technique prior to chromatographic analysis. However, in this work, this was done in a systematized way, which allowed defining the best HS-SPME/GC-MS methodology for coffee volatile aroma compounds profile determination, according to the roasting conditions (chromatic values) and coffee origin (chapter 7, figure 45). Nevertheless, coffee aroma is a mixture of volatile compounds with a wide range of polarity which may compromise the capacity and efficiency of SPME. For this reason, a new polymeric phase based on polyurethane foams (PU) was applied, for the first time, to characterize coffee aroma profiles, demonstrating high analytical efficiency (chapter 7, figure 45). This was evident in relation to the most relevant chemical classes for the roasted coffee aroma, particularly in the case of furans and pyrazines (chapter 7, figure 45). These are some of the most important volatile aroma compounds of roasted coffee, responsible for the well-known sweet, earthy and caramel notes (Berlitz *et al.*, 2004). The methodology HSSE(PU)/LVI-GC-MS was proposed as a novel alternative for coffee aroma analysis, and was applied in the discrimination of different roasting conditions, and *gourmet* blends (chapter 7, figure 47) with promising results.

9. General conclusions

In this work, the spectroscopic analytical techniques applied were fundamental to achieve the discrimination between coffee types, and of certain geographical origins of green coffee beans. Fourier transform Raman spectroscopy allowed the unequivocally discrimination between *Arabica* and *Robusta* coffee types, independently of their geographical origin, based on the content of kahweol, an important component of the coffee bean with reported antioxidant and anticarcinogenic properties. But the market value of coffee does not vary solely on the basis of its type but also of its geographical origin. In this work, isotope ratio analysis of C, N, O, S and Sr eventually combined with multi element analysis proved to be the best analytical tool for the geographical origin discrimination of the green coffee bean. Coffees from East Timor, from several countries in South America and originating from different coffee-producing islands were discriminated according to their isotopic composition. Isotope ratio analysis (by IRMS and ICP-MS) is the best spectroscopic approach to achieve the green coffee bean geographical origin discrimination. From the series of analysis performed, O and Sr isotopes were the most relevant to reach this goal. The coffee bean isotopic composition of O and Sr was related with local meteoric water O isotopic composition ($\delta^{18}O_{prec}$), and with Sr isotopic composition of local parent rock. The combination of these two elements reflects the hydrology and geology of the location where the green coffee bean is produced.

Moreover, the isotopic composition of the green coffee bean yielded important understanding on the relationships between environmental factors and the coffee plant. Environmental factors, *e.g.* altitude, latitude, distance to the coast, precipitation amount and volcanic activity, as well as the above mentioned factors determine the isotopic signature of the coffee plant seed, *i.e.* the coffee bean. This was confirmed whether at regional and global scale. Additionally, isotope ratio analysis was applied to a specific compound extracted from the green coffee bean. Caffeine presented itself as a novel alternative to cellulose and/or 'bulk' green coffee bean isotope ratio analysis in coffee plant ecophysiology studies. The $\delta^{18}O_{caff}$ values may eventually work as a 'correction' factor of model predicted $\delta^{18}O_{prec}$ and plant water $\delta^{18}O$ values. At last, in what refers to the characterization of roasted coffee aroma compounds, PU foams, applied in the HS mode, proved to be a suitable enrichment approach in comparison to other conventional analytical techniques. The HSSE(PU)/LVI-GC-MS methodology showed increased extraction efficiency in the case of the most relevant chemical families that characterize roasted coffee aroma, that result from lipid peroxidation (*Maillard* reaction), and related *Strecker* degradation of aminoacids occurring during the roasting process.

10. Trends for the future

The future of this work is inherent to the ongoing research project, IsoGeoCoffee (PTDC/AGR-AAM/104357/2008; Fundação para a Ciência e Tecnologia, Portugal), initiated in January of 2010. Research is being developed in smaller coffee-producing regions (*e.g.* Lavras and Mogiana in Brazil as well as Hawai'i) in order to develop the potentialities of isotope and multi element analysis for the characterization of *gourmet*/certified coffees. The goal of this research project is also to evaluate the effects of environmental change in the coffee bean isotopic composition. For this reason, the study of multiyear harvests of coffee will be also addressed. Additionally, real time experiments have been initiated with coffee plants in greenhouse to yield better understanding on isotope fractionation in different coffee plant organs, and how this is related with different water availability conditions. The final goal of IsoGeoCoffee project is to achieve the first maps of isotope patterned distribution of the green coffee bean. At the same time, the application of Raman spectroscopy for kahweol determination in coffee beans from different geographical origins will continue. As already stated, depending on the regional system under study, other analytical techniques may provide important information contributing to more robust coffee origin discrimination (*e.g.* NMR, LC-MS, etc.). In what refers to the application of PU foams to characterize the coffee aroma composition in detail, and how this relates to roasting conditions, future research should include experiments from mid to large scale, at industry, to evaluate the performance of HSSE(PU)/LVI-GC-MS analytical approach for the quality control and optimization of the roasting process.

11. List of figures

12. List of tables

13. References

Ággarwal, J., Araguás-Araguás, L., Groening, M., Kulkani, K., Kurthas, T., Newman, B., & Vitvar, T. (2010). Global hydrological isotope data and data networks. In: J. West, G. Bowen, T. E. Dawson, & K. P. Tu, *Isoscapes, understanding movement, pattern, and process on earth through isotope mapping.* New York: Springer.

Ággarwal, J., Habich-Mauche, J., & Juarez, C. (2008). Application of heavy stable isotopes in forensic isotope geochemistry: a review. *Applied Geochemistry*, *23*, 2658-2666.

Akiyama, M., Murakami, K., Ikeda, M., Iwatsuki, K., Kokubo, S., Wada, A., Tokuno, K., Onishi, M., Iwabuchi, H., & Tanaka, K. (2005). Characterization of flavor compounds released during grinding of robusta coffee beans. *Food Science and Technology Research*, *11*, 298-307.

Akiyama, M., Murakami, K., Ohtani, N., Iwatsuki, K., Sotoyama, K., Wada, A., Tokuno, K., Iwabuchi, H., & Tanaka, K. (2003). Analysis of volatile compounds released during the grinding of roasted coffee beans using solid-phase microextraction. *Journal of Agricultural and Food Chemistry*, *51*, 1961-1969.

Allègre, C. (2008). Radiogenic isotope geochemistry. *Isotope Geology*. Cambridge: Cambridge University Press.

Almeida, C., Nogueira, J.M.F. (2006). Determination of steroid sex hormones in water and urine matrices by stir bar sorptive extraction and liquid chromatography with diode array. *Journal of Pharmaceutical and Biomedical Analysis*, *41*, 1303-1311.

Almeida, C.M., & Vasconcelos, M.T.S.D. (2001). ICP-MS determination of strontium isotope ratio in wine in order to use it as a fingerprint of its regional origin. *Journal of Analytical Atomic Spectrometry*, *16*, 607-611.

Almeida, C.M.R., & Vasconcelos, M.T.S.D. (2004). Does the winemaking process influence the wine 87Sr/86Sr? a case study. *Food Chemistry*, *85*, 7-12.

Alonso-Salces, R.M., Moreno-Rojas, J.M., Holland, M.V., Reniero, F., Guillou, C., & Héberger, K.R. (2010). Virgin olive oil authentication by multivariate analyses of ^{1}H NMR fingerprints and $\delta^{13}C$ and $\delta^{2}H$ data. *Journal of Agricultural and Food Chemistry*, *58*, 5586-5596.

Alves, M.R., Casal, S., Oliveira, M.B.P.P., & Ferreira, M.A. (2003). Contribution of FA profile obtained by high resolution GC/chemometric techniques to the authenticity of green and roasted coffee varieties. *Journal of American Oil Chemistry*, *80*, 511-517.

Alves, R.C., Casal, S., Alves, M.R., & Oliveira, M.B. (2009). Discrimination between arabica and robusta coffee species on the basis of their tocopherol profiles. *Food Chemistry*, *114*, 295-299.

Alves, R.F., Nascimento, A.M.D., & Nogueira, J.M.F. (2005). Characterization of the aroma profile of Madeira wine by sorptive extraction techniques. *Analytica Chimica Acta*, *546*, 11-21.

Amstalden, L.C., Leite, F., & Menezes, H.C. (2001). Identificação e quantificação de voláteis de café através de cromatografia gasosa de alta resolução/espectrometria de massa empregando um amostrador automático de headspace. *Ciências Tecnológicas Alimentares*, *21*, 123-128.

Amundson, R., Austin, A.T., & Schuur, A.G. (2003). Global patterns of the isotopic composition of soil and plant nitrogen. *Global Biogeochemical Cycles*, *17*, 1031.

Anderson, K.A., & Smith, B.W. (2002a). Chemical profiling to differentiate geographic growing origins of coffee. *Journal of Agricultural and Food Chemistry*, *50*, 2068-2075.
Anderson, W.T., Bernasconi, S.M., Mckenzie, J.A., Sauer, M., & Schweingruber, F. (2002b). Model evaluation for reconstructing the oxygen isotopic composition in precipitation from three ring cellulose over the last century. *Chemical Geology*, *2002*, 121-137.
Andrade, P.B., Leitao, R., Seabra, R.M., Oliveira, M.B., & Ferreira, M.A. (1998). 3,4-dimethoxy-cinnamic acid levels as a tool for differentiation of *Coffea canephora* var *robusta* and *Coffea arabica*. *Food Chemistry*, *61*, 511-514.
Ariyama, K., Aoyama, Y., Mochizuki, A., Homura, Y., Kadokura, M., & Yasui, A. (2006). Determination of the geographic origin of onions between three main production areas in Japan and other countries by mineral composition. *Journal of Agricultural and Food Chemistry*, *55*, 347-354.
Arthur, C.L., Pawliszyn, J. (1990). Solid phase microextraction with thermal desorption using fused silica optical fibers. *Analytical Chemistry*, *62*, 2145-2148.
Ashihara, H., Monteiro, A.M., Gillies, F.M., & Crozier, A. (1996). Biosynthesis of caffeine in leaves of coffee. *Plant Physiology*, *111*, 747-753.
Ashihara, H., Sano, H., & Crozier, A. (2008). Caffeine and related purine alkaloids: biosynthesis, catabolism, function and genetic engineering. *Phytochemistry*, *69*, 841-856.
Ashihara, H., Zheng, X.-Q., Katahira, R., Morimoto, M., Ogita, S., & Sano, H. (2006). Caffeine biosynthesis and adenine metabolism in transgenic *Coffea canephora* plants with reduced expression of N-methyltransferase genes. *Phytochemistry*, *67*, 882-886.
Augusti, A., & Schleucher, J. (2007). The ins and outs of stable isotopes in plants. *New Phytologist*, *174*, 473-475.
Badeck, F.-W., Tcherkez, G., Nogués, S., Piel, C., & Ghashghaie, J. (2005). Post-photosynthetic fractionation of stable carbon isotopes between plants organs - a widespread phenomenon. *Rapid Communications in Mass Spectrometry*, *19*, 1381-1391.
Baltussen, E., Sandra, P., David, F., Cramers, C. (1999) Stir bar sorptive extraction (SBSE), a novel extraction technique for aqueous samples: Theory and principles. *Journal of Microcolumn Separations*, *11*, 737-747.
Barbaste, M., Halicz, L., Galy, A., Medina, B., Emteborg, H., C. Adams, F., & Lobinski, R. (2001). Evaluation of the accuracy of the determination of lead isotope ratios in wine by ICP MS using quadrupole, multicollector magnetic sector and time-of-flight analyzers. *Talanta*, *54*, 307-317.
Barbaste, M., Robinson, K., Guylfoile, S., Medina, B., & Lobinski, R. (2002). Precise determination of the strontium isotope ratios in wine by inductively coupled plasma sector field multicollector mass spectrometry. *Journal of Analytical Atomic Spectrometry*, *17*, 135-137.
Barbour, M. M. (2007a). Stable oxygen isotope composition of plant tissue: a review. *Functional Plant Biology*, *34*, 83-94.
Barbour, M. M., Andrews, T. J., & Farquhar, G. D. (2001). Correlations between oxygen isotope ratios of wood constituents of *Quercus* and *Pinus* samples from around the world. *Australian Journal of Plant Physiology*, *28*, 335-348.
Barbour, M. M., Cernusak, L. A., & Farquhar, G. D. (2005a). Factors affecting the oxygen isotope ratio of plant organic material. In: L.B. Flanagan, J.R. Ehlereinger, & D.E. Pataki, *Stable Isotopes and Biosphere-Atmosphere Interactions Processes and Biological Controls*. Oxford: Elsevier.

Barbour, M.M., Cernusak, L.A., & Farquhar, G.D. (2005b). Factors affecting the oxygen isotope ratio of plant organic material. In: L.B. Flanagan, J.R. Ehleringer, & D.E. Pataki, *Physiological ecology: a series of monographs, texts and treatises*. Oxford: Elsevier.

Barbour, M.M., & Farquhar, G.D. (2000a). Relative humidity- and ABA-induced variation in carbon and oxygen isotope ratios of cotton leaves. *Plant, Cell and Environment*, *23*, 473-485.

Barbour, M.M., Schurr, U., Henry, B.K., Wong, S.C., & Farquhar, D. (2000b). Variation in the oxygen isotope ratio of phloem sap sucrose from castor bean. Evidence in support of the Péclet effect. *Plant Physiology*, *123*, 671-679.

Barwick, V.J., Ellison, S.L.R., Lucking, C.L., & Burn, M.J. (2001). Experimental studies of uncertainties associated with chromatographic techniques. *Journal of Chromatography A, 918*, 267-276.

Baumann, T. W. (2006). Some thoughts on the physiology of caffeine in coffee and a glimpse of metabolite profiling. *Brazilian Journal of Plant Physiology*, *18*, 243-251.

Berlitz, H.-D., Grosch, W., & Schieberle, P. (2004). Food Chemistry. Berlim: Springer-Verlag.

Bertrand, B., Etienne, H., Lashermes, P., Guyot, B., & Davrieux, F. (2005). Can near-infrared reflectance of green coffee be used to detect introgression in Coffea Arabica cultivars? *Journal of Science and Food Agriculture*, *85*, 955-962.

Bicchi, C.P., Binello, A.E., Pellegrino, G.M., Vanni, A.C. (1995). Characterization of green and roasted coffees through the chlorogenic acid fraction by HPLC-UV and principal component analysis. *Journal of Agricultural and Food Chemistry*, *45*, 1549-1555.

Bicchi, R.A., Panero, O.M., Pellegrino, G.M., & Vanni, A.C. (1997). Characterization of roasted coffee and coffee beverages by solid-phase microextraction - gas chromatography and principal component analysis. *Journal of Agricultural and Food Chemistry*, *45*, 4680-4686.

Bicchi, C., Cordero, C., Liberto, E., Rubiolo, P., Sgorbini, B., David, F., & Sandra, P. (2005). Dual-phase twisters: a new approach to headspace sorptive extraction and stir bar sorptive extraction. *Journal of Chromatography A, 1094*, 9-16.

Boons, F. (2009). *Creating ecological value, an evolutionary approach to business strategies on the natural environment*. Cheltenham, UK: Edward Elgar Publishing Limited.

Borella, S., & Sauer, M. (1999). Analysis of $\delta^{18}O$ in tree rings: wood-cellulose comparison and method dependent sensitivity. *Journal of Geophysical Research*, *104*, 19267-19273.

Bowen, G.J., & Revenaugh, J. (2003a). Interpolating the isotopic composition of modern meteoric precipitation. *Water Resources Reseach*, *39*, 1299.

Bowen, G., & Wilkinson, B. (2003b). Spatial distribution of $\delta^{18}O$ in meteoric precipitation. *Geology*, *30*, 315-318.

Bowen, G.J. (2010). The Online Isotopes in Precipitation Calculator, version 2.2. http://www.waterisotopes.org

Bowen, G.J., Wassenar, I.I., & Hobson, K.A. (2005). Global application of stable hydrogen and oxygen isotopes to wildlife forensics. *Oecologia*, *143*, 337-348.

Bowen, G.J., West, J.B., & Hoogewerff, J. (2009). Isoscapes: Isotope mapping and its applications. *Journal of Geochemical Exploration*, *102*, v-vii.

Bowen, G.J., West, J.B., Vaughn, B.H., Dawson, T.E., Ehleringer, J.R., Fogel, M.L., Hobson, K.A., Hoogewerff, J., Kendall, C., Lai, C.T., Miller, C.C., Noone, D.,

Schwarcz, H.P., & Still, C.J. (2009b). Isoscapes to address large-scale Earth science challenges. *Eos*, *90*, 109-116.
Bowen, G.J., & Wilkinson, B. (2002). Spatial distribution of δ18O in meteoric precipitation. *Geology*, *30*, 315-318.
Bradbury, A.G.W. (2001). Chemistry I: Non-volatile compounds. 1A: Carbohydrates. In: R. J. Clarke, & O. G. Vitzthum, *Coffee, Recent Developments*. Oxford: Blackwell Science.
Brando, C. (2004). Harvesting and green coffee processing. In: W. J, *Coffee: Growing, processing, sustainable production. A guidebook for growers, processors, traders, and researchers.* Weinheim.: Wiley-VVCH.
Brandt, S., von Stetten, D., Günther, M., Hildebrandt, P., & Frankenberg-Dinkel, N. (2008). The fungal phytochrome Fph A from *Aspergillus nidulance*. *Journal of Biological Chemistry*, *283*, 34605-34614.
Briandet, R., Kemsley, E.K., & Wilson, R.H. (1996). Discrimination of arabica and robusta in instant coffee by Fourier transform infrared spectroscopy and chemometrics. *Journal of Agricultural and Food Chemistry*, *44*, 170-174.
Bröhan, M., Huybrighs, T., Wouters, C., & Van der Bruggen, B. (2009). Influence of storage conditions on aroma compounds in coffee pads using static headspace GC-MS. *Food Chemistry*, *116*, 480-483.
Brugnoli, E., & Farquhar, G.D. (2000). Photosynthetic fractionation of carbon isotopes. In: R.C. Leegood, T.D. Sharkey, & S. von Caemmerer, *Advances in Photosynthesis and Respiration: Photosynthesis, Physiology and Metabolism*. The Netherlands: Springer.
Brunner, M., Katona, R., Stefánka, Z., & Prohaska, T. (2010). Determination of the geographical origin of processed spice using multielement and isotopic pattern on the example of Szegedi paprika. *European Foods Research and Technology*, *231*, 623-634.
Buffo, R.A., & Cardelli-Freire, C. (2004). Coffee flavour: an overview. *Flavour and Fragance Journal*, *19*, 99-104.
Callejón, R.M., Tesfaye, W., Torija, M.J., Mas, A., Troncoso, A.M., & Morales, M.L. (2009). Volatile compounds in red wine vinegars obtained by submerged and surface acetification in different woods. *Food Chemistry*, *113*, 1252-1259.
Câmara, J.S., Marques, J.C., Perestelo, R.M., Rodrigues, F., Oliveira, L., Andrade, P., & Caldeira, M. (2007). Comparative study of the whisky aroma profile based on headspace solid phase microextraction using different fiber coatings. *Journal of Chromatography A*, *1150*, 198-207.
Camin, F., Larcher, R., Perini, M., Bontempo, L., Bertoli, D., Gagliano, G., Nicolini, G., & Versini, G. (2010). Characterisation of authentic Italian extra-virgin olive oils by stable isotope ratios of C, O and H and mineral composition. *Food Chemistry*, *118*, 901-909.
Capo, R.C., Stewart, B.W., & Chadwock, O.A. (1998). Strontium isotopes as tracers of ecosystem processes: theory and methods. *Geoderma*, *82*, 197-225.
Carelli, M.L.C., Fahl, J.I., & Ramalho, J.D.C. (2006). Aspects of nitrogen metabolism in coffee plants. *Brazilian Journal of Plant Physiology*, *18*, 9-21.
Carrera, F., Leon-Camacho, M., Pablos, F., & Gonzalez, A.G. (1998). Authentication of green coffee varieties according to their sterolic profile. *Analytical Chimica Acta*, *370*, 131-139.
Casal, S., Alves, M.R., Mendes, E., Oliveira, M.B.P.P., & Ferreira, M.A. (2003). Discrimination between Arabica and Robusta coffee species on the basis of their amino acid enantiomers. *Journal of Agriculture and Food Chemistry*, *51*, 6495-6501.

Casal, S., Oliveira, M.B.P.P., Alves, M.R., & Ferreira, M.A. (2000). Discriminate analysis of roasted coffee varieties for trigonelline, nicotinic acid, and caffeine content. *Journal of Agricultural and Food Chemistry*, *48*, 3420-3424.

Cavin, C., Holzhaeuser, D., Scharf, G., Constable, A., Huber, W.W., & Schilter, B. (2002). Cafestol and kahweol, two coffee specific diterpenes with anticarcinogenic activity. . *Food Chemistry*, *40*, 1155-1163.

Cerling, T., Bowen, G., Ehleringer, J.R., & Sponheimer, M. (2007). The reaction progress variable and isotope turnover in biological systems. In: T.E. Dawson, & T.W. Siegwolf, *Stable isotopes as indicators of ecological change*. London: Elsevier.

Chadwick, O.A., Derry, L.A., Bern, C.R., Vitousek, P.M. (2009). Changing sources of strontium to soils and ecosystems accross the Hawaiian Islands. *Chemical Geology*, *267*, 64-76.

Chen, Y., Begnaud, F., Chaintreau, A., & Pawliszyn, J. (2007a). Analysis of flavor and perfume using an internally cooled coated fiber device. *Journal of Separation Science*, *30*, 1037-1043.

Choi, W.-J., Ro, H.-M., & Lee, S.-M. (2003). Natural ^{15}N abundances of inorganic nitrogen in soil treated with fertilizer and compost under changing soil moisture regimes. *Soil Biology & Biochemistry*, *35*, 1289-1298.

Cocchi, M., Durante, C., Marchetti, A., Armanino, C., & Casale, M. (2007). Characterization and discrimination of different aged ‘Aceto Balsamico Tradizionale di Modena' products by head space mass spectrometry and chemometrics. *Analytica Chimica Acta*, *589*, 96-104.

Coelho, E., Perestrelo, R., Neng, N.R., Câmara, J.S., Coimbra, M.A., Nogueira, J.M.F., & Rocha, S. (2008). Optimization of stir bar sorptive extraction and liquid desorption combined with large volume injection - gas chromatography - quadrupole mass spectrometry for the determination of volatile compounds in wines. *Analytica Chimica Acta*, *624*, 79-89.

Coetzee, P., & Vanhaecke, F. (2005a). Classifying wine according to geographical origin via quadrupole-based ICP–mass spectrometry measurements of boron isotope ratios. *Analytical and Bioanalytical Chemistry*, *383*(6), 977-984.

Coetzee, P.P., Steffens, F.E., Eiselen, R.J., Augustyn, O.P., Balcaen, L., & Vanhaecke, F. (2005b). Multi-element analysis of South African wines by ICP-MS and their classification according to geographical origin. *Journal of Agricultural and Food Chemistry*, *53*, 5060-5066.

Collomb, M., Bütikofer, U., Sieber, R., Jeangros, B., & Bosset, J.-O. (2002). Composition of fatty acids in cow's milk fat produced in the lowlands, mountains and highlands of Switzerland using high resolution gas chromatography. *International Dairy Journal*, *12*, 649-659.

Correia, A.M.N.G. (1990). A influência da torra na evolução dos ácidos clorogénicos do café. *Instituto Superior de Agronomia*, vol. PhD. Lisboa: Universidade Técnica de Lisboa.

Costa Freitas, A.M., Parreira, C., & Vilas-Boas, L. (2001). The use of an electronic aroma-sensing device to assess coffee differentiation-comparison with SPME gas chromatography-mass spectrometry aroma patterns. *Journal of Food Composition and Analysis*, *14*, 513-522.

Craig, H. (1961). Isotopic variation in meteoric waters. *Science*, *133*, 1702-1703.

Critteren, R.G., Andrew, A.S., LeFournour, M., Young, M.D., Middleton, H., & Stockmann, R. (2007). Determining the geographic origin of milk in Australasia using multi-element stable isotope ratio analysis. *International Dairy Journal*, *17*, 421-428.

Czerny, M., Mayer, F., & Grosch, W. (1999). Sensory study on the character impact odorants of roasted arabica coffee. *Journal of Agricultural and Food Chemistry*, *47*, 605-699.
DaMatta, F. (2004). Ecophysiological constraints on the production of shaded and unshaded coffee: a review. *Field Crops Research*, *86*, 99-114.
DaMatta, F., & Ramalho, J. (2006). Impacts of drought and temperature stress on coffee physiology and production: a review. *Brazilian Journal of Plant Physiology*, *18*, 55-81.
Dansgaard, W. (1964) Stable isotopes in precipitation. Tellu, *16*, 436-438.
Dawson, T. E. (1993). Hydraulic lift and water-use by plants - Implications for water-balance, performance and plant-plant interactions. *Oecologia*, *95*, 565-574.
Dawson, T.E., & Ehleringer, J.R. (1998). Plants, isotopes, and water use: A catchment-level perspective. In: C. Kendall, & J. J. McDonnell, *Isotope Tracers in Catchment Hydrology*. The Netherlands: Elsevier Science Publications.
Dawson, T.E., Mambelli, S., Plamboek, H., Templer, P.H., & Tu, K.P. (2002). Stable isotopes in plant ecology. *Annual Review of Ecology and Systematics*, *33*, 507-559.
Dawson, T.E., & Siegwolf, R.T.W. (2007). Using stable isotopes as indicators, tracers, and recorders of ecological change: some context and background. In: T.E. Dawson, & R.T.W. Siegwolf, *Stable Isotopes as Indicators of Ecological Change*. Burlington: Elsevier.
De Castro, R.D., & Marraccini, P. (2006). Cytology, biochemistry and molecular changes during coffee fruit development. *Brazilian Journal of Plant Physiology*, *18*, 175-199.
de Roos, B., van der Weg, G., Urgert, R., Van de Bovenkamp, P., Charrier, A., & Katan, M. B. (1997). Levels of cafestol, kahweol, and related diterpenoids in wild species of the coffee plant coffea. . *Journal of Agricultural and Food Chemistry*, *45*, 3065-3069.
Descroix, F., & Snoeck, J. (2004). Environmental factors suitable for coffee cultivation. In: J. N. Wintgens, *Coffee: Growing, processing, sustainable production. A guidebook for growers, processors, traders, and researchers*. Weinheim: Wiley-VCH.
Dias, R.C.E., Campanha, F.C., Vieira, L.G.E., Ferreira, L.P., Pot, D., Marraccini, P., & de Toldedo Benassi, M. (2010). Evaluation of kahweol and cafestol in coffee tissues and roasted coffee by a new high-performance liquid chromatography methodology. *Journal of Agricultural and Food Chemistry*, *58*, 88-93.
Döpner, S., Hildebrandt, P., Mauk, A. G., Lenk, H., & Stempfle, W. (1996). Analysis of vibrational spectra of multicomponent systems. Application to a resonance Raman spectroscopic study of cytochrome c. *Spectrochimica Acta Part A: Molecular and Biomolecular Spectroscopy*, *51*, 573-584.
Downey, G., Boussion, J., & Beauchene, D. (1994). Authentication of whole and ground coffee beans by near infrared reflectance spectroscopy. *Journal of Near Infrared Spectroscopy*, *2*, 85-92.
Downey, G., Briandet, R., Wilson, R.H., & Kemsley, E.K. (1997). Near- and Mid-infrared spectroscopies in food authentication: coffee varietal identification. . *Journal of Agricultural and Food Chemistry*, *45*, 4357-4361.
Downey, G., McIntyre, P., & Davies, A.N. (2003). Geographical classification of extra virgin olive oils from the Eastern mediterranean by chemometric analysis of visible and near/infrared spectroscopy data. *Applied Spectroscopy*, *57*, 158-163.
Drake, P.L., Franks, P.J. (2003). Water resource partitioning, stem xylem hydraulic properties and plant water use strategies in a seasonally dry riparian tropical rainforest. *Oecologia*, *137*, 321-329.

Drouet, T., Herbauts, J., & Demaiffe, D. (2007). Change of the origin of calcium in forrest ecosystems in the twentieth century highlighted by natural Sr isotopes. In: T. E. Dawson, & R. T. W. Siegwolf, *Stable Isotopes As Indicators of Ecological Change*. London: Elsevier.

Dunbar, J., & Wilson, A.T. (1982). Determination of geographic origin of caffeine by stable isotope analysis. *Analytical Chemistry*, *54*, 590-592.

Dupuy, N., Le Dréau, Y., Ollivier, D., Artaud, J., Pinatel, C., & Kister, J. (2005). Origin of French virgin olive oil registered designation of origins predicted by chemometric analysis of synchronous excitation-emission fluorescence spectra. *Journal of Agricultural and Food Chemistry*, *53*, 9361-9368.

EarthChem (2003). Advanced Data Management in Solid Earth Geochemistry. http://www.earthchem.org/

Eggers, R., & Pietsch, A. (2001). Technology I: Roasting. In: R.J. Clarke, & O.G. Vitzthum, *Coffee, Recent Developments*. Oxford: Balckwell Science.

Ehleringer, J.R., & Dawson, T.E. (1992). Water uptake by plants. Perspectives from stable isotope composition. *Plant, Cell and Environment*, *15*, 1073-1082.

Eira, M.T.S., Amaral da Silva, E.A., de Castro, R.D., Dussert, S., Walters, C., Bewley, J.D., & Hilhorst, H.W.M. (2006). Coffee seed physiology. *Brazilian Journal of Plant Physiology*, *18*, 149-163.

Emura, M., Nohara, I., Toyoda, T., & Kanisawa, T. (1997). The volatile constituents of the coffee flower (*Coffea arabica* L.). *Flavour and Fragance Journal*, *12*, 9-13.

Esteban-Diez, I., Gonzalez-Saiz, J.M., & Pizarro, C. (2004). An evaluation of orthogonal signal correction methods for the characterization of arabica and robusta coffee varieties by NIRS. . *Analytical and Bioanalytical Chemistry*, *514*, 57-67.

Esteban-Diez, I., Gonzalez-Saiz, J.M., Saenz-Gonzalez, C., & Pizarro, C. (2007). Coffee varietal differentiation based on near infrared spectroscopy. *Talanta*, *71*, 221-229.

Etiévant, P., Schlich, P., Cantagrel, R., Bertrand, M., & Bouvier, J.-C. (2006). Varietal and geographic classification of French red wines in terms of major acids. *Journal of Science of Food and Agriculture*, *46*, 421-438.

EuDASM (2005). European Digital Archive of Soil Maps. Maps are holdings of ISRIC. http://eusoils.jrc.ec.europa.eu/esdb_archive/eudasm/EUDASM.htm.

EURACHEM/CITAC (2000). EURACHEM/CITAC Guide (http://measurementuncertainty.org/). Quantifying Uncertainty in Analytical Measurement.

Evans, R. (2001). Physiological mechanisms influencing plant nitrogen isotope composition. *Trends in Plant Science*, *6*, 121-126.

Farquhar, G.D., Ehleringer, J.R., & Hubik, K.T. (1989). Carbon isotope discrimination and photosynthesis. *Annual Review of Plant Physiology and Plant Molecular Biology*, *40*, 503-537.

Farquhar, G.D., & Lloyd, J. (1993). Carbon and oxygen isotope effects in the exchange of carbon dioxide between terrestrial plants and the atmosphere. In: J.R. Ehleringer, A.E. Hall, & G.D. Farquhar, *Stable isotopes and plant carbon-water relations*. San Diego: Academic Press.

Fay, L.B., & Brevard, H. (2005). Contribution of mass spectrometry to the study of Maillard reaction in food. *Mass Spectrometry Reviews*, *24*, 487-507.

Ferreira, L., Perestrelo, R., & Câmara, J.S. (2009). Comparative analysis of the volatile fraction from *Annona chemiola* Mill. cultivars by solid-phase microextraction and gas chromatography-quadrupole mass spectrometry detection. *Talanta*, *77*, 1087-1096.

Fischer, M., Reimann, S., Trovato, V., & Redgwell, R.J. (2001). Polysaccharides of green Arabica and Robusta coffee beans. *Carbohydrate Research*, *330*, 93-101.
Flament, I. (2002). *Coffee Flavour Chemistry*. Chichester Wiley.
Flanagan, L.B. (2005). *Stable isotopes and biosphere-atmosphere interactions, processes and biological controls*. Oxford: Elsevier.
Flanagan, L.B., & Ehleringer, J.R. (1991). Stable isotope composition of stem and leaf water: applications to the study of plant water use. *Functional Ecology*, *5*, 270-277.
Food Standards Agency (2007). What consumers want – A literature review. Labelling and Packing. Labelling Research. Retrieved in 25.09.2007: http://www.food.gov.uk/foodlabelling/researchreports/litreview.
Ford, D. (2008). Global warming pushes Peru to pick coffee earlier. *Reuters News*: Reuters.
Fortunato, G., Mumic, K., Wunderli, S., Pillonel, L., Bosset, J.O., & Gremaud, G. (2004). Application of strontium isotope abundance ratios measured by MC-ICP-MS for food authentication. *Journal of Analytical Atomic Spectrometry*, *19*, 227-234.
Franca, A.S., Oliveira, L.S., Oliveira, R.C.S., Agresti, P.C.M., & Augusti, R. (2009). A preliminary evaluation of the effect of processing temperature on coffee roasting degree assessment. *Journal of Food Engineering*, *92*, 345-352.
García-Ruiz, S., Moldovan, M., Fortunato, G., Wunderli, S., & García Alonso, J.I. (2007). Evaluation of strontium isotope abundance ratios in combination with multi-elemental analysis as a possible tool to study the geographical origin of ciders. *Analytica Chimica Acta*, *590*, 55-66.
Gibson, J.J., Birks, S.J., & Edwards, T.W.D. (2008). Global prediction of δ_A and δ^2H-$\delta^{18}O$ evaporation slopes for lakes and soil water accounting for seasonality. *Global Biogeochemical Cycles*, *22*(GB2031).
Gibson, J.J., Fekete, B., & Bowen, G. (2009). Stable isotopes in large scale hydrological applications. In: J. West, & G. Bowen, *Isoscapes: Understanding movement, pattern, and process on Earth through isotope mapping*: Springer.
Gleixner, G., Scrimgeour, C., Schmidt, H.L., & Viola, R. (1993). Correlations between the ^{13}C content of primary and secondary plant products in different cell compartments and that in decomposing basidiomycetes. *Plant Physiology*, *102*, 1287-1290.
Global Gazetter. (2006). Global Gazetteer. Falling Rain Genomics, Inc.
González, A.G., Pablos, F., Martín, M.J., Léon-Camanho, M., Valdenebro, M.S. (2001). HPLC analysis of tocopherols and triglycerides in coffee and then use as authentication parameters. *Food Chemistry*, *73*, 93-101.
González-Miret, M., Ayala, F., Terrab, A., Echávarri, J.F., Negueruela, A.I., & Heredia, F.J. (2007). Simplified method for calculating colour of honey by application of the characteristic vector method. *Food Research International*, *40*, 1080-1086.
González-Rios, M., Suarez-Quiroz, M.L., Boulanger, R., Barel, M., Guyot, B., Guirard, J.P., & Schrorr-Galindo, S. (2007). Impact of 'ecological' post-harvest processing on coffee aroma: II. Roasted coffee. *Journal of Food Composition and Analysis*, *20*, 297-307.
Goodman, D. (2008). *Confronting the Coffee Crisis, Fair Trade, Sustainable Livelihoods and Ecosystems in Mexico and Central America*. Cambridge: The MIT Press.
Górecki, T., Yu, X., & Pawliszyn, J. (1999). Theory of analyte extraction by selected porous polymer SPME fibers. *Analyst*, *124*, 643-649.
Grainger, S. (2010). Central America coffee land to shrink as globe warms. *Reuters News*: Reuter.

Grosch, W. (2001). Chemistry III: Volatile Compounds. In: R.J. Clarke, & O.G. Vitzthum, *Coffee, Recent Developments* (pp. 68-89). Oxford: Blackwell Science.
Harmon, A.D. (2002). *Solid-phase microextraction for the analysis of aromas and flavours*. New York: Marcel Dekker.
Hatanaka, M., Bain, C., & Busch, L. (2005). Third-party certification in the global agri-food system. *Food Policy*, *30*, 354-369.
Hatchett, D.W., Kodippili, G., Kinyanjui, J. M., Benincasa, F., & Sapochak, L. (2005). FTIR analysis of thermally processed PU foam. *Polymer degradation and stability*, *87*, 555-561.
Hernandéz, J.A., Heyd, B., Irles, C., Valdovinos, B., & Trystram, G. (2007). Analysis of the heat and mass transfer during coffee batch roasting. *Journal of Food Engineering*, *78*, 1141-1148.
Higgins, V., Dibden, J., & Coklin, C. (2008). Building alternative agri-food networks: Certification, embeddedness and agro-environmental governance. *Journal of Rural Studies*, *24*, 15-27.
Hobbie, E., & Werner, R. (2004). Intramolecular, compound-specific, and bulk carbon isotope patterns in C_3 and C_4 plants: a review and synthesis. *New Phytologist*, *161*, 371-385.
Horacek, M., & Min, J.S. (2010). Discrimination of Korean beef from beef of other origin by stable isotope measurements. *Food Chemistry*, *121*, 517-520.
Hu, Y., Zheng, Y., Zhu, F., Li, G. (2007). Sol-gel coated polydimethylsiloxane/β-cyclodextrin as novel stationary phase for stir bar sorptive extraction and its application to analysis of estrogens and bisphenol A. *Journal of Chromatography A, 1148,* 16-22.
Huang, L.-F., Wu, M.-J., Zhong, K.-J., Sun, X.-J., Liang, Y.-Z., Dai, Y.-H., Huang, K.-L., & Guo, F.-Q. (2007). Fingerprint developing of coffee flavor by gas chromatography-mass spectrometry and combined chemometrics methods. *Analytica Chimica Acta*, *588*, 216-223.
Hue, N.V., Fox, R.L., & Wolt, J.D. (1990). Sulfur status of volcanic ash-derived soils in Hawaii. *Communications in Soil Science and Plant Analysis*, *21*, 299-310.
IAEA (2001). GNIP Maps and Animations, International Atomic Energy Agency, Vienna. Accessible at http://isohis.iaea.org
ICO (2009). International Coffee Organization (ICO) ICO indicator prices. http://www.ico.org/prices/pr.htm.
Ingraham, N., & Taylor, B. (1991). Light stable isotope systematics of large-scale hydrologic regimes in California and Nevada. *Water resources research*, *27*, 77-90.
Ishikawa, M., Ito, O., Ishizaki, S., Kurobayashi, Y., & Fujita, A. (2004). Solid-phase aroma concentrate extraction (SPACETM): a new headspace technique for more sensitive analysis of volatiles. *Flavour and Fragance Journal*, *19*, 183-187.
Jaffe, D. (2007). *Brewing Justice, Fair Trade Coffee, Sustainability, and Survival*. Berkeley: University of California Press.
Kabata-Pendias, A. (2001). *Trace elements in soils and plants*. Boca Raton: CRC Press.
Karoui, R., Bosset, J.-O., Mazerolles, G., Kulmyrzaev, A., & Dufour, E. (2005). Monitoring the geographic origin of both experimental French Jura hard cheeses and Swiss Gruyère and L'Etivaz PDO cheeses using mid-infrared and fluorescence spectroscopies: A preliminary investigations. *International Dairy Journal*, *15*, 275-286.
Kelly, S., Heaton, K., & Hoogewerff, J. (2005). Traccing the geographical origin of food: The application of multi-element and multi-isotope. *Trends in Food Science & Technology*, *16*, 555-567.

Kemsley, E.K., Ruault, S., & Wilson, R.H. (1995). Discrimination between Coffea arabica and Coffea canephora variant robusta beans using infrared spectroscopy. *Food Chemistry*, *54*, 321-326.
Kennedy, M.J., Chadwick, O.A., Vitousek, P.M., Derry, L.A., & Hendricks, D.M. (1998). Replacement of weathering with atmospheric sources of base cations during ecosystem development, Hawaiian Islands. *Geology*, *26*, 1015-1018.
Kölling-Speer, I., Strohschneider, S., & Speer, K. (1999). Determination of free diterpenes in green and roasted coffees. *Journal of High Resolution Chromatography*, *22*, 43-46.
Koshiro, Y., Zheng, X.-Q., Wang, M.-L., Nagai, C., & Ashihara, H. (2006). Changes in content and biosynthetic activity of caffeine and trigonelline during growth and ripening of *Coffea arabica* and *Coffea canephora* fruits. *Plant Science*, *2006*, 242-250.
Krivan, V., Barth, P., & Morales, A. (1993). Multielement analysis of green coffee and its possible use for the discrimination of origin. *Mikrochimica Acta*, *110*, 217-236.
Krouse, H.R., Stewart, J.W.B., & Grinenko, V.A. (1991). Pedosphere and biosphere. In: H.R. Krouse, & V.A. Grinenko, *Stable Isotopes: Natural and Anthropogenic Sulfur in the Environment, SCOPE 43*. New York: Wiley.
Kurzrock, T., & Spear, K. (2001). Diterpenes and diterpene esters in coffee. *Food Reviews International*, *17*, 433-450.
Lakatos, M., Hartard, B., Máguas, C. (2007). The stable isotopes $\delta^{13}C$ and $\delta^{18}O$ of lichens can be used as tracers of microenvironmental carbon and water sources. In: T.E. Dawson, R.T.W. Siegwolf, *Stable isotopes as indicators of ecological change*. Amsterdam: Academic Press, Elsevier.
Lajtha, K., & Marshall, J.D. (1994). Sources of variation in the stable isotopic composition of plants. In: K. Lajtha, & R.H. Michener, *Stable Isotopes in Ecology and Environmental Science*. Oxford: Blackwell Scientific Publications.
Lee, K.-G., & Shibamoto, T. (2002). Analysis of volatile components isolated from Hawaiian green coffee beans (*Coffea arabica* L.). *Flavour and Fragance Journal*, *17*, 349-351.
Lin, G., Sternberg, L. (1992). Comparative study of water uptake and photosynthetic gas exchange between scrub and fringe red mangroves, *Rhizophora mangle* L.. *Oecologia*, *90*, 399-403.
Loader, N.J., McCarroll, D., Gagen, M., Robertson, I., & Jalkanene, R. (2007). Extracting climatic information from stable isotopes in tree rings. In: T.E. Dawson, & T.W. Siegwolf, *Stable isotopes as indicators of ecological change*. Amsterdam: Academic Press, Elsevier.
Luykx, D.M.A.M., & van Ruth, S.M. (2008). An overview of analytical methods for determining the geographical origin of food products. *Food Chemistry*, *107*, 897-911.
Macko, S., Estep, M., & Engle, M. (1986). Kinetic fractionation of stable nitrogen isotopes during amino acid transamination. *Geochimica et Cosmochimica Acta*, *50*, 2143-2146.
Máguas, C., & Griffiths, H. (2003). Applications of stable isotopes in plant ecology. In: K. Esser, U. Lüttge, W. Beyschlag, *Progress in Botany*. Berlin: Springer.
Mannina, L., Patumi, M., Proietti, N., Bassi, D., & Segre, A.L. (2001). Geographical chracterization of Italian extra virgin oils using high-field ^{1}H NMR spectroscopy, *Journal of Agricultural and Food Chemistry*, *49*, 2687-2696.
Marshall, J. D., Renée Brooks, J., & Lajtha, K. (2007). Sources of variation in the stable isotopic composition of plants. In: R. Michener, & K. Lajtha, *Stable Isotopes in Ecology and Environmental Science*. Oxford: Blackwell Publishing.

Martín, M., Pablos, F., González, A., Valdenebro, M., & León-Camacho, M. (2001). Fatty acid profiles as discriminant parameters for coffee varieties differentiation. *Talanta*, *54*, 291-297.
Martín, M., Pablos, F., & González, A.G. (1998). Discrimination between arabica and robusta green coffee varieties according to their chemical composition. *Talanta*, *46*, 1259-1264.
Martin, M.J., Pablos, F., & Gonzalez, A.G. (1999). Characterization of arabica and robusta roasted coffee varieties and mixture resolution according to their metal content. *Food Chemistry*, *66*, 365-370.
McPhaul, J. (2008). Global warming moves Costa Rica coffee land higher. *Reuters News*: Reuter.
Mehdinla, A., Mouravi, M.F. (2008). Enhancing extraction rate in solid-phase microextraction by using nano-structure polyaniline coating. *Journal of Separation Science*, *31*, 3565-3572.
Mendes, L.C., Menezes, H.C., Aparecida, M., & da Silva, A.P. (2001). Optimization of the roasting of robusta coffee (*C. canephora* conillon) using acceptability tests and RSM. *Food Quality and Preference*, *12*, 153-162.
Mendonça, J.C.F., Franca, A.S., & Oliveira, L.S. (2009). Physical characterization of non-defective and defective Arabica and Robusta coffees before and after roasting. *Journal of Food Engineering*, *92*, 474-479.
Mendonça, J.C.F., Franca, A.S., Oliveira, L.S., & Nunes, M. (2008). Chemical characterisation of non-defective and defective green arabica and robusta coffees by electrospray ionization-mass spectrometry (ESI-MS). *Food Chemistry*, *111*, 490-497.
Mendoza, F., Dejmek, P., & Aguilera, J.M. (2006). Calibrated color measurements of agricultural foods using image analysis. *Postharvest biology and technology*, *41*.
Meng, Q., & Liang, T. (2007). HNRIS (Hawaii Natural Resource Information System) for Windows. Honolulu (HI): University of Hawaii at Manoa.
Mizota, C., & Sasaki, A. (1996). Sulfur isotope composition of soils and fertilizers: Differences between Northern and Southern Hemispheres. *Geoderma*, *71*, 77-93.
Moire, A., & Wadleigh, M.A. (2003). Lichens and atmospheric sulphur: what stable isotopes reveal. *Environmental Pollution*, *126*, 345-351.
Muik, B., Lendl, B., Molina-Díaz, A., Ayora-Cañada, M.J. (2005). Direct monitoring of lipid oxidation in edible oils by Fourier-transform Raman spectroscopy. *Chemistry and Physics of Lipids*, *134*, 173-182.
Murray, A.P., Edwards, D., Hope, J.M., Boreham, C.J., Booth, W.E., Alexander, R.A., & Summons, R.E. (1998). Carbon isotope biogeochemistry of plant resins and derived hydrocarbons. *Organic Geochemistry*, *29*, 1199-1217.
Neng, N.R., Pinto, M.L., Pires, J., Marcos, P.M., & Nogueira, J.M.F. (2007). Development, optimisation and application of polyurethane foams as new polymeric phases for stir bar sorptive extraction. *Journal of Chromatography A*, *1171*, 8-14.
O'Leary, M., Madhavan, S., & Paneth, P. (1992). Physical and chemical basis of carbon isotope fractionation in plants. *Plant, Cell and Environment*, *15*, 1099-1104.
Oka, H., Tokunaga, Y., Masuda, T., Kiso, H., & Yoshimura, H. (2006). Characterization of local structures in flexible polyurethane foams by solid-state NMR and FTIR spectroscopy. *Journal of Cellular Plastics*, *42*, 307-323.
Ollivier, D., Artaud, J., Pinatel, C., Durbec, J.P., & Guérère, M. (2003). Triacylglycerol and fatty acid compositions of French virgin olive oils. Characterisation by chemometrics. *Journal of Agricultural and Food Chemistry*, *51*, 5723-5731.
Pawliszyn, J. (1997). *Solid-phase microextraction - theory and practice*. New York: Wiley-VCH.

Perez, A.L., Smith, B.W., & Anderson, K.A. (2006). Stable isotope and trace element profiling combined with classification models to differentiate geographic growing origin for three fruits: effects of subregion and variety. *Journal of Agricultural and Food Chemistry*, *54*, 4506-4516.

Pilgrim, T.S., Watling, R.J., & Grice, K. (2010). Application of trace element and stable isotope signatures to determine the provenance of tea (Camellia sinensis) samples. *Food Chemistry*, *118*, 921-926.

Pizarro, C., Esteban-Diez, I., & Gonzalez-Saiz, J.M. (2007). Mixture resolution according to the percentage of robusta variety in order to detect adulteration in roasted coffee by near infrared spectroscopy. *Analytica Chimica Acta*, *585*, 266-276.

Portugal, F.C.M., Pinto, M.L., & Nogueira, J.M.F. (2008). Optimization of polyurethane foams for enhanced stir bar sorptive extraction of triazinic herbicides in water matrices. *Talanta*, *77*, 765-773.

Portugal, F.C.M., Pinto, M.L., Pires, J., Nogueira, J.M.F. (2010). Potentialities of polyurethane foams to trace level analysis of triazinic metabolites in water matrices by stir bar sorptive extraction. *Journal of Chromatography A*, *1217*, 3707-3710.

Portugal, F.C.M. (2010). Desenvolvimento, Optimização e Aplicação de Novas Fases Poliméricas (Poliuretanos) para Extracção Sortiva em Barra de Agitação (SBSE). Doutoramento em Química. Lisboa: Faculdade de Ciências da Universidade de Lisboa.

Powers, M.D., Pregitzer, K.S., & Palik, B.J. (2008). $\delta^{13}C$ and $\delta^{18}O$ trends across overstory environments in whole foliage and cellulose of three *Pinus* species. *Journal of American Society for Mass Spectrometry*, *19*, 1330-1335.

Prohaska, T., Wenzel, W., & Stingeder, G. (2005). ICP-MS-based tracing of metal sources and mobility in a soil depth profile via the isotopic variation of Sr and Pb. *International Journal of Mass Spectrometry*, *242*, 243-250.

Rhodes, C.N., Heaton, K., Goodall, I., & Brereton, P.A. (2009). Gas chromatography carbon isotope ratio mass spectrometry applied to the detection of neutral alcohol in Scotch whisky: an internal reference approach. *Food Chemistry*, *114*, 697-701.

Risticevic, S., Carasek, E., Pawliszyn, J. (2008). Headspace solid-phase microextraction-gas chromatographic-time-of-flight mass spectrometric methodology for geographical origin verification of coffee. *Journal of Agriculture and Food Chemistry*, *617*, 72-84.

Roberts, D.D., Pollien, P., & Milo, C. (2000). Solid-phase microextraction method development for headspace analysis of volatile flavor compounds. *Journal of Agricultural and Food Chemistry*, *48*, 2430-2437.

Robinson, D. (2001). $\delta^{15}N$ as an integrator of the nitregon cycle. *Trends in Ecology & Evolution*, *16*, 153-162.

Rocha, S., Maetzu, L., Barros, A., Cid, C., & Coimbra, M.A. (2003). Screening and distribution of coffee brews based on headspace solid phase microextraction/gas chromatography/principal component analysis. *Journal of the Science of Food and Agriculture*, *84*, 43-51.

Roden, J.S., Lin, G., & Ehlereinger, J.R. (2000). A mechanistic model for interpretation of hydrogen and oxygen isotope ratios in tree-ring cellulose. *Geochimica et Cosmochimica Acta*, *64*, 21-35.

Rodrigues, C., Máguas, C., & Prohaska, T. (2011). Strontium and oxygen isotope fingerprinting of green coffee beans and its potential to proof authenticity of coffee. *European Food Research and Technology*, 232, 361-373.

Rodrigues, C., Maia, R., Miranda, M., Ribeirinho, M., Nogueira, J.M.F., & Máguas, C. (2009). Stable isotope analysis for green coffee bean: a possible method for geographic origin discrimination. *Journal of Food Composition and Analysis*, *22*, 463-471.

Rodrigues, C., Marta, L., Maia, R., Miranda, M., Ribeirinho, M., Máguas, C. (2007). Application of solid-phase extraction to brewed coffee caffeine and organic acid determination by UV/HPLC. *Journal of Food Composition and Analysis*, *20*, 440-448.
Rosário, P., Nogueira, J.M.F., (2006) Combining stir bar sorptive extraction and MEKC for the determination of polynuclear aromatic hydrocarbons in environmental and biological matrices. *Electrophoresis*, *27*, 4694-4702.
Rose, K.L., Graham, R.C., Parker, D.R. (2003). Water source utilization by *Pinus jeffreyi* and *Anctostaphylos patula* on thin soils over bedrock. *Oecologia*, *134*, 46-54.
Rossmann, A., Haberhauer, G., Holzl, S., Horn, P., Pichlmayer, F., & Voerkelius, S. (2000). The potential of multielement stable isotope analysis for regional origin assignment of butter. *European Food Research and Technology*, *211*, 32-40.
Rubayiza, A.B., & Meurens, M. (2005). Chemical discrimination of Arabica and Robusta coffees by Fourier transform Raman spectroscopy. *Journal of Agricultural and Food Chemistry*, *53*, 4654-4659.
Ruiz del Castillo, M.L., Caja, M.M., Blanch, G.P., & Herriaz, M. (2003). Enantiometric distribution of chiral compounds in orange juices according to their geographical origins. *Journal of Food Protection*, *66*, 1448-1454.
Sakai, H., Casadevall, T.J., & Moore, J.J. (1982). Chemistry and isotope ratios of sulfur in basalts and volcanic gases at Kilauea volcano, Hawaii. *Geochimica et Cosmoquimica Acta*, *46*, 729-738.
Sanz, C., Ansorena, D., Bello, J., & Cid, C. (2001). Optimizing headspace temperature and time sampling for identification of volatile compounds in ground roasted Arabica coffee. *Journal of Agricultural and Food Chemistry*, *49*, 1364-1369.
Sanz, C., Maetzu, L., Zapelena, M.J., Bello, J., & Cid, C. (2002). Profiles of volatile compounds and sensory analysis of three blends of coffee: influence of different proportions of Arabica and Robusta and influence of roasting coffee with sugar. *Journal of the Science of Food and Agriculture*, *82*, 840-847.
Saranga, Y., Flash, I., Paterson, A.H., & Yakir, D. (1999). Carbon isotope ratio in cotton varies with growth stage and plant organ. *Plant Science*, *142*, 47-56.
Scheidegger, Y., Sauer, M., Bahn, M., & Siegwolf, R.T.W. (2000). Linking stable oxygen and carbon isotopes with stomatal conductance and photosynthetic capacity: a conceptual model. *Oecologia*, *125*, 350-357.
Schmidt, H.-L., Werner, R. A., & Rossman, A. (2001). ^{18}O Pattern and biosynthesis of natural plant products. *Phytochemistry*, *58*, 9-32.
Schmidt, O., Quilter, J.M., Bahar, B., Moloney, A.P., Scrimgeour, C.M., Begley, I.S., & Monahan, F.J. (2005). Inferring the origin and dietary history of beef from C, N and S stable isotope ratio analysis. *Food Chemistry*, *91*, 545-549.
Scholl, M.A., Ingebritsen, S.E., Janik, C.J., & Kauahikaua, J.P. (1996). Use of precipitation and groundwater isotopes to interpret regional hydrology on a tropical volcanic island: Kilauea volcano area *Water resources research*, *32*, 3525-3537.
Schultheis, G. (2003). Analysis of isotope ratios in anthropological and archaeological samples by high resolution inductively coupled plasma mass spectrometry (HR-ICP-MS). PhD. Vienna: Universität für Bodenkultur am Institut für Chemie.
Sekiya, N., Yano, K. (2002). Water acquisition from rainfall and groundwater by legume crops developing deep rooting systems determined with stable hydrogen isotope compositions of xylem waters. *Field Crop Research*, *8*, 133-137.
Serôdio, P., Nogueira, J.M.F. (2004). Multi-residue screening of endocrine disrupters chemicals in water samples by stir bar sorptive extraction-liquid desorption-capillary gas chromatography-mass spectrometry detection. *Analytica Chimica Acta*, *517*, 21-32.

Serôdio, P., Nogueira, J.M.F. (2005) Development of a stir-bar-sorptive extraction-liquid desorption-large-volume injection capillary gas chromatographic-mass spectrometric method for pyrethroid pesticides in water samples. *Analytical and Bioanalytical Chemistry*, *382*, 1141-1151.

Serôdio, P., Cabral, M.S., Nogueira, J.M.F. (2007). Use of experimental desings in the optimization of stir bar sorptive extraction for the determination of polybrominated diphenyl ethers in environmental matrices. *Journal of Chromatography A*, *1141*, 259-270.

Serra, F., Guillou, C., Reniero, F., Ballarin, L., Cantagallo, M., Wieser, M., Iyer, S., Héberger, K., & Vanhaecke, F. (2005a). Determination of the geographical origin of green coffee by principal component analysis of carbon, nitrogen and boron stable isotope ratios. *Rapid Communications in Mass Spectrometry*, *19*, 2111-2115.

Shulthess, B. H., & Baumann, T. W. (1995). Stimulation of caffeine biosynthesis in suspension-cultured coffee cells and the *in situ* existence of 7-methylxanthosine. *Phytochemistry*, *38*, 1381-1386.

Silva, A. R. M., & Nogueira, J. M. F. (2008a). New approaches on trace analysis of triclosan in personal care products, biological and environmental matrices. *Talanta*, *74*, 1298-1504.

Silva, A.R.M., Portugal, F.C.M., & Nogueira, J.M.F. (2008b). Advances in stir bar sorptive extraction for the determination of acidic pharmaceuticals in environmental water matrices. Comparison between polyurethane and polydimethylsiloxane polymeric phases. *Journal of Chromatography A*, *1209*, 10-16.

Silva, E., DaMatta, F., Ducatti, C., Regazzi, A., & Barros, R. (2004). Seasonal changes in vegetative growth and photosynthesis of Arabica coffee trees. *Field Crops Research*, *89*, 349-357.

Smith, A.W. (1985). Introduction. In: R.J. Clarke, & R. Macrae, *Coffee. Volume 1: Chemistry*. London: Elsevier.

Smith, D.M., Jarvis, P.G., Odongo, J.C.W. (1997). Sources of water used by trees and millet in Sahelian windbreak systems. *Journal of Hydrology*, *198*, 140-153.

Smith, R.M. (2003). Before the injection--modern methods of sample preparation for separation techniques. *Journal of Chromatography A*, *1000*, 3-27.

Sondahl, M., & Baumann, T. (2001). Agronomy II: Developmental and Cell Biology. In: R. Clark, & O. Vitzthum, *Coffee, Recent Developments*. Oxford: Blackwell.

Steiman, S. (2008). *The Hawai'i Coffee Book. A Gourmet's Guide from Kona to Kaua'i*. Honolulu: Watermark Publishing.

Stein, M., Starinsky, A., Katz, A., Goldstein, S. L., Machlus, M., & Schramm, A. (1997). Strontium isotopic, chemical, and sedimentological evidence for the evolution of Lake Lisan and the Dead Sea. *Geochimica and Cosmochimica Acta*, *61*, 3975-3992.

Stratton, L.C., Goldstein, G., Meinzer, F.C. (2000). Temporal and spatial partitioning of water resources among eight woody species in a Hawaiian dry forest. *Oecologia*, *124*, 304-317.

Suchanek, M., Filipova, H., Volka, K., Delgadillo, I., & Davies, A.N. (1996). Qualitative analysis of green coffee by infrared spectrometry. *Fresenius Journal of Analytical Chemistry*, *354*, 327-332.

Suzuki, Y., Chikaraishi, Y., Ogawa, N. O., Ohkoushi, N., & Korenaga, T. (2008b). Geographical origin of polished rice based on multiple element and stable isotope analysis. *Food Chemistry*, *109*, 470-475.

Swoboda, S., Brunner, M., Boulyga, S. F., Galler, P., Horacek, M., & Prohaska, T. (2008). Identification of Marchfeld asparagus using Sr isotope ratio measurements by MC-ICP-MS. *Analytical and Bioanalytical Chemistry*, *390*, 487-494.

Tanz, N., & Schmidt, H.-L. (2010). d34S-Value Measurements in Food Origin Assignments and Sulphur Isotope Fractionations in Plants and Animals. *Journal of Agricultural Food Chemistry*, *58*, 3139-3146.
Tcherkez, G.S., Nogue, S., Bleton, J., Cornic, G., Badeck, F., & Ghashghaie, J. (2003). Metabolic origin of carbon isotope composition of leaf dark-respired CO2 in french bean. *Plant Physiology*, *131*, 237-244.
Techer, I., Lancelot, J., Descroix, F., & Guyot, B. (2011). About Sr isotopes in cofee 'Bourbon Pointu' of the Réunion Island *Food Chemistry*, *126*, 718-724.
Trust, B. A., & Fry, B. (1992). Stable sulphur isotopes in plants: a review. *Plant, Cell and Environment*, *15*, 1105-1110.
Vallano, D.M., & Sparks, J.P. (2007). Foliar $\delta^{15}N$ values as indicators of foliar uptake of atmospheric nitrogen pollution. In: T.E. Dawson, & T.W. Siegwolf, *Stable Isotopes and Indicators of Ecological Change*. London: Elsevier.
Van der Vossen, H. (2001). Agronomy I: Coffee Breeding Practices. In: R. Clark, & O. Vitzthum, *Coffee, Recent Developments*. Oxford: Blackwell.
Vitousek, P.M., Kennedy, M.J., Derry, L.A., & Chadwick, O.A. (1999). Weathering versus atmospheric sources of strontium in ecosystems on young volcaninc soils. *Oecologia*, *121*, 255-259.
Wadleigh, M.A. (2003). Lichens and atmospheric sulphur: what stable isotopes reveal. *Environmental Pollution*, *126*, 345-351.
Wadleigh, M.A., & Blake, D.M. (1999). Tracing sources of atmospheric sulphur using epiphytic lichens. *Environmental Pollution*, *106*, 265-271.
Weckerle, B., Richling, E., Heinrich, S., & Schreier, P. (2002). Origin assessment of green coffee (*Coffea arabica*) by multi-element stable isotope analysis of caffeine. *Analytical and Bioanalytical Chemistry*, *374*, 886-890.
Weltzin, J.F., McPherson, G.R. (1997). Spatial and temporal soil moisture resource partitioning ny trees and grasses in a temperate savanna, Arizona, USA. *Oecologia*, *112*, 156-164.
Werner, R.A., & Schmidt, H.-L. (2002). The *in vivo* nitrogen isotope discrimination among organic plant compounds. *Phytochemistry*, *61*, 465-484.
West, J.B., Bowen, G.J., Cerling, T.E., & Ehleringer, J.R. (2006). Stable isotopes as one of nature's ecological recorders. *Trends in Ecology and Evolution*, *21*, 408-414.
West, J.B., Kreuzer, H.W., & Ehleringer, J.R. (2010). Approaches to plant hydrogen and oxygen isoscapes generation In: J.B. West, G.J. Bowen, T.E. Dawson, & K.P. Tu, *Isoscapes, Understanding movement, pattern, and process on Earth through isotope mapping*. Dordrecht: Springer.
West, J.B., Sobek, A., & Ehleringer, J.R. (2008). A simplified GIS approach to modeling global leaf water isoscapes. *PlosOne*, *3*, e2447.
Whipkey, C.E., Capo, R.C., Chadwick, O.A., & Stewart, B.W. (2000). The importance of sea spray to the caption budget of a coastal Hawaiian soil: a strontium isotope approach. *Chemical Geology*, *168*, 37-48.
White, J.W.C., Cook, E.R., Lawrence, J.R., & Broecker, W.S. (1985). The D/H ratios of sap in trees: implications for water sources and tree ring D/H ratios. *Geochimica and Cosmochimica Acta*, *49*, 237-246.
Wieser, E., Iyer, S., Krouse, H., & Cantagallo, M. (2001). Variations in the boron isotope composition of coffea arabica beans. *Applied Geochemistry*, *16*, 317-322.
Wihlborg, R., Pippitt, D., & Marsili, R. (2008). Headspace sorptive extraction and GC-TOFMS for the identification of volatile fungal metabolites. *Journal of Microbiological Methods*, *75*, 244-250.

Williams, D.G., Coltrain, J.B., Lott, M., English, N.B., & Ehleringer, J.R. (2005). Oxygen isotopes in cellulose identify source water for archaeological maize in the American Southwest. *Journal of Archaeological Science*, *32*, 931-939.
Wintgens, J. (2004a). The Coffee Plant. In: J. Wintgens, *Coffee: Growing, Processing, Sustainable Production. A Guidebook for Growers, Processors, Traders, and Researchers*. Weinheim: Wiley-VCH.
Wintgens, J. (2004b). Factos influencing the quality of green coffee. In: J. Wintgens, *Coffee: Growing, processing, sustainable production. A guidebook for growers, processors, traders, and researchers.* Weinheim.: Wiley-VCH.
Yakir, D. (1992). Variations in the natural abundance of oxygen-18 and deuterium in plant carbohydrates. *Plant, Cell and Environment*, *15*, 1005-1020.
Yakir, D., & DeNiro, M. J. (1990). Oxygen and hydrogen isotope fractionation during cellulose metabolism in *Lemna gibba* L. *Plant Physiology*, *93*, 325-332.
Yakir, D., & Sternberg, L. d. S. L. (2000). The use of stable isotopes to study ecosystem gas exchange. *Oecologia*, *123*, 297-311.
Yang, H., Irudayaraf, J., Paradkar, M. (2005). Discriminant analysis of edible oils and fats by FTIR, FT-NIR and FT-Raman spectroscopy. *Food Chemistry*, *93*, 25-32.
Yeretzian, C., Jordan, A., Badoud, R., & Lindinger, W. (2002). From the green bean to the cup of coffee: investigating coffee roasting by on-line monitoring of volatiles. *European Food Research and Technology*, *214*, 92-104.
Zambonin, C. G., Balest, L., De Benedetto, G. E., & Palmisano, F. (2005). Solid-phase microextraction-gas chromatography mass spectrometry and multivariate analysis for the characterization of roasted coffees. *Talanta*, *66*, 261-265.
Zhang, C., Zhang, J., Zhao, B., Zhang, H., Huang, P. (2009). Stable isotope studies of crop carbon and water relations: a review. *Agricultural Sciences in China, 8,* 578-590.
Zhou, Y., Stuart-Williams, H., Farquhar, G. D., & Hocart, C. H. (2010). The use of natural abundance stable isotopic ratios to indicate the presence of oxygen-containing chemical linkages between cellulose and lignin in plant cell walls. *Phytochemistry*, *71*, 982-993.
Zunin, P., Salvadeo, P., Boggia, R., & Lanteri, S. (2009). Study of different kinds of 'Pesto Genovese' by the analysis of their volatile fraction and chemometric methods. *Food Chemistry*, *114*, 306-309.

APPENDIX

Spectroscopic techniques applied in this work

Isotope ratio mass spectrometry (IRMS)

Stable Isotopes and Instrumental Analysis Facility (SIIAF), FCUL, Lisbon, Portugal

Gas isotope ratio mass spectrometry (GIRMS or simply IRMS; figure 1) was probably the first type of mass spectrometry used in analytical chemistry. IRMS has been the standard tool in areas such as geochemistry, quaternary sciences and environmental sciences (Meier-Augenstein, 2004). In contrast to organic mass spectrometers (MS) that yield structural information by scanning a mass range over several hundred Dalton for characteristic fragment ions, IRMS instruments achieve highly accurate and precise measurement of isotopic abundance at the expense of the flexibility of scanning. Scanning mass spectrometers use a single detector and therefore cannot simultaneously detect particular isotope pairs for isotope ratio measurement.

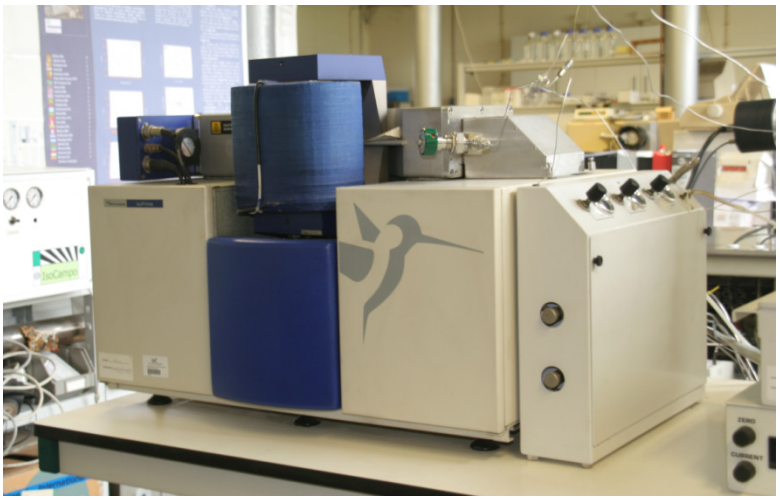

Figure 1. Isoprime (Micromass, UK) isotope ratio mass spectrometer (SIIAF, FCUL).

For isotope ratio measurement, the organic/scanning MSs are best operated in selected ion monitoring mode (SIM) to optimize sensitivity to selected masses. Even in SIM mode, limited accuracy and precision of such isotope ratio measurements impose a minimum working enrichment for ^{13}C and ^{15}N of at least 0.5 atom % excess (APE). In other words, organic MS cannot provide reliable quantitative information in cases where low turnover or low rate of incorporation results in isotopic enrichment of less than 0.5 APE (Meier-Augenstein, 2004). However, in IRMS, it is possible to measure

isotopic composition at low enrichment and natural abundance level. This means that minute variations in very small amounts of the heavier (or less abundant) isotope are detected in the presence of large amounts of the lighter isotope. Since the very small variations of the heavier isotope habitually measured by IRMS are of the order of -0.07 to + 1.09 APE (Meier-Augenstein, 2004), the δ-notation in units of per mil (‰) has been adopted to report changes in isotopic abundance as a per mil deviation compared to a designated isotopic standard. It is also important to remember that IRMS, in fact, determines the difference isotope ratio with great precision and accuracy rather than the absolute isotope ratio (as in ICP-MS).

For isotope ratio measurement the analyte must either be a simple gas as CO_2 or N_2, or must be converted into a simple gas, isotopically representative of the original sample, before entering the ion source of an IRMS. Sample conversion into simple gas molecules was firstly achieved via offline combustion or thermal degradation, the resulting gases being separated in a triple-trap cryogenic separation system associated with a dual-inlet valve system for sample admission into the IRMS (known as "static" IRMS). With the advent of higher yield Dumas-combustion/thermal conversion Elemental Analyzers (EA), it became possible to couple such instruments directly to the IRMS source, via an open split interface, thus using the EA for sample combustion or thermal degradation (figure 2). This technique, currently employed at SIIAF lab, F.C.U.L., allows for higher sample throughput, although for some applications, especially in Geology, offline preparation and dual-inlet analysis is still preferred.

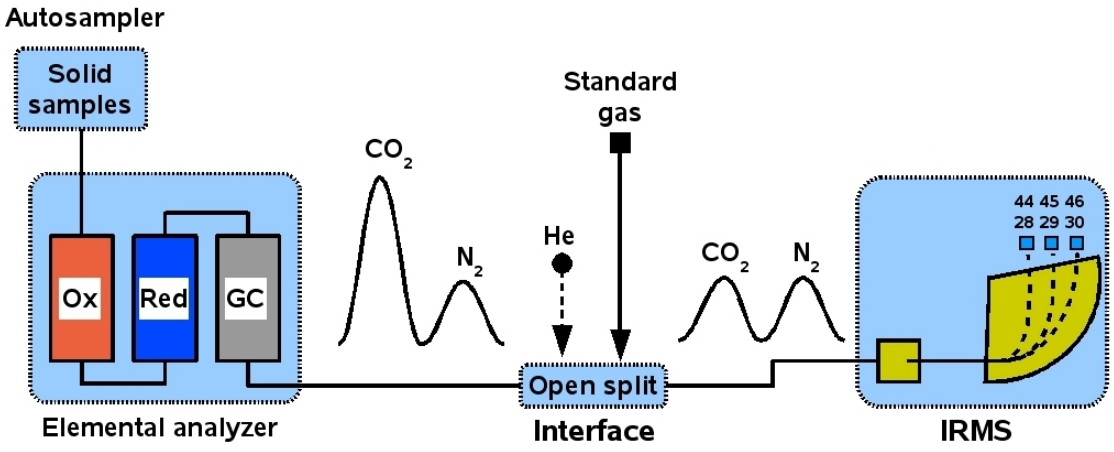

Figure 2. Setup for EA-IRMS for simultaneously measurement of $\delta^{13}C$ and $\delta^{15}N$.

For sample preparation with an EA, sample material is weighted into tin capsules (figure 3) and loaded into a multiple sample carousel on the EA.

Figure 3. Tin capsules utilized to weight the coffee samples and introduce them in the elemental analyzer.

The whole sample including the tin capsule is combusted (1020 °C) in the presence of O_2. The resultant gases are oxidized in the elemental analyzer furnace at 1020 ºC loaded with Cr_2O_3 and Co_3O_4/CoO. The NO_x gases are further reduced to N_2 in a quartz glass tube that is typically filled with copper oxide (CuO) and maintained at a temperature of approximately 600 □C and located downstream from the oxidation furnace; copper will also act as a scrub to remove excess O_2. To remove water vapor generated during combustion, a water trap (magnesium perchlorate) is required. Quantitative water removal prior to admitting the combusting gases into the ion source of the MS is essential because any water residue would lead to protonation of CO_2 to produce HCO_2^+, which interferes with analysis of $^{13}CO_2$ (isobaric interference) (Meier-Augenstein, 2004). The gases (CO_2, N_2) resulting from combustion are swept over on a He carrier gas stream, to be separated on a gas chromatography column (typically a Poropack packed column, with length and internal diameter varying according to the manufacturer) (figure 4). The gases are then introduced into the IRMS, and both $\delta^{13}C$ and $\delta^{15}N$ values can be obtained from the same sample. It is good laboratory practice to analyze a laboratory standard after every 5 samples to check precision, and ideally the standard should be similar in elemental composition to the sample of interest (Teece & Fogel, 2004). IRMS measurements yield the information of isotopic ratio of the analyte gas relative to the measured isotope ratio of a standard or reference gas. This is done to compensate for mass discrimination effects that may fluctuate with time and from instrument to instrument. The external reference gas pulses compensate for isotopic fractionation that might occur at the IRMS itself. Additionally, laboratory reference-materials are used, as those reflect all the potential sources of fractionation, e.g. due to sample injection, chromatographic isotope effects and peak distortion, the combustion process and changing flow conditions at the open-split prior to the IRMS. Owning to its unique design, it is not possible in EA-IRMS to calibrate sample isotope ratio against a standard of known isotopic composition, introducing the standard in *exactly* the same way as the analyte.

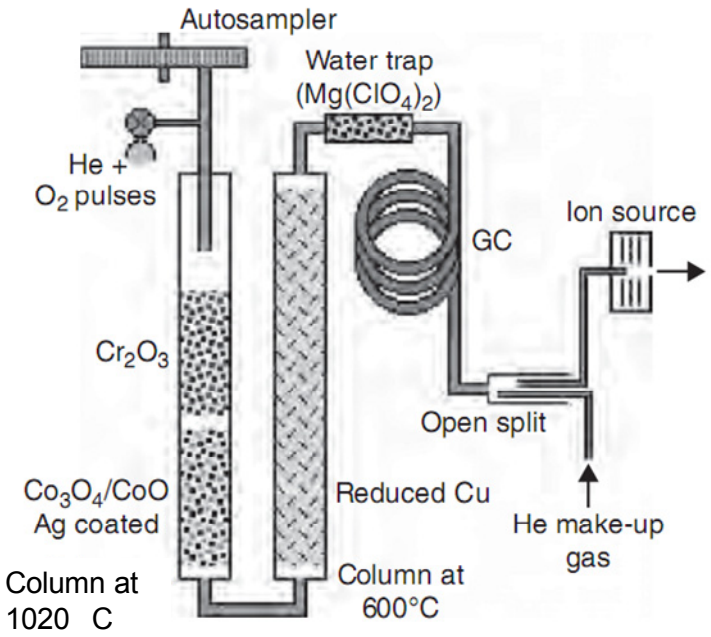

Figure 4. Diagram showing a CF-EA-IRMS device for oxidation of organic compounds and reduction of surplus O_2 and NO_x for C- and N-isotope determination (adapted from Midwood & McGraw, 1999 *in* de Groot, 2009).

There are only three feasible means of introducing a standard; (a) addition of reference compounds to the sample, (b) introduction of reference gas pulses to the carrier gas stream or (c) introduction of reference gas pulses directly into the ion source. Therefore, international reference materials (typically originated from the International Agency for Atomic Energy, IAEA-Vienna) are sequentially analyzed prior to or after the samples, thus allowing for cross-calibration, in addition to laboratory standards that allow for drift correction and precision verification along a sequence of analysis. At SIIAF, the reference gas is added to the He carrier gas flow via the open-split interface. The molecules composing the gaseous samples that are introduced in the ion source of the IRMS are ionized by an electron impact, forming positive ions, and the electron emission is tuned for maximum ion yield. Ion source electrically repels ions, and ion optics downstream from the source, along the ion path, are tuned for maximum collimation of the ion beams. Ions are afterwards subjected to a magnetic field for the separation of the different masses. The path followed by the different masses of interest will be more or less deflected depending on their lower or higher mass (figure 5). After separation, the different masses are detected. This occurs in the Faraday cups that constitute the IRMS detector.

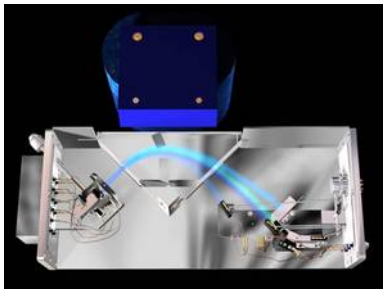

Figure 5. Ion beam path inside the IsoPrime IRMS detector (Micromass, UK).

The ions hit the Faraday cups, and the transference of their electric charge will result in an electric current, which will be amplified and converted to a digital signal.

For sulfur, a system of combined combustion-oxidation is used applying the Dumas method (DEA-IRMS). Samples were oxidized at 1030 ºC in the presence of O_2 and Tungsten oxide catalyst. Combustion gases were swept over heated reduced Cu, to reduce traces of SO_3 into SO_2 and NO_x into N_2, and remove excess O_2, by a He carrier. Water was removed in a magnesium perchlorate trap. The He + SO_2 gas stream was lead into the ion source of the MS. Nearly coincident peaks of N_2 and CO_2 is separated from SO_2 peak by GC. Memory effects for consequent samples (SO_2 is a chemical reactive compound) with large difference in isotopic values can be solved by passing a number of dummy samples before measuring the next sample.

In the case of oxygen isotope ratio measurements, there are some modifications to the previously described technical setup. In this case, the material is thermally decomposed in an oxygen-free atmosphere (pyrolysis) and all of the sample oxygen is converted to CO (figure 6). This is performed at the elemental analyzer in a glassy carbon tube coaxially installed in a ceramic tube. The pyrolysis reaction occurs in the presence of hot carbon (the carbon tube is filled up to half of the height with glassy carbon chips). The furnace temperature is 1230 ºC, which according to the manufacturer corresponds to 1300 ºC in the tube hot spot. The temperature of 1300 ºC is necessary to obtain complete conversion into CO. The samples are weighed into silver capsules (cleaned of any contamination oxides by treatment at 450ºC, for 4 hours, in a furnace) and then are dropped into the pyrolysis furnace by the autosampler, without addition of oxygen. The produced gases (mostly CO, H_2) are swept by the helium carrier gas through a CO_2-trap (soda-lime) and a water trap (magnesium perchlorate). Nitrogen present in the samples is separated from CO by a molecular sieve (5A, 1,5m). The CO masses 28 and 30 are measured for isotope ratio determination. The isotope ratios are calculated from the time integrals of the peak areas of the ion intensities m/z 30 and 28 (i.e. $^{12}C^{18}O^{+}$ and $^{12}C^{16}O^{+}$). Each sample is analyzed in four or three consecutive runs,

with the first discarded to account for memory effects. For every sample, the 30/28-ratio is related to the 30/28-ratio of a CO standard gas.

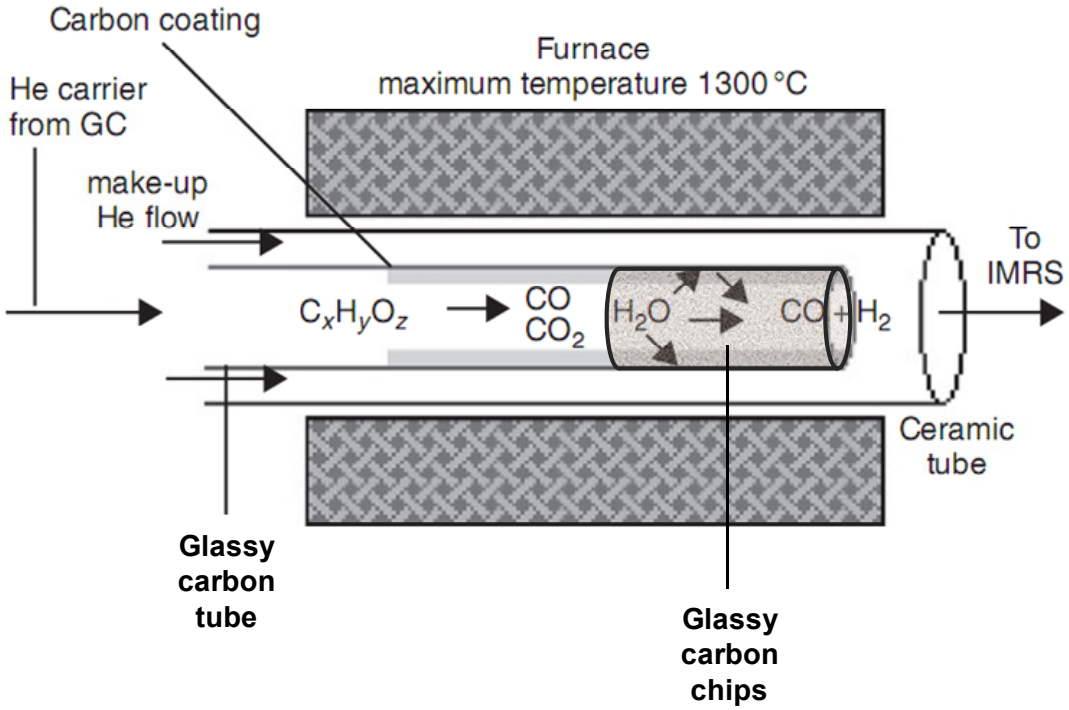

Figure 6. Pyrolysis setup for the EA prior to the determination of oxygen isotope ratio in the IRMS.

The calibration *versus* VSMOW is done by cross-calibration with IAEA reference materials IAEA-601 and IAEA 602 (Benzoic acid). When measuring isotope ratios of any chemical element, there are several masses of interest that may correspond to different chemical species. This demands the use of correction factors (algorithms) to correct for small contribution to the δ of the measured element. The isotope correction for CO measurement and the oxygen and carbon isotope correction for C measurement are presented by Pier A. de Groot in the Volume II, Chapter 19 of the Handbook of Stable Isotope Analytical Techniques (de Groot, 2009). Corrections for O isotope composition of SO_2 for sulfur isotopic measurements are presented in Volume I, Part 2, Chapter 45 of the Handbook of Stable Isotope Analytical Techniques by by C. Leckrone and M. Ricci (Leckrone & Ricci, 2004). In practice, the algorithms applied for data correction are automatically applied to the measured masses raw ratios by the instrument software. The equations and algorithms used for the corrections applied in this work (particularly for the presence of oxygen) are presented in the IsoPrime User's Guide (GV Instruments, 2005). Continuous-flow measurement of sulfur isotopes are measured based on the mass spectrum of the SO_2^+ molecular ion. Since both sulfur and oxygen are multi-isotope, all measurable ion currents above the molecular ion (m/z) 64 represent sums of multiple isotopic contributions. The masses 65 and 66 depend on the oxygen isotope composition of the SO_2 as well as that of sulfur. The aim of the

correction is to remove the effects of oxygen isotope composition to reveal the true sulfur isotope values. There are also carbon and oxygen isotopic corrections and calibrations in CO_2 for MS measurements. Here, measured ion currents above the molecular ion (m/z) 44 represent sums of multiple contributions. The mass 45 depends on the oxygen isotope composition of CO_2 as well as that of carbon. For the correction of oxygen isotopic composition, the mass 46 is measured versus the combined mass 44 and 45.

Sr isotope ratio and multielement measurements by inductively coupled plasma mass spectrometry (ICP-MS)

VIRIS Laboratory, BOKU University, Vienna, Austria

The Sr isotope system

Natural Sr consists of 4 isotopes of the approximate atomic weights 84, 86, 87 and 88 (de Laeter *et al*., 2003). Isotope abundances as recommended by the International Union of Pure and Applied Chemistry (IUPAC) (Rosman & Taylor, 1998) can be found in table 1.

Table 1. Natural Sr isotope abundances.

Isotope	Abundance [%]
^{84}Sr	0.56
^{86}Sr	9.86
^{87}Sr	7
^{88}Sr	82.58

However, natural isotope abundances may vary significantly owing to either radioactive decay processes or mass dependent chemical and physical processes such as dissolution or precipitation of Sr containing minerals. Sr is among the most abundant trace elements found on earth (Capo, Stewart & Chadwock, 1998). ^{87}Sr is the only radiogenic of all 4 naturally occurring Sr isotopes, and is the product of the radioactive β^- decay of ^{87}Rb, with an approximate half life of $t_{1/2} = 4.88 \pm 0.05 \times 10^{10}$ years; decay constant $\lambda = 1.42 \times 10^{-11}$ years (Bentley, 2006). Within a given geologic matrix, the radioactive decay of ^{87}Rb will lead to an increase of the ^{87}Sr abundance over time, while the abundances of ^{84}Sr, ^{86}Sr and ^{88}Sr remain constant. The absolute amount of ^{87}Sr within a geologic matrix is therefore a function of the initial Rb/Sr concentration ratio as well as the time Rb and Sr spent together within the given geologic matrix (Galler, 2008). Older rocks have higher $^{87}Sr/^{86}Sr$ ratio than younger rocks and the ratio can be used as an indicator for provenance, age and geologic interactions. The measurand for estimation of ^{87}Sr abundance is traditionally the $^{87}Sr/^{86}Sr$ isotope ratio (Bentley, 2006). The $^{87}Sr/^{86}Sr$ isotope ratio reflects the local environment, exhibits significant variation in nature, and is typically close to 0.7. The lowest natural $^{87}Sr/^{86}Sr$ isotope ratio

representative for the upper mantle of the Earth is 0.703. Sr is released from geologic matrices by weathering processes, dissipated and subsequently cycled in nature. It is also deposited in marine carbonate and a small amount exhausts directly to the atmosphere and is released to the continents in precipitation (Capo et al., 1998). Only bioavailabile or exchangeable Sr will be taken up by plants. Strontium isotopes are taken up by the roots of plants as the same isotopic proportions as their existence in the soil (Almeida & Vasconcelos, 2004). Because of the slight mass ratio between the Sr isotopes, biological and chemical processes have neglected isotopic fractionation compared to low-mass isotopic systems such as O, C, N and S. Variations in the Sr isotopic composition in the different components of forest ecosystems are therefore caused entirely by the mixing of Sr derived from sources with specific $^{87}Sr/^{86}Sr$ ratio. For this reason, the $^{87}Sr/^{86}Sr$ ratio can be used to identify and quantify the contribution of different Sr sources to a forest vegetation (Drouet, Herbauts & Demaiffe, 2007). So, in this sense, it is generally accepted that the isotopic composition of Sr does not undergo measurable change when it passes from bedrock into soil further via water into plants and finally along the food chain into animal tissues. Therefore, Sr isotopic analysis provides a valuable tool to trace provenance of goods, agricultural products, food or even animals (Bentley, 2006; Capo et al., 1998; Pett-Ridge, Derry & Kurtz, 2009). Animals also cycle or store strontium in their teeth, bones and shells as Sr acts as a proxy for Ca. Especially for animals, strontium may reveal their environment and dietary habits (Capo et al., 1998). Additionally, differences in the strontium signature between bones and teeth are an indicator for mobility during humans life (Prohaska, Latkoczy, Schultheis, Teschler-Nicola & Stingeder, 2002). Strontium isotopes ratios have also been applied for authentication of the origin of different food products and beverages.

Inductively coupled plasma mass spectrometry (ICP-MS)

The fundamental principle of ICP-MS is to use inductively coupled argon plasma to generate positively charged ions which are separated according to their mass/charge ratio in a mass spectrometer. The sample, typically in liquid form, is pumped into the sample introduction system, which is made up of a spray chamber and nebulizer. After the sample enters the nebulizer, the liquid is broken up into a fine aerosol by the pneumatic action of gas flow (usually argon), and the smaller droplets pass through the central tube of the spray chamber and are transported into the sample injector (figure 7). As the sample travels through the different heating zones of the plasma torch it is dried, vaporized, atomized, and ionized. The ionization process occurs under atmospheric pressure. When the sample reaches the analytical zone of the plasma, it exits as excited atoms and ions, representing the elemental composition of the sample.

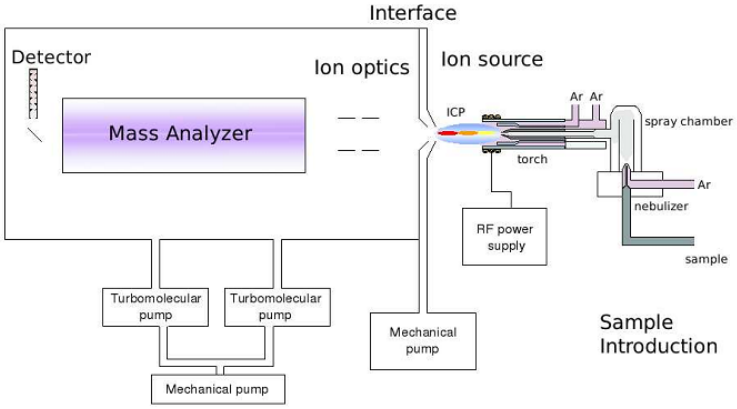

Figure 7. Schematic view of an ICP-MS instrument (Horsky, 2010).

A plasma discharge is formed when a tangential (spiral) flow of argon gas is directed between the outer and middle tube of a quartz torch. A load coil surrounds the top end of the torch and is connected to a radio frequency (RF) generator. An RF is applied at the top of the torch. With argon gas flowing through the torch, a high-voltage spark is applied to the gas. Electrons are stripped from argon atoms, accelerated in a magnetic field and collide with argon atoms, stripping more electrons in a chain reaction called Collision Induced Ionization. This is what forms an Inductively Coupled Plasma discharge. The ICP discharge is then sustained within the torch. The ions emerging from the plasma are directed into the interface of the mass spectrometer. It consists of two metallic cones maintained under vacuum of with a mechanical pump. The first cone is called the sampler cone and the second cone is the skimmer cone. Flow through the sampler cone is characterized as continuum, and the central core of this expansion is skimmed at the skimmer. The flow downstream of the skimmer is supersonic, and the ions gain energy from the expansion that is proportional to their mass. This yields an ion beam characterized by mass-dependent kinetic energies (Tanner, Baranov & Bandura, 2002). It is very important that the plasma is kept at zero potential in order to transfer the ions efficiently from the plasma to the mass spectrometer analyzer region. When the ions emerge from the argon plasma, they will have different kinetic energies based on their mass-to-charge ratio. However, their velocities should be similar because they are controlled by the rapid expansion of the bulk plasma, which is neutral as long as it is maintained at zero potential in order to keep ion energy spread low. This will facilitate ion focusing by ion optics. The energy spread of the ions entering the mass spectrometer must be as low as possible to ensure that they can all be focused efficiently and with full electrical integrity by the ion optics and the mass separation devices. The ion optics is positioned between the skimmer cone and the mass separation device (figure 7). It consists of one or more electrostatically controlled lens components made up of a series of metallic plates, barrels, or cylinders that have a voltage placed on them.

The function of the lens system is to take ions from the environment of the plasma which is at atmospheric pressure via the interface cones and steer them into the mass analyzer which is under vacuum. When the ions generated in the plasma emerge from the skimmer cone, there is a rapid expansion of the ion beam as the pressure is reduced from $\approx 10^5$ Pa (atmospheric pressure) to approximately 1.3×10^{-2} to 1.3×10^{-1} Pa in the lens chamber with a turbomolecular pump. With this rapid drop in pressure in the lens chamber, electrons diffuse out in preference to ions with medium (mid-mass) or low (low-mass) kinetic energy. By placing voltages on one or more ion lens components it is possible to electrostatically steer the ions of interest back into the center of the ion beam. Again, this is only possible if the interface is kept at zero potential which ensures a neutral gas-dynamic flow through the interface and maintains the compositional integrity of the ion beam. The mass analyzer is positioned between the ion optics and the detector and maintained at a vacuum of approximately 1.3×10^{-4} Pa. Assuming the ions are emerging from the ion optics at the optimum kinetic energy, they are ready to be separated according to their mass-to-charge ratio by the mass analyzer.

In the present work, two different ICP-MS instruments were used for testing the efficiency of the offline Sr/matrix separation procedure and multielement analysis, and for $^{87}Sr/^{86}Sr$ measurements in green coffees. The two instruments differ on the type of mass analyzer and detector. For this reason, a more detailed description on each instrument will be given separately.

Quadrupole mass spectrometry (ICP-QMS)

An ELAN DRC-e (PerkinElmer, Ontario, Canada) ICP-MS instrument was used for the determination of Sr and Rb concentration multi-element analysis in the different green coffee bean samples. The instrument is equipped with a quadrupole mass analyzer. A direct current (DC) voltage applied on one pair of rods is superimposed to a radio frequency (RF) voltage applied to the opposite pair. Ions of a selected mass are allowed to pass through the rods to the detector, while the others are ejected. This scanning process is then repeated for another analyte at a different mass-to-charge ratio until all the analytes in a multielement analysis have been measured. This consists of a sequential analysis of the ions with different m/z. Several interferences may occur during routine ICP-MS analysis, i.e. non-spectral (due to matrix effects) and spectral ones. The latter may be isobaric interferences or polyatomic/molecular overlaps. Isobaric interferences are caused by isotopes of a neighboring element having close masses (e.g. between ^{87}Sr and ^{87}Rb) or by molecular (cluster) ions of matrix elements (e.g. $^{80}Se^+$ and $^{40}Ar_2^+$: $m/\Delta m \approx 9\ 500$). Spectral interferences can bring difficulties in analyzing some critical elements. To minimize these interferences, the Elan DRC-e

instrument has a Dynamic Reaction Cell™ (DRC) next to the focusing lens and photon stop and in front of the quadrupole analyzer. The DRC is a high precision quadrupole that is enclosed and may be pressurized with a reactive gas. Ions of interest are fragmented in collisions with an inert gas at energies that exceed the bond strength of the parent ion. Different ions have different reactivity toward many reaction gases. The difference in reactivity between isobaric ions is an essential feature of method development for interference reduction (Tanner et al., 2002). For a detailed review on reaction and collision cells please refer to Tanner *et al*. 2002. In this work, the DRC mode was not used when screening the samples for Sr as well as for multi-element analysis. This setup is specially used when measuring, e.g. the sulfur (S) element. In our case, the reaction cell acted as an open cell letting the ions move free to the analyzer. In ELAN DRC-e the detection system consists of a discrete secondary electron multiplier. The positively charged ions that leave the quadrupole analyzer are attracted to a negative charged dynode. The impact of the ions on the dynode causes the emission of electrons that are attracted to a positively charged second dynode and this chain reaction is repeated for a total of 20 dynodes. The result is the amplification of the signal due to ions entering the detector.

Multicollector sector field mass spectrometry (HR-MC-ICP-SFMS)

Green coffee beans Sr isotope ratios were performed on a multicollector ICP-MS (MC-ICPMS) (figure 8). The following paragraphs discuss the basic background of data acquisition and handling used with the Nu Plasma HR™ MC-ICP-MS system (Nu Instruments Ltd., Wrexham, UK).

Figure 8. Nu Plasma HR™ instrument setup at VIRIS laboratory, BOKU University, Vienna, Austria.

The liquid sample is introduced into the plasma as a dry aerosol generated by a desolvating membrane nebulizer "DNS 100" (Nu Instruments Ltd.) which enables efficient removal of water from the sample aerosol (figure 9).

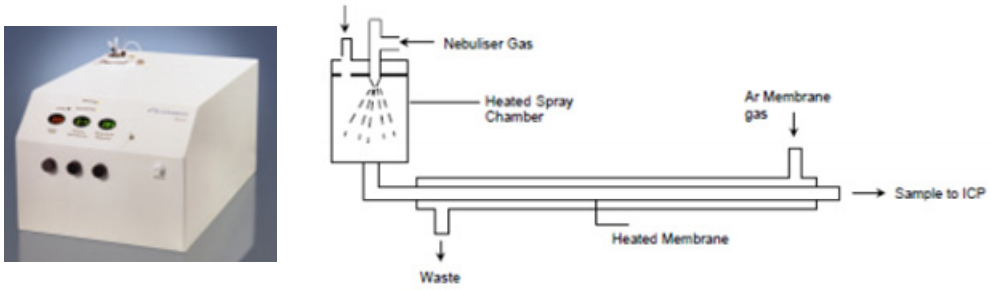

Figure 9. DNS 100 desolvating membrane nebulizer (Nu Instruments, 2007).

The sample solution is introduced via a conventional low flow nebulizer (PFA nebulizer) into a heated spray chamber and subsequently transported through a heated membrane, where water vapor is removed from the sample aerosol. Outside the membrane a heated counter current Ar gas flow is removing the water vapor. The sample leaves the membrane desolvating nebulizer as dried aerosol and is directly introduced into the ICP. A high capacity interface rotary pump "E2M80" (BOC Edwards, West Sussex, Great Britain) is permanently installed, resulting in lower pressure in the interface region between sampler and skimmer cone compared to when a default interface pump with lower evacuation capacity is installed. This as a favorable effect on instrumental sensitivity as a significantly smaller number of ions will be scattered due to collision with neutral species in the interface region (Galler, 2008; Nelms, 2005). As in the case of ICP-QMS, the sample ionization occurs in the torch and the ions are transferred to the interface region consisting of a sampler and skimmer cones (figure 10). In order to work with a multiple collector detector, a sector field analyzer is necessary to measure different masses simultaneously. The sector field in Nu Plasma HR is composed by two analyzers, an electrostatic sector analyzer (ESA) and a magnetic sector analyzer (MSA) of Nier-Johnson geometry (figure 11). In the ESA a voltage is applied to promote ions kinetic energy focusing (Nelms, 2005; Prohaska, Wenzel & Stingeder, 2005). Different ions (with different masses) come from the plasma with different kinetic energies. The kinetic energy focusing will set the same kinetic energy for all ions and, as a result, the velocities of the ions change. Then, through the electromagnet, ions will move in a certain angle depending on their *m/z*. The Nu Plasma HR is a double focusing sector field instrument because it involves focusing in both ion angles and energies.

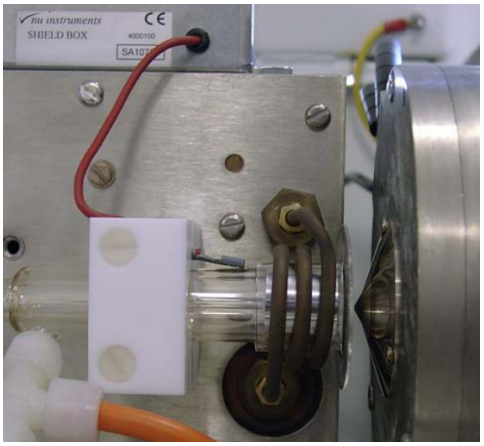

Figure 10. Nu Plasma HR^{TM} torch and sampler cone.

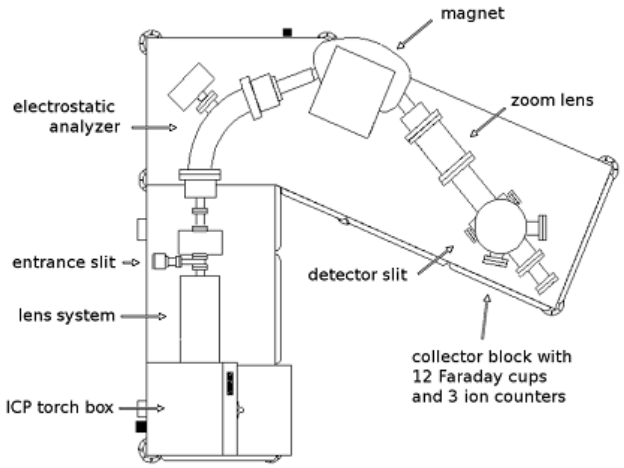

Figure 11. Schematic of Nu Plasma instrument (Nu Instruments, 2007).

Following the magnet are two zoom lens assemblies. These are designed to produce quadrupolar fields using an array of plates above and below the ion beam path on which a series of quadratically increasing voltages are applied. The lens systems focus the ion beam to hit specific Faraday cups at the detector. A multiple collector instrument includes more than one detector allowing the simultaneous detection of ions with different m/z after separation by the magnet sector. The advantage in relation to ICP-QMS is that this array of detectors improves precision of isotope ratio measurements by one order of magnitude because instabilities due to plasma fluctuations are compensated. The detection of ions in the Nu Plasma HR may be held by three multiple ion counting detectors and twelve Faraday cups. A Faraday detector is an electrode from which electrical current is measured while a charge particle bean

(electrons or ions) impinges on it. The Faraday detectors used on the Nu Plasma HR^{TM} are boxed and the ion beam enters and strikes the back of the detector (figure 12a). Up to 12 Faraday detectors can be fitted into what is called the collector block located inside the collector housing (figure 12b).

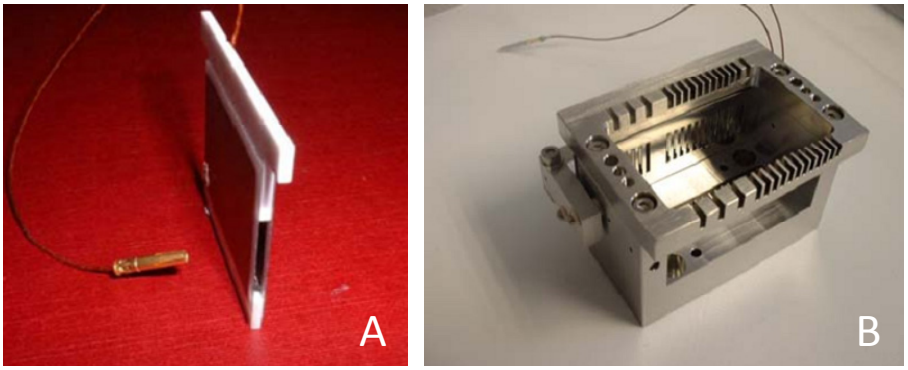

Figure 12. Nu Plasma HRTM Faraday detector (A) and collector block (B).

A screen is placed in front of the collector block to stop any scattered ions getting behind it. The signal leads of each Faraday detector are connected to feed-troughs that are then connected to the amplifier electronics below the collector housing (figure 13).

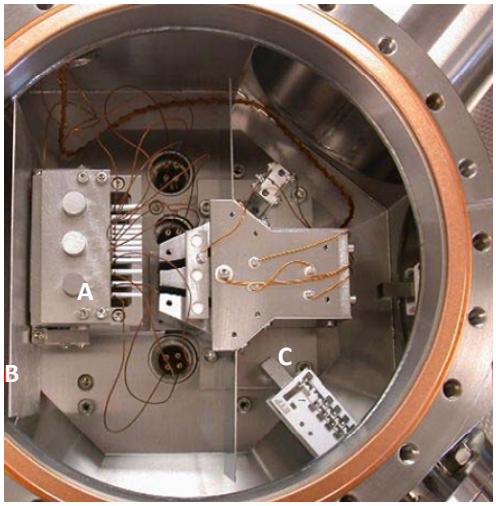

Figure 13. Nu Plasma HR^{TM} collector housing with collector block (A), screen (B) and ion-counting multipliers (C).

Sample preparation

The aim of the sample preparation preceding solution based measurements is to obtain the sample in a form suitable for the employed mass spectrometric technique. Ideally the sample digest is a clear, colourless solution without presence of suspended or sedimented particulate matter. Energy for sample digestion can be delivered by e.g. UV-lamps, microwave systems or simple hot plates (Galler, 2008). All coffee beans were grinded in a ball mill (Retsch, Germany) to reach a particle size of less than 1 mm before they are used for microwave digestion. The grinded coffee samples were digested in a high performance microwave digestion unit (MLS 1200 mega, Leutkirch im Allgäu, Germany). Approximately 0.5 g of grinded coffee beans was weighed into Teflon digestion bombs and 6 mL concentrated double-subboiled HNO_3 65% (w/w) and 1 mL H_2O_2 31% (w/w) were added as digestion reagents. The time and temperature program of digestion is shown in table 2. A blank digestion was always performed in each digestion batch. The digested samples were transferred into 50 mL flasks and filled up to 20 g with double-subboiled H_2O and stored at room temperature. ForThe digested samples were filtered using a 5 mL syringe through 0.22 µm filters (Minisart RC 25, non-sterile, RC membrane, PP-housing) to remove solid residuals.

Table 2. Temperature and power program for microwave assisted digestion.

Time	Temperature
2 min	250 W
2 min	0 W
6 min	250 W
5 min	400 W
5 min	600 W
10 min	Vented

Sr/matrix separation

Generally Sr/matrix separation is a pre-requisite for solution based high precision Sr isotope ratio measurements to avoid interferences or matrix effects (Albarède, Telouk, Blichert-Toft, Boyet, Agranier & Nelson, 2004). Here, the signal for ^{87}Sr is interferred with the ^{87}Rb (Balcaen, De Schrijver, Moens & Vanhaecke, 2005)

Traditionally Sr/matrix separation is performed off-line as batch procedure before the actual samples investigation. In this work, sample matrix separation was achieved exclusively by using the Sr specific solid phase extraction as originally proposed by Horwitz and co-authors (Horwitz, Dietz & Fisher, 1991). This procedure is performed using a commercially available product called "Sr Spec resin" (Eichrom, USA). The resin is received in dry powder form and it has to be soaked prior to use with a 1 % (w/w) nitric acid solution. It was found to be worthwhile pre-cleaning the Sr resin with water before conditioning the resin with the sample media (Vonderheide et al., 2004). Sr retention is strongly increased with the nitric acid concentration of the sample and washing solution (Horwitz, Chiarizia & Dietz, 1992). Typically nitric acid concentrations between 6 and 8 $mol.L^{-1}$ were found to be sufficient for the sample medium and the washing solution (Galler, Limbeck, Boulyga, Stingeder, Hirata & Prohaska, 2007; Swoboda, Brunner, Boulyga, Galler, Horacek & Prohaska, 2008a). When loading the sample into the extraction column, the flow rate should not exceed 0.5 $mL.min^{-1}$ in order to allow the sample solution to equilibrate with the sorbent. Washing cycles necessary to remove all matrix components depend on the Sr/Rb concentration ratio as well as on their absolute concentrations and may have to be optimised for each sample type. After sample elution, the resin is washed well with several column volumes of water and stored as slurry in PE vessels at 4º C in dilute nitric acid. The separation was done with Sr specific resin (ElChrom Industries, Inc., Darien, IL, USA) with particle size of 100 µm – 150 µm, and based on previous work (Swoboda et al., 2008b). The powdered resin was slurred with HNO_3 1% (w/w) for a minimum of 30 minutes or, if possible, overnight. After this, the supernatant was removed and the flask containing the resin was refilled with fresh HNO_3 1% (w/w). This resin could be used up to four times although, before each usage, it had to be washed with 50 mL HNO_3 1% (w/w), and then with subboiled water. This procedure was repeated twice. The Sr/matrix is performed in 3 mL columns (Separtis, Grenzach-Wyhlen, Germany) equipped with 10 µm filters (Separtis, Grenzach-Whylen, Germany). Approximately 0.5 mL of bed volume of Sr resin was pipetted to the column. The following standard separation procedure was applied. Resin wash: 4 times with 0.5 mL of subboiled H_2O;

- Conditioning: 5 times with 0.5 mL of 6 $mol.L^{-1}$ HNO_3
- Sample loading: 2 mL of acidified sample solution
- Washing: 12 - 15 times with 0.5 mL of 8 $mol.L^{-1}$ HNO_3
- Elution: 4 times with 0.5 mL of subboiled H_2O

After usage, the filters are cleaned with HNO_3 5% (w/w) in an ultrasonic bath (Transsonic T80, Elma Hans Schmidbauer GmbH & Co. KG, Singen, Germany) and

stored in HNO3 (5 % (w/w). The columns were flushed with HQ water, stored in 10% HNO3 overnight, rinsed again with HQ-water and stored in HNO_3 5% (w/w).

Multielement analysis

After microwave digestion and filtration, the coffee samples were diluted 1:10 with subboiled H_2O and the internal standard In was added to reach a final concentration of 10 ng g-1 before proceeding to multielement analysis. Microwave digestion blanks were also measured in order to control possible contaminations through the sample preparation. All samples were screened for the following isotopes: ^{10}B, ^{23}Na, ^{26}Mg, ^{27}Al, ^{52}Cr, ^{55}Mn, ^{56}Fe, ^{59}Co, ^{60}Ni, ^{63}Cu, ^{66}Zn, ^{69}Ga, ^{85}Rb, ^{88}Sr, ^{98}Mo, ^{137}Ba, ^{138}Ba, ^{208}Pb and ^{209}Bi. Determination of element concentrations in digested coffee samples was performed with the ELAN DRC-e quadrupole mass spectrometer. The operational conditions used are described in table 3. Nine calibration levels were prepared with the standard solution VI (MERCK KGaA, Damrstadt, Germany) with concentrations of 0.05 $ng.g^{-1}$, 0.1 $ng.g^{-1}$, 0.5 $ng.g^{-1}$, 1 $ng.g^{-1}$,5 $ng.g^{-1}$,10 $ng.g^{-1}$, 25 $ng.g^{-1}$, 50 ng g-1 and 100 ng g-1 respectively. Indium standard solution (110 $ng.g^{-1}$) was added for internal normalization to get a final concentration in samples of 10 $ng.g^{-1}$. A HNO_3 1% (w/w) solution was chosen for blank correction and surveillance of possible memory effects during the measurement series. The blank corrected concentrations of the different isotopes in each sample were calculated by the instrumental software through external calibration, based on linear regression and/or weighted regression and internal normalization after blank subtraction.

Screening of Sr and Rb

In order to control Sr/matrix separation efficiency it is necessary to screen the separated samples for Sr and Rb content. The eluted samples obtained after Sr/matrix separation were diluted 1:10 with HNO_3 1% (w/w) to a final volume of 1 mL prior to measurement. The ELAN DRC-e operational conditions are shown in table 4. The Multi-Element Standard Solution VI (MERCK KGaA, Darmstadt, Germany) was used to prepare the calibration standards for the Sr and Rb quantification. A nine-point calibration with concentrations of 0.05 $ng.g^{-1}$, 0.1 $ng.g^{-1}$,0.5 $ng.g^{-1}$,1 $ng.g^{-1}$,5 $ng.g^{-1}$,10 $ng.g^{-1}$, 25 $ng.g^{-1}$, 50 $ng.g^{-1}$, and 100 $ng.g^{-1}$ was done. Indium was also added to each sample as internal normalization standard to reach a final concentration of 10 $ng.g^{-1}$ In.

After evaluating Rb concentration in the digested and separated green coffee bean samples (which should below 0.2 % Rb compared to Sr), samples are diluted to a Sr concentration of approximately 20 $ng.g^{-1}$. If the Sr concentrations in the separated

samples were below 20 ng.g^{-1}, no further sample dilution was performed prior to MC-ICP-MS measurements.

Table 3. Operating parameters of Elan DRC-e for multielement analysis of green coffee samples.

Parameter	
RF Power	1250 W
auxiliary gas flow	0.6 L min^{-1}
plasma gas flow	15 L min^{-1}
nebuliser gas flow rate	0.98 – 1.02 L min^{-1}
sample cone	Nickel
skimmer cone	Nickel
nebuliser	Glass (Micromist)
spray chamber	cyclonic spray chamber
number of sweeps	10
number of readings	1
number of replicates	5
lens settings	< 12 V
sample uptake rate	500 µl min^{-1}
signal intensity (In per 10 ng g-1)	650 000 – 800 000cps
flush delay	60 sec
wash time	120 sec
pump velocity	20 rpm
measurement	dual mode

Table 4. Operational conditions of Elan DRC-e for Sr/Rb screening.

Parameter	
RF Power	1250 W
nebuliser gas flow rate	0.98 – 1.02 L min^{-1}
auxiliary gas flow	0.6 L min^{-1}
plasma gas flow	15 L min^{-1}
sample cone	nickel
skimmer cone	nickel
nebulizer	PFA
spray chamber	cyclonic spray chamber
number of sweeps	8
number of readings	1
number of replicates	5
lens settings	< 12 V
sample uptake rate	100 µl min^{-1}
signal intensity In	350 000-450 000
flush delay	80 sec
wash time	80 sec
pump velocity	20 rpm
measurement	dual mode

MC-ICP-MS measurement of $^{87}Sr/^{86}Sr$ isotope ratios

The Nu Plasma operational parameters used for $^{87}Sr/^{86}Sr$ determination of green coffee bean samples are shown in table 5. A 20 ng g-1 NIST SRM 987 solution was used for quality control purpose and was measured after every fifth sample. The arrangement of the Faraday collector block for simultaneous measurement of Sr masses 86, 87 and 88 is shown in table 6. Possible isobaric interferences and their isotopic abundances are also included in this table. Additionally krypton isotopes were monitored.

Table 5. Nu Plasma HR^{TM} operational parameters used for Sr isotope ratio measurement.

Parameter	
axial mass	86
RF power	1300 W
lens settings	optimal sensitivity
sample uptake rate	40 – 100 µl min^{-1}
plasma gas flow	13 L min^{-1}
auxiliary gas flow rate	1.2 L min^{-1}
cool gas flow rate	13 L min^{-1}
sample cone	nickel
skimmer cone	nickel
instrumental sensitivity	~200-400 V ppm^{-1}
dwell time	5 sec.
measurement per block	10
number of blocks	6
nebuliser	PFA
nebulizer pressure	~ 30 psi
DSN hot gas flow	0.09 L min^{-1}
DSN membrane gas flow	~ 3 L min^{-1}
DSN membrane temperature	120 °C
membrane temperature	112 °C

Table 6. Faraday collector blocks setup for simultaneous measurement of Sr isotopes.

Cups	L5	IC2	L4	IC1	L3	IC0	L2	L1	Ax	H1	H2	H3	H4	H5	H6
Mass	82		83		84		85		86		87		88		
Sr (%)					0.56				9.86		7.00		82.58		
Rb (%)							72.20				27.8				
Kr (%)	11.60		11.50		57				17.3						

Blank correction, mass bias correction and Rb correction for $^{87}Sr/^{86}Sr$ determination by MC-ICP-MS

Data correction of MC-ICP-MS measurements is a complex matter. Given below are only the steps that are routinely performed when processing a set of raw data. Some of the corrections of the data are performed automatically by the instrument software of the Nu Plasma. Mass bias describes mass fractionation effects that occur in the instrument. Ions with lighter mass are preferentially transmitted resulting in inaccurate measured isotope ratios (Niu & Houk, 1996). This effect is measured in the range of a few percent for Sr on the Nu Plasma (Galler, 2008). The crucial step is the sampling of ions from the plasma and their extraction through the interface. The space charge effect in this region appears to have a major influence. The underlying processes are not fully understood, however. Nonetheless, corrections are required in order to receive better estimates of the true isotope ratio. Various laws are applied like the linear law, the power law and the exponential law (Albarède et al., 2004; Ingle, Sharp, Horstwood, Parrish & Lewis, 2003). The latter is used in this work. An exponential mass bias correction was performed using a mass dependent exponential correction algorithm, identical to the one used by Balcaen et al 2005. Mass bias can be externally corrected for by monitoring and evaluating the mass bias drift of a standard solution of known isotopic composition, measured before and after samples. In this case matrices of standard and sample solutions should be matched as close as possible, as matrix components can lead to a change of mass bias behavior by affecting the charge density in the ICP (Ingle et al., 2003). If the investigated isotopic system provides a stable, invariable isotope ratio that is constant in nature, internal mass bias correction may be applied by evaluating the mass bias of this ratio. Subsequently the observed mass bias for this isotope pair may be applied for mass bias correction of another isotope pair of the same element. In the case of Sr the presumably invariant $^{86}Sr/^{88}Sr$ isotope ratio is routinely applied for internal mass bias correction of the measurand $^{87}Sr/^{86}Sr$ (Cavazzini, 2005). The use of an $^{86}Sr/^{88}Sr$ isotope ratio of 0.1194 for this purpose has a long history in literature and can be considered as convention (Bizzarro, Simonetti,

Stevenson & Kurszlaukis, 2003). A constant $^{86}Sr/^{88}Sr$ isotope ratio of 0.1194 was assumed throughout this work. The first step is a blank or baseline correction of the raw signals. Solution based measurements of samples formerly processed by off-line batch Sr/matrix separation are baseline corrected with procedural blanks. It is necessary to introduce washing times between the measurement of samples and blanks to minimize influence of memory effects from the sample introduction system. The blank is measured using an 'on-peak-zero' method and defines the background voltage for each cup, which is consequently subtracted from all measured voltages. The NIST CRM 987 certified for its Sr isotopic composition is evaluated like a sample and reveals if mass bias correction results in accurate isotope ratios and if precision requirements are met. After obtaining the blank corrected intensities, it is necessary to calculate the fractionation factor (equation 1) to account for mass fractionation according to the exponential law (Albarède et al., 2004; Ingle et al., 2003) using the measured $^{86}Sr/^{88}Sr$ ratio, which is assumed to be stable and not interfered. *U* signifies the measured voltages on the respective masses, while m is the mass of the respective isotope.

$$ff = log\left(\frac{U_{86}}{U_{88}}\left(\frac{^{86}Sr}{^{88}Sr}\right)\right)^{-1}_{true} \times \left(log\left(\frac{m_{Sr86}}{m_{Sr88}}\right)\right)^{-1} \qquad \text{Equation 9}$$

Not properly taking care of the isobaric interference of ^{87}Rb on ^{87}Sr will inevitably lead to inaccurate measurement results. The Rb correction procedure is based on the knowledge of the measured intensity of a non interfered Rb isotope (^{85}Rb) and calculation of contribution of ^{87}Rb to the total measured intensity at mass 87. The $^{87}Rb/^{85}Rb$ isotope ratio is a well defined constant and may be used to estimate the ^{87}Rb signal intensity from the measured ^{85}Rb intensity. Only the ^{85}Rb isotope being available for interference free measurement, the mass bias between ^{87}Rb and ^{85}Rb has to be estimated from the measured mass bias for $^{86}Sr/^{88}Sr$. Assuming a constant fractionation factor for Rb and Sr, the fractionation factor calculated in equation 1 can also be applied to calculating the signal on mass 87, which is caused by ^{87}Rb, as described in equation 2 (Ehrlich, Gavrieli, Dor & Halicz, 2001a):

$$U_{Rb87} = 0.38506 \times U_{85} \times \left(\frac{m_{Rb85}}{m_{Rb87}}\right)^{f} \qquad \text{Equation 10}$$

Subtraction of U_{Rb87} from the total signal on mass 87 gives the net signal for ^{87}Sr (equation 3):

$$U_{Sr87} = U_{87} - U_{Rb87} \qquad \text{Equation 11}$$

The blank and ^{87}Rb corrected ^{87}Sr signal intensity ($^{87}Sr_{meas}$) is subsequently used for calculating an $^{87}Sr/^{86}Sr$ isotope ratio which will be corrected for mass bias using equation 4:

$$\frac{^{87}Sr}{^{86}Sr} = \frac{U_{Sr87}}{U_{86}} \times \left(\frac{m_{Sr87}}{m_{Sr86}}\right)^{f} \qquad \text{Equation 12}$$

Although it is possible to correct for the isobaric ^{87}Rb interference, Rb levels should be kept as low as possible by thorough conduction of Sr/matrix separation as described before. It is known from experience and literature that increase of the Rb/Sr concentration ratio will lead not only to larger measurement uncertainties as a result of the uncertainty of the $^{87}Rb/^{85}Rb$ isotope ratio, but also to a linear increase of the finally determined $^{87}Sr/^{86}Sr$ isotope ratio (Fortunato et al., 2004; Galler et al., 2007).

Validation and total combined uncertainty

The limits of detection (LOD) and quantification (LOQ) were calculated as three and ten times de standard deviation of the method blanks, respectively. The uncertainty of the multi-element measurements was calculated using GUM Workbench Pro (version 1.2, Metrodata GmbH, Germany). The Guide to the Expression of Uncertainty in Measurement (GUM) was published by ISO and establishes the general rules for evaluating and expressing uncertainty (Barwick, Ellison, Lucking & Burn, 2001). The strontium isotope ratio uncertainty was calculated with Excel software (Microsoft Office, 2007) using the Kragten-spreadsheet approach (Kragten, 1994). For more detailed information on this approach, please refer to the EURACHEM/CITAC Guide Quantifying Uncertainty in Analytical Measurement (EURACHEM/CITAC, 2000).

Brief introduction to Raman spectroscopy theory

Max-Volmer Institute, Technical University of Berlin, Germany

Vibrational spectroscopy probes the periodic oscillations of atoms within the molecule. These oscillations do not occur randomly but in a precisely defined manner. This can easily be understood by taking into account that an N-atomic molecule has *3N* degrees of freedom, of which three refer to translations and three (two) correspond to rotations in the case of a nonlinear (linear) molecule structure. The remaining degrees of freedom represent *3N-6* (*3N-5*) vibrations of a non-linear (linear) molecular, the so-called normal modes. In each normal mode, atoms oscillate with the same frequency, the first observable in vibrational spectroscopy (although with different amplitudes that quantifies the displacements of each atom). The frequency depends on the forces acting on the individual atoms and on the respective masses. These forces do not only result from the chemical bonds connecting the individual atoms but also include contributions from non-bonding interactions within the molecule and with the molecular environment. In this way, the frequencies of the normal modes constitute a characteristic signature of the chemical constitution, the structure, and electron density distribution of the molecule in a given chemical environment, i.e., all the parameters required for a comprehensive atomic-scale description of a molecule. These parameters also control the second important observable parameter in the vibrational spectrum, the intensities of the bands, which, unlike the frequencies, are not independent of the method by which the vibrational spectrum is probed. The intensity is simply proportional to the probability of the transition from a vibrational energy level *n* to the vibrational level *m*, typically (but not necessarily) corresponding to the vibrational ground and excited states, respectively. The two main techniques used to obtain vibrational spectra, Infrared (IR) and Raman spectroscopy, are based on different physical mechanisms. In IR spectroscopy, molecules are exposed to a continuum of IR radiation and those photons that have energies corresponding to the frequencies of the normal modes can be absorbed to excite the respective vibrations. In Raman spectroscopy, these vibrational transitions are induced upon inelastic scattering of monochromatic light by the molecule, such that the frequency of the scattered light is shifted by the frequency of the molecular vibration. For a given molecule, absorption- and scattering-induced vibrational transitions are associated with different probabilities; hence, IR and Raman spectra may display different vibrational band patterns, which are an additional source of information about the structural and electronic properties of the molecule. In contrast to IR spectroscopy, the scattering mechanism for exciting molecular vibrations requires monochromatic irradiation. A portion of the incident photons is scattered inelastically such that the energy of the scattered photons differs from that of the incident photons. The electric

field of incident excitation radiation (usually highly polarized laser light) can induce a dipole moment in the molecule which is related to the polarisability. This quantity describes the response of the electron distribution to the movements of the nuclei that oscillate with the normal mode frequency (ν_k). Three different cases have to be distinguished, depending on the initial (i) and final state (f) of the scattering process. If f = i, the frequency ν_0 of the incident radiation is identical to that of the scattered radiation. This case refers to elastic or Rayleigh scattering in contrast to (inelastic) Raman scattering for which $f \neq i$. For Raman scattering we have to distinguish the cases $f < i$ and $f > i$ which corresponds to frequencies of the scattered light of $\nu_0+\nu_k$ (anti-Stokes) and $\nu_0-\nu_k$ (Stokes), respectively. At ambient temperature, thermal energy is lower than the energies of most of the vibrational transitions, such that molecules predominantly exists in the vibrational ground state and Stokes scattering represents the most important case of Raman scattering. When we observe spectra we read in ordinates the extent of absorbed (IR) or scattered (Raman) light intensity related to the energy of the vibrational transition (abscissa) that corresponds to the frequency of the absorbed light (IR) or to the frequency difference between the exciting and scattered light (Raman), usually expressed in wavenumbers (IR) or relative wavenumbers (Raman). For a more detailed theoretical treatment of vibrational spectroscopy, the reader is referred to Siebert & Hildebrandt (2008).

Gas chromatography-mass spectrometry

Chromatography and Capillary Electrophoresis Laboratory of Center of Chemistry and Biochemistry (CQB), FCUL, Lisbon, Portugal).

Gas chromatography-mass spectrometry (GC-MS) (figure 14) is a hyphenated combination of two powerful analytical techniques. The gas chromatograph separates the components of a mixture in time, and the mass spectrometer provides information that aids in the structural identification of each component.

Figure 14. GC-MS in the chromatography and capillary electrophoresis laboratory (CQB, FCUL).

The basic operating principle of a gas chromatograph involves volatilization of the sample in a heated inlet port (injector), separation of the components of the mixture in a specially prepared column, and detection of each component by a detector. An important facet of the gas chromatograph is the use of a carrier gas, such as helium, to transfer ha sample from the injector, through the column, and into the detector. The column, or column packing, contains a coating of a stationary phase. A component that spends less time in the stationary phase will elute quickly. There are several types of sample introduction systems available for GC analysis. These included gas sampling valves, split and splitless injectors, on-column injection systems, programmed-temperature injectors, and concentration devices. The sample device used depends on the application. For example, in the present work, the injection of the sample after SPME was a splitless injection. In splitless injection, the splitter vent of the injector is

closed so that the entire sample flows onto the head of the column. After a specific time called purge activation time, the splitter vent is opened to purge solvent from the injector (this is the case; in SPME there is no solvent) and any low boiling components of the sample that are not adsorbed by the column. Splitless injection, therefore, concentrates the sample onto the head of the column. In the gas chromatograph, separation of the different components of the sample occurs within a heated column. The column contains a thin layer of nonvolatile chemical that is coated onto the walls of the column (capillary column). The compounds are carried onto the column by the carrier gas and selectively retarded by the stationary phase. The temperature of the oven in which the GC column resides is usually increased at 4°-20°/minute so that higher boiling and more strongly retained components are successively released. The effluent from the gas chromatograph is transported to the mass spectrometer through the interface device. This must be done in such a manner that the analyte neither condenses in the interface nor decomposes before entering the mass spectrometer ion source. In addition, the gas load entering the ion source must be within the pumping capacity of the mass spectrometer. The interface must be heated above the boiling point of the highest-boiling component of the sample. In the ion source (figure 15), molecules can be ionized by different ionization techniques. In the present work, electron energy was the ionization method used. Electrons are produced from a filament and accelerated typically by 70 eV before entering the ion source through a small aperture. When the electrons pass near neutral molecules, they may impact sufficient energy to remove outer shell electrons, producing additional free electrons and positive (molecular) ions. The energy impacted by this type of ionization is high and causes part of or all of the molecular ions to break apart into neutral atoms and fragment ions.

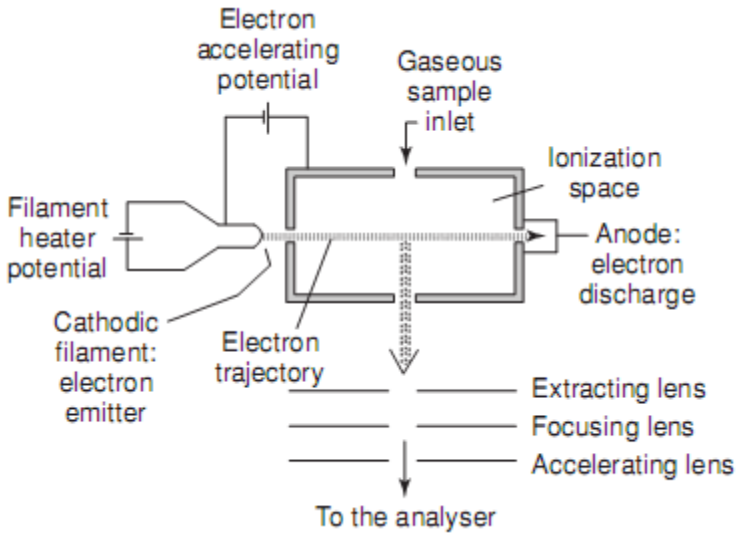

Figure 15. Diagram of an electron ionization source (from Hoffman & Stroobant, 2007).

The mass spectrometer is the instrument that measures the mass-to-charge ratio (*m/z*) of gas phase ions and provides a measure of the abundance of each ionic species.

The measurement is calibrated against ions of known *m/z*. In GC-MS, the charge is almost always 1, so that the calibrated scale is in Dalton or atomic mass units. The atomic mass units u or Da have the same fundamental definition (Hoffmann & Stroobant, 2007) :

$$1\ u = 1\ Da = 1.660\ 540 \times 10^{-27}\ kg \pm 0.59\ ppm$$

All mass spectrometers operate by separating gas phase ions in a low pressure (high vaccum) environment by the interaction of magnetic or electrical field on the charged particles. The most common mass spectrometers interfaced to gas chromatography use quadrupole and ion-trap analyzers. The instrument used for GC-MS analysis of the coffee aroma was a quadrupole mass filter. This name derives from the four precisely machined rods that the ions must pass in order to reach the detector. By screening the RF and dc fields on diagonally apposed rods, usually from low to high voltages, ions of successively higher masses follow a stable path to the detector. At a given filed strength, only ions in a narrow *m/z* range reach the detector. All others are deflected into the rods. In GC-MS, the chromatographic information is reconstructed from spectral analysis data. The representation of the sum of all *m/z* in time generates the total ion chromatogram (TIC) similar to a GC chromatogram obtained with a conventional detector. Each peak of the TIC will correspond to one component of the sample (if there are no overlapping peaks from different compounds) and correspond to a certain range of *m/z* values, which are represented by the mass spectrum. The output is in the form of an x, y plot in which the x-axis is the mass-to-charge scale and the y-axis is the intensity scale. If an ion is observed at an *m/z* value, a line is drawn representing the response of the detector to that ionic species. The mass spectrum will contain peaks that represent fragment ions as well as the molecular ion. Interpretation of a mass spectrum identifies, confirms, or determines the quantity of specific compounds. Both the intensity and *m/z* are important in interpreting a mass spectrum and when performing a spectra library search. The compound may be identified either by analyzing the pure compound and comparing the spectrum with the spectral library. In the present work, the compounds were identified by spectral library search as for many compounds for coffee aroma, no pure standards are available in the market. For a more detailed information on the fundamentals of GC-MS the reader can consult the work of Fulton and co-authors (Fulton, Barbara & Charles, 1996), Hans-Joachim Hübschmann (Hübschmann, 2001), and Hoffmann and Stroobant (Hoffmann et al., 2007).

References

Albarède, F., Telouk, P., Blichert-Toft, J., Boyet, M., Agranier, A., & Nelson, B. (2004). Precise and accurate isotopic measurements using multiple-collector ICPMS. *Geochimica and Cosmochimica Acta*, *68*, 2725-2744.

Almeida, C. M., & Vasconcelos, M. T. S. D. (2001). ICP-MS determination of strontium isotope ratio in wine in order to used as a fingerprint of its regional origin. *Journal of Analytical Atomic Spectrometry*, *16*, 607-611.

Almeida, C. M. R., & Vasconcelos, M. T. S. D. (2004). Does the winemaking process influence the wine 87Sr/86Sr? A case study. *Food Chemistry*, *85*, 7-12.

Balcaen, L., De Schrijver, I., Moens, L., & Vanhaecke, F. (2005). Determination of the $^{87}Sr/^{86}Sr$ isotope ratio in USGS silicate reference materials by multi-collector ICP-mass spectrometry. *International Journal of Mass Spectrometry*, *242*, 251-255.

Barbaste, M., Robinson, K., Guylfoile, S., Medina, B., & Lobinski, R. (2002). Precise determination of the strontium isotope ratios in wine by inductively coupled plasma sector field multicollector mass spectrometry. *Journal of Analytical Atomic Spectrometry*, *17*, 135-137.

Barwick, V. J., Ellison, S. L. R., Lucking, C. L., & Burn, M. J. (2001). Experimental studies of uncertainties associated with chromatographic techniques. *Journal of Chromatography A*, *918*, 267-276.

Bentley, R. A. (2006). Strontium isotopes from the Earth to the archaeological skeleton: A review. *Journal of Archaeological Method and Theory*, *13*, 135-187.

Bizzarro, M., Simonetti, A., Stevenson, R. K., & Kurszlaukis, S. (2003). In situ $^{87}Sr/^{86}Sr$ investigation of igneous apatites and carbonates using laser-ablation MC-ICP-MS. *Geochimica and Cosmochimica Acta*, *67*, 289-302.

Brach-Papa, C., Van Bocxstaele, M., Ponzevera, E., & Quétel, C. R. (2009). Fit for purpose validated method for the determination of the strontium isotopic signature in mineral water samples by multi-collector inductively coupled plasma mass spectrometry. *Spectrochimica Acta Part B: Atomic Spectroscopy*, *64*, 229-234.

Capo, R. C., Stewart, B. W., & Chadwock, O. A. (1998). Strontium isotopes as tracers of ecosystem processes: theory and methods. *Geoderma*, *82*, 197-225.

Cavazzini, G. (2005). A method for determining isotopic composition of elements by thermal ionization source mass spectrometry - Application to Sr. *International Journal of Mass Spectrometry*, *240*, 17-26.

Critteren, R. G., Andrew, A. S., LeFournour, M., Young, M. D., Middleton, H., & Stockmann, R. (2007). Determining the geographic origin of milk in Australasia using multi-element stable isotope ratio analysis. *International Dairy Journal*, *17*, 421-428.

de Groot, P. A. (2009). Mass Spectrometer Correction and Calibration Procedures. In: P. A. de Groot, *Handbook of Stable Isotope Analytical Techniques*, vol. II. Oxford: Elsevier.

de Laeter, J. R., Böhlke, J. K., P., D. B., Hidaka, H., Peiser, H. S., Rosman, K. J. R., & Taylor, P. D. P. A. w. o. t. e. R. I. T. R. (2003). Atomic weights of the elements. Review 2000 (IUPAC Technical Report). *Pure and Applied Chemistry*, *75*, 683-800.

Drouet, T., Herbauts, J., & Demaiffe, D. (2007). Change of the Origin of Calcium in Forrest Ecosystems in the Twentieth Century Highlighted by Natural Sr Isotopes. In: T.

E. Dawson, & R. T. W. Siegwolf, *Stable Isotopes As Indicators of Ecological Change* (pp. 333-343). London: Elsevier.

Ehrlich, S., Gavrieli, I., Dor, L.-B., & Halicz, L. (2001a). Direct high-precision measurements of the $^{87}Sr/^{86}Sr$ isotope ratio in natural water, carbonates and related materials by multiple collector inductively coupled plasma mass spectrometry (MC-ICP-MS). *Journal of Analytical Atomic Spectrometry*, *16*, 1389-1392.

Ehrlich, S., Gavrieli, I., Dor, L.-B., & Halicz, L. (2001b). Direct high-precision measurements of the 87Sr/86Sr isotope ratio in natural water, carbonates and related materials by multiple collector inductively coupled plasma mass spectrometry (MC-ICP-MS). . *Journal of Analytical Atomic Spectrometry*, *16*, 1389-1392.

EURACHEM/CITAC (2000). EURACHEM/CITAC Guide. Quantifying Uncertainty in Analytical Measurement. vol. 9.

Fortunato, G., Mumic, K., Wunderli, S., Pillonel, L., Bosset, J. O., & Gremaud, G. (2004). Application of strontium isotope abundance ratios measured by MC-ICP-MS for food authentication. *Journal of Analytical Atomic Spectrometry*, *19*, 227-234.

Fulton, G. K., Barbara, S. L., & Charles, N. M. (1996). *Gas chromatography and Mass Spectrometry, A Practical Guide*. San Diego: Academic Press.

Galler, P. (2008). Precise Sr Isotope Ratio Measurements by Multiple Collector Inductively Coupled Plasma Mass Spectrometry. *Analytical Chemistry Division, VIRIS Laboratory* vol. PhD. Vienna: BOKU, Universität für Bodenkultur.

Galler, P., Limbeck, A., Boulyga, S. F., Stingeder, G., Hirata, T., & Prohaska, T. (2007). Development of an on-line flow injection Sr/matrix separation method for accurate, high-thourghput determination of Sr isotope ratios by multiple collector-inductively coupled plasma-mass spectrometry. *Analytical Chemistry*, *79*, 5023-5029.

García-Ruiz, S., Moldovan, M., Fortunato, G., Wunderli, S., & García Alonso, J. I. (2007). Evaluation of strontium isotope abundance ratios in combination with multi-elemental analysis as a possible tool to study the geographical origin of ciders. *Analytica Chimica Acta*, *590*, 55-66.

GV_Instruments (2005). IsoPrime User's Guide, Code 666700, Issue 2. In: G. Instruments. Manchester: GV Instruments.

Hoffmann, E. d., & Stroobant, V. (2007). *Mass spectrometry, Principles and Applications*. West Sussex: Wiley.

Horsky, M. (2010). Determination of the provenance of prehistoric wood by isotopic fingerprinting. *Department of Chemistry*, vol. Diplomarbeit. Vienna: Universität für Bodenkultur.

Horwitz, E. P., Chiarizia, R., & Dietz, M. L. (1992). A Novel Strontium-selective extraction chromatographic resin. *Solvent Extraction and Ion Exchange*, *10*, 313-336.

Horwitz, E. P., Dietz, M. L., & Fisher, D. E. (1991). Separation and Preconcentration of Strontium from Biological, Environmental, and Nuclear Waste Samples by Extraction Chromatography using a Crown Ether. *Analytical Chemistry*, *63*, 522-525.

Hübschmann, H.-J. (2001). *Handbook og GC/MS - Fundamentals and Applications* Weinheim: Wiley.

Ingle, C. P., Sharp, B. L., Horstwood, M. S. A., Parrish, R. R., & Lewis, D. J. (2003). Instrument response functions, mass bias and matrix effects in isotope ration measurements and semi-quantitative analysis by sinlge and multi-collector ICP-MS. *18*(219-229).

Kragten, J. (1994). Calculating standard deviations and confidence intervals with a universally applicable spreadsheet approach. *Analyst*, *119*, 2661-2666.

Leckrone, K., & Ricci, M. (2004). Oxygen Isotope Corresctions in Continuous-Flow Measurements of SO_2. In: P. A. de Groot, *Handbook of Stable Isotope Analytical Technique*, vol. I. Oxford: Elsevier.

Montgomery, J., Evans, J. A., & Wildman, G. (2006). $^{87}Sr/^{86}Sr$ isotope composition of bottled British mineral waters for environmental and forensic purposes. *Applied Geochemistry*, *21*, 1626-1634.

Nelms, S. M. (2005). *ICP Mass Spectrometry Handbook*. Oxford: Blackwell Publishing, CRC Press.

Niu, H., & Houk, R. S. (1996). Fundamental aspects of ion extraction in inductively coupled plasma mass spectrometry. *Spectrochimica Acta Part B*, *51*, 779-815.

Pett-Ridge, J. C., Derry, L. A., & Kurtz, A. C. (2009). Sr isotopes as a tracer of weathering processes and dust inputs in a tropical granitoid watershed, Luquillo Mountains, Puerto Rico. *Geochimica and Cosmochimica Acta*, *73*, 25-43.

Prohaska, T., Latkoczy, C., Schultheis, G., Teschler-Nicola, M., & Stingeder, G. (2002). Investigation of Sr isotope ratios in prehistoric human bones and teeth using laser ablation ICP-MS and ICP-MS after Rb/Sr separation. *Journal of Analytical Atomic Spectrometry*, *17*, 887-891.

Prohaska, T., Wenzel, W., & Stingeder, G. (2005). ICP-MS-based tracing of metal sources and mobility in a soil depth profile via the isotopic variation of Sr and Pb. *International Journal of Mass Spectrometry*, *242*, 243-250.

Rodushkin, I., Bergman, T., Douglas, G., Engström, E., Sörlin, D., & Baxter, D. C. (2007). Authentication of Kalix (N.E. Sweden) vendance caviar using inductively coupled plasma-based analytical techniques: Evaluation of different approaches. *Analytica Chimica Acta*, *583*, 310-318.

Rosman, K. J. R., & Taylor, P. D. P. (1998). Isotopic compositions of the elements. *Pure and Applied Chemistry*, *70*, 217-236.

Rummel, S., Hoelzl, S., Horn, P., Rossman, A., & Schlicht, C. (2008). The combination of stable isotope abundance ratios of H, C, N and S with 87Sr/86Sr for the origin assignment of orange juices. *Food Chemistry*, *118*, 890-900.

Swoboda, S., Brunner, M., Boulyga, S., Galler, P., Horacek, M., & Prohaska, T. (2008a). Identification of marchfeld asparagus using sr isotope ratio measurements by MC-ICP-MS. . *Analytical and Bioanalytical Chemistry*, *390*, 487-494.

Swoboda, S., Brunner, M., Boulyga, S. F., Galler, P., Horacek, M., & Prohaska, T. (2008b). Identification of Marchfeld asparagus using Sr isotope ratio measurements by MC-ICP-MS. *Analytical and Bioanalytical Chemistry*, *390*, 487-494.

Tanner, S. D., Baranov, V. I., & Bandura, D. R. (2002). Reaction cells and collision cells for ICP-MS: a tutorial review. *Spectrochimica Acta Part B*, *57*, 1361-1452.

Voerkelius, S., Lorenz, G. D., Rummel, S., Quétel, C. R., Heiss, G., Baxter, M., Brach-Papa, C., Deters-Itzelsberger, P., Hoelzl, S., Hoogewerff, J., Ponzevera, E., Bocxstaele, M. V., & Ueckermann, H. (2009). Strontium isotopic signatures of natural mineral waters, the reference to a simple geological map and its potential for authentication of food. *Food Chemistry*, *118*, 933-940.

Vonderheide, A. P., Zoriy, M. V., Izmer, A. V., Pickhardt, C., Caruso, J. A., Ostapczuk, P., Hille, R., & Becker, J. S. (2004). Dtermination of ^{90}Sr at ultratrace levels in urine by ICP-MS. *Journal of Analytical Atomic Spectrometry*, *19*, 675-680.